

https://dspace.org/

Molecular characterisation of understudied Anopheles species using morphological and DNA-based approaches

Langa, Zandile

2025

University of the Witwatersrand, Johannesburg

https://hdl.handle.net/10539/49895

Langa, Zandile. (2025). Molecular characterisation of understudied Anopheles species using morphological and DNA-based approaches [Master's dissertation, University of the Witwatersrand, Johannesburg]. WIReDSpace. https://hdl.handle.net/10539/49895

Downloaded from a DSpace repository. https://dspace.org/

Molecular characterisation of understudied *Anopheles* species using morphological and DNA-based approaches.



ZANDILE LANGA

758103

School of Pathology

A Dissertation submitted to the Faculty of Health Sciences, University of the Witwatersrand, Johannesburg, in fulfilment of the requirements for the degree of Master of Science in Medicine.

Johannesburg – 2025

DECLARATION

I Zandile Langa declare that this dissertation is my own independent work. It is being submitted for the Degree of Master of Science in Medicine at the University of the Witwatersrand, Johannesburg. It has not been submitted before for any degree or examination at any other University.



29th day of May in 2025.

DEDICATION

To my late father, ***Bhekuyise Noqhayi Langa***

You were my biggest cheerleader and greatest supporter. Your unwavering belief in me gave me the confidence to overcome challenges and pursue my dreams fearlessly. Your love, guidance, and encouragement have been my constant source of inspiration, even in your absence. Although you are no longer here to share this moment, I carry your spirit with me in every step of this journey.

This work is for you, Dad. I hope I've made you proud.

PUBLICATIONS ARISING FROM THIS DISSERTATION

1. **Gebhardt, M. E., Krizek, R. S., Coetzee, M., Koekemoer, L. L., Dahan-Moss, Y., Mbewe, D., ... & Southern Africa International Centers of Excellence for Malaria Research.** (2022). Expanded geographic distribution and host preference of *Anopheles gibbinsi* (*Anopheles species 6*) in northern Zambia. *Malaria Journal*, 21(1), 211.

Role: I was responsible for conducting the *ITS2* PCR for sequencing analysis.

2. **Oduola, A. O, Inyama, P. U., Samdi, L. M., Okeke, I., Uhomoibhi, P., Adeogun, A., Oyale, O., Inyang, A., Ambrose, K., Hendershot, A., Ngaruro, C., Mihigo, J., Rogers, J., Yoshimizu, M., Koekemoer, L. L., Langa, Z., Erlank, E., Coetzee, M., and Seyoum, A.** Importance of *Anopheles marshallii* group identification as a secondary vector of malaria in the forest ecozone of Akwa Ibom State, Southern Nigeria. (*Currently in preparation for publication*)

Role: My contributions included conducting the *ITS2* and *COI* assays for molecular characterization, as well as performing the phylogenetic analysis.

ABSTRACT

Accurate identification of *Anopheles* species is critical for effective malaria vector surveillance and control. *A priori* morphological identification forms the basis for species identification. However, it is time-consuming, and identification is incomplete if specimens have lost important external taxonomic features. Therefore, it is vital to use molecular techniques in conjunction with morphology for identification. This study aimed to use both morphological and molecular methods for the identification of understudied *Anopheles* species. Focus was placed on *An. marshallii* group and *An. maculipalpis* specimens from KwaZulu-Natal (KZN), South Africa, as well as *An. hargreavesi* and *An. gibbinsi* from Nigeria and Zambia, given their potential roles as overlooked or secondary malaria vectors.

Morphological identification of *An. marshallii* group and *An. maculipalpis* individual female specimens and their first filial generation (F_1) progeny was conducted using established taxonomic keys. Molecular analysis was performed by sequencing the *Internal Transcribed Spacer 2 (ITS2)* and *Cytochrome Oxidase I (COI*) regions of these species. Phylogenetic trees were constructed using the Neighbor-Joining (NJ) method to assess the evolutionary relationships among the different species. Additionally, the presence of *Plasmodium falciparum* in female specimens of the *An. marshallii* group and *An. maculipalpis* from KZN was assessed using a hydrolysis probe assay to determine their potential role as vectors in the region.

The morphological identification of *An. hargreavesi* and *An. gibbinsi* specimens was based on their distinctive traits. There was low genetic variation observed in *An. hargreavesi ITS2* and *COI* sequences. *Anopheles hargreavesi ITS2* and *COI* sequences from this study could not be aligned with previously published reference sequences due to the absence of available sequence data for this species in existing databases. The generated *An. hargreavesi* sequences from this study represent the first published molecular data for this species, highlighting the importance of expanding genetic reference databases. The *ITS2* region of *An. gibbinsi* revealed high homology with a 100% match to a previously published "*Anopheles sp. 6*" from Kenya, suggesting that they are the same species. Morphological analysis of *An. marshallii* group adults from KZN isofemale families confirmed their classification within the *An. marshallii* group, with no notable differences observed between families. However, the use of egg and larval morphology to identify *An. marshallii* group specimens from KZN presented several challenges, limiting their usefulness as a reliable diagnostic tool in this study. Molecular sequencing of these specimens revealed unique *ITS2* and *COI* sequences,

indicating that the families belonged to the same species. The *An. marshallii* group specimens from KZN exhibited a low level of DNA variation and formed distinct clades in phylogenetic trees, indicating their novelty and divergence from other known species. Misidentification posed a significant practical challenge as specimens initially identified *as An. pretoriensis* were later confirmed through molecular analysis to be *An. maculipalpis*, highlighting the limitations of morphological techniques in distinguishing closely related or cryptic species. Moreover, high intraspecific genetic variation in sequences complicated species delineation in certain groups, underlining the need for multi-locus approaches in future studies. None of the female specimens tested positive for *Plasmodium falciparum*, indicating no evidence of infection among the tested populations at the time of collection.

The findings have significant implications for malaria control, as secondary vectors or understudied species may be overlooked in surveillance efforts due to misidentification or underrepresentation in reference databases. This study highlights the importance of using morphological and molecular identification techniques to intensify vector surveillance and improve our understanding of the *An. marshallii* group and *An. maculipalpis* species, given their potential role in malaria transmission and the difficulties associated with accurately identifying these species using morphological methods alone. While generating large-scale DNA barcode data for anophelines is comparatively easy, this information becomes valuable when linked to accurate morphological species identification. By establishing this linkage between morphology and molecular data, this research provides the foundation for developing rapid identification assays, such as multiplex PCR, to streamline and enhance vector surveillance efforts for species like the *An. marshallii* group and *An. maculipalpis.*

ACKNOWLEDGMENTS

I would like to express my deepest appreciation to my supervisor, Prof. Lizette L. Koekemoer for offering me the opportunity to conduct my Master's project at the Wits Research Institute for Malaria (WRIM) and the Vector Control Reference Laboratory (VCRL). Her guidance, support, and expertise have been invaluable throughout this research. I'm grateful for the trust and confidence she placed in me, which allowed me to grow academically and professionally during my time at both institutions. I would also like to extend my sincere gratitude to my co-supervisor, Dr Yael Dahan-Moss. The experience of working under her mentorship has been enriching and has significantly contributed to the development of my skills in malaria research. Your constructive criticisms and patience have been instrumental in refining my work and helping me grow as a researcher. Your words of encouragement have consistently motivated me to push boundaries and strive for excellence.

I am also grateful to Prof. Maureen Coetzee for being generous with her time and expertise and providing critical insights whenever we needed clarification or additional information. Her knowledge and willingness to assist have greatly contributed to the success of this work. I also want to thank the Jozini Provincial Department of Health entomological field team for assisting with specimen collections for this project. I would also like to acknowledge the Southern Africa ICEMR team in Zambia and the PMI Vectorlink team in Nigeria for providing me with specimens used in this project. Their insights have been instrumental in shaping the outcomes of my research. I express my gratitude to Mr Nelius Venter and Mrs Erica Erlank for their tremendous assistance with the morphological analysis of my specimens. I also extend my appreciation to Mr. Donald McCallum for kindly allowing me to use the scanning electron microscope at the Department of Animal, Plant, and Environmental Sciences. Furthermore, I thank my colleagues at WRIM and VCRL for their unwavering support and assistance.

This research would not have been possible without the significant financial support from the National Research Foundation (FBIS2204224239 and in part by SRUG2203311457) awarded to Prof. Koekemoer. I must thank my family for their unconditional support throughout these past intense academic years. Your belief in my dreams and sacrifices have been invaluable, and I am truly fortunate to have you by my side.

TABLE OF CONTENTS

DECLARATION ..... **ii**
DEDICATION ..... **iii**
PUBLICATIONS ARISING FROM THIS DISSERTATION ..... **iv**
ABSTRACT ..... **v**
ACKNOWLEDGMENTS ..... **vii**
TABLE OF CONTENTS ..... **viii**
LIST OF FIGURES ..... **xi**
LIST OF TABLES ..... **xiv**
ABBREVIATIONS ..... **xvi**

CHAPTER ONE - INTRODUCTION **1**
1.1 MALARIA BURDEN GLOBALLY 1
1.2 MALARIA VECTOR CONTROL IN SOUTH AFRICA 3
1.3 REPRODUCTIVE ISOLATION 5
1.4 CRYPTIC SPECIES 6
1.5 TECHNIQUES USED FOR MOSQUITO IDENTIFICATION 6
1.5.1 Morphological Methods 8
1.5.2 Cytological Methods 9
1.5.3 Iso-enzyme Electrophoretic Variation 11
1.5.4 DNA-Based Methods 12
1.5.4.1 Polymerase Chain Reaction (PCR) 12
1.5.4.2 DNA Barcoding and Sequencing 13
1.6 THE *ANOPHELES MARSHALLII* GROUP 19
1.6.1 *Anopheles marshallii* Group Summary Overview 19
1.6.2 Historical Synopsis of the *Anopheles marshallii* group 19
1.6.3 Role of *Anopheles marshallii* group in Malaria Transmission: 21
1.6.4 Distribution and Biology of Members of the *Anopheles marshallii* Group 22
1.6.5 Morphological Differences between Members of the *Anopheles marshallii* group 28
1.6.5.1 Differences in Egg Stages 28
1.6.5.2 Differences in Larval Stages 29
1.6.5.3 Differences in Pupal Stages 32
1.6.5.4 Adult Morphological Description 33
1.7 *ANOPHELES MACULIPALPIS* SPECIES 42

1.7.1 Biology and Distribution 42
1.7.2 Morphological Description 43
1.8 STUDY RATIONALE 44
1.9 STUDY AIM AND OBJECTIVES 46

CHAPTER TWO – MATERIALS & METHODS 47
2.1 COLLECTION OF BIOLOGICAL MATERIAL USED AND *A PRIORI* IDENTIFICATION 48
2.2 MOSQUITO REARING 50
2.3 MOUNTING OF LARVAL AND PUPAL PELTS 53
2.3.1 Morphology Data Analysis 54
2.4 MOLECULAR ANALYSIS 56
2.4.1 Species Identification 56
2.4.2 DNA Extraction 56
2.4.3 *Anopheles funestus* PCR 56
2.4.4 *Plasmodium* Detection using Hydrolysis Probe Assay 58
2.5 DNA AMPLIFICATION AND SEQUENCING OF THE *ITS2* AND *COI* REGIONS 60
2.5.1 DNA Extraction 60
2.5.2 *Internal Transcribed Spacer 2 (ITS2)* PCR 61
2.5.3 *Cytochrome C Oxidase Subunit I (COI)* PCR 62
2.5.4 Gel Purification 64
2.5.5 Sequence Analysis 65
2.5.6 Phylogenetic Analysis 66

CHAPTER THREE - RESULTS 67
3.1 IDENTIFICATION OF SAMPLES FROM NIGERIA: *ANOPHELES HARGREAVESI* 67
3.1.1 Morphological Identification 67
3.1.2 *Anopheles hargreavesi* Sequence Analysis 67
3.2 IDENTIFICATION OF SAMPLES FROM ZAMBIA: *ANOPHELES GIBBINSI* 72
3.2.1 Morphological Identification 72
3.2.2 *Anopheles gibbinsi* Sequence Analysis 72
3.3 IDENTIFICATION OF SAMPLES FROM SOUTH AFRICA: *ANOPHELES MARSHALLII* GROUP 75
3.3.1 Morphological Identification (A *priori* identification) 75
3.3.1.1 *Anopheles marshallii* Group Egg Morphology 75
3.3.1.2 *Anopheles marshallii* Group Larval Morphology 76
3.3.1.3 *Anopheles marshallii* group Adult Morphology 77
3.3.1.4 *Anopheles marshallii* group Leg Morphology 81

3.3.1.5 *Anopheles marshallii* group Palp Morphology 82
3.3.1.6 *Anopheles marshallii* Group Wing Morphology 85
3.3.2 *Anopheles marshallii* Group Molecular Identification 89
3.3.2.1 *Anopheles funestus* group Species Identification 89
3.3.2.2 Sequence Variation of rDNA *ITS2* Subunit of *An. marshallii* group samples from KwaZulu-Natal 90
3.3.2.3 Sequence Variation of rDNA mtDNA *COI* of *An. marshallii* group samples from KwaZulu-Natal 92
3.3.2.4 Analysis of BLAST Statistics for *ITS2* and *COI* Contig Sequences in *An. marshallii* group 95
3.4 SEQUENCE ALIGNMENT OF *ITS2* AND *COI* CONTIGS IN THE *ANOPHELES MARSHALLII* GROUP AND RELATED SPECIES 97
3.5 PHYLOGENETIC ANALYSIS 101
3.6 SAMPLES FROM SOUTH AFRICA: *ANOPHELES MACULIPALPIS* 104
3.6.1 Morphological Identification 94
3.6.2 *Anopheles maculipalpis* Molecular Identification 104
3.6.2.1 *Anopheles funestus* group Species Identification 104
3.6.2.2 Sequence Variation of rDNA *ITS2* Subunit and mtDNA *COI* of *Anopheles maculipalpis* samples from KwaZulu-Natal 105
3.7 SPOROZOITE DETECTION IN *AN. MARSHALLII* GROUP AND *AN. MACULIPALPIS* FROM KWAZULU-NATAL 110

CHAPTER FOUR - DISCUSSION 111
4.1 MORPHOLOGICAL ANALYSIS 111
4.2 MOLECULAR ANALYSIS 115
4.2.1 Sequence Analysis 115
4.2.2 Phylogenetic Relationship 119
4.2.3 Sporozoite Detection 121
4.3 FUTURE DIRECTIONS 122

CHAPTER FIVE - CONCLUSIONS 124
REFERENCES 127
APPENDICES 142

LIST OF FIGURES

CHAPTER 1

Figure 1.1: Global trends in malaria cases and mortality rate (per 100 000 population at risk) from 2000 – 2022 2

Figure 1.2: Schematic representation of a transcription unit of eukaryotic rDNA 15

Figure 1.3: Illustration of a typical mitochondrial genome 17

Figure 1.4: Map showing the distribution of *Anopheles marshallii* group species across Africa. Adapted from Gillies and De Meillon (1968) and Gillies and Coetzee (1987) 23

Figure 1.5: Illustration of *Anopheles marshallii s.s.* egg. Sourced from (Gillies and De Meillon, 1968) 29

Figure 1.6: Larval morphological features of *Anopheles marshallii s.s.* 31

Figure 1.7: Dorsal view of *Anopheles* pupae abdominal segments 32

Figure 1.8: Morphological characters (wing and palps) of a female *Anopheles marshallii* group mosquito 33

Figure 1.9: *Anopheles marshallii* group mesonotal scales 34

CHAPTER 2

Figure 2.1: Outline of Chapter 2 to achieve objectives listed in Chapter 1 47

Figure 2.2: Map showing sampling sites where *An. hargreavesi* and *An. gibbinsi* specimens were collected in Nigeria and Zambia 48

Figure 2.3: Map of the uMkhanyakude district showing locations of sampling sites where specimens were collected in KZN 49

Figure 2.4: Glass vials containing damp filter paper with wild-caught female mosquitoes for egg-laying 51

Figure 2.5: Plastic bowls partially filled with distilled water used for larval hatching 52

Figure 2.6: Bug-dorm cage with the placement of sugar water on top, labelled with a unique number to identify each iso-female family 52

Figure 2.7: Illustration of a pinned *Anopheles* adult 53

Figure 2.8: Diagram illustrating slide mounting steps 54

Figure 2.9: Laboratory procedure for gel extraction using the QIAquick Gel Extraction Kit 65

CHAPTER 3

Figure 3.1: Scutal scale pattern of *Anopheles hargreavesi* 67

Figure 3.2: Amplification of *ITS2* and *COI* regions in *Anopheles hargreavesi* specimens using PCR, visualised on 2.5% agarose gels 68

Figure 3.3: Multiple sequence alignment of the *ITS2* region from *Anopheles hargreavesi* specimens collected in Nigeria sequence alignment 70

Figure 3.4: Multiple sequence alignment of the *COI* region from *Anopheles hargreavesi* specimens collected in Nigeria. 71

Figure 3.5: Amplification of the *ITS2* and *COI* regions in *Anopheles gibbinsi* specimens using PCR, visualised on 2.5% agarose gels 73

Figure 3.6: Multiple sequence alignment of the *ITS2* region in *Anopheles gibbinsi* specimens collected in Zambia 74

Figure 3.7: Comparative egg morphology of *Anopheles marshallii* group specimens from KZN 76

Figure 3.8: Larval morphology of fourth-instar larvae from the *Anopheles marshallii* group 77

Figure 3.9: *Anopheles marshallii* group female morphological characters 78

Figure 3.10: *Anopheles marshallii* group hind legs with apical pale bands on joints 82

Figure 3.11: Illustration of the measured palp segments 83

Figure 3.12: Measured costal wing spots of *Anopheles marshallii* group specimens 85

Figure 3.13: Measured wing length of *Anopheles marshallii* group specimens 88

Figure 3.14: Comparison of the mean wing length between the families 88

Figure 3.15: Species-specific PCR amplification of *Anopheles funestus* group on a 2.5% agarose gel stained with ethidium bromide 89

Figure 3.16: PCR amplification of the *ITS2* region in *Anopheles marshallii* group specimens, visualised on a 2.5% agarose gel 91

Figure 3.17: Multiple sequence alignment of the *ITS2* region from *Anopheles marshallii* group specimens 92

Figure 3.18: PCR amplification of the *COI* region in *Anopheles marshallii* group specimens, visualised on a 2.5% agarose gel 93

Figure 3.19: Multiple sequence alignment of the *COI* region sequences of *Anopheles marshallii* group specimens 94

Figure 3.20: Multiple Sequence alignment of the *ITS2* region from *Anopheles marshallii* group specimens and related species 98

Figure 3.21: Multiple Sequence alignment of the *COI* region from *Anopheles marshallii* group specimens and related species 99

Figure 3.22: Phylogenetic tree of the *Anopheles marshallii* group and related species based on rDNA *ITS2* sequence data 102

Figure 3.23: Phylogenetic tree of the *Anopheles marshallii* group based and related species on mtDNA *COI* sequence data 103

Figure 3.24: Species-specific PCR amplification of *Anopheles funestus* group on a 2.5% agarose gel stained with ethidium bromide 105

Figure 3.25: PCR amplification of the *ITS2* and *COI* region in *An. maculipalpis* specimens, visualised on a 2.5% agarose gel 106

Figure 3.26: Alignment of *ITS2* nucleotide sequences from *Anopheles maculipalpis* samples collected in KwaZulu-Natal 108

Figure 3.27: Multiple sequence alignment of the *COI* region from *Anopheles maculipalpis* group specimens 109

LIST OF TABLES

CHAPTER 1

Table 1.1: Morphological differences within adult members of the *Anopheles marshallii* group 39

CHAPTER 2

Table 2.1: Species-specific primer sequences for members of the *An. funestus* group 57

Table 2.2: TaqMan assay primer sequences for *Plasmodium* detection 60

Table 2.3: *Internal Transcribed Spacer 2* primer sequences 61

Table 2.4: *Internal Transcribed Spacer 2* PCR protocol 62

Table 2.5: *Cytochrome C Oxidase Subunit I* primer sequences 63

Table 2.6: *Cytochrome C Oxidase Subunit I* PCR protocol 64

CHAPTER 3

Table 3.1: Comparisons of palp spots (widths and lengths in mm) between the families 84

Table 3.2: Measurements (mm) of wing spots of three members of the *Anopheles marshallii* group 86

Table 3.3: Wing spot measurements (mm) for morphological comparison with members of the *Anopheles marshallii* group 87

Table 3.4: *Internal Transcribed Spacer 2* and *Cytochrome C Oxidase Subunit I* database comparisons for consensus sequences of each family used to determine species 96

Table 3.5: Percentage Identity (%) Matrix of *ITS2* Sequences among *Anopheles* species 100

Table 3.6: Percentage Identity (%) Matrix of *COI* Sequences among *Anopheles* species 100

Table 3.7: GenBank Accession Numbers for species used for phylogenetic analysis in this study 101

Table 3.8: Summary of *Plasmodium* infectivity results 110

ABBREVIATIONS

rDNA	Ribosomal Deoxyribonucleic Acid
%	Percentage
µl	Microlitre
µM	Micromolar
ANOVA	Analysis of Variance
BLAST	Basic Local Alignment Search Tool
BLASTn	Nucleotide BLAST
BOLD	Barcode of Life Database
bp	Base pair
CO_2	Carbon dioxide
COI	*Cytochrome C Oxidase* Subunit 1
Covid-19	Coronavirus disease 2019
CSP	Circumsporozoite Protein
Ct	Cycle threshold
DNA	Deoxyribose Nucleic Acid
dNTP	Dinucleotide triphosphate
ELISA	Enzyme-Linked Immunosorbent Assay
F_1	First filial generation
g/ml	grams per milliliter
HSD	Honestly significant difference
IRS	Indoor Residual Spraying
ITNs	Insecticide-Treated Nets
ITS2	*Internal Transcribed Spacer Region 2*
kb	Kilobyte
$MgCl_2$	Magnesium chloride
ml	milliliter
mm	millimetre
mtDNA	Mitochondrial Deoxyribonucleic Acid
Na_2EDTA	Disodium ethylenediaminetetraacetate dihydrate
NaOH	Sodium hydroxide
NCBI	National Center for Biotechnology Information
NICD	National Institute for Communicable Diseases

nM	Nanomolar
PCR	Polymerase chain reaction
RFLP	Restriction Fragment Length Polymorphism
RFU	Relative fluorescence units
rmp	Revolutions per minute
s.l.	*Sensu lato*
s.s.	*Sensu stricto*
SMRS	Specific Mate Recognition System
TAE	Tris(hydroxymethyl) aminomethane-acetate
Taq	Thermus aquaticus polymerase
Tris-HCl	Tris(hydroxymethyl)aminomethane hydrochloride
UN	Universal
UV	Ultraviolet
VCRL	Vector Control Reference Laboratory
WHO	World Health Organization
WRIM	Wits Research Institute for Malaria

CHAPTER 1

INTRODUCTION

1.1 MALARIA BURDEN GLOBALLY

Malaria is a deadly, mosquito-transmitted disease that has devastating consequences globally (WHO, 2023). About 94% of malaria infections and deaths globally occur in Africa, particularly in underdeveloped tropical and subtropical areas (WHO, 2023). The World Health Organization (WHO) reported 249 million malaria cases globally in 2022, five million more than the anticipated figure due to the COVID-19 pandemic (WHO, 2023).
Nigeria, the Democratic Republic of the Congo, Uganda, and Mozambique accounted for approximately half of the 249 million cases that were reported in 2022 (WHO, 2023). In 2022, there were an estimated 608 000 deaths globally, leading to a mortality rate of 14.3 deaths per 100 000 individuals at risk (**Figure 1.1**). Children below the age of five accounted for the majority of these deaths in sub-Saharan Africa, where the disease is most prevalent (Adum *et al.,* 2023). Malaria mortality among children under five years old decreased from 87% in 2000 to 76% in 2015, then slightly increased to 77% in 2020 (WHO, 2023). Since then, it has remained unchanged.

Progress towards malaria elimination has accelerated over the past two decades, preventing roughly 2.1 billion malaria cases and 11.7 million malaria-related fatalities worldwide (WHO, 2023). Between 2000 and 2019, malaria cases decreased from 81.1 per 1 000 population at risk to 57 cases per 1 000 population at risk (**Figure 1.1**). During the same period, global estimated malaria deaths declined substantially from 864,000 to 576,000 (WHO, 2023). Despite the dramatic increase in global malaria cases and fatalities in 2020 brought on by COVID-19 induced interruptions of vital malaria services, the WHO reported that the number of malaria cases continued to increase between 2020 and 2022, although more slowly than it did from 2019 to 2020 (WHO, 2023). The COVID-19 pandemic resulted in a diversion of resources toward the response, resulting in decreased investment budgets for malaria programs and widespread shortages of medical supplies. Key malaria control interventions, such as indoor residual spraying (IRS), long-lasting insecticidal net (LLIN), and distribution campaigns, were delayed or interrupted due to logistical challenges, movement restrictions, and the reallocation of health personnel. The availability and

distribution of curative and preventive malaria commodities were also severely impacted, leading to stockouts in some regions.

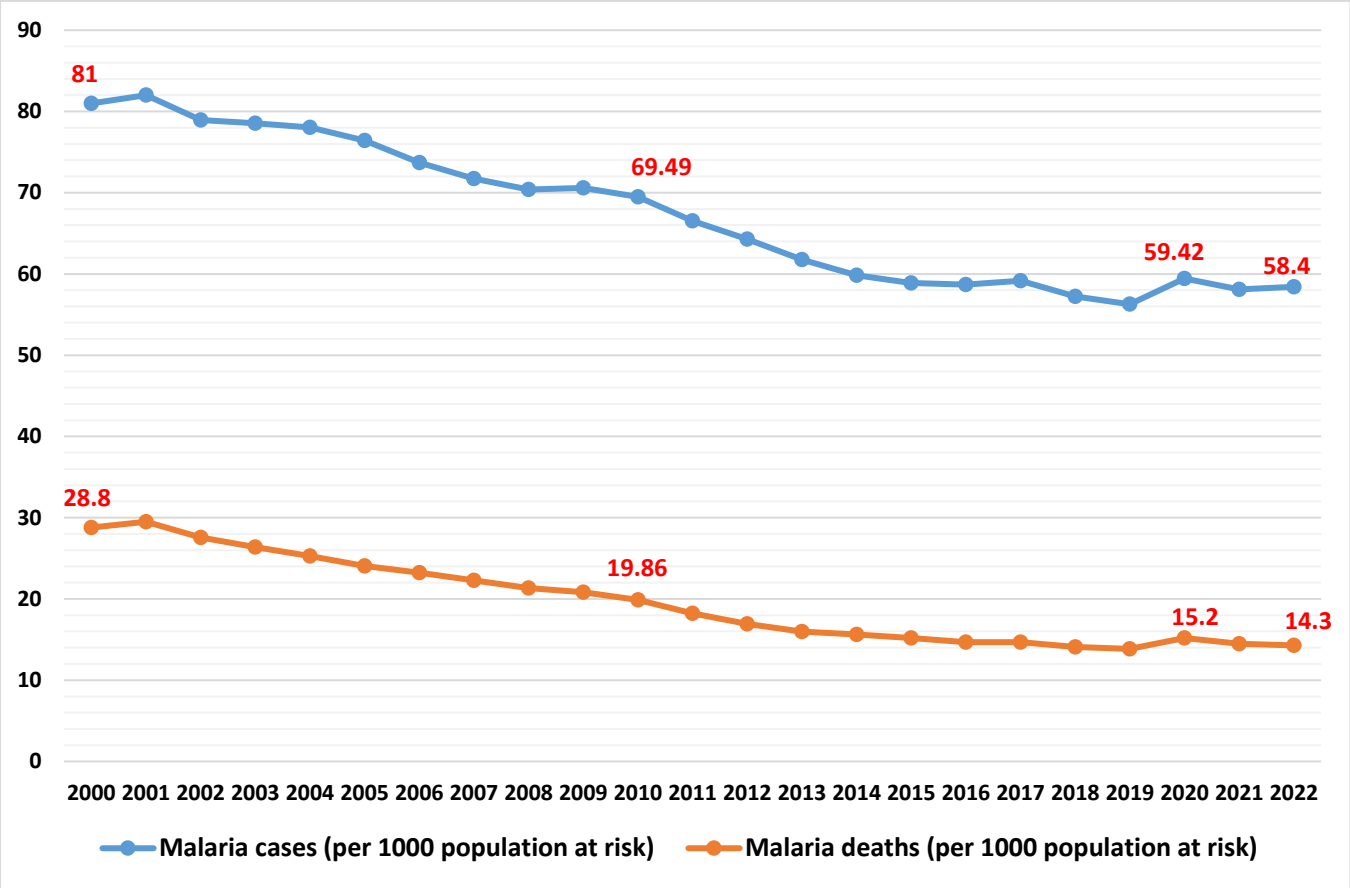


Figure 1.1 - Global trends in malaria cases and mortality rate (per 100 000 population at risk) from 2000 – 2022. Data adapted from WHO Malaria Report (2023).

Given the information above, it is clear that many people are still in danger of contracting the malaria parasite, mainly *Plasmodium falciparum.* This parasite remains the predominant species associated with severe malaria and death (Singh and Daneshvar, 2013; WHO, 2022). Humans transmit malaria from infected female mosquito vectors of the *Anopheles* genus (*Diptera: Culicidae*). There are currently 500 recognised *Anopheles* species, many of which belong to species complexes of closely related species that share morphological characteristics (Harbach, 1994; Sinka, 2012). These species complexes often contain both primary vectors and non-vector species that may only be distinguished by molecular or cytogenetic methods. Understanding these complexes is essential because failing to distinguish vector from non-vector species may compromise control efforts. However, of the 500 *Anopheles* species, only approximately 40 are known to be carriers of human malaria

parasites, and 15 of them are believed to be major vector species or species complexes that have the capacity to transmit malaria at a level that poses a threat to the well-being of everyone (Service and Townson, 2002; Hay *et al*., 2010; Sinka *et al*., 2012; Whittaker *et al*., 2023). In Africa, the most dominant and well-studied malaria vector species include *Anopheles gambiae*, *Anopheles coluzzii*, *Anopheles arabiensis*, and *Anopheles funestus* which are member of such species complexes (Gillies and De Meillon, 1968; Gillies and Coetzee; 1987 Sinka *et al*., 2012; Asmare *et al*., 2022).

1.2 MALARIA VECTOR CONTROL IN SOUTH AFRICA

Malaria vector control has historically been the key to eradicating malaria in many parts of the world. Today's vector control initiatives include the use of chemical, biological, natural plant products, and environmental management. In sub-Saharan Africa, the most critical definitive hosts for human *Plasmodium* are mosquitoes of the *Anopheles gambiae* complex and *An. funestus* group (Dia *et al*., 2013; Ogola *et al*., 2018). A definitive host is the organism in which a parasite reaches its mature, reproductive stage. In this case, it is the *Anopheles* mosquito, where the sexual reproduction of *Plasmodium* occurs. The predominant vector in South Africa at present is *An. arabiensis*, a member of *An. gambiae* complex (Gillies and De Meillon, 1968; Gillies and Coetzee, 1987; Brooke *et al*., 2013; Adeola *et al*., 2016; Dandalo *et al*., 2017; Munhenga *et al*., 2022). During previous control interventions and sporadic outbreaks, *An. funestus* has also been a dominant vector in this country. (Gillies and De Meillon, 1968; Gillies and Coetzee, 1987; Brooke *et al.*, 2013). The primary strategies for controlling malaria vectors in South Africa are targeted larval source management and indoor residual spraying (IRS) of insecticide (Brooke *et al*., 2013; Brooke *et al*., 2020). IRS entails applying insecticide to the walls and ceilings of dwellings where mosquitoes rest. The insecticide has a duration of several months (6- 12 months, depending on the insecticide) and kills mosquitoes that come into contact with the treated surfaces (Brooke *et al.*, 2013; Coetzee *et al.*, 2013a). The residual efficacy of IRS varies depending on the kind of insecticide used, environmental conditions, and the nature of the wall surface.

In addition to IRS, South Africa (SA) also uses larviciding during winter in certain areas, such as game reserves (Coetzee, 2013). Larviciding is the practice of applying insecticides or biological control agents to bodies of water, such as stagnant pools, where mosquitoes thrive

to eradicate mosquito larvae before they develop into adults. In South Africa, the prevalence of malaria has been effectively reduced by IRS-based vector control to the point that the eradication of all locally acquired cases is a plausible prospect (Brooke *et al.*, 2013*;* Coetzee *et al.*, 2013*;* Coetzee and Koekemoer, 2013). South Africa is in the pre-elimination stage of the malaria epidemic and has committed to eradicating the disease by 2028 although previous targets aimed to do so by 2023 (Oyegoke *et al*., 2022; Kleinhans *et al.*, 2024). However, this has yet to be accomplished, and local transmission continues at low levels in a number of districts and towns throughout the impacted provinces with conducive transmission climates.

A systematic review by Zhou *et al.* (2022) found that IRS can significantly reduce malaria transmission when properly executed, leading to notable declines in parasite prevalence and case incidence. Similarly, Irish *et al*. (2024) discovered that targeted IRS, concentrating on transmission hotspots rather than broad areas, can improve efficiency and lower operational costs while achieving similar results. Nonetheless, both studies emphasise that the effectiveness of IRS largely relies on strategic implementation, timing, and the local epidemiological context. In South Africa, IRS has proven effective when high coverage is achieved. However, its long-term sustainability faces several challenges that could hinder elimination. Insecticide resistance, particularly to pyrethroids, is a growing concern, and the requirement for regular rotation of insecticide classes increases costs and logistical difficulties (Brooke *et al.*, 2020). Resistance can reduce the efficacy of IRS and allow vector populations to persist despite interventions. Additionally, vector behavioural adaptation is an increasing concern. *Anopheles arabiensis* is known for its ecological adaptability, often resting outdoors or feeding on animals, which reduces IRS contact and thus undermines its efficacy (Afrane *et al.*, 2016; Alafo, 2021). Alafo (2021) highlights the importance of implementation strategies and residual efficacy for achieving adequate coverage. Poor timing, inconsistent application, insecticide degradation, and logistical challenges, such as community resistance or limited access to remote areas, can adversely affect the overall impact of IRS.

Malaria is prevalent in certain parts of South Africa, particularly in the north-eastern provinces such as Mpumalanga, Limpopo, and KwaZulu-Natal, where active malaria transmission is primarily due to the presence of *An. arabiensis* species (Brooke *et al.*, 2013; Dandalo *et al*., 2017; Dahan-Moss *et al*., 2022). As South Africa shares borders with countries that have high malaria burdens, such as Mozambique, Zimbabwe and Eswatini,

there is a chance that drug-resistant parasites and insecticide-resistant mosquitoes will be imported into South Africa, contributing to high rates of malaria transmission. Each year, affected districts and municipalities in each province conduct malaria vector control to scale up towards elimination**.** Major mosquito vector species are typically the most comprehensively researched and understood in terms of their physiology and taxonomy due to their role in disease transmission (Harbach, 2004; Becker *et al*., 2010). Research into cryptic *Anopheles* species and disease vector speciation is essential for vector management, as they could have profound public health implications (Zheng, 2020). To define species is complex and is defined by various theories. One of these is based on reproductive isolation which will be discussed in more detail below.

1.3 REPRODUCTIVE ISOLATION

The *Anopheles* genus contains cryptic species that appear morphologically similar but exhibit genetic differences (Zheng, 2020). The prevalence of morphologically identical species that have diverse roles in spreading diseases and parasites makes it challenging to easily and accurately identify mosquitoes (Müller *et al*., 2013). Reproductive isolation plays a pivotal role in species formation, making it important to understand how a single interbreeding species separates into two reproductively distinct species. Hence, understanding the specific isolating attributes and the rates at which they evolve is necessary for understanding the emergence and persistence of species (Zheng, 2020).

Reproductive isolation is a critical mechanism in speciation, where two or more separate species cannot interbreed and produce fertile offspring. According to Coetzee (1982), species are "groups of distinct organisms that have a common preferred habitat and specific mate recognition system (SMRS)". The SMRS could be in the form of optical, auditory, chemical or other types of signals. Specific mate recognition system has the unintended consequence of confining gene pools into compartments. Nevertheless, genetic variation among individuals in nature may be explained as gaps/interruptions caused by a lack of gene flow between two or more sympatric gene pools (i.e., populations that occur in the same geographic area), due to various SMRS (Coetzee, 1982). The formation of reproductive isolation between populations with different genetic make-up is how speciation develops over time. Reproductive isolation results from the combined effect of all barriers that prevent and hinder

gene flow. This can occur through various factors, including geographical isolation, genetic drift, and natural selection (Zheng, 2020).

Reproductive isolation plays a key role in the emergence of cryptic species. It prevents gene flow between populations, allowing genetic differences to accumulate over time. When these differences become substantial enough to prevent successful interbreeding, cryptic species emerge. These differences may result in one species being an efficient malaria vector while its sibling species is not. For instance, two reproductively isolated species may occupy the same area (sympatry) but exhibit different host preferences, resting behaviour or insecticide susceptibility, all of which directly affect their role in transmission and the success of vector control interventions such as IRS or insecticide-treated nets. Therefore, understanding reproductive isolation and the resulting genetic divergence among cryptic taxa is essential for improving targeted surveillance, developing effective control strategies, and ultimately contributing to effective malaria elimination efforts.

1.4 CRYPTIC SPECIES

Numerous species complexes within the genus *Anopheles* have been uncovered, and the use of the term “sibling” or “cryptic” species by researchers has become widespread. While most authors use the terms interchangeably, some authors argue that the term "sibling" indicates a sister-species relationship and denotes more recent shared ancestry than the term "cryptic" (Knowlton, 1986; Sáez and Lozano, 2005; Bickford *et al.,* 2007). Cryptic species are biologically distinct groups that lack discernible physical distinctions identified through genetic data from populations previously assumed to belong to a single species (Collins and Paskewitz, 1996; Zheng, 2020). Mayr (1969) described sibling species as sympatric forms that are reproductively isolated, yet have unique biological traits, and are physically similar or indistinguishable, a definition that has been supported by other researchers (Singh, 2016; Zheng, 2020).

Extensive studies have identified cryptic mosquito species, and most of these studies concentrate on the *An. gambiae* complex. This complex consists of closely related species historically considered a single species. However, advances in molecular genetics and DNA analysis have revealed that this complex is composed of multiple cryptic species (Barrón *et al*., 2019). The *An. gambiae* complex includes several mosquito species, among them *An.*

gambiae sensu stricto (previously known as *An. gambiae* S molecular form), *An. coluzzii* (previously known as *An. gambiae* M molecular form), and *An. arabiensis*, which are the major malaria vectors (Dahan-Moss *et al.*, 2020; Rants'o *et al.*, 2023). Additionally, there are minor localised vectors, such as *An. melas*, *An. merus*, and *An. bwambae*, whereas *An. quadriannulatus*, *An. fontenillei* and *An. amharicus* are not known to transmit malaria (Gillies and Coetzee, 1987; Brooke *et al*., 2013; Coetzee *et al.*, 2013; Barrón *et al*., 2019). These cryptic species vary in ecological characteristics, including host feeding preferences, breeding locations, feeding behaviour, insecticide susceptibility and their contribution to malaria transmission (Barrón *et al*., 2019). In a study investigating the genetic basis for reproductive isolation in populations of the sub-Saharan African mosquito species *An. coluzzii*, White *et al*., (2011) reported that there were significant genetic differences between populations of *An. coluzzii* that were geographically separated and these differences were associated with differences in the timing of mating and reproductive behaviour. Their findings suggests that reproductive isolation may play a significant role in the emergence of cryptic *Anopheles* mosquito species.

Another well-documented example of a cryptic species is the *Anopheles funestus* group, which comprises of several morphologically similar (sibling) member species. *Anopheles funestus s.s.* (*sensu stricto*) is the main species responsible for malaria transmission in Africa (Harbach, 2003; Stevenson *et al*., 2016; Odero *et al*., 2023). Other members of the group such as *An. parensis*, *An. vaneedeni* and *An. rivulorum* are considered potential vectors. *Anopheles rivulorum* can be misidentified at its adult stage as *An. funestus*. In a study conducted in Cameroon, Cohuet *et al.* (2003) identified a non-vector species in Cameroon with biological, morphological and genetic characteristics similar to *An. rivulorum* and named it *An. rivolorum*-like (Vezenegho, 2012). Spillings *et al.* (2009) reported cytogenetic differences among closely related populations of *An. funestus* in Malawi suggesting that this species may comprise a complex of cryptic species. Their findings suggested that *An. funestus s.s.* itself may represent a complex of genetically distinct taxa. In the same study, a morphologically similar but genetically distinct species was identified and assigned the name *An. funestus-like*.

The *Anopheles* genus contains numerous species. Some of these belong to species groups or complexes, as indicated above. Identifying and describing these species are vital in order for researchers and vector control managers to target control interventions effectively and adjust their strategies to specific mosquito populations. Research on cryptic species within the *Anopheles* genus is particularly crucial in malaria transmission because these

morphologically indistinguishable species may differ greatly in their vectorial capacity, biting behaviour, ecological preferences, and insecticide resistance. Misidentification of such species or failing to recognise an emerging vector within a cryptic complex can lead to inaccurate inferences about transmission dynamics and the persistence of transmission hotspots and hinder targeted vector control efforts. It is essential to study these cryptic species in order to design precise, evidence-based malaria control strategies that are responsive to the true vector landscape.

1.5 TECHNIQUES USED FOR MOSQUITO IDENTIFICATION

The accurate identification of mosquito species has significant clinical and practical ramifications and it is crucial for the implementation of vector control strategies (Murugan *et al.,* 2016). One of the most important steps in monitoring and controlling malaria is identifying species in the *Anopheles* genus. As mentioned above, many complexes of closely related cryptic species in mosquitoes share the same morphology but differ in their ecology and preferred hosts and, hence, their role in disease transmission. Precise identification is vital since species groups and complexes exhibit considerable behavioural and vectorial diversity (Gillies and Coetzee, 1987). Several methods for identifying mosquitoes include morphological, molecular (Polymerase Chain Reaction and nucleic acids sequencing), proteomics techniques, and isozyme analysis (Jourdain *et al.,* 2018).

1.5.1 Morphological Methods

Morphological identification remains the first step prior to molecular methods for both research and operational entomological surveillance because it does not need costly specialised equipment and is easy to use in the field, even when a large number of specimens need to be identified (Chan *et al.,* 2014). Morphological identification is the conventional and accepted approach for classifying mosquito species based on their external characteristics and morphological features using taxonomic keys (Chan *et al.,* 2014). Morphological identification of mosquitoes collected during entomological surveillance is an essential prerequisite for effective malaria vector control programs (Sinka *et al*., 2010; Garros and Dujardin, 2013; Erlank *et al*., 2018).

Before the development of molecular identification techniques, *a priori* morphological identification formed the basis for species identification. This means that in order to identify a species, female specimens needed to be captured from the wild and brought to an insectary facility. These females were then blood-fed, and the eggs they produced were reared until they reached the adult stage. Thereafter, the eggs, fourth instar larval skins and pupal pelts are examined. However, this technique is time-consuming, and identification takes long to complete (Gillies and Coetzee, 1987; Coetzee, 2020). For this reason, it is important to combine morphological identification with molecular approaches (Garros and Dujardin, 2013; Erlank *et al.*, 2018).

Morphological keys for the Afrotropical Anophelinae (Coetzee, 2020) are used to identify adult female *Anopheles* mosquitoes. The keys provide a rapid means of mosquito identification, but they also have several limitations. Misidentification can result when mosquitoes are too damaged to clearly visualise key distinguishing features or due to human error. As mentioned above, another drawback of this approach is the existence of intraspecific morphological differences and the presence of novel or cryptic species (Gillies and Coetzee, 1987; Koekemoer *et al*., 2002; Harbach, 2004; Zhang, 2022). The dichotomous keys are restricted to identifying the adult female mosquitoes, pupa and fourth instar larvae, which may prevent accurate identification of male mosquitoes, and this gap may underestimate the abundance and distribution of the species (Gillies and Coetzee, 1987; Chan *et al*., 2014; Coetzee, 2020).

1.5.2 Cytological Methods

Although not applied in the current study, historical approaches to *Anopheles* identification, such as cytological analysis and iso-enzyme electrophoresis, have contributed significantly to the characterisation of *Anopheles* species and provided crucial context for developing modern molecular techniques. Historically, cytogenetics has undoubtedly been one of the most essential methods for distinguishing morphologically similar sibling species within Anopheles complexes. This method is based on the analysis of polytene chromosome banding patterns, usually obtained from the ovarian nurse cells of half-gravid females or larval salivary glands. Polytene chromosomes are large chromosomes that arise from repeated rounds of DNA replication without subsequent cell division, resulting in thick, aligned bundles of chromatids (Alberts *et al.*, 2002). Their unique structure makes them easily observable under a microscope, revealing distinct banding patterns along the chromosomal

arms. In addition to exhibiting species-specific banding patterns, polytene chromosomes are valuable for identifying chromosomal inversions and structural rearrangements, which serve as stable genetic markers. These markers are instrumental in distinguishing closely related species and have been extensively used to study genetic divergence and speciation in *Anopheles* mosquitoes (Sharakhov *et al.,* 2001; Subbarao, 1994).

According to Subbarao (1994), the majority of anopheline mosquitoes contain cells that generate polytene chromosomes with observable banding patterns, which allowed researchers to differentiate cryptic species that may be indistinguishable using classical morphological traits (Walton *et al*., 1999). The ovarian nurse cells of half-gravid females and the salivary glands of fourth-instar larvae contain these polytene chromosomes (Green, 1970; Artemov *et al.,* 2018). They result from repetitive chromosome replication at interphase without nuclear division. After division, chromosomes remain attached and thicken, resulting in long ribbon-like structures with dark and light horizontal segments representing band and interband regions, respectively (Baimai, 1975; Subbarao, 1994). The identification process involves staining chromosomes with propionic acid and lacto-acetic orcein to make the banding patterns visible (Hunt, 1973; Hunt and Coetzee, 1986; Sharakhov *et al*., 2001). These patterns are then compared to known reference patterns for different *Anopheles* species. Each species' unique chromosomal banding pattern distinguishes it from other species, and each species has its unique chromosome banding pattern.

Polytene chromosomes are incredibly informative and useful for both species identification and population structure analysis (Sharakhov *et al.,* 2014). Additionally, it has been used to identify previously unknown species within complexes like *An. gambiae* in Africa (Coluzzi *et al.,* 1979) and *An. dirus* in Southeast Asia (Baimai *et al.,* 1988). The *Anopheles maculatus* group consists of eight recognized species in Southeast Asia, which are difficult to differentiate from one another due to overlapping physical traits (Rattanarithikul and Green, 1986; Rattanarithikul and Harbach, 1991). Cytological procedures were the primary means of resolving the presence of many species within the group. Although the *An. maculatus* group is known to contribute to the spread of malaria, prior research has not determined the vectorial potential of particular species because it is challenging to identify species based solely on morphology (Baimai and Green, 1988; Walton *et al.,* 2007).

The primary advantage of cytological techniques was their ability to reveal genetic structure at the chromosomal level. Anopheline species with poor ovarian polytenes can use the

chromosomes from the salivary glands or fourth-instar larvae. The advantage of using adult females' ovaries is that they can be removed, fixed in modified Cornoy's fluid (made with acetic acid and methanol), and analysed whenever required (Baimai and Green, 1988; Subbarao, 1996). Another benefit is the ability to examine the same adult female for several factors, such as host preferences and the presence of sporozoites. However, this method has the disadvantage of only allowing the identification of half-gravid females, which excludes males, unfed females, or fully gravid females. Moreover, this method is time-consuming and labour intensive.

1.5.3 Iso-enzyme Electrophoretic Variation

Iso-enzyme electrophoresis represents another historical method that was frequently employed in the study of species complexes. This technique involved the separation of enzymes based on their mobilities which was influenced by their molecular structure and electric charge (Ayala *et al.,* 1972; Green and Hunt, 1980). The result of this separation was a pattern of enzyme bands known as a zymogram. These bands corresponded to different protein variants (allozymes), each coded by distinct alleles at specific loci. The banding patterns were examined to find variations in the isoenzymes (enzyme variants) between the samples. The zymogram could be examined to identify variations in the isoenzymes between samples, which could then be used to infer genetic variation within and between populations. It was suggested by Ayala and Powell (1972) that allozymes would be helpful in identifying sister species after they demonstrated diagnostic allozymes for the identification of members of the *Drosophila willistoni* species group (Mahon *et al.,* 1976; Coetzee, 1982). The first description of isoenzyme electrophoresis for the intent of identifying *An. gambiae* complex members was provided by Mahon *et al*. (1976), but it is no longer in use due to the development of new molecular techniques such as the species-specific PCR test (Scott *et al*., 1993). This technique allows for large-scale screening of natural populations. It is immensely useful as a diagnostic tool in the routine species identification procedure due to the ease of data processing and interpretation. In addition to identifying isomorphic species, electrophoretic differences at enzyme loci can be used to correctly identify species with distinctive morphology. Species-specific electromorphs also served as valuable markers for studying gene flow among natural populations (Green and Hunt, 1980; Coetzee, 1982). Although iso-enzyme analysis provided valuable insights into the study of species complexes,

its utility was limited by several factors. It requires the use of live mosquitoes, alternatively, mosquitoes preserved at low temperatures using liquid nitrogen, which is not always easily accessible in the field (Miles, 1979). In addition, females of a specific age (3-5 days) are used, thus excluding the use of larvae, males and females of unknown age. Although this technique is useful for identifying variations in enzyme expression it does not provide information about the specific gene responsible for the variation.

Both cytological and iso-enzyme approaches have established an important foundation for understanding species complexes in *Anopheles* mosquitoes. Their contributions underscore the need for more accessible, precise, and scalable identification tools, such as the molecular markers (*ITS2* and *COI*) used in this study. The limitations of these methods have led to their gradual replacement by molecular tools, including PCR-based assays and sequence analysis. These modern approaches not only provide higher resolution but also facilitate species identification across all life stages and from a broader range of sample preservation conditions. As a result, the molecular methods utilised in this dissertation continue the foundational work established by cytological and iso-enzyme techniques while addressing their limitations.

1.5.4 DNA-Based Methods

1.5.4.1 Polymerase Chain Reaction (PCR)

Molecular methods are preferred for species identification as they are comparatively quick, easy to use, and accurate. PCR is the standard technique used for separating between species that are morphologically identical or similar. Five members of the *An. gambiae* complex can be distinguished using PCR techniques developed by Scott *et al*. (1993). In the same manner, the six most prevalent members of the *An. funestus* group can be differentiated by the multiplex PCR assay established by Koekemoer *et al.* (2002) and Cohuet *et al.* (2003). These PCR assays are crucial tools in both primary and practical research. The sensitivity of PCR means that it can detect low concentrations of DNA, making it suitable for analysing small amounts of genetic material extracted from a single leg or wing *Anopheles* specimens, and it can be applied to identify specimens of any gender and at all life stages, including eggs, larvae, and pupae, which may be challenging or impossible to identify morphologically (Scott *et al*., 1993; Walton *et al.*, 1999; Koekemoer *et al.*, 2002). PCR primers are designed to target

specific regions of the *Anopheles* genome, enabling highly specific identification even among closely related species. This technique is useful to detect and identify pathogens transmitted by *Anopheles* mosquitoes. Furthermore, PCR can be combined with sequencing techniques to analyse specific genetic markers, such as mitochondrial DNA, which aids in studying population genetics.

However, the limitation of species-specific PCR is that the primers are designed to target specific sequences, as a result, some of the diversity within a species group can be missed (Hong *et al.,* 2006). Over time, genetic changes, like mutations in the primer binding regions, may diminish the assay's efficiency or specificity, potentially causing false-negative or ambiguous results (Suzuki and Giovannoni, 1996). Similarly, though infrequent, genetic recombination events could change the genomic regions that the primers target, making species identification more complex (Martin *et al.,* 2011). In such cases, relying solely on these genetic markers might lead to inaccurate species identification. These theoretical concerns highlight the necessity of periodically validating primer sets against up-to-date population data. Nonetheless, such complications have not yet been reported since the development of these assays. Another limitation is that PCR is sensitive and prone to contamination where even trace amounts of foreign DNA can result in false-positive outcomes. To mitigate these limitations, researchers can enhance PCR results with DNA sequencing, which aids in confirming ambiguous identifications and uncover cryptic genetic variation (Garros and Dujardin, 2013; Panda and Barik, 2021; Hadebe *et al.,* 2023). Additionally, the use of multiplex or nested PCR assays that target multiple genetic loci can improve diagnostic accuracy and minimize the risk of misidentification. To tackle the issue of false positives resulting from contamination, it is essential to adhere to strict laboratory protocols and ensure regular decontamination of workspaces and equipment.

1.5.4.2 DNA Barcoding and Sequencing

DNA barcoding is a supplementary identification technique that can address the limitations associated with conventional morphology-based taxonomy. DNA barcoding is a molecular method used to confirm insect species that are difficult to identify by morphological methods (Frézal and Leblois, 2008; Batovska *et al.,* 2016). This method utilizes a short, standardized region of DNA (about 400–800 base pairs) present within the genome, where the sequence varies distinctly between species, and is used for the genetic identification of a species

(Herbert and Gregory, 2005; Frézal and Leblois, 2008, Chan *et al.*, 2014). The process of DNA sequencing is used to determine the precise nucleotide order within a DNA molecule. DNA barcoding is an effective technique that complements the traditional taxonomic identification of mosquito species, significantly reducing the time required for identification (Kress and Erickson, 2008). This contemporary method of species identification is especially useful when working with small quantities of starting material from juvenile stages or incomplete specimens (Batovska *et al.*, 2016). However, reference databases containing sequences from recognised species are necessary for DNA barcoding to be effective. Accurate species identification can be hindered by inadequate or insufficient sequences, particularly for newly discovered or poorly researched species, leading to a lack of credibility (Chan *et al.*, 2014; Chaiphongpachara *et al*., 2022).

Two quickly evolving genetic loci, the mitochondrial DNA *Cytochrome Oxidase Subunit 1* (mtDNA *COI*) and the ribosomal DNA *Internal Transcribed Spacer Region 2* (rDNA *ITS2*), have been used to create reference sequences and unique barcodes that identify and differentiate *Anopheles* species as well as to differentiate members of species complexes. (Herbert and Gregory 2005; Chan *et al.*, 2014; St Laurent *et al.*, 2016; Rathnayake *et al*., 2023).

a) *Internal Transcribed Spacer 2* (*ITS2*)

The *Internal Transcribed Spacer 2* (*ITS2*) is a region within the ribosomal DNA (rDNA) array that separates the 5.8S and 28S rRNA genes in eukaryotic organisms (**Figure 1.2**). *ITS2* is part of the larger ribosomal DNA array, located between the conserved coding regions of the rRNA genes (Paskewitz and Collins, 1997). This region is crucial for ribosomal RNA transcription and subsequent ribosome assembly. The rDNA array consists of both transcribed and non-transcribed spacer regions, which show significant interspecific and low intraspecific variation, while the coding regions are mostly conserved. In most organisms, the rDNA consists of multiple tandem repeats of a specific DNA sequence that includes genes for the three major types of ribosomal RNA: 18S, 5.8S, and 28S (in eukaryotes), and 16S and 23S (in prokaryotes) (Gerbi, 1986; Wilkerson; Reinert and Li, 2004).

The *ITS2* region has been widely used in mosquito systematics due to its high interspecific variation and low intraspecific variability, making it particularly useful for distinguishing closely related or cryptic species. The primary advantage of the *ITS* region is that it mutates at a higher rate making it useful for distinguishing closely related species where

morphological identification may fail (Gonzalez *et al*., 1985). This gene has become valuable for molecular taxonomy and phylogenetic analysis due to its high variability among species (Coleman, 2003). The *ITS2* gene has proven valuable for studying relationships of closely related species and serves as a foundation a basis for PCR identification, contributing to efficient and cost-effective species diagnostics in vector surveillance programs. It has frequently been used to uncover cryptic *Anopheles* species, and ribosomal DNA-based PCR assays have been developed for several species complexes such as the *An. funestus* complex, the *An. punctulatus* complex and the *An. quadrimaculatus* complex (Cornel *et al.*, 1996; Beebe *et al.*, 1999; Hackett *et al.*, 2000; Koekemoer *et al*., 2002). Due to their great intraspecific homogeneity and interspecific diversity, spacer sequence analysis enables unequivocal species identification in a variety of closely related mosquito species (Carter *et al.*, 2019). However the use of *ITS2* has limitations, in some organisms, incomplete concerted evolution can result in multiple *ITS2* variants within an individual. Additionally, amplification may be hindered by complex secondary structures or length variations in the spacer region, complicating sequencing and alignment. Moreover, reference databases for *ITS2* may be incomplete or poorly annotated, particularly for lesser-studied mosquito species, which can undermine species identification reliability.

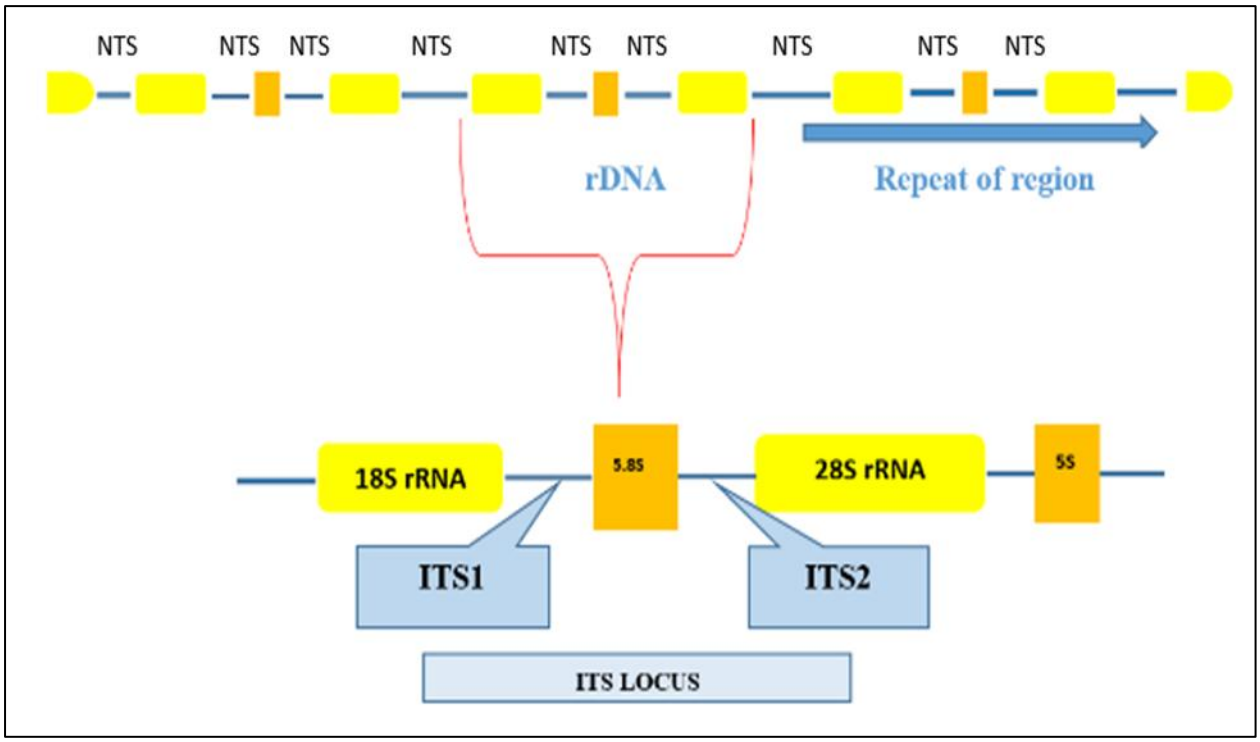


Figure 1.2 - Schematic representation of a transcription unit of eukaryotic DNA. Showing tandems of the rDNA locus separated by non-transcribed spacer regions (NTS) and regions coding for

18S rRNA, 5.8S rRNA and 28S rRNA and *Internal Transcribed Spacer regions* (*ITS1* and *ITS2*). Modified from (Paskewitz and Collins, 1997).

b) *Cytochrome c Oxidase Subunit I (COI)*

The *COI* gene is found in the mitochondrial DNA (mtDNA) of numerous organisms and has been used to successfully discriminate mosquitoes genetically (Hebert *et al*., 2003; Iyiola *et al*., 2021). The standard region used for DNA barcoding in mosquitoes is a ~658 bp fragment located near the 5′ end of the mitochondrial *COI* gene, commonly known as the Folmer region which provides sufficient interspecific variation for reliable species-level identification. The mitochondrial marker, *COI* gene, produces a protein component of the *Cytochrome C Oxidase* complex, essential for the mitochondrial respiratory pathway's electron transport chain and energy production (Rodrigues *et al*., 2017). The structure of a typical mitochondrial genome consists of several subunits and genes involved in cellular respiration that form a compact and circular genome (**Figure 1.3).** The *COI* gene serves as a molecular marker for analysing genetic diversity, species identification, and investigating phylogenetic relationships among animals. The mitochondrial genome shows significant diversity across species but little variation within species because of the high percentage of nucleotide substitution brought about by evolution (Tobe *et al*., 2010).

The major advantages of *COI* are its high interspecific divergence and relatively conserved priming sites, which make it effective for identifying a wide range of species with a single universal primer set. Mitochondrial genes are regarded as better markers to nuclear genes due to their high abundance (thousands of copies per cell), restricted exposure to recombination, and haploid inheritance (Saccone *et al.,* 1999; Murugan, *et al.,* 2016). The high copy number of the mitochondrial genome allows *COI* to be amplified from small or degraded samples, like mosquito legs or wings. Its maternal inheritance and lack of recombination make it an excellent marker for studying population structure and evolution. The *COI* gene serves as a crucial tool in identifying mosquitoes via DNA barcoding, allowing researchers to differentiate between morphologically similar or cryptic species by analysing sequence variation. It proves especially beneficial in vector surveillance initiatives, helping confirm species from degraded specimens and track the spread of invasive mosquito species. *COI* data can be matched with curated reference databases like BOLD or GenBank for species verification.

Although *COI* has several advantages, it also has limitations. One significant drawback is its lower effectiveness in distinguishing species that have recently diverged or those affected by mitochondrial introgression. This gene flow between species can result in shared haplotypes, which can obscure species boundaries and lead to misidentification. Furthermore, because *COI* only reflects the maternal lineage, it does not capture the complete genomic history of hybrid or recombinant individuals. In cases of nuclear-mitochondrial discordance, the results from *COI* should be interpreted with caution. Like *ITS2*, the accuracy of identification relies heavily on the quality and comprehensiveness of reference sequences available in public databases.

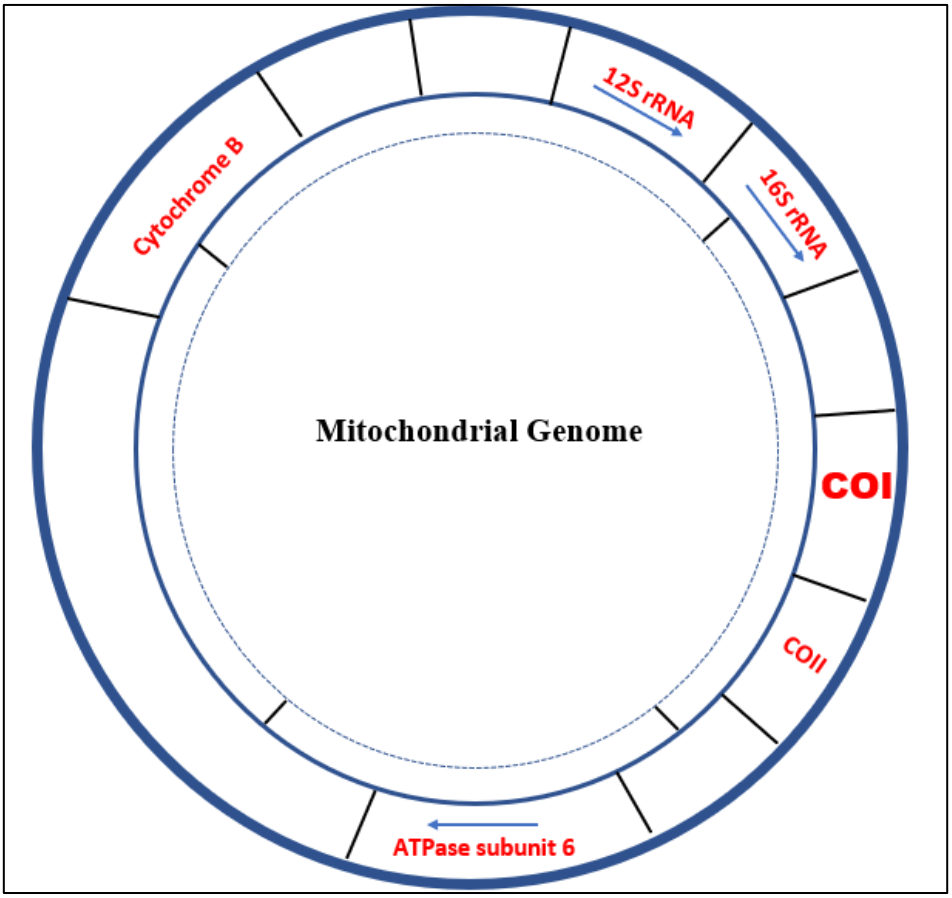


Figure 1.3 - Illustration of a typical mitochondrial genome (Modified from Trivedi, *et al.*, 2016).

Murugan and other researchers (2016) examined ten mosquito vector species from three genera (*Aedes, Culex*, and *Anopheles*) in India to evaluate the effectiveness of the *COI* gene for species identification. The study found that the generated sequences had no insertions or deletions (INDELS) and lacked stop or nonsense codons, a characteristic feature of

mitochondrial genes, allowing for clean sequence alignments. All the sequences accurately matched their haplotypes in the National Center for Biotechnology Information (NCBI) with a significant percentage of identities. Maximum identity values for the chosen species ranged from 93% to 100% in the Basic Local Alignment Search Tool (BLAST) and NCBI, supporting their precise identification. The NCBI manages the GenBank database, a collection of annotated nucleotide and protein sequences accessible to the general public. Researchers can evaluate which sequences in the GenBank database are most comparable to the obtained sequences, which can aid in validating the identity of the target species. Carter *et al.* (2019) explored the usefulness of the *ITS2* and *COI* loci for the detection of *Anopheles* species from understudied parts of eastern Ethiopia and two species, *An. arabiensis* and *An. pretoriensis* were identified. Both species were distinguished through examination of the *ITS2* locus. *Anopheles pretoriensis* sequences could be distinguished from sibling taxa, however, *An. arabiensis* could not be distinguished from other *An. gambiae* complex species using *COI* locus analysis. *Anopheles pretoriensis* could be identified using the *COI* locus, as it is not part of a species complex and shows a greater degree of mitochondrial divergence from other *Anopheles* species. In contrast, *An. arabiensis* is part of the *An. gambiae* complex, which consists of morphologically indistinguishable sibling species that have only recently diverged in their evolutionary development. The unclear results of *COI* sequencing analysis show potential difficulties in identifying species within closely related species complexes (Carter *et al.*, 2019).

A small number of studies have integrated morphological data with *ITS2* and *COI* sequencing to provide insight into previously undetected anophelines in southern and east Africa (Lobo *et al*., 2015; St Laurent *et al*., 2016; Stevenson *et al*., 2016). Although these genes are similar enough to be easily recognizable across species, they also exhibit enough variation to distinguish between different species. This variation occurs due to mutations that accumulate over time, which allows for the differentiation of closely related species. The *COI* and *ITS2* genes are suitable tools for phylogenetic and evolutionary studies because they evolve at rates that are suitable for distinguishing between closely related species while maintaining enough similarity within species. Given that both the *An. marshallii* group and *An. maculipalpis* are part of this study, additional background information on each species will be provided to emphasise their significance and clarify their roles in the research.

1.6 THE *ANOPHELES MARSHALLII* GROUP

1.6.1 *Anopheles marshallii* Group Summary Overview

A "complex" is defined as a group of species that are morphologically similar or indistinguishable but are genetically distinct. The term "group" refers to a group of species that share many adult physical characteristics but can be distinguished at juvenile stages (Coetzee, 2020). Theobald (1903) described the *Anopheles marshallii* group [*An. marshallii senso lato* (*s.l.*)] from a single female in Salisbury, Mashonaland, Rhodesia, and placed it in the genus *Pyretophorus.* Over time, numerous species that were initially described as varieties of *An. marshallii* group are now considered to consist of distinct species by most authors. There are 16 species in the *An. marshallii* group namely: *An. austenii, An. berghei, An. brohieri, An. gibbinsi, An. hancocki, An. hargreavesi, An. harperi, An. mortiauxi, An. mousinhoi, An. njombiensis, An. seydeli, An. upemba, An. marshallii s.s., An. letabensis, An. hughi* and *An. kosiensis* (Gillies and De Meillon, 1968; Lambert, 1979; Gillies and Coetzee, 1987; Harbach, 2004). The latter four species can also be differentiated from each other by cytogenetic variations (Lambert, 1981; Lambert and Coetzee, 1982).

Species belonging to the *An. marshallii* group are present in different sub-Saharan African regions, which include South Africa. Species found in southern Africa include *An. marshallii s.s., An. letabensis, An. hughi, An. kosiensis, An. mousinhoi* and *An. seydeli.* The current distribution of members of the *An. marshallii* group in South Africa are concentrated in specific regions. The most significant populations have been reported in the north-eastern parts of the country, particularly in provinces such as Mpumalanga, KwaZulu-Natal, and Limpopo (Dahan-Moss *et al.,* 2021). These areas have suitable climates, with warm temperatures and high rainfall, making them conducive to mosquito breeding. The significance of these populations lies in their potential ability to act as secondary vectors of malaria transmission. The *An. marshallii* group species reproduce in streams and wetlands, with the majority of the species being primarily zoophilic and exophilic, preferring to feed on non-human vertebrates (Gillies and De Meillon, 1968; Gilles and Coetzee, 1987).

1.6.2 Historical Synopsis of the *Anopheles marshallii* group

Earlier research on the *An. marshallii* group involved in-depth examinations of physical characteristics of the mosquitoes within this group, which was instrumental in differentiating the members of this group from each other. Extensive research has been conducted on the

morphology and population genetics of this species. A few studies have been conducted to understand the population structure, genetic diversity, and phylogenetic relationship of *An. marshallii* group with other *Anopheles* species.

Lambert (1979) conducted a cytogenetic analysis of the *An. marshallii* group individuals from localities in Zimbabwe and South Africa to identify three geographically widespread species (randomly defined as Species A, B and C) within the taxon. One of his objectives was to provide evidence of the existence of cryptic species within the *An. marshallii* group using the ovarian polytene chromosomal method. It was discovered that these species differ in chromosomal structure, exhibiting fixed inversion differences in sex chromosomes and autosomes on polytene chromosomes derived from ovarian nurse cells. A further study revealed another chromosomally distinct population (Species E) of individual females from Kosi Bay in Northern KwaZulu-Natal (Lambert 1981, 1983). These species were described and named as *An. letabensis* (Species A), *An. marshallii s.s.* (Species B), *An. hughi* (Species C), and *An. kosiensis* (Species E), respectively (Lambert and Coetzee, 1982; Coetzee *et al.*, 1987). *Anopheles kosiensis* (Species E) was identified based on a new X chromosome inversion arrangement previously unknown to science (Lambert, 1983; Coetzee *et al.*, 1987). *Anopheles marshallii s.s., An. hughi,* and *An. kosiensis* were found to have no floating inversions in their chromosomes. However, *An. letabensis* was found to have two inversions on chromosome 5 (Lambert and Coetzee, 1982; Lambert, 1983). Although the fixed sequence differences between the sex chromosomes of the four species indicated that species B, C, and E are closely related, it was discovered that these species were unique and did not interbreed in nature, suggesting that they were separate species (Lambert and Coetzee, 1982; Lambert, 1983). Two other varieties, *An. pitchfordi* and *An. pseudocostalis*, were formerly considered to be distinct species due to variations in their physical features. However, this conclusion came from statistical analysis of these characteristics rather than genetic evidence. Lambert and Coetzee (1982) decided to regard *An. pitchfordi* and *An. pseudocostalis* as a synonym of *An. marshallii s.s* for the time being until more research yields more definitive answers, and until genetic data can be correlated with morphological features (M Coetzee, *pers comm*).

This historical ambiguity regarding the taxonomy of the *An. marshallii* group has hindered clear understanding of its role in malaria transmission in Southern Africa. As secondary vectors gain recognition and the potential for overlooked transmission dynamics comes to light, there is a renewed interest in reassessing the group's taxonomic and epidemiological significance using robust molecular techniques. Therefore, this study sets out to clarify the

identity of *An. marshallii* group specimens collected in South Africa through a combination of morphological and molecular tools. This research offers a revised framework for understanding the group's composition and potential significance in local vector surveillance.

1.6.3 Role of *An. marshallii* group in Malaria Transmission:

According to Lambert and Coetzee (1982), adult female *An. marshallii* group specimens were considered both zoophilic and exophilic, and their occasional appearance in homes may have been due to the presence of animals besides humans. However, Bafort (1985) conducted a study that demonstrated that *An. marshallii* group could be a secondary malaria vector and may be responsible for low-level transmission in some regions of Africa, necessitating further research on these vectors (Bafort *et al*., 1985). The study collected blood-fed *Anopheles* mosquitoes from huts in small villages around Lwiro (Democratic Republic of the Congo). He postulated that *An. letabensis* may be the species concerned due to its man-biting tendency. In addition to its anthropophilic behaviour, *An. letabensis* has been found to bite in nocturnal patterns and in close proximity to human dwellings; both traits that are commonly associated with malaria vectors. Unfortunately, no chromosomal identification was possible for any specimens to validate this hypothesis. Out of the 1 212 *An. marshallii* group samples that were examined for sporozoites, only three (0.24%) harboured malaria sporozoites (Bafort *et al*., 1985). This demonstrates that certain vectors can only be identified by using appropriate molecular techniques along with detailed morphological identification. A molecular PCR assay would provide a more precise and efficient way of distinguishing between these species and determining which of the 16 *An. marshallii* group species are potential vectors.

Entomological surveys were carried out in Olama (Cameroon) where one *An. marshallii* group specimen was infected with the parasite *P. falciparum* (Antonio-Nkondjio *et al*., 2005). In another study, the vectorial diversity of *An. marshallii* group and their infectivity across various seasons and altitudes in relation to parasite prevalence around the slopes of Mount Cameroon. The prevalence of *Plasmodium* infection was assessed in 313 anophelines using circumsporozoite antigen ELISA and 12 (3.8%) *An. hancocki* specimens carried *P. falciparum* circumsporozoites (Kwi *et al*., 2022).

Although a substantial number of *An. marshallii* group specimens have been collected from sentinel sites in the KwaZulu-Natal malaria-endemic province over the past years, it has not been identified as a malaria vector in South Africa, as it has in other regions of Africa (Dahan-Moss *et al*., 2021). This may stem from their zoophilic tendencies, low population densities, or historical underrepresentation in vector incrimination studies. However, the absence of incriminating evidence in South Africa does not rule out a potential future role, especially if ecological conditions or vector behaviours change. Accurately identifying *An. marshallii* group specimens remains crucial in areas where malaria persists. This research aims to enhance species resolution and lay the groundwork for future studies that may evaluate the group's role in malaria transmission, particularly under changing environmental or epidemiological conditions, through the use of iso-female lines and molecular analysis.

1.6.4 Distribution and Biology of Members of the *Anopheles marshallii* Group

a. *Anopheles marshallii s.s.*

Anopheles marshallii s.s. is a widespread species distributed in East and South Africa (**Figure 1.4**). They also occur in specific areas along the southern edge of the West African savanna (Gillies and De Meillon, 1968). These species are both zoophilic and exophilic, and there is evidence that their sporadic presence inside homes is linked to the presence of domestic animals nearby, however, contact with humans appears to be rare. *Anopheles marshallii s.s* specimens were identified by Bruce-Chwatt and Gockel (1960) as a possible secondary vector when 29.5% of the group's specimens tested positive for human blood, however, no sporozoite infections have been documented. Their larvae are usually found in fresh backwaters of streams and seepage areas in weeds and grass (Gillies and De Meillon, 1968; Gillies and Coetzee, 1987).

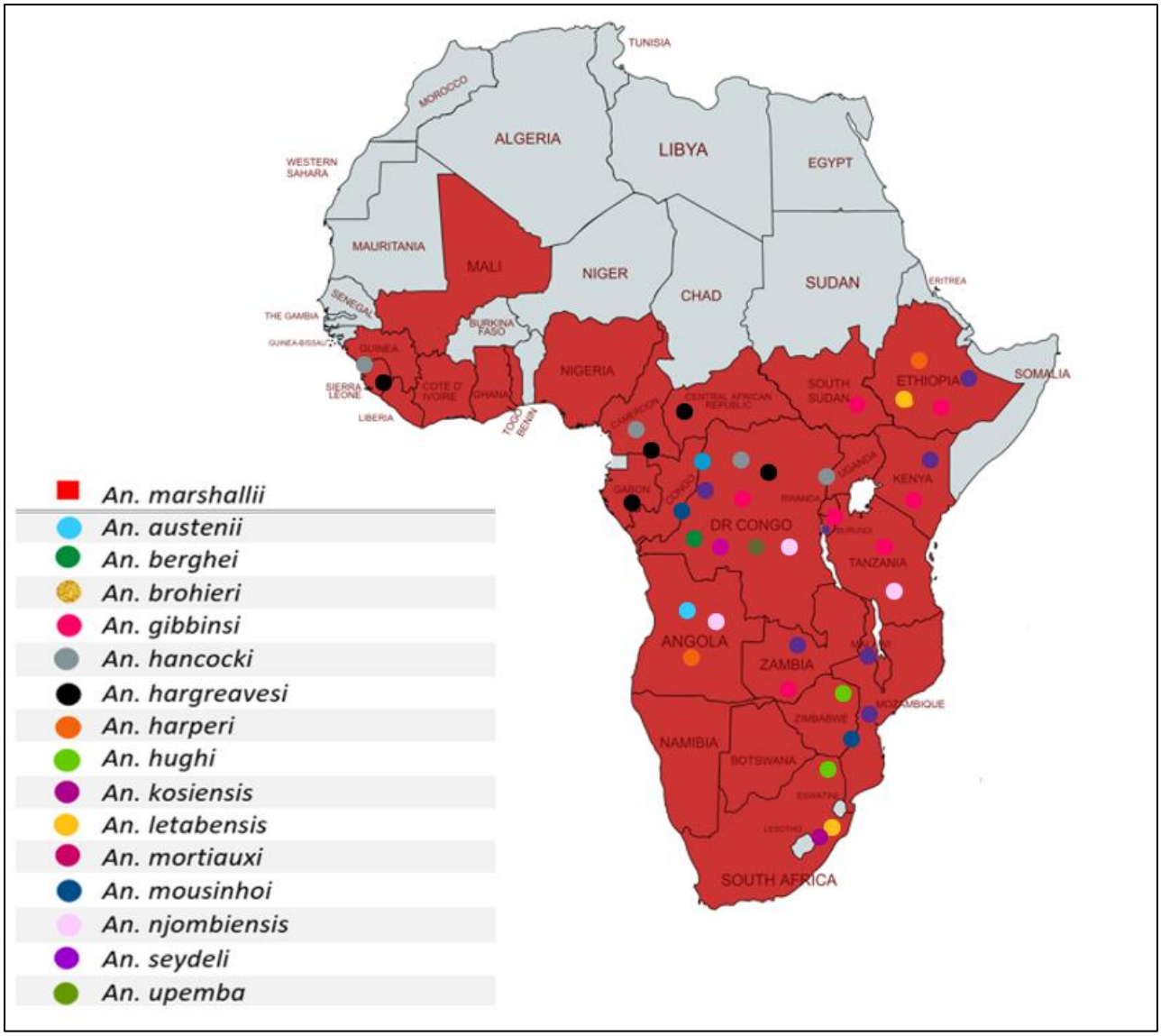


Figure 1.4 - Map showing the distribution of *Anopheles marshallii* group species across Africa. Adapted from Gillies and De Meillon (1968) and Gillies and Coetzee (1987).

b. *Anopheles austenii*

Anopheles austenii species were recorded from Katanga (Congo) and Angola (**Figure 1.4**). Ribiero and Ramos (1975) reported a small number of adults biting humans at night in Angola, making it a potential malaria vector. No *Plasmodium* infections have been reported in spite of this. Larvae were discovered in a shallow well dug in a grass-covered pit (Gillies and De Meillon, 1968).

c. *Anopheles berghei*

This species is found in Katanga, Democratic Republic of Congo (**Figure 1.4**). The adults have been discovered resting low on the trunks of trees or in the spaces between their roots in a humid forest (Vincke and Leleup, 1949). There is a possibility that *An. berghei* may be a subspecies of *An. mortiauxi,* as proposed by Vincke and Leleup (1949). This is supported by their close morphological resemblance, including similarities in wing spot patterns and scaling on the legs. However, both forms have been treated as distinct species due to a lack of extensive study on their early stages with a larger sample size. No reports of human bites or sporozoite discovery exist for this species. The adult biology of this species is unknown (Gillies and De Meillon, 1968).

d. *Anopheles brohieri*

This species lives in the savanna and is widely distributed from Mali to northern Nigeria, Cameroon to northern Uganda, and the far south of Sudan (**Figure 1.4**). *Anopheles brohieri* are primarily zoophilic, however, they are occasionally captured outside using humans as bait. According to Hamon *et al*. (1964), adult mosquitoes have been seen resting outside in dirt crevices. Studies have not shown consistent human blood feeding or sporozoite positivity. As a result, it is not currently regarded as a vector. The larvae develop in swamps and slowly moving streams (Gillies and De Meillon, 1968).

e. *Anopheles gibbinsi*

This highland species is found in eastern Africa that ranging from Ethiopia and southern Sudan to Rwanda, Burundi, Kenya, Tanzania and the Democratic Republic of Congo (**Figure 1.4**). It is mainly zoophilic and exophilic. However, it has been documented that it occasionally feeds on humans, indicating that it is likely to ingest human malaria parasites. Their larvae have been found in Kenya in ditches without trees to provide shade or in slow, shallow streams (Evans, 1938; Gillies and De Meillon, 1968). According to studies from the Kenyan highlands, 7.7% of *An. gibbinsi* specimens tested positive for *Plasmodium falciparum* sporozoites by CSP ELISA, indicating that this species is a malaria vector. (Cooke *et al*., 2015). Gebhardt *et al*. (2022) recently showed that *An. gibbinsi* were also collected in Zambia. However, none of the samples was found to be infected.

f. *Anopheles hancocki*

Anopheles hancocki species mainly inhabit the mosaic forest-savanna zones of West Africa, which stretch from Sierra Leone to Cameroon and the Congo basin to Uganda (**Figure 1.4**). This species, which is anthropophilic across its habitat, enters homes to feed on people and then rests inside. Although *An. hancocki* has been implicated as a malaria vector in a number of locations, such as Uganda, Cameroon, and Nigeria, its infection rates are rarely high enough to be significant when compared to the primary vectors (Gillies and De Meillon, 1968). Their larval habitat constitutes clear water in densely vegetated swamps, seepages, and slowly flowing streams and rivers.

g. *Anopheles hargreavesi*

Anopheles hargreavesi is a forest zone species primarily found in West Africa, extending from Sierra Leone to Cameroon to Congo, across western Uganda, Gabon and Central African Republic (**Figure 1.4**). It is a slightly anthropophilic species that readily bite people indoors and outdoors, especially when no cattle are around. The larvae can be found in open forest regions in grassy wetlands or slow-flowing streams (Gillies and De Meillon, 1968). No other positive gland dissections have been documented since Barber *et al.* (1931) discovered that 5.4% of 92 dissected mosquitoes in southern Nigeria had sporozoites and declared it a significant malaria vector. Hamon and Mouchet (1961) observed that despite the ongoing presence of *An. hargreavesi* biting outside, malaria was eliminated in the Cameroun Forest through residual spraying (Gillies and De Meillon, 1968).

h. *Anopheles harperi*

Anopheles harperi is a rare highland species that is most likely more widespread than earlier reports suggested. It is distributed in Ethiopia, Kenya, and Angola (**Figure 1.4**). Nothing is known about its adult biology. The larvae of *An. harperi* are found in shallow ponds with standing grass under the shelter of plants and trees, as well as in the swamps (Gillies and De Meillon, 1968). It is unlikely to be a malaria vector based on the evidence available, as there is no information on human bite or infection.

i. *Anopheles hughi*

The distribution of *Anopheles hughi* is restricted to Limpopo (formerly Transvaal) and Zimbabwe (formerly Rhodesia) (**Figure 1.4**). This species is primarily found outdoors, where

it is predominantly caught on animals (Gillies and Coetzee, 1987). To date, no studies have conclusively identified its host preferences and its vector status remains unknown.

j. *Anopheles kosiensis*

This species was first described from a single location in Kosi Bay, KwaZulu-Natal, South Africa (**Figure 1.4**). Fully engorged female specimens were collected in a cattle enclosure, suggesting a significant tendency to feed on animals (Gillies and Coetzee, 1987). Since its initial description, there have been very few additional reports, and its distribution seems to be highly localized, with no confirmed sightings beyond the original collection site. The limited data makes it challenging to assess its potential role in malaria transmission.

k. *Anopheles letabensis*

Anopheles letabensis exhibits a widespread distribution ranging from Ethiopia to KwaZulu Natal, typically found at lower altitudes than *An. marshallii s.s.* They are sometimes seen biting people outdoors or resting inside houses (Gillies and Coetzee, 1987). According to previous reports, *An. letabensis* has been found to exhibit human biting characteristics (Chwatt and Gockel, 1960; Lambert, 1981; Lambert and Coetzee, 1982). Bruce-Chwatt and Gockel (1960), demonstrated that 29.5% of *An. marshallii* group individuals collected across a wide geographic area tested positive for human blood. Most of these individuals were *An. letabensis*, which commonly bite humans, unlike the other species. Lambert (1979) proposed that *An. letabensis* should be studied due to its anthropophilic biting behaviour, to determine its vectorial capacity for malaria. Furthermore, this species is able to adapt to various habitats and its efficient transmission of the *Plasmodium* parasite could potentially contribute to the higher risk of malaria transmission.

l. *Anopheles mortiauxi*

Anopheles mortiauxi is a rare mosquito species that was described by Edwards in 1938. Its distribution is primarily limited to Kinshasa Province in Congo (see Figure 1.4). The type specimens, which include both male and female mosquitoes, are housed in the British Museum, where the males are labeled as cotypes (Gillies and De Meillon, 1968). To date, no studies have documented the host preferences, breeding ecology, or adult feeding behaviors

of this species. Its rarity and the absence of collection records indicate that it may have a limited distribution or specific habitat requirements.

m. *Anopheles mousinhoi*

Anopheles mousinhoi is a rare species of mosquito found in South Africa, Mozambique, Zimbabwe, and the Democratic Republic of Congo (**Figure 1.4**) (Gillies and De Meillon, 1968; Coetzee and Le Seur, 1988). However, it is likely that this mosquito also inhabits neighboring countries due to ecological similarities and the availability of suitable habitats across borders. Although no formal collection records confirm its presence beyond these four countries, the shared bioclimatic zones and wetland environments in adjacent areas make its occurrence plausible. There is currently no data available regarding its adult biology or host preferences. Until more information is available, *An. mousinhoi* is classified as a non-vector species because there is no evidence of human contact or *Plasmodium* detection. The larvae of *An. mousinhoi* are typically found in slow-moving, clear water that contains grass and reeds, or in permanent wetlands with grass and aquatic vegetation.

n. *Anopheles njombiensis*

Anopheles njombiensis is only found Angola and in the southern Highlands of Tanzania, Katanga Province (Congo) (**Figure 1.4**). There is no information on the biology of this species other than that the few specimens captured were either unfed in houses or overfed at night in cattle sheds (Gillies and De Meillon, 1968). Its vector status is unknown since no research has found sporozoite infection, however zoophilic bias might indicate a low risk of human transmission. Nothing is known about the larval habitat of this species.

o. *Anopheles seydeli*

Anopheles seydeli covers a wide distribution in eastern Africa, from Ethiopia, Burundi, Tanzania, Katanga Province (Congo), Malawi, Mozambique and Zambia (**Figure 1.4**) (Gillies and De Meillon, 1968). While outdoor human-biting behavior by small populations of females has been observed in Tanzania, no sporozoite-positive specimens have been reported to date. As such, no sporozoite-positive specimens have been reported, so its role in transmission remains unconfirmed. Their larvae are generally found in the grassy margins of slow- or fast-moving streams.

p. *Anopheles upemba*

This species was identified from a single incomplete female lacking fore legs and the last two hind tarsal segments found in Katanga, Zaire, in 1947. Mattingly (1955) described it but did not give it a name. However, he recognised it as a unique species. Lips (1960) subsequently provided the name in an appendix to one of several studies on the anopheline fauna of Zaire (Gillies and Coetzee, 1987). Gillies and De Meillon (1968) failed to mention the existence of this name. This species has yet to be studied extensively, thus, information about its adult biology, infection status and host preference is unavailable.

1.6.5 Morphological Differences between Members of the *Anopheles marshallii* group

The study of the physical characteristics of *An. marshallii* group species requires examining all its life-stages. This is because identifying the *An. marshallii* group species based solely on adult females is difficult due to overlapping adult morphological traits. To accurately identify them, examining their juvenile characteristics, which can be observed in their eggs, larvae or pupae, is necessary. The analysis of these characters allows for a clearer distinction between species in the *An. marshallii* group. Each developmental stage presents unique features, and when assessed collectively, they enhance the reliability of morphological identification. **Table 1.1** highlights the variations among adult species, while detailed descriptions of these species can be found in Gillies and Demeilon (1968) and Gillies and Coetzee (1987). To further examine the differences between species at different stages, please refer to **Appendix 1A**, **1B**, and **1C** for information on egg, larval and pupal stages. An overview of the morphological variations observed across these stages is provided below:

1.6.5.1 Differences in Egg Stages

The egg is the first life stage that is examined. The dorsal surface of *Anopheles marshallii s.s.* eggs have two visible decks, each encircled by a narrow frill (**Figure 1.5**) (Gillies and De Meillon, 1968). However, variation in egg morphology reported or absence of egg morphology recorded or published provide challenges for species identification (M Coetzee, *pers comm*). *Anopheles letabensis* eggs are similar but with slightly more rounded deck openings (Gillies and Coetzee, 1987). The eggs of *An. kosiensis* and *An. hughi* are similar, they have well-separated floats with a single deck continuous between them. *Anopheles*

gibbinsi eggs are larger than *An. marshallii s.s.* eggs and have a discontinuous chorion between the floats (Gillies and De Meillon, 1968). *Anopheles hancocki* eggs have a finely sculptured chorion and floats with multiple ridges. *Anopheles hargreavesi* eggs have two fully developed frills surrounding the polar enclosed sections in an oval shape. *Anopheles seydeli* eggs resemble *An. marshallii s.s.* but they have three decks (Gillies and De Meillon, 1968). However, the egg morphology of *An. austenii, An. berghei, An. brohieri, An. harperi, An. mortiauxi, An. mousinhoi, An. njombiensis* and *An. upemba* is still unknown **(**see **Appendix 1A)**. The lack of published data on these species presents a significant gap in knowledge, and further research is needed to determine their egg morphology for proper identification.

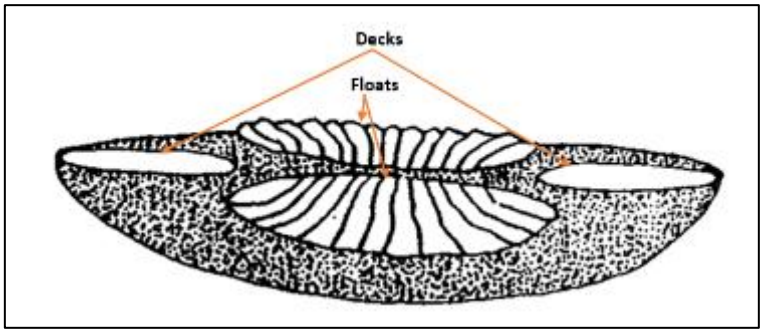


Figure 1.5 – Illustration of *Anopheles marshallii s.s.* egg. Sourced from (Gillies and De Meillon, 1968).

1.6.5.2 Differences in Larval Stages

Following the egg stage, larval morphology provides additional traits that can help distinguish between species. *Anopheles marshallii* group mosquito larvae of different species exhibit varying features in terms of their hair and setae (see **Appendix 1B**). Particularly valuable are the setae, which are specialised bristle-like hairs found on the thorax, abdomen, and head (clypeal area). These hairs are dependable diagnostic features in morphological keys because they differ structurally between species in terms of position, length, branching pattern, and attachment base (Gillies & De Meillon, 1968). The abdominal palmate hairs, which are comb-like structures located laterally on the abdominal segments, are used to distinguish species based on the filament shape and length (Appendix 1B). **Figure 1.6A** illustrates the abdominal segments and palmate hairs of *An. marshallii s.s.*, showcasing their typical structure: short, sharply pointed filaments. These structures serve as a reference for

comparing similar species. In Southern African specimens like *An. marshallii s.s.,* the filaments are generally short and sharply pointed (Gillies and De Meillon, 1968), consistent with the features shown in **Figure 1.6A**. In contrast, larvae from other regions may display longer or more variable filament shapes, indicating regional variation. For instance, *An. brohieri* larvae have longer palmate hair filaments and broader abdominal plates than those seen in **Figure 1.6A.** Additionally, *An. mousinhoi* exhibits undifferentiated abdominal palmate hairs on its first two segments. *Anopheles austenii* larvae show similarities to *An. marshallii s.s.,* but their tergal plates differ in size (Gillies and De Meillon, 1968).

Figure 1.6B displays the posterior and outer clypeal hairs of *An. marshallii s.s*. are critical for differentiating this species from others in the group. The outer clypeal hairs of *An. hargreavesi* are relatively short and abruptly pointed, differing in length and shape from those of *An. marshallii s.s.* shown in the figure. Similarly, *An. harperi* larvae, which resemble *An. hargreavesi*, can be differentiated by the presence of arms on the scoop's middle plate, a feature not observed in **Figure 1.6B**. In *An. letabensis*, the posterior clypeal hair is simple, and the inner shoulder hairs are mounted on a small tubercle (Gillies and Coetzee, 1987). *Anopheles hughi* larvae are similar; however, their abdominal hairs consist of branches that primarily arise from one side of the hair stem. *Anopheles kosiensis* and *An. hughi* larvae are comparable, but *An. kosiensis* has a significantly smaller larval thoracic palmate seta when compared to *An. marshallii s.s.* (Gillies and Coetzee, 1987). *Anopheles gibbinsi larvae* resemble *An. marshallii s.s.,* while *An. hancocki* larvae have more sharply pointed inner clypeal hairs and more primitive palmate hairs on their abdominal segments. *Anopheles mousinhoi* larvae are similar to *An. marshallii s.s.,* except the posterior clypeal hair is slightly shorter. In *An. njombiensis*, the posterior clypeal hairs are slightly longer than the outer hairs, while in *An. seydellii* larvae, the posterior clypeal hairs are simple, very short, and stumpy. Unfortunately, there is currently no available information on the larval morphology of *An. berghei, An. mortiauxi*, and *An. upemba* (Gillies and De Meillon, 1968).

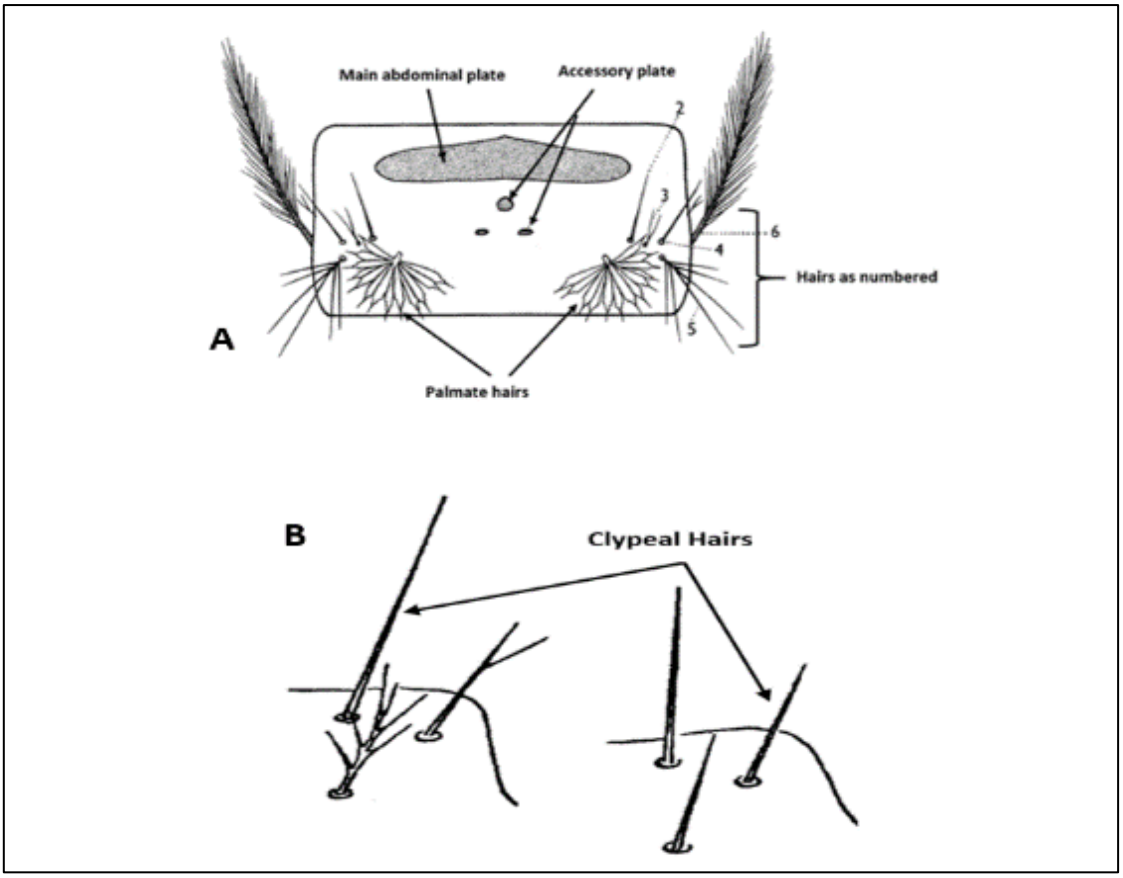


Figure 1.6 - Larval morphological features of *Anopheles marshallii s.s*. (A) *An. marshallii s.s*. larval abdominal segments. (B) *An. marshallii s.s.* clypeal hairs. Sourced from (Gillies and De Meillon, 1968).

1.6.5.3 Differences in Pupal Stages

Lastly, the pupae are examined, using subtle morphological features such as paddle fringe structures and setal patterns to distinguish the species. The apical paddle hair is a crucial characteristic that varies both qualitatively and quantitatively between species. In *An. marshallii s.s.*, the apical paddle hair is of moderate length, straight, and tapers evenly to a point. In contrast, other members of the group exhibit varying apical paddle hair morphologies; for instance, *An. hargreavesi* has shorter, slightly curved apical hairs, whereas *An. austenii* has longer and more flexuous apical paddle hairs. These differences are often species-specific and are employed in taxonomic keys to distinguish closely related species during pupal identification. Additionally, the paddle fringe in *An. marshallii s.s*. consists of spines that gradually transition into fine hairs without extending beyond the apical paddle hair (**Figure 1.7**). Variations in this fringe pattern, along with differences in the length, branching, and location of pupal setae (as detailed in **Appendix 1C**), also provide valuable characteristics for species identification. However, pupal morphology has yet to be documented for *An. berghei, An. brohieri, An. mortiauxi,* and *An. upemba*, highlighting gaps in the current literature (Gillies and De Meillon, 1968; Gillies and Coetzee, 1987).

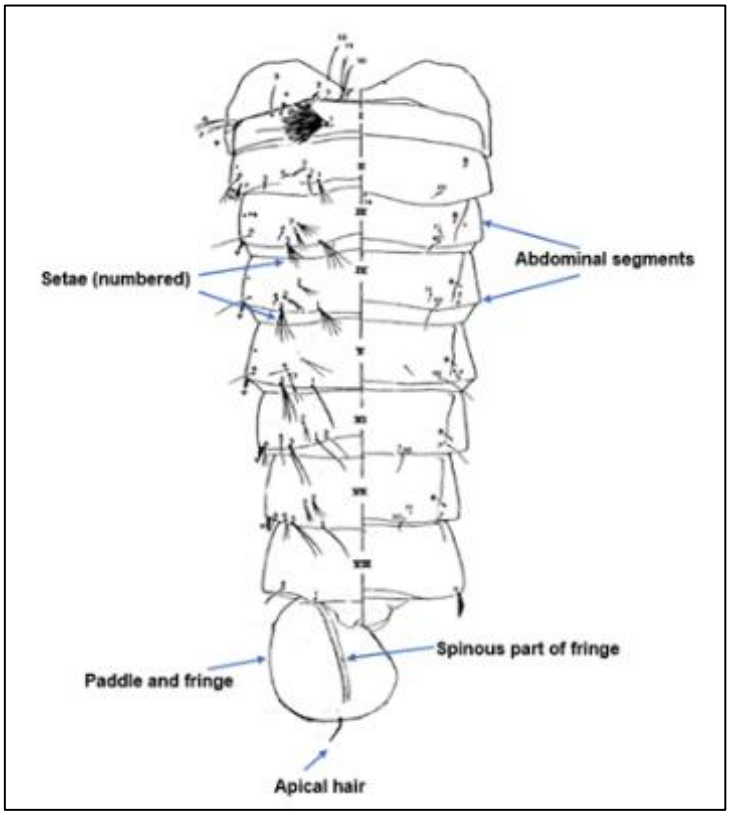


Figure 1.7 - Dorsal view of *Anopheles* pupae abdominal segments. Sourced from (Gillies and Coetzee, 1987).

1.6.5.4 Adult Morphological Description

a. *Anopheles marshallii s.s.*

In adult forms, the width of the apical dark palpal band and the amount of pale scaling in the wing vary greatly (**Figure 1.8A** and **B**). The palps are smooth with a few suberect scales basally, and the apical dark band is about the same width as the adjacent pale bands. The third main dark section of the first vein in the wing always has a pale interruption (**Figure 1.8A**). The tarsal segments of the legs are very narrowly pale apically, with some geographic variation in the extent of the pale markings across populations. The scutal scales of *Anopheles marshallii s.s.* are white, ranging from linear to narrowly lanceolate in shape, measuring approximately 0.06–0.08 mm in width, slightly curved, and neither truncate nor flattened according to Gillies and De Meillon (1968) (**Figure 1.9**).

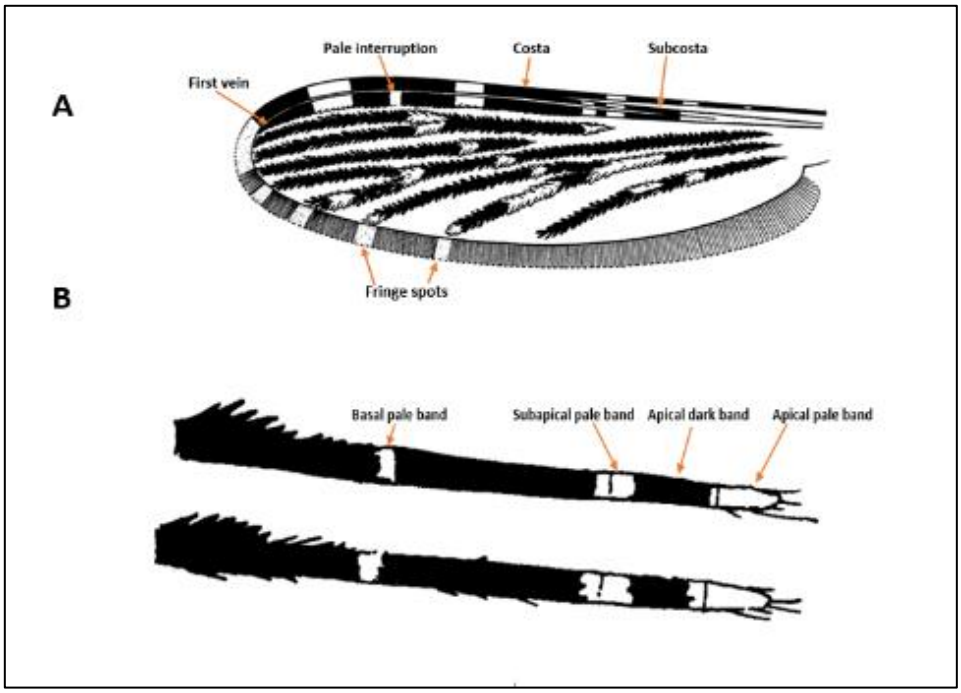


Figure 1.8 - Morphological characters of a female *Anopheles marshallii* group. (A) wing and (B) palps. Sourced from (Gillies and De Meillon, 1968).

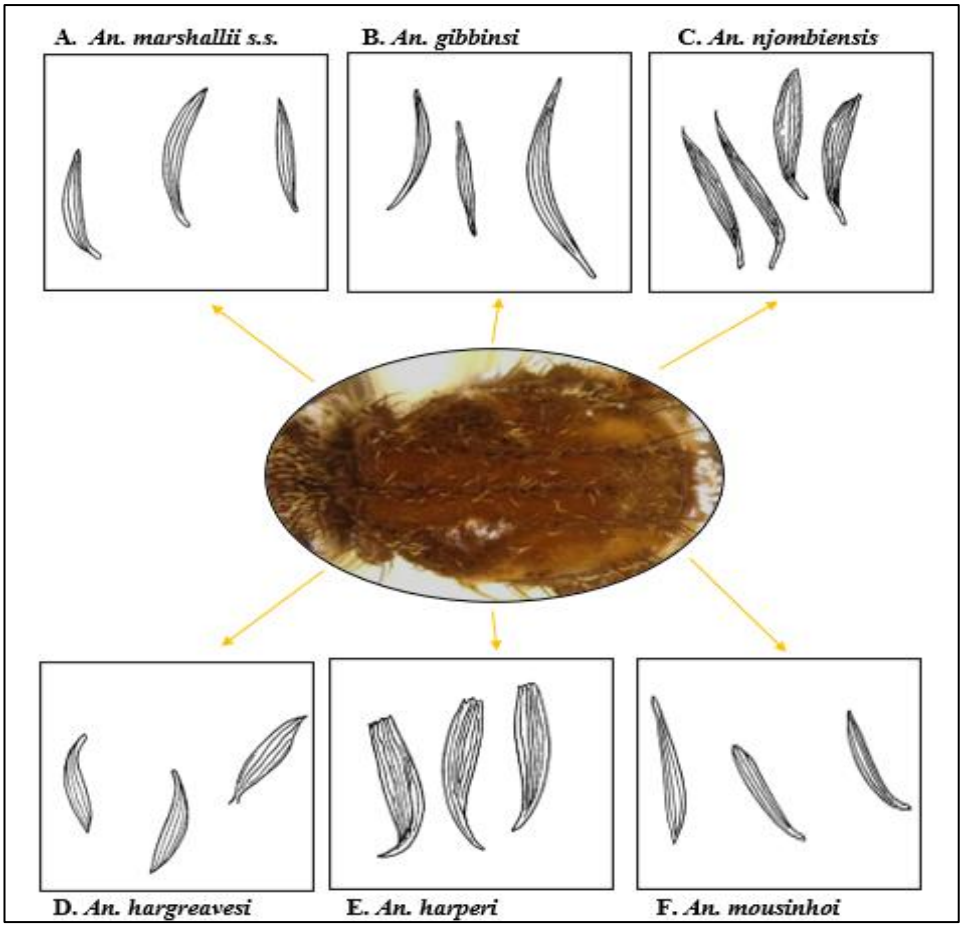


Figure 1.9 - *Anopheles marshallii* group mesonotal scales (Gillies and De Meillon, 1968).

b. *Anopheles austenii*

There are distinct apical pale patches on the femur and tibia of the adults. The apexes of each of the four tarsal segments have comparatively broad white bands; the fore and hind tarsi's bands are at least twice as wide as those of the mid-tarsi. Variation in the size and prominence of these bands has been noted in different populations (Gillies and De Meillon, 1968). The mesonotum is quite heavily covered in wide, white scales that cover the entire scutellum and scutum (Gillies and De Meillon, 1968).

c. *Anopheles berghei*

This species closely resembles *An. mortiauxi*. In contrast to *An. mortiauxi*, the pale scales on the fore tibia and tarsal segments do not extend over the joints onto the bases of the subsequent segments, and they are extremely narrowly pale at the apex (Gillies and De Meillon, 1968). The apex of the mid-femur is black and lacks a subapical pale patch, the

tibial and tarsal apices are narrowly pale. The degree of pale scaling varies somewhat by location, with specimens from different regions exhibiting slight differences in the prominence of pale bands on the legs. Compared to other members of the *An. marshallii* group, their wing field often appears significantly darker. In contrast to *An. mortiauxi* species, they do not have a pale fringe spot across from the sixth vein. The mesonotum is covered by golden scales that are falcate to lanceolate in shape, with widths averaging 0.07 mm and tapering to a curved, acute apex (Gillies and De Meillon, 1968).

d. *Anopheles broheiri*

This species is very closely related to *An. hancocki* however, the hind tarsi are variable. In contrast to *An. marshallii s.s.*, the third segment of the hind tarsus may be entirely white or have light scaling confined to the segment's base and apex (Gillies and De Meillon, 1968). The size of pale patches on the costa of the wing varies more from specimen to specimen. The pre-sector and humeral spots are present in the lightest forms, but the darkest forms have no presence of pale spots. The anterior quarter of the mesonotum is covered in very narrow, curved white scales (approximately 0.04 mm in width), while the rest has somewhat broad, curved, and pointed white scales (Gillies and De Meillon, 1968).

e. *Anopheles gibbinsi*

An. gibbinsi closely resembles *An. marshallii s.s.* but the wing markings are where variety is most noticeable. The third vein may be entirely dark, or it may be dark only at the apex and base. There is variation in the presence and prominence of pale markings across populations. The mesonotum is draped in extremely thin golden scales (**Figure 1.9**). In some populations, the golden scales on the mesonotum may be more prominent, while in others, they may be slightly less pronounced (Gillies and De Meillon, 1968).

f. *Anopheles hancocki*

A faint pale band may be present basally on the second hind tarsal segment, specimens from Kampala show this particularly clearly. The pale costal wing areas vary significantly in size, though less than in *An. brohieri*, as noted by Evans (1938) and Adam (1956) (Gillies and De Meillon, 1968). Specimens of *An. hancocki* from southern Nigeria often lack the dark band at

the tip of their palps. The scutal scales resemble those of *An. brohieri* (Gillies and De Meillon, 1968).

g. *Anopheles hargreavesi*

All tarsi, except the fifth, have apical pale bands, while those on fore tarsal segments one and two are longer than broad, while those on the hind tarsals resemble those of *An. marshallii s.s.* (Gillies and De Meillon, 1968). The fringe spots opposing all veins are well-marked but short, except those opposite the sixth vein, which may be quite weak. The third main dark area of the first vein is disrupted, and the costal markings on the wings are short but well-marked. Broad, pale scales, many of which are truncated with round apices, cover the mesonotum evenly (**Figure 1.9**). The scutal scales on the posterior part of the mesonotum are as broad as those on the anterior (Gillies and De Meillon, 1968).

h. *Anopheles harperi*

The adult closely resembles *An. marshallii s.s.* but can be differentiated by the reduced pale markings on all legs (Gillies and De Meillon, 1968). The last three segments of the hind tarsi are often completely dark, with a few pale scales at the apices of the preceding two segments creating narrow rings. The dark hind tarsi distinguish it from all other members of the *An. marshallii* group except *An. njombiensis*. The sixth pale fringe spot is often absent on the wings. The scutal scales are cream or yellow in colour and range in width from relatively broad to narrow (**Figure 1.9**) (Gillies and De Meillon, 1968).

i. *Anopheles hughi*

Their distinguishing characteristics are the pale bands on hind tarsi being more prominent than in either *An. letabensis* or *An. marshallii s.s.* The female palps feature a dark apical band that is the same width to the adjacent pale bands (Gillies and Coetzee, 1987). There is some variation in the pale scaling on the tarsi across different populations, with some specimens showing more pronounced pale markings than others.

j. *Anopheles kosiensis*

The adults closely resemble *An. hughi* with slight differences in the size of palp spots and the banding on the hind tarsomeres. The fore and mid-legs of *An. kosiensis* show some pale

scaling, with the pale bands on the tarsi being most prominent on the forelegs. The pale bands on the fore tarsal segments are generally broader compared to those on the hind and mid-tarsal segments. Compared to *An. hughi,* the banding on the hind tarsal segments of *An. kosiensis* tends to be narrower and less distinct (Gillies and Coetzee, 1987).

k. *Anopheles letabensis*

The main diagnostic characters in adult forms are the more prominent pale bands on tarsi compared to those of *An. marshallii s.s.* The apical dark bands on palps are very narrow, much less than the width of pale bands (Gillies and Coetzee, 1987).

l. *Anopheles mortiauxi*

The fore tarsal segments 1-4 exhibit prominent apical and basal pale bands, in contrast to the mid and hind tarsi, which have narrow apical pale bands that sometimes slightly overlap the bases of the following segments (Gillies and De Meillon, 1968). Their wings are darker than in *An. marshallii s.s.* with less pale areas, the upper branch of the fifth vein has a small second pale patch of scales and a sixth pale fringe spot. Moderately broad, pointed, curved golden scales cover the mesonotum fairly densely (Gillies and De Meillon, 1968).

m. *Anopheles mousinhoi*

This species is very closely related to *An. marshallii s.s.* The females of *An. mousinhoi* have broad apical and subapical pale bands on the palps, but unlike *An. marshallii s.s.,* they lack a pale interruption in the third main dark area of the first vein (Gillies and De Meillon, 1968). The mesonotum is covered in somewhat broad white scales, typically elliptical to lanceolate in shape and measuring approximately 0.07–0.09 mm in width, similar to those of *An. marshallii s.s.* (**Figure 1.9**). The tarsal segments of the legs exhibit variable patterns in the extent of pale scaling, with the forelegs typically displaying broad apical pale bands. The forelegs typically have broad apical pale bands; however, in some populations, the pale bands on the hind tarsi may be narrower or less distinct, indicating potential variation across different geographic regions (Gillies and De Meillon, 1968).

n. *Anopheles njombiensis*

Anopheles njombiensis looks very similar to *An. harperi*. It can be recognised from the latter by the mesonotum's vast white scales, which, in contrast to those of other *An. marshallii*

group members, are dispersed over the lateral regions and the fossae (Gillies and De Meillon, 1968). Palps have a pale subapical band that is nearly as long as the apical band.

o. *Anopheles seydeli*

The amount of pale scaling on the tarsal segments varies among adult forms. De Meillon and Pereira (1940) identified a male specimen in which the dark band on hind tarsal segment four was greatly reduced, in contrast to the typical broad pale scaling on the hind tarsi from prior material. The tarsus of the forelegs has broad apical pale bands, although these bands appear significantly shorter in the mid-legs (Gillies and De Meillon, 1968). Mesonotum is covered in a few yellowish hairs and a few sparse, narrow, curved white scales (Gillies and De Meillon, 1968).

p. *Anopheles upemba*

Mattingly (1955) states this species is typically similar to *An. hargreavesi*, but the scutal integument in *An. upemba* is entirely dark, the posterior two-thirds of the median area have darker golden brown scutal scales, which are noticeably smaller (Gillies and Coetzee, 1987). The palps have a subapical pale band that is twice as large as the apical band and takes up the entire fifth segment, distinguishing it from *An. hargreavesi*. Even though the authors were unaware of the patterns on the hind tarsal segments, the dimensions of the pale bands on the palps are quite different from those of any other Afrotropical *Anopheles* and made it possible to identify this species (Gillies and Coetzee, 1987).

Table 1.1 - Morphological differences within adult members of the *Anopheles marshallii* group.

Species name	Palps	Mesotonum	Legs	Wings
An. marshallii s.s.*	The surface is smooth with a few suberect scales basally. The apical dark band is approximately the same width as the adjacent pale bands. There is considerable variation in the width of the apical dark palpal band, which is typically as broad as the pale bands it separates, though it can sometimes be narrower.	With broad or thin whitish scales, slightly curved, covering the anterior half or the whole surface.	Segments 1-3 of the fore and mid-tarsals are somewhat pale apically. The tibiae are strikingly pale apically.	Pale scales white or creamy. There is a pale interruption in the third main dark section of the first vein that occasionally overlaps with the subcostal pale area, though its location varies.
An. austenii *	Features 3 pale bands, with the apical and subapical being broad and roughly equal in width.	With broad white scales that cover the entire scuteum.	The femor and tibia have visible apical pale spots. Tarsal segments (1-4) have wide white stripes at the apexes.	Same as *An. marshallii s.s.* There may be fewer or no basal pale spots on the costa.
An. berghei	Same as in *An. marshallii s.s.*	Same as in *An. mortiauxi.*	The apex of the foretibia is pale. Tarsal segments 1–3 are somewhat pale apically. The mid-femur lacks a subapical pale spot and is dark at the apex.	Darker than in other *An. marshallii* group members. There is no pale fringe spot located opposite the sixth vein.
An. brohieri	Resembles *An. hancocki.*	Resembles *An. hancocki.*	Hind tarsus variable, with 3rd segment wholly white or with dark banding.	There is variation in the size of the pale areas along the costa.
An. gibbinsi	Resembles *An. marshallii s.s.*	Covered with very narrow golden scales.	Same as *An. marshallii s.s.*	Darker than in *An. marshallii s.s.* The sector and basal costal pale spots are reduced. Reduced fringe spots.
An. hancocki	There are three pale bands, with the one at the apex of the second segment being narrow proximally. The apical dark band is narrower compared to the pale bands.	White scales on the anterior part of the body are somewhat broad, curved, and pointy.	The tarsus 1-3 of the forelegs is widely pale apically. Tibiae narrowly tipped with pale scales.	There is variation in the size of the pale areas along the costa.

An. hargreavesi	Same as in *An. marshallii s.s.*	Covered with thickly distributed broadish pale scales, most of them are truncated.	Every tarsus has apical pale bands, with the exception of the fifth. The foretarsal segments 1 and 2 are longer than the broad ones.	The costa spots are distinct but short, and the third main dark area on the first vein is interrupted.
An. harperi	Subapical pale band distinctly narrower than apical.	The scales are moderately broad to narrow and are either cream or yellow in colour.	All legs have reduced pale marks. It can be distinguished from other members of the *An. marshallii s.s.* group by its dark hind tarsi.	The sixth pale fringe spot is often absent.
An. hughi*	The apical dark band and the nearby pale bands are roughly the same width.	Same as *An. marshallii s.s.*	The hind tarsi have more noticeable pale bands than in *An. marshallii s.s.* or *An. letabensis.*	Same as *An. marshallii s.s.*
An. kosiensis*	Closely resembles *An. hughi* but there are distinct differences in the size of palp spots.	Same as *An. hughi*	There is banding on the hind tarsomeres and pale scaling on the fore and mid-legs.	There is noticeable variation in the size of some of the spots on the costa.
An. letabensis*	The apical dark band is very narrow, much less than the width of pale bands.	Same as *An. marshallii s.s.*	Pale bands on tarsi rather more prominent than in *An. marshallii s.s.*	Same as *An. marshallii s.s.*
An. mortiauxi	Same as *An. marshallii s.s.*	Heavily covered in yellowish scales that are pointy and curved, and they are moderately broad.	There is a tiny subapical pale spot on the posterior surface of the mid-femur. Every tibia has small apical spots.	Darker than those of *An. marshallii s.s.* The pale areas tend to be generally reduced.
An. mousinhoi*	Apical and subapical pale bands both broad.	Same as in *An. marshallii s.s.*	Tarsus 1-4 have pronounced apical pale bands on all legs.	Same as *An. marshallii s.s.*
An. njombiensis	Same as *An. harperi.*	With very broad white scales.	Palps have a pale subapical band that is as long as the apical band.	Same as *An. harperi.*

An. seydeli *	Has three pale bands. The subapical and apical bands are about the same width. The apical dark band is narrower than the pale bands.	It is covered with scattered, narrow, curved whitish scales and some yellowish hairs. The anterior promontory has a well-developed white tuft.	The hind legs' segment 1 has a long pale apical band, segments 2 and 4 have broad pale apical and basal bands, segment 5 is completely white.	The wing has creamy pale scales. The base of the costa has two visible interruptions. The fringe features clearly defined pale spots located opposite each vein.
An. upemba	The 5th segment is taken up by a subapical pale band that is twice as wide as the apical band.	Scutal integument are dark throughout. Scutal scales much smaller. Those on the posterior two-thirds of the median area are dark golden brown.	No information	No information

(Gillies and De Meillon, 1968; Gillies and Coetzee, 1987).

No information = Mosquito feature has been studied, but no data was recorded.

Unknown = The mosquito feature has yet to be looked into.

***** *Anopheles marshallii* group species found in South Africa.

1.7 *ANOPHELES MACULIPALPIS* SPECIES

Another species of interest from KwaZulu-Natal that was investigated in this study is *Anopheles maculipalpis*. Even though the prevalence of *An. maculipalpis* in South Africa is relatively low compared to that of other mosquito species, with only 20 adults collected during the 2022 surveillance period (Dahan-Moss *et al*., 2022), this species was assessed for the possible risk of parasite transmission because a number of *Anopheles* species play a secondary role in the spread of malaria. It is likely that *An. maculipalpis* is a malaria vector as it has previously been reported that this species is capable of carrying malaria parasites (Ingram and De Meillon, 1927; Vaucel and Campourcy, 1943; Nyirakanani *et al.,* 2017). According to De Meillon (1951), MacGregor (1924) was able to successfully infect *P. vivax* in the adult *An. maculipalpis* specimens in a lab setting in Mauritius. In Cameroon, Vaucel and Campourcy (1943) discovered an 8% sporozoite rate out of 206 *An. maculipalpis* adults that were dissected. Although its lower prevalence and uncommon association with malaria cases demonstrate it is not a major vector, changes in environmental conditions or mosquito population structure may increase its role as a vector in the future. *Anopheles maculipalpis* was examined alongside the *An. marshallii* group due to their shared ecological niches, which can sometimes lead to misidentification in field research. This study aimed to increase the precision of species-specific identification and to better understand the potential vector, especially in areas where malaria transmission is endemic and both species coexist.

1.7.1 Biology and Distribution

Anopheles maculipalpis is a generally scarce savanna species found across tropical Africa, from Senegal to southern Sudan, Madagascar, South Africa, Mauritius and Zambia. These are occasionally seen resting at night in animal shelters, feeding on domestic animals or biting humans outdoors. Although this species is primarily caught outdoors, it has also been found resting indoors. (Reid and Woods, 1957; Gilles and De Meillon, 1968). It was discovered that this species was comparatively more zoophilic than other species in Katanga, Congo (Gilles and De Meillon, 1968). The larvae inhabit a wide range of water types, including ponds and wetlands between rice fields and reeds (Gilles and De Meillon, 1968).

1.7.2 Morphological Description

Anopheles maculipalpis is characterised by the following traits: the femora, tibiae, and first tarsal segment of all legs are speckled; the spots often merge to form long white patches; and the hind tarsomeres 4 and 5 are completely pale (Gilles and De Meillon, 1968; Coetzee, 2020). The palps have three pale bands, with segments 3 and 4 speckled to some extent. The proximal pale band is narrow at the intersection of segments 2-3. The subcostal pale spot on the first wing vein is often completely absent, whereas the apical half of vein 6 is dark, and the base of the upper branch of vein 5 is pale, vein 1 has two accessory sector pale spots. The mesonotum is primarily covered in wide, flat white scales (Gilles and De Meillon, 1968).

Although there is no evidence showing that *An. maculipalpis* belongs to a species complex, the iso-female line approach was still necessary to ensure accurate tracking of genetic traits from the mother to her offspring. This method reduces genetic variability within each line, providing a clearer view of how specific traits are inherited and expressed. Keeping the mother and her F_1 progeny as individuals can be beneficial if future research reveals unexpected genetic diversity. Molecular analysis was performed to confirm species identity and to detect sporozoite infection.

1.8 STUDY RATIONALE

Anopheles arabiensis, Anopheles coluzzii, Anopheles funestus and *Anopheles gambiae,* are four major species that are recognised as significant malaria vectors since they account for more than 95% of the continent's overall malaria transmission (Mouchet *et al*., 2004). The remainder is transmitted by "secondary" or "vectors of local interest," which have a significant impact locally since they can prolong or increase the duration of malaria transmission (Mouchet *et al*., 2004; Antonio-Nkondjio *et al.*, 2006; Afrane *et al*., 2016). It is crucial to understand the role of secondary malaria vectors in the transmission of the parasite. Primary vectors are typically easy to identify since they are abundant, frequently feed on humans, and have quantifiable sporozoite rates. It is more challenging to incriminate secondary vectors because these species may be rare and have low sporozoite rates (Oaks *et al*., 1991). However, secondary vectors may be seasonally abundant and, at times, play a vital role in malaria transmission. Despite the extensive research on malaria in Africa, very little is known about secondary vectors and how they contribute to malaria transmission.

Understanding the role of secondary vectors is crucial for current malaria control and elimination strategies. Recent research indicates that these vectors can maintain residual transmission due to their varied behaviours, including exophilic (resting outdoors), zoophilic (feeding on animals), and nocturnal activity patterns, which enable them to evade traditional indoor-focused interventions like IRS and ITNs (Afrane *et al.,* 2016; Katusi *et al.,* 2022). For instance, in Tanzania, Katusi *et al.* (2022) discovered that secondary vectors such as *Anopheles coustani* and *An. pharoensis* displayed seasonal population fluctuations and different host preferences, suggesting they can sustain transmission when primary vectors decline. Likewise, Mustapha *et al.* (2021) reported unexpectedly high densities and Plasmodium infection rates in secondary and novel *Anopheles* species in western Kenya, reinforcing the idea that these vectors can be highly competent and abundant, even in regions with intensive vector control measures. These findings highlight the risk of underestimating transmission potential by neglecting secondary vectors, which can lead to ineffective control strategies. As primary vector populations decline, secondary vectors may occupy the ecological niche and sustain transmission, potentially jeopardising progress towards malaria elimination.

Due to the number of vector species and their role in malaria transmission in many areas, it is essential to plan and implement a vector control program that requires quick and reliable identification, along with data on the composition and abundance of vector species (Mishra *et al*., 2020; Loonen *et al.,* 2020). It is evident that there is a significant gap in knowledge regarding the *An. marshallii* group and *An. maculipalpis* species, even though species in the group have been implicated as malaria vectors. Developing efficient malaria control methods requires a deeper understanding of the ecology, traits, and description of *An. maculipalpis* and members of the *An. marshallii* group.

There is a current drive to provide and obtain DNA barcode sequence information on anophelines to aid in the rapid and easy identification of mosquitoes. However, the data will be of limited value without proper morphological information linked to the sequencing information. This was clearly seen when Jones *et al*. (2021) identified a number of "unknown species." One of these was identified as "*An. species 6*". This species was only recently confirmed to be a member of the *An. marshallii* group, *An. gibbinsi* (Gebhardt *et al.,* 2022). The importance of DNA sequencing should not be disregarded as it provides valuable insight into the genetic diversity of species and their relationship to other species.

1.9 STUDY AIM AND OBJECTIVES

The primary aim of this study is to use *a priori* iso-female lines to generate a DNA barcode database for the *An. marshallii* group and other anopheline species (e.g., *An. maculipalpis*) collected from South Africa.

Objective 1: Employ morphological identification techniques to identify *Anopheles marshallii* group and other locally understudied anopheline species including *An. maculipalpis* from South Africa.

Objective 2: Generate preliminary DNA barcode data using *ITS2* and *COI* sequences to aid in identifying collected *Anopheles* species and contribute to developing a reference database for understudied taxa.

Objective 3: To employ phylogenetic analysis to study the evolutionary relationship and for phylogenetic comparison between anophelines collected across SA regions.

CHAPTER TWO

MATERIALS & METHODS

This chapter provides an outline of the research methods that were used in this study. As shown in **(Figure 2.1)**, it begins with collecting mosquito samples and then describes the specific research methods and the employed data analysis methods.

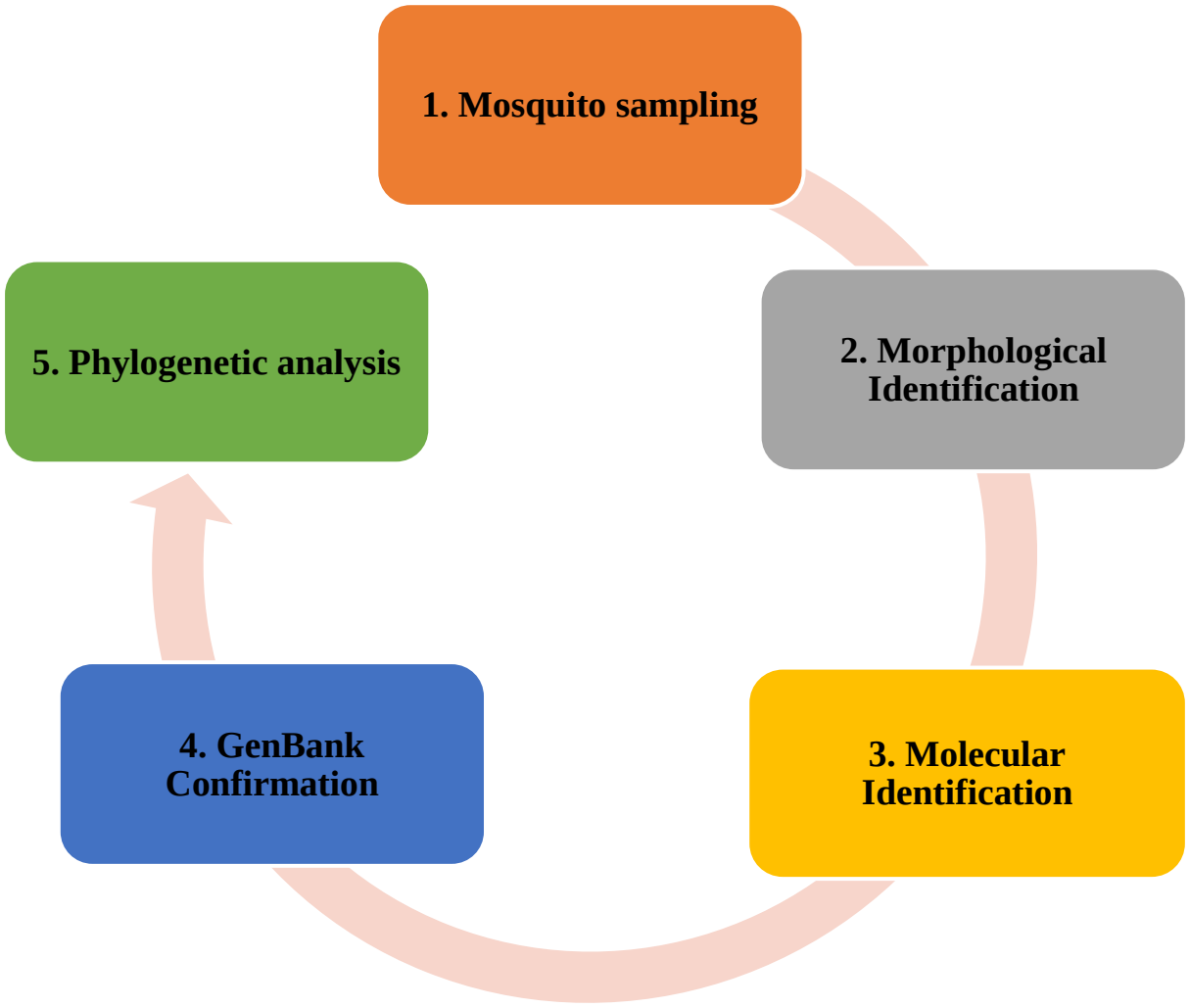


Figure 2.1 - Outline of Chapter 2 to achieve objectives listed in Chapter 1.

2.1 COLLECTION OF BIOLOGICAL MATERIAL USED AND *A PRIORI* IDENTIFICATION

2.1.1 Samples from Nigeria

A total of 59 *Anopheles hargreavesi* mosquito samples collected during a study in Nigeria were preserved in silica gel and sent to the Wits Research Institute for Malaria (WRIM) at the University of the Witwatersrand, Johannesburg, South Africa, for species confirmation. The study took place in the Ibekwe Akpayan community, Mkpat Enin Local Government Area (LGA), Akwa Ibom State. Akwa Ibom is located in the mangrove/tropical rainforest ecological zone of southern Nigeria (**Figure 2.2**). Mkpat Enin LGA is approximately situated at (5.25°N, 7.50°E), about 60 kilometres south of Uyo, the state capital.

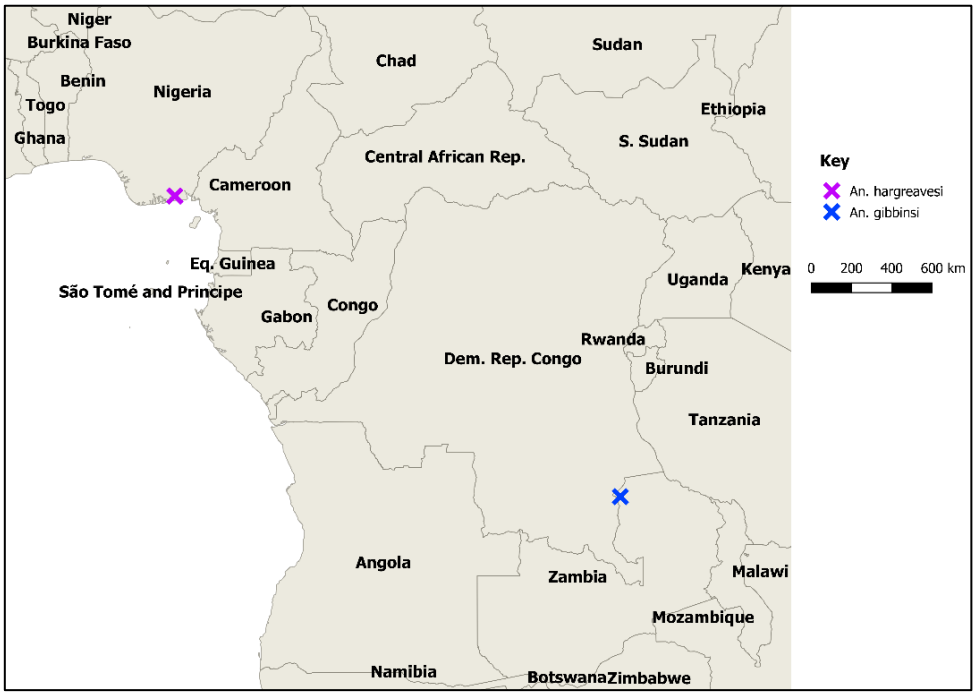


Figure 2.2 - Map showing sampling sites where *An. hargreavesi* and *An. gibbinsi* specimens were collected in Nigeria and Zambia (QGIS Geographic Information System http://www.qgis.org).

2.1.2 Samples from Zambia

A study was conducted in Nchelenge District, Luapula Province, northern Zambia (**Figure 2.2**), to understand the significance of *Anopheles gibbinsi* as an understudied species, including determining its genetic identity and role in transmission. (Gebhardt *et al*., 2022). Seventeen samples, morphologically identified as *Anopheles gibbinsi*, were sent to the Wits

Research Institute for Malaria (WRIM) in partnership with the International Centers of Excellence for Malaria Research (ICEMR) to confirm their identity. Nchelenge District is situated alongside Lake Mweru and features several streams and rivers that persist during the dry season, leading to numerous marshy habitats conducive to mosquito breeding.

2.1.3 Samples from South Africa

A total of 112 wild-caught *Anopheles* mosquitoes identified as *An. marshallii* group were collected from the uMkhanyakude District of KwaZulu-Natal (KZN) province, South Africa, between January and August 2022 (**Figure 2.3**). The samples that were subsequently used in this study were collected from three sections of the Mamfene locality: Section 7 (S27°39'14.2", E032°22'49.8"), Section 8 (S27°27'34.3", E032°10'43.7") and Section 9 (S27°23'50.5", E032° 12'20.1"). The specimens were successfully collected by the entomology team of Jozini local municipality in the KZN province. Most of the houses in the study area are constructed out of brick and mud with corrugated or thatched roofs and no ceilings. Domesticated pets and livestock are kept in the area. Host-seeking females were collected outdoors using carbon dioxide (CO_2) bait net traps between 6:00 PM and 11:00 PM over five consecutive nights for each collection period. Live adult *Anopheles* mosquitos were retrieved from the carbon dioxide-baited traps by mouth aspiration.

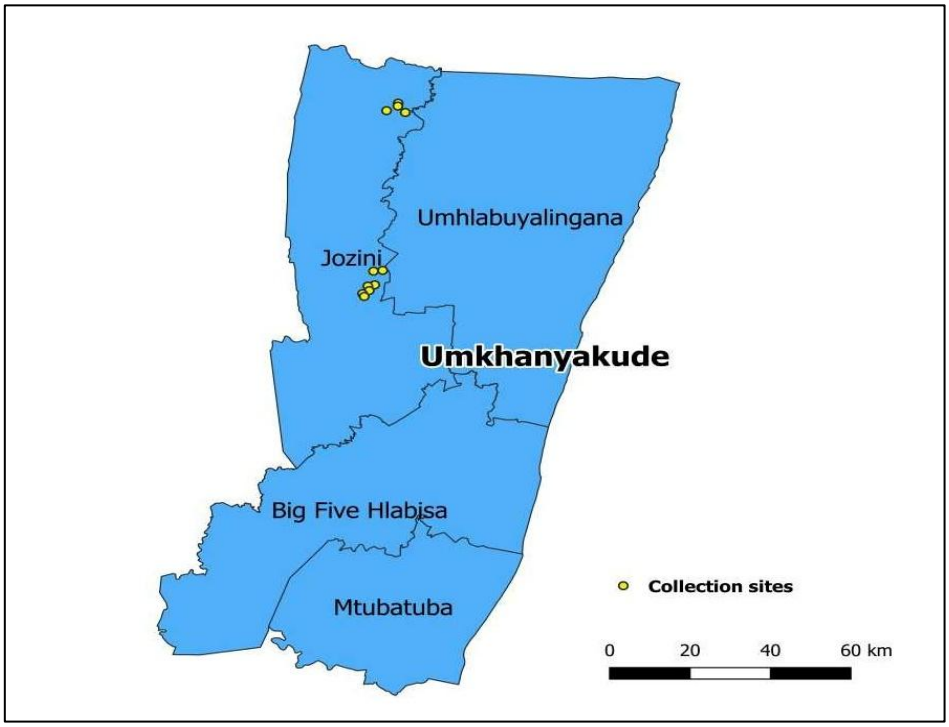


Figure 2.3 - Map of the uMkhanyakude district showing locations of sampling sites where specimens were collected in KZN (QGIS Geographic Information System http://www.qgis.org).

Wild-caught female mosquitoes were maintained in 250 ml polystyrene cups (sand-papered prior to use), and sugar pads soaked in 10% sugar water were placed on each cup for the mosquitoes to feed on to prevent them from dying during transport back to the Vector Control Reference Laboratory (VCRL) and the Wits Research Institute for Malaria (WRIM) insectary - Johannesburg, South Africa.

2.2 MOSQUITO REARING

The collected mosquitoes were housed at the Botha de Meillon insectary at the NICD and the Maureen Coetzee insectary located at the WRIM institution. They were maintained under standard insectary conditions, which included a temperature of 25°C ± 2°C, 85% relative humidity and a photoperiod of 12:12 hours light/darkness. Due to logistical issues, the project was officially transferred from NICD to WRIM in October 2022. The transition between the two labs was seamless, as the WRIM lab provided the necessary resources and expertise to continue working effectively. There were no changes in the environmental conditions, rearing protocols, or sample handling procedures at both facilities, ensuring consistent mosquito treatment across the two locations. The integrity of the research was not jeopardised, and the research objectives were met with guidance from the supervisors. Morphological identification of wild-caught, blood-fed female mosquitoes was performed on live adults using the appropriate taxonomic keys (Gillies and De Meillon, 1968; Gillies and Coetzee, 1987; Coetzee, 2020). The Olympus SZ61 microscope was used to identify the distinguishing characters such as the wings, palps and hind legs. After morphological identification, a subset of live, wild-caught female samples required for this research were separated from those used for entomological surveillance at NICD. Once in the insectary, the live females were transferred from polystyrene cups to glass vials containing damp filter paper to allow the mosquito to lay eggs (Hunt and Coetzee, 1989; Choi *et al.*, 2014) (**Figure 2.4 A and B**). These glass vials were stored in an insectary room with controlled temperature and humidity, maintained by standard air conditioning and humidity control systems. This environment ensured the physiological comfort of the females.

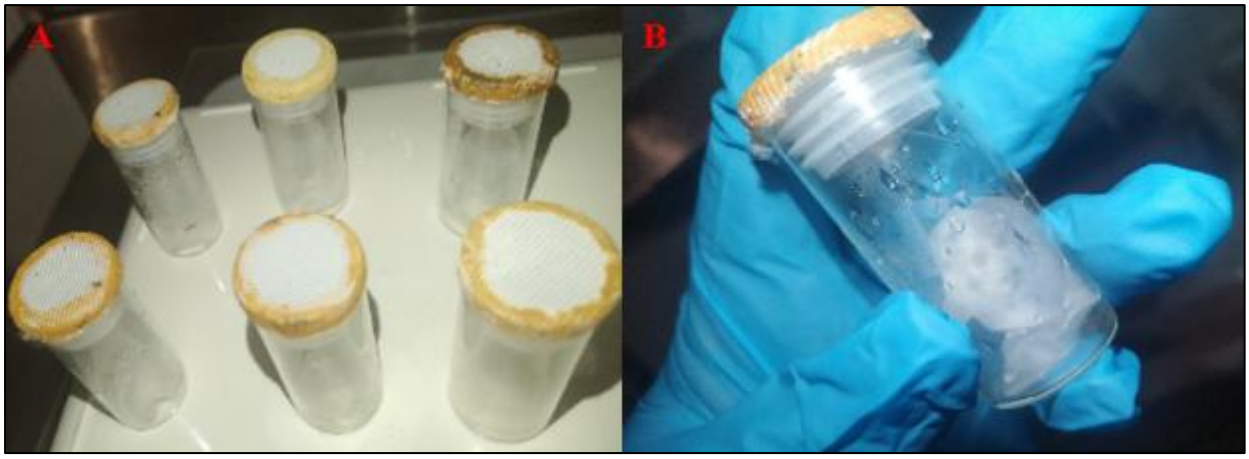


Figure 2.4 - Glass vials containing damp filter paper with wild-caught female mosquitoes for egg-laying (A). An egg-laying vial containing a wild-caught female mosquito (B). Each family was reared separately.

Egg batches were collected on filter paper and examined under a microscope. Their images were captured using Olympus Stream Basic version 1.9.3 software and morphologically identified. Egg batches were then transferred to 250 ml plastic bowls (diameter = 12 cm, height = 7 cm) partially filled with about 100 ml of distilled water to induce larvae hatching (**Figure 2.5**). In most cases, larvae hatched after 2-3 days, but for those that did not hatch, the small larval bowls were placed in a larger bowl with warm water (36-40°C) for about 20-30 minutes to assist in egg hatching. Emerging larvae were fed a fine mixture of brewer's yeast (Vital Health Foods, South Africa) and ground dog biscuits (West's Beeno Traditional Crunchy Biscuit Treats, Martin and Martin, South Africa) prepared at a ratio of 3:1. The dog biscuits contain approximately 16% protein, crude fat (2.5%) and other essential vitamins and minerals (Zengenene *et al*., 2021). In instances where larvae were overfed or bacterial growth was seen to be accumulating on the water's surface, larvae were transferred to fresh, clean water.

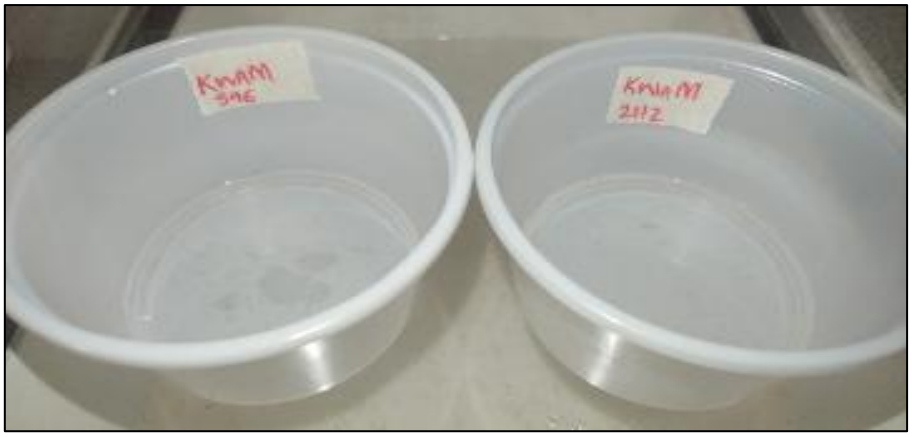


Figure 2.5 - Plastic bowls partially filled with distilled water used for larval hatching. Each iso-female family had a unique number, and bowls were marked accordingly.

Fourth instar larval skins were collected immediately after pupation and stored in micro-centrifuge tubes with 80% ethanol to preserve them. Pupae were transferred to a small bowl (diameter = 12 cm, height = 7 cm) and placed into a 17.5cm (L) x 17.5cm (W) x 17.5cm (H) Bug-Dorm-1 meshed cage (MegaView Science Co., Ltd. Taiwan) for adults to emerge (**Figure 2.6**).



Figure 2.6: Bug-dorm cage with the placement of sugar water on top, labelled with a unique number to identify each iso-female family.

Pupal pelts were collected every 24 hours after the adult emergence and kept in 80% ethanol for future use. Adult mosquitoes were fed on cotton pads moistened with a 10% sucrose solution to keep them alive. After being maintained alive for just 48 hours, the adults were

put in a freezer at -70°C for 4 hours to freeze to death. The first generation of offspring (F_1) from each mosquito family was preserved in silica tubes for further morphological and molecular identification. The mother and four F_1 offspring (two males and two females) from each family were carefully pinned and labelled with their correlating data. The adults were glued to triangles cut from stiff paper and held on insect pins **(Figure 2.7**). DNA was extracted from the rest of the adults and stored for subsequent molecular assays.

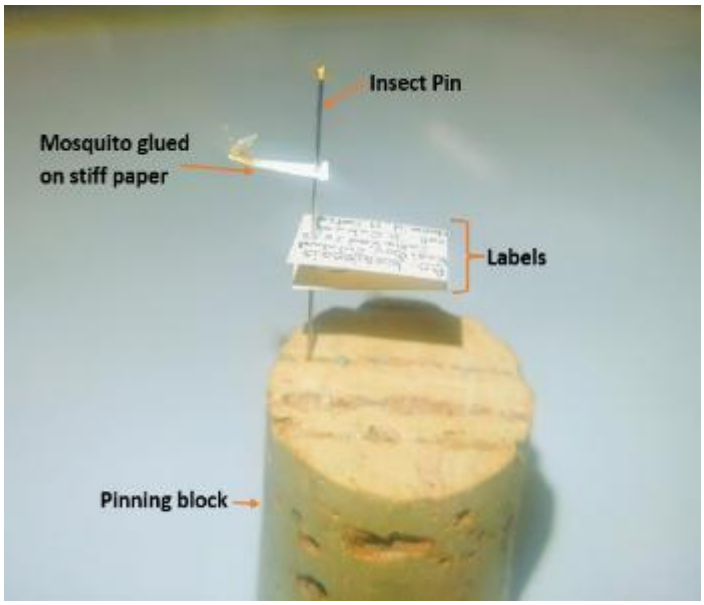


Figure 2.7: Illustration of a pinned *Anopheles* adult.

2.3 MOUNTING OF LARVAL AND PUPAL PELTS

The fourth instar larval and pupal pelts were transferred from 80% to 100% ethanol for 10-15 minutes to remove all traces of water and then transferred to xylene for 15-20 minutes (Merck cat. no. 108298). Thereafter, the pelts were mounted on microscope slides containing entellen (Merck cat. no. 107961) and then covered with coverslips (**Figure 2.8**). The clypeal plate is one of the crucial anatomical structures in mosquito larvae that contains specialised features used for larval morphology (Gillies and Coetzee, 1987). However, it is not the only feature used for species identification. Other key morphological structures, such as the antennae, head setae, mouth brushes, and abdominal setae, are also considered when examining anopheline larvae (Gillies and De Meillon, 1968; Harbach, 2004). The mounted slides and the pinned adults were viewed under an Olympus SZ61 microscope, and the images were captured using DinoCapture 2.0 software for morphological identification.

About 2-3 slides from each family were labelled with their species name, locality, collector, date and unique code identifying the family (Koekemoer, 1999). The data on the slides correlated with the data on the pinned adults. The slides and pinned adults are stored at the National Institute for Communicable Diseases (NICD) museum.

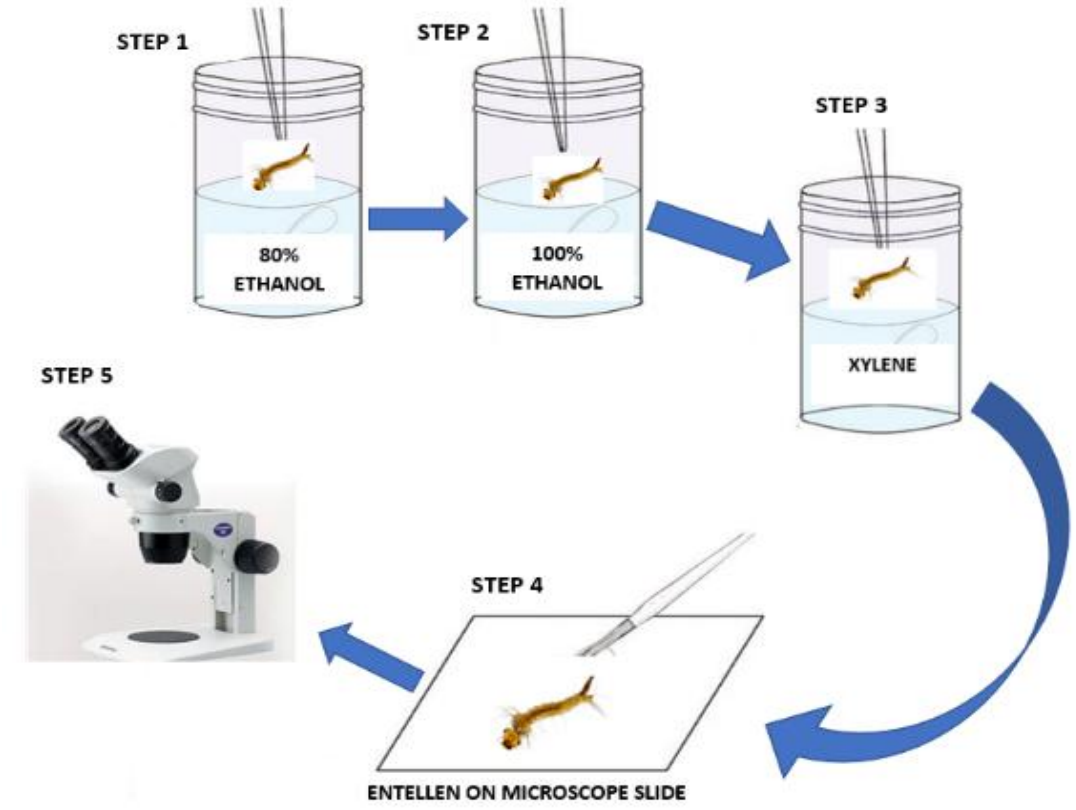


Figure 2.8: Diagram illustrating slide mounting steps.

2.3.1 Morphology Data Analysis

The external morphology of the different developmental stages was assessed using various diagnostic characteristics.

1. **Egg stage**

The external morphology of the eggs was examined by examining the shape and size of the eggs with special attention to distinctive features such as floats and ridges.

2. **Larval stage**

The larval pelts were examined for differences in the clypeal patterns, clypeal hairs, and abdominal and accessory plates. The keys in Gillies and Coetzee (1987) were used to aid identification.

3. Adult stage

Leg morphology: The hind legs were examined for pale bands on the joints of the tarsomeres, while the complete leg was observed for any diagnostic characteristics.

Palp morphology: The length and width of the palp spots (apical dark band, apical pale band, and subapical pale band) on each female mosquito were measured using DinoCapture 2.0 software.

Wing morphology: The wing length was measured from the base (where it attaches to the mosquito's body) to the tip**.** The sub-coastal pale spot, pre-apical dark spot, and sub-apical dark spot were measured to determine the wing spot ratio.

The wing spot ratio was calculated as follows:

$$\frac{\text{Length of costa spot 3 + Length of costa spot 5}}{\text{Length of costa spot 4}}$$

These morphological traits have historically played a crucial role in both field and laboratory identifications, particularly in situations where molecular methods are not readily available. Specific egg features, such as shape, the structure of floats, and the arrangement of ridges, are unique to each species and have proven valuable for differentiating among members of various species complexes. Larval clypeal patterns, the arrangement of setae, and the structure of abdominal plates are crucial for distinguishing closely related species, as these features are consistent and well-documented in regional taxonomic keys (Gillies and Coetzee, 1987). In adult specimens, leg banding patterns, wing spot ratios, and the size and position of pale and dark spots on the palps are commonly used to differentiate morphologically similar species.

One-way analysis of variance (ANOVA) was used to assess variation in morphological characters (leg, palp and wing) within and between members of each family. All statistical analysis was done using GraphPad Prism 10.

2.4 MOLECULAR ANALYSIS

2.4.1 Species Identification

Specific members of the *An. marshallii* group, but not all, have previously been misidentified using the *An. funestus* multiplex PCR assay as *An. leesoni*, a zoophilic member of the *An. funestus* group (Koekemoer, *pers comm).* This is most likely due to some degree of cross-reactivity of the *An. funestus* group PCR primers with the DNA of specific *An. marshallii* group species. With this in mind, the *An. funestus* group multiplex PCR assay (Koekemoer *et al*., 2002) was performed as one of the steps to determine if this cross-hybridisation is consistent within the *An. marshallii* group.

2.4.2 DNA Extraction

Using the prepGEM Insect DNA extraction kit (ZyGEM™, cat. no. PUN1000) (Dahan-Moss *et al.,* 2020), genomic DNA was extracted from a leg or wing of individual F_1 mosquitoes of the *An. marshallii* group following the manufacturer's instructions, with a minor modification in that the reagent volumes were only used at a quarter of the recommended volumes for each DNA extraction. This modification was implemented to conserve reagents and to accommodate the small sample size, specifically individual mosquito legs or wings. This did not compromise DNA quality and has been previously validated in other studies (Erlank *et al.*, 2018; Dahan-Moss *et al.*, 2020). The components of each 10 µl mastermix were prepGEM enzyme, 10x extraction buffer and distilled water **(Appendix 2A)**. After that, each leg or wing was submerged in the extraction mixture and heated to 75 °C for 15 minutes followed by 95 °C for 5 minutes in a thermocycler (Bio-Rad T100). The extracted DNA was either processed immediately or stored at -20 °C.

2.4.3 *Anopheles funestus* PCR

Specimens identified using morphological keys belonging to the *Anopheles marshallii* group were subjected to a species-specific *An. funestus* multiplex PCR to confirm how many of the samples produced *An. leesoni* (member of the *An. funestus* group) fragments (Koekemoer *et al*., 2002; Cohuet *et al*., 2003). This assay was performed using *An. funestus* species-specific primers and a universal forward primer **(Table 2.1).** The species specificity of this assay is

mainly attributed to the reverse primer, which is designed to target a region unique to *An. funestus* species.

DNA was extracted from a single mosquito leg or wing from the insectary-reared FUMOZ colony (as per section 2.4.2) and was used as a positive control in the PCR. A negative control consisting of DNA extraction with 1 µl deionised water (DNA extraction negative control) was used to detect possible contamination during the extraction stage. A PCR buffer with no DNA template was used as a no-template control for PCR. The PCR mixture consisted of 10x buffer (500 mM KCl, 100 mM Tris-HCl pH 8.3), 1.5 mM $MgCl_2$, 200 µM of each dNTP, 8.25 pmol of each primer, and two units of the thermostable Taq DNA polymerase (Koekemoer *et al.*, 2002). The volume of each PCR component was multiplied by the total number of samples and controls and added to a microcentrifuge tube. The tube containing the PCR master mix was then vortexed briefly and centrifuged at 10 000 rpm for 10 seconds. Aliquots of 12 µl were then prepared and placed into labelled PCR tubes along with 0.5 µl of the sample DNA template to make a total volume of 12.5 µl (**Appendix 2B**).

Table 2.1: Species-specific primer sequences to identify members of the *An. funestus* group (Koekemoer *et al.*, 2002; Cohuet *et al.*, 2003).

Primer Name	Sequence (5' - 3')	Amplicon sizes to identify *An. funestus* group species (bp)	Tm (°C)
Universal	TGT GAA CTG CAG GAC ACA T	-	55.3
Fun	GCA TCG ATG GGT TAA TCA TG	505	52.4
Van	TGT CGA CTT GGT AGC CGA AC	587	58.0
Riv	CAA GCC GTT CGA CCC TGA TT	411	58.8
Riv-like	CCG CCT CCC GTG GAG TGG GGG	313	60.7
Par	TGC GGT CCC AAG CTA GGT TC	252	60.5
Lees	TAC ACG GGC GCC ATG TAG TT	146	60.2

The PCR tubes were then placed in the thermal cyclers (Bio-Rad T100, Bio-Rad C1000), which were programmed according to the following cycling conditions: One cycle of 94℃ for 2 minutes and 30 cycles of the following conditions: 94℃ for 30 seconds, 45℃ for 30 seconds, 72℃ for 40 seconds and one cycle of 72℃ for 5 minutes. The PCR products were electrophoresed on a 2.5% agarose gel that contained 1X Tris-acetate-ethylene diamine tetraacetic acid (TAE) buffer (**Appendix 2C**) and stained with 12 µl ethidium bromide (0.5 g/ml) (Lot no. MKCL8014, Sigma-Aldrich, South Africa). A Gel-doc system (Syngene-Gensys) was used to view the gels, and the amplicon sizes were then compared to the relevant molecular weight markers. The specimens that yielded no amplicons were labelled (Species A), and the specimens that had an amplicon corresponding to the size of *An. leesoni* (146 bp) were labelled (Species B), and the specimens with multiple bands were labelled (Species C).

2.4.4 *Plasmodium* detection using the Hydrolysis probe assay

The four *Plasmodium* species (*P. falciparum, P. vivax, P. ovale* and *P. malariae*) that cause malaria in humans can successfully be detected by the hydrolysis probe (TaqMan) assay, which also distinguishes the most dangerous species, *P. falciparum,* from the others (Bass *et al*., 2008). This assay uses two species-specific probes to detect the presence of a specific *Plasmodium* genome. The *P. falciparum* is detected by the first probe labelled with FAM, and the second probe labelled with VIC detects the presence of *P. vivax, P. ovale* or *P. malariae.* These probes are designed to differentiate between *P. falciparum* and non-*falciparum* species by utilizing specific fluorescence signals in conjunction with the unique binding characteristics of the probes to targeted DNA sequences. The excitation (absorption) of VIC is 530 nM and its fluorescence is at 555 nM, whereas the excitation and fluorescence wavelengths of FAM are 470/510 nM, respectively (Bass *et al*., 2008). Extracted DNA is mixed with primers and probes unique to *Plasmodium* and the necessary PCR reagents. The probes are designed to bind to a target DNA sequence. When the fluorescently labelled probe hybridises with the target DNA during amplification, it releases a fluorescent signal. This signal is picked up during the PCR polymerisation step, when the DNA polymerase cleaves the probe, separating the fluorescent dye from the quencher. This results in an emitted fluorescent signal (Heid *et al.*, 1996; Ginzinger, 2002). A fluorescence detector monitors the fluorescence emitted during each PCR cycle. The increase in fluorescence over cycles indicates the accumulation of PCR products, and the point at which the fluorescence signal

crosses a certain threshold (known as the cycle threshold/Ct value) is used to determine the initial amount of target DNA in the sample.

I. DNA extraction

DNA was extracted from the head and thorax of single female mosquitoes using the HotShot extraction technique (**Appendix 2D**). In this method, samples were incubated for 30 minutes at 95°C in an alkaline lysis buffer (pH 12) containing 100 mM NaOH (Lot no. 30385, ACE, South Africa) and 50 mM Na_2EDTA (Lot no. 1052966, Sigma-Aldrich). After that, the samples were allowed to cool on ice for 3-4 minutes and then neutralised by a Tris-HCl buffer (40mM, pH 5) (Lot no. 3255466, EMD Millipore Corporation). The resulting DNA was kept in the freezer (-20 °C) until processing.

II. Real-time RT-PCR

A PCR mastermix containing primers, probe and other PCR components was prepared according to the number of reactions desired (**Appendix 2E**). Aliquots of 18µl of the PCR mastermix and 2 µl of genomic DNA were added to a 96-well plate with one positive control (DNA extracted from cultured *P. falciparum* parasite stages) and one negative control (PCR master mix without DNA template) included. Reactions were run on a thermal cycler (CFX96 Real-time System, BioRad) using cycling conditions of 10 minutes at 95°C followed by 40 cycles of 95°C for 10 seconds and 60°C for 45 seconds. The VIC and FAM fluorescence increase was observed in real-time by acquiring each cycle on the yellow (530 nM excitation and 555 nM emission) and green channel (470 nM excitation and 510 emission) of the real-time machine, respectively (Bass *et al*., 2008). The cycle threshold (Ct) value indicates the specific PCR cycle number at which the fluorescence signal produced by the amplified DNA surpassed the predefined detection threshold. This threshold is crucial for determining the presence of target DNA sequences in a sample. The Ct value displays an inverse correlation with the quantity of parasitic DNA present - lower Ct values are indicative of higher concentrations of parasite DNA, while higher Ct values suggest lower parasite loads. For any samples that tested positive (Ct value <30, RFU value >500) in the initial run, the assay was carried out again to rule out false positives and validate the prior positive results. This additional step ensured the reliability and accuracy of the results.

Table 2.2: Primers and probes for Bassman PCR assay specific for *Plasmodium* detection.

Reagents		Sequence (5' - 3')
Primers	PlasFwd (10µM)	GCTTAGTTACGATTAATAGGAGTAGCTTG
	PlasRev (10µM)	GAAAATCTAAGAATTTCACCTCTGACA
Probes	PlasF-probe (10µM)	TCTGAATACGAATGTC
	OVM+probe (10µM)	CTGAATACAAATGCC

2.5 DNA AMPLIFICATION AND SEQUENCING OF THE *ITS2* AND *COI* REGIONS

2.5.1 DNA Extraction

The legs were removed using clean forceps, sterilised using 70% ethanol. Total DNA was extracted using the DNeasy Blood and Tissue kit (Lot no. 172045050, Qiagen) following the manufacturer's instructions **(Appendix 2F).** This kit was the preferred extraction method because it is known for its ability to yield high-quality DNA suitable for sequencing. The kit includes reagents used to effectively eliminate contaminants like proteins, salts, and inhibitors from the extracted DNA and ensure it is free of any elements that can impede further analysis. The isolated DNA was maintained at -20°C. This method was used to extract DNA from tissue samples, specifically for the *ITS2* and *COI* PCR. Only 2 µl of the extracted DNA was used for *ITS2* PCR, and 5 µl of DNA was used for *COI* PCR. To prevent contamination during the DNA extraction process, all procedures were conducted using stringent sterile techniques within a designated clean workspace. Filtered pipette tips, sterile tubes, and decontaminated surfaces were utilised throughout the procedure to avoid cross-contamination.

2.5.2 *Internal Transcribed Spacer 2 (ITS2)* PCR

The ribosomal DNA *Internal Transcribed Spacer Region 2* (rDNA *ITS2*) region of the *An. marshallii* group specimen was amplified using the *ITS2* PCR with *ITS2A* (5´ TGTGAACTGCAGGACACAT-3´) as the forward primer and *ITS2B* (5´-TATGCTTAAATTCAGGGGGT-3´) as the reverse primer (Koekemoer *et al*., 2002) (**Table 2.3**). These universal *ITS2* primers target conserved regions of ribosomal DNA and amplify the highly variable *ITS2* region, providing species-level resolution (Koekemoer *et al.,* 2002; Makunin *et al.,* 2022). Each PCR reaction contained 2.5 µl of 10× buffer, 200 µM of each dNTP, 0.5 units of Taq DNA polymerase, and 0.75 µl of 10 pmol/µl of forward and reverse primers (**Table 2.4**). Each volume of the PCR reagents was multiplied by the total number of samples to be analysed, including the positive control, the negative extraction control (NEC) and the PCR no template control (NTC). DNA extracted from an insectary-reared *An. funestus* mosquito (FUMOZ colony) was used as a positive control, whereas the negative control only consisted of the PCR mix without a DNA template. Aliquots of 23 µl of the PCR mastermix and 2 µl of the sample DNA template were added to labelled PCR tubes. The tubes were vortexed and centrifuged.

Table 2.3: *Internal Transcribed Spacer 2* Primer sequences (Koekemoer *et al*., 2002).

Primer Name	Sequence (5' - 3')	Annealing temperature (°C)	Product size (bp)
ITS2 A	TGTGAACTGCAGGACACAT	50	≈ 500
ITS2 B	TATGCTTAAATTCAGGGGGT		

Table 2.4: *Internal Transcribed Spacer 2* PCR protocol. The PCR mastermix for ***ITS2*** **PCR** was prepared using the below protocol:

Reagents	**1X reaction**	**Cat. Number and Supplier**
10x PCR buffer	2.5 µl	ALE2493A, Separations, South Africa
dNTPs (2.5 mM)	2.0 µl	AJ30387A, Separations, South Africa
MgCl2 (25 mM)	3.0 µl	ALE2495A, Separations, South Africa
Primers: *ITS2A* (10 µM)	0.5 µl	00312829-1, Inqaba Biotec
ITS2B (10 µM)	0.5 µl	00312829-2, Inqaba Biotec
Taq-polymerase (5U/µl)	0.2 µl	ALE2492A, Separations, South Africa
dH_2O	14.3 µl	–
DNA template	2 µl	_
Total:	**25 µl**	–

The PCR tubes were placed on the designated thermal cyclers (Bio-Rad T100, Bio-Rad C1000). The PCR machines were programmed according to the following cycling conditions: an initial denaturation of 94°C for 2 minutes, followed by 40 cycles of denaturation at 94°C for 30 seconds, annealing at 50°C for 30 seconds, an extension at 72°C for 40 seconds, and a final extension at 72°C for 10 minutes. The PCR tubes were removed from the PCR machines once the program had been completed. Only 10 µl of the PCR product was loaded on a 2.5% agarose gel and was electrophoresed and viewed as described in **section 2.4.2** above. The remaining PCR products (15 µl) was used for subsequent sequencing only after successful amplification was confirmed through agarose gel electrophoresis.

2.5.3 *Cytochrome C Oxidase Subunit I (COI)* PCR

The desired *COI* fragments were amplified using LCO1490 (5´GGATTTGGAAATTGATTAGT TCCT-3´) as the forward and HCO2198 (5´-AAAAATTTTAATTCCAGTTGGAACAGC -3´) as the reverse primers (Chan *et al.*, 2014) (**Table 2.5**). The total reaction mixture was 50 µl and comprised of: 10× PCR buffer, 1.5 mM of $MgCl_2$, 0.2 mM of the dNTP mixture, 1.5 U of DNA Taq polymerase plus 0.3 µM of each primer and 5 µl of DNA template (**Table 2.6**). Similar to the *ITS2* PCR, the positive control

for this assay was DNA acquired from an *An. funestus* mosquito, while the negative control was just the PCR mixture without a DNA template. After determining the number of necessary amplifications required, including the positive and negative controls, the PCR mastermix was prepared, mixed well and added into labelled individual PCR tubes. The PCR reaction conditions included an initial denaturation of 95°C for 5 minutes, followed by five cycles of denaturation at 94°C for 40 seconds, annealing at 45°C for 1 minute and extension at 72°C for 1 minute. This was followed by an additional 35 cycles of denaturation at 94°C for 40 seconds, annealing at 51°C for 1 minute and extension at 72°C for 1 minute, with a final extension at 72°C for 10 minutes. Amplified DNA was electrophoresed on a 2.5% agarose gel containing TAE and 12 µl ethidium bromide (0.5 g/ml) to verify product band size.

Table 2.5: *Cytochrome C Oxidase Subunit I* Primer sequences (Chan *et al.*, 2014).

Primer Name	**Sequence (5' - 3')**	**Annealing temperature (**°C**)**	**Product size (bp)**
***COI* Forward (LCO1490)**	GGATTTGGAAATTGATTAGTTCCT	51	≈ 900
***COI* Reverse (HCO2198)**	AAAAATTTTAATTCCAGTTGGAACAGC		

Table 2.6: *Cytochrome C Oxidase Subunit I* PCR protocol (Chan *et al.*, 2014).

Reagents	1x Reaction	Cat. Number and Supplier
10x PCR Buffer	5 µl	ALE2493A, Separations, South Africa
dNTPs (2.5 mM)	4 µl	AJ30387A, Separations, South Africa
$MgCl_2$ (25 mM)	3 µl	ALE2495A, Separations, South Africa
LCO1490 Primer (10 µM)	4.5 µl	220110-027-E6, Integrated DNA Technologies
HCO2198 Primer (10 µM)	4.5 µl	220110-027-E7, Integrated DNA Technologies
Taq-polymerase (5U/µl)	0.5 µl	ALE2492A, Separations, South Africa
dH_2O	23.5 µl	–
DNA template	5 µl	–
Total:	**50 µl**	–

2.5.4 Gel Purification

PCR products that produced more than one PCR amplicon were purified from a low melting point agarose gel (Lot. No. 0001122915, SeaKem® LE Agarose). The PCR products were loaded on a 1% low melting agarose gel containing TAE and stained with 12 µl ethidium bromide (0.5 g/ml). The gel was electrophoresed at a voltage of 60V for 2.5 hours. Thereafter, the gel was viewed on an open ultraviolet (UV) box in the Gel-doc system. The UV light illuminated all the ethidium bromide-stained, allowing for the desired DNA fragments to be excised from the agarose gel using gel cutters (Lot no. 3110, Sigma-Aldrich) and placed in a microcentrifuge tube.

The QIAquick Gel Extraction Kit protocol (Lot no. 172031860, Qiagen), which purifies up to 10µg DNA (70bp – 10kb), was used to perform gel extraction. The excised gel slices were placed on 1.5ml microcentrifuge tubes and weighed using Adam weighing balance (AE439L180, Adam Equipment,). Buffer QG (solubilisation and binding buffer) was added to the tubes, and thereafter, the tubes were incubated at 50°C for 10 minutes. Once the gel slice had dissolved, isopropanol was added to each tube. The sample was then transferred to a QIAquick spin column and centrifuged for 1 minute at 13 000 rpm. The samples were allowed to stand at room temperature (15–25°C) after an addition of 750 µl Buffer PE (wash

buffer) was added to each QIAquick spin column. The columns were centrifuged for 1 minute to remove residual wash buffer. The spin columns were then placed on a clean 1.5ml micro-centrifuge tube. The DNA was eluted using 50 µl elution buffer (**Figure 2.9**). After adding elution buffer, the spin columns were allowed to stand for 4 minutes to increase the yield of purified DNA. After that, the purified DNA was mixed with 6x TriTrack loading dye (Cat. no. 01122392, Thermo Scientific) and loaded on a 2.5% agarose gel that contained TAE and stained with 12 µl ethidium bromide (0.5 g/ml). PCR products that could be seen on the gel were then sent to Inqaba Biotec™ for sequencing for species confirmation. Sanger sequencing was performed to determine the sequence of nucleotide bases of a DNA molecule. Each DNA sample was sequenced separately in both directions using forward and reverse primers.

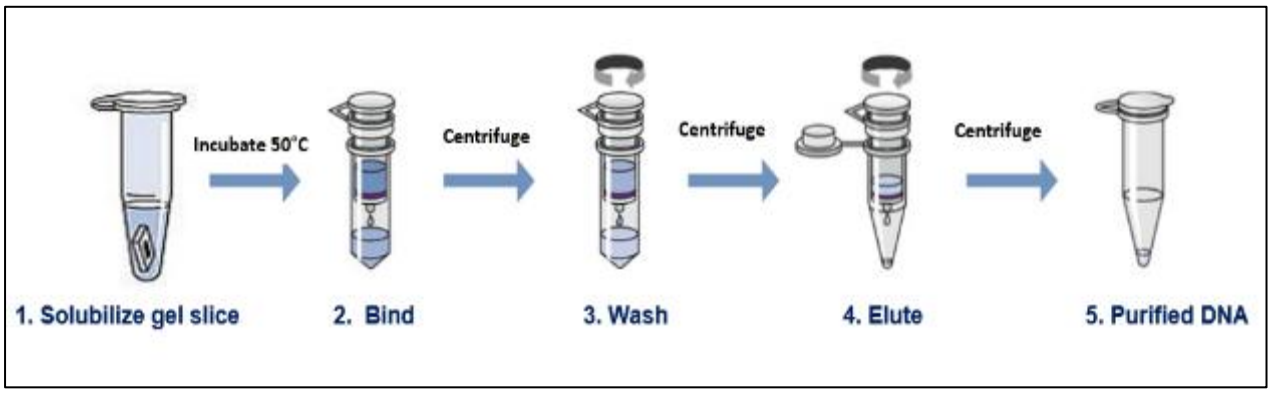


Figure 2.9: Laboratory procedure for gel extraction using the QIAquick Gel Extraction Kit. (Modified from QIAquick Gel Extraction Kit, QIAGEN®, South Africa).

2.5.5 Sequence Analysis

The BioEdit Sequence Alignment Editor (version 7.2.5) program was used to trim and manually edit nucleotide sequences (Hall, 1999). BioEdit was selected for its user-friendly interface and powerful features that facilitate visual inspection, manual editing, and alignment of nucleotide sequences, making it particularly well-suited for DNA barcoding and small-scale sequence analyses. Sequences of poor quality or unclear chromatograms were not included in the study. Individual mosquito forward and reverse primer sequences were aligned and assembled into a consensus (contig) sequences using the BioEdit and Emboss Needle pairwise sequence alignment tool (https://www.ebi.ac.uk/Tools/psa/emboss needle/). Comparison of the examined *ITS2* and *COI* sequences with previously established reference

sequences were retrieved using NCBI's Basic Local Alignment Search tool (BLAST) (http://www.ncbi.nlm.nih.gov/WebSub/index.cgi?tool=barcode). The BLASTn search was subsequently used to evaluate the complete sequences of the mosquitoes' *COI* and *ITS2* regions against a non-redundant nucleotide collection for species identification.

2.5.6 Phylogenetic Analysis

Phylogenetic analysis was used to determine the evolutionary relationships among the different species. The sequenced *ITS2* and *COI* regions were compared to reference sequences from GenBank and used for analysis and phylogenetic tree construction using Molecular Evolutionary Genetics Analysis (MEGA XI) software (Kumar *et al*., 2016). The Maximum Likelihood and Neighbor-Joining (NJ) techniques were used to create phylogenetic trees in Mega XI. The NJ method was chosen for its computational efficiency and reliability in generating phylogenies based on genetic distance data. It is especially effective for visualising evolutionary relationships when analysing *ITS2* and *COI* sequence data across closely related species. The Maximum Likelihood approach utilises evolutionary models to find the evolutionary trees that have the highest probability of explaining the sequence relationships (Felsenstein, 1981), while the Neighbor-Joining method constructs a tree using the matrix of genetic distances between the downloaded and analysed samples (Gascuel and Steel, 2006). Bootstrap support was computed for both trees using 1 000 replications**.**

CHAPTER THREE

RESULTS

3.1 IDENTIFICATION OF SAMPLES FROM NIGERIA: *ANOPHELES HARGREAVESI*

3.1.1 Morphological Identification

A total of 59 samples belonging to the *Anopheles marshallii* group were received from Nigeria as part of the PMI VectorLink project. Morphological identification conducted by E. Erlank classified these samples as *Anopheles hargreavesi* (a member of the *An. marshallii* group). Scale morphology was used to confirm the identity of several samples that were missing vital parts such as legs and wings. Morphologically, *An. hargreavesi* are distinguished by a mesonotum thickly and uniformly coated in truncated, broadish scales (**Figure 3.1**).

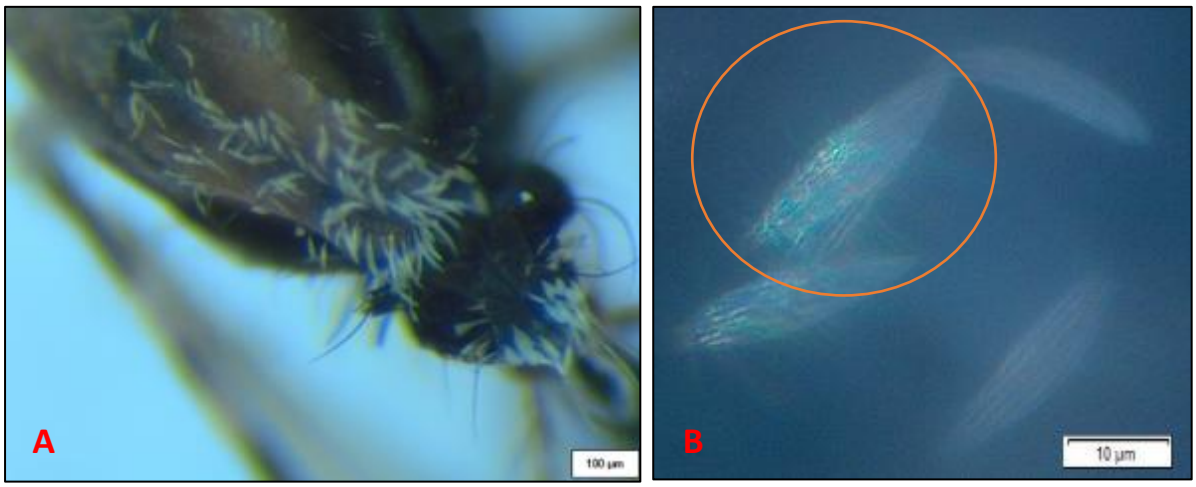


Figure 3.1: Scutal scale pattern of *Anopheles hargreavesi*. A: Arrangement of *An. hargreavesi* scutal scales on the mesonotum. **B:** Close-up view of *An. hargreavesi* scutal scales.

3.1.2 *Anopheles hargreavesi* Sequence Analysis

Five *An. hargreavesi* female adults from Nigeria were analysed by *ITS2* and *COI* PCR. The *ITS2* and *COI* sequences were amplified from these specimens to confirm species identity. After electrophoresis of the PCR products on a 2.5% agarose gel, double bands migrating at approximately ≈485 bp to ≈560 bp were visible on the *ITS2* PCR gel **(Figure 3.2A)**, whereas single bands migrating at approximately 900 bp were observed on the *COI* PCR gel **(Figure 3.2B).** The *ITS2* specimens that generated double fragments required gel purification in order

to isolate and sequence individual bands, ensuring precise characterisation of the amplified *ITS2* regions. The PCR products of these specimens were subsequently sequenced, and contiguous sequences of each specimen based on forward and reverse sequences were created. For the purpose of species identification, the *ITS2* and *COI* contigs were compared (BLASTn) to the NCBI database.

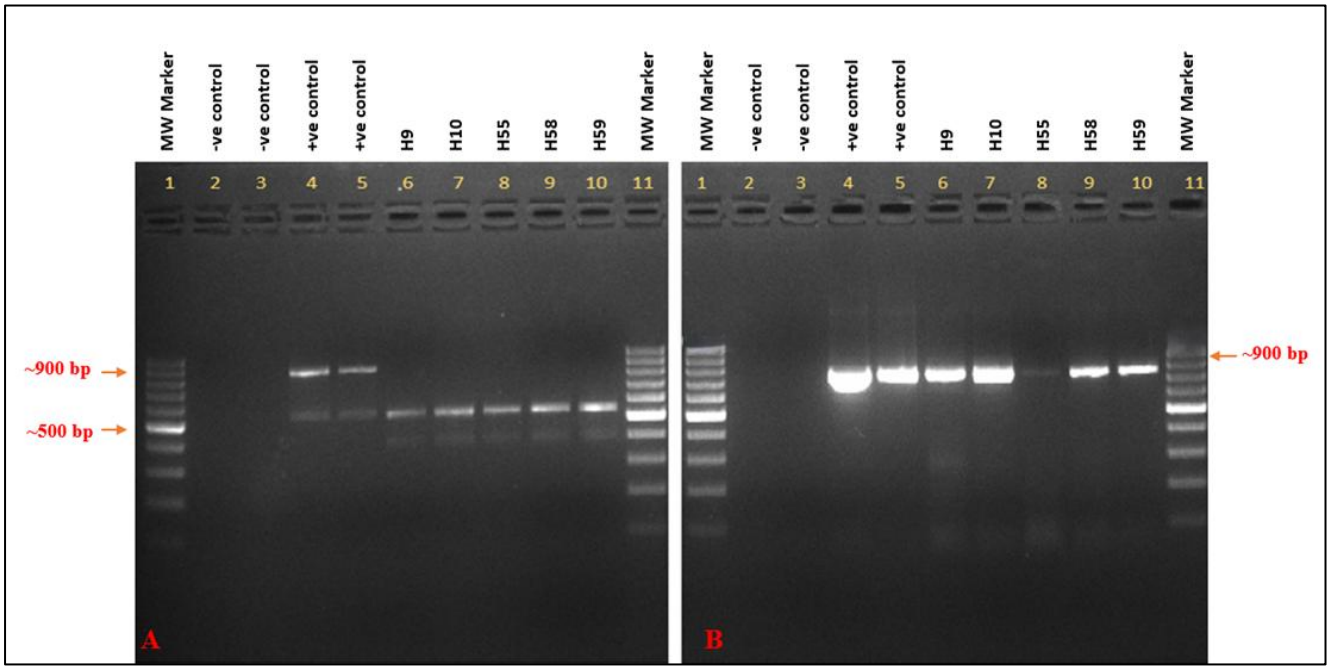


Figure 3.2: Amplification of *ITS2* and *COI* regions in *Anopheles hargreavesi* specimens using PCR, visualised on 2.5% agarose gels. A) *ITS2* PCR Amplification. Lanes 1 and 11: Molecular weight marker of 1000 bp. Lanes 2 and 3: PCR and DNA extraction negative controls. Lane 4 and 5: *An. funestus* positive controls (~900 bp). Lanes 6-10: *An. hargreavesi ITS2* amplicons, with band sizes ranging from ~485 bp to ~560 bp. **B) *COI* PCR Amplification.** Lanes 1 and 11: Molecular weight marker of 1000 bp. Lanes 2 and 3: PCR and DNA extraction negative controls. Lanes 4 and 5: *An. funestus* positive control (~900 bp). Lanes 6-10: *An. hargreavesi COI* amplicons (~900 bp). A faint band was observed in lane 5, likely due to low DNA concentration. Upon retesting this sample still failed to yield a bright visible amplicon.

Five *ITS2* rDNA sequences were obtained from these mosquitoes, whereas only four *COI* mtDNA sequences were obtained. The *ITS2* sequences showed a 81% sequence identity to *Anopheles marshallii* isolate MAR.2019CAM.ABDOMEN459 *ITS2* partial sequence in GenBank (Sequence ID: MW257138.1). The multiple sequence alignment for the *ITS2* sequences shows a high level of identity (>99% percentage identity) among all the *An. hargreavesi* samples **(Figure 3.3).**

The *COI* sequences revealed a 93% sequence identity to *Anopheles marshallii* mitochondrion, complete genome (Sequence ID: NC064607.1) based on 745 bp fragment.

The *COI* sequence alignment revealed variable residues in some sequences **(Figure 3.4).** The *COI* sequences were 98.29% identical to each other. Overall, both markers were effective but the *COI* region was more consistent across specimens, producing single, clean bands and high-quality sequence data, while *ITS2* required additional processing due to the double bands. However, *An. hargreavesi ITS2* and *COI* sequences could not be aligned with a previously published reference sequence from GenBank because up until now, no DNA sequence analyses have been reported for *An. hargreavesi*, and hence the sequence of the rDNA and mtDNA is unknown. As such, the *ITS2* and *COI* sequences obtained here represent the first published reference data for this species. These sequences were deposited to the NCBI GenBank as new sequences. **Appendix 3A** shows the BLAST search results and accession numbers obtained for the *An. hargreavesi* specimens.

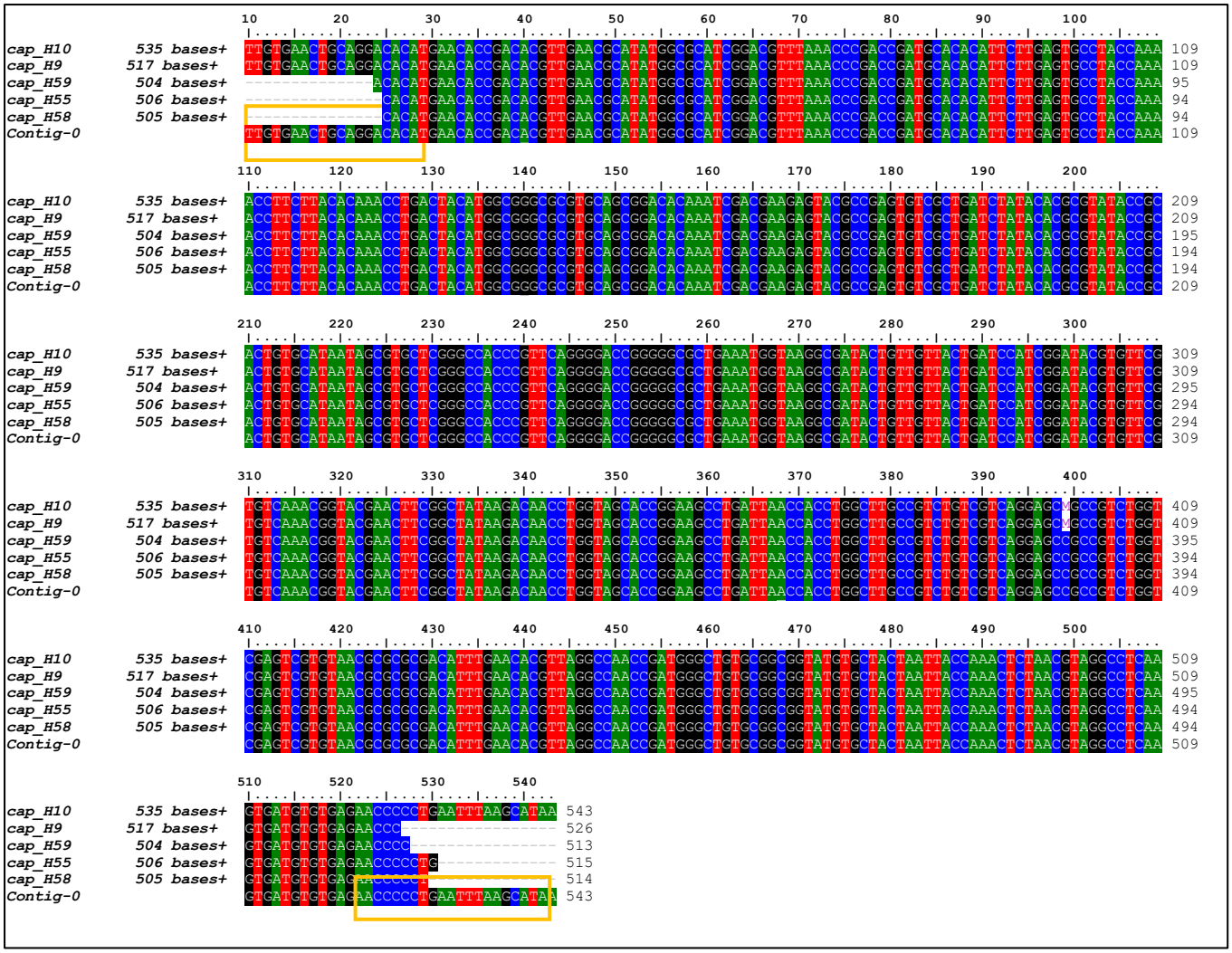


Figure 3.3: Multiple sequence alignment of the *ITS2* region from *Anopheles hargreavesi* specimens collected in Nigeria. Forward and reverse sequencing reads were assembled into contiguous sequences for five *An. hargreavesi* specimens. The alignment was generated using BioEdit, revealing a high level of conservation among the sequences. Sequences highlighted in yellow rectangular boxes indicate the locations of the *ITS2* forward and reverse primer binding sites employed during PCR amplification.

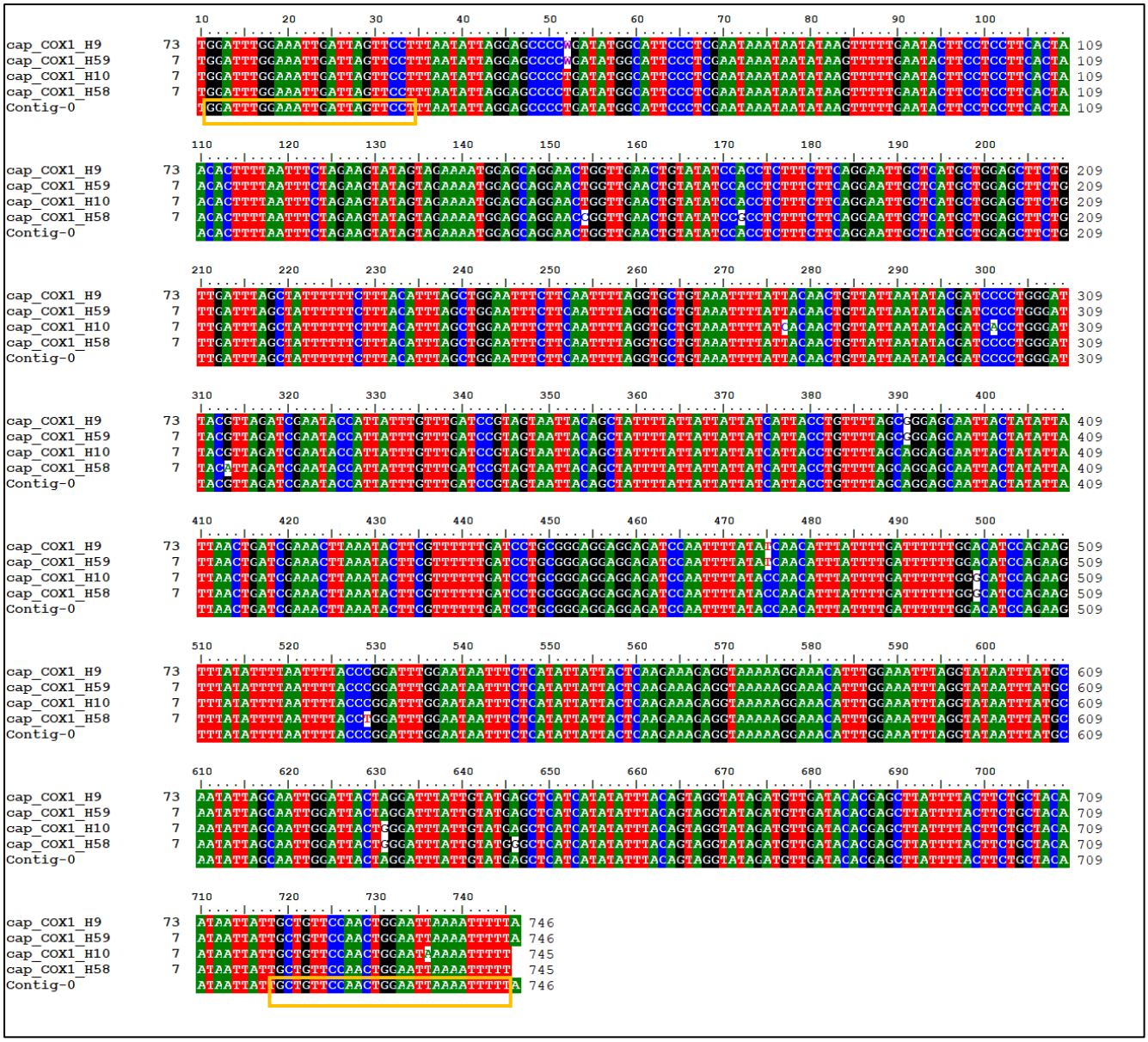


Figure 3.4: Multiple sequence alignment of the *COI* region from *Anopheles hargreavesi* specimens collected in Nigeria. Forward and reverse sequencing reads were assembled into contiguous sequences for four *An. hargreavesi* specimens. Sequences highlighted in yellow rectangular boxes indicate the locations of the *COI* forward and reverse primer binding sites employed during PCR amplification.

3.2 IDENTIFICATION OF SAMPLES FROM ZAMBIA: *ANOPHELES GIBBINSI*

3.2.1 Morphological Identification

Seven of the seventeen samples that were received were morphologically confirmed to be *An. gibbinsi*, two were recognised as belonging to the *An. marshallii* group, one sample was identified as belonging to the *An. funestus* group and six were unable to be confirmed due to the lack of essential body parts. The extent of the physical damage to these six specimens hindered a clear classification. The morphology of these specimens was confirmed by Prof. M. Coetzee. *Anopheles gibbinsi* samples could be identified by the presence of three pale bands on the palps, narrow pale bands on hind tarsomeres 1–4 and a pale interruption in the third main dark area of the first vein in the wing.

3.2.2 *Anopheles gibbinsi* Sequence Analysis

The *ITS2* PCR and sequencing were successful on all the samples that were confirmed as *An. gibbinsi.* The *ITS2* PCR product size for all samples was ≈507 bp **(Figure 3.5A).** All *ITS2* sequences matched to the previously reported *An. gibbinsi* sequences deposited in NCBI as *Anopheles sp. 6.* The NCBI BLAST result for all *ITS2* samples revealed a 99% identity with *Anopheles sp.* 6 BSL-2014 *Internal Transcribed Spacer 2*. The *ITS2* sequences were deposited in GenBank. **Appendix 3B** shows the BLAST search results and the accession numbers obtained for the *An. gibbinsi* specimens.

The *COI* amplicons on the PCR gel were faint due to DNA degradation **(Figure 3.5B).** Consequently, these samples were retested to verify the findings. Upon retesting, the samples still failed to yield visible amplicons. As a result, these samples were not sequenced. The *ITS2* multiple sequence alignment of *An. gibbinsi* was highly similar and highlighted conserved regions in *ITS2* sequences, though a single base substitution was observed at the 519 bp position (**Figure 3.6**). The *ITS2* sequences shared 96.85% identity with each other.

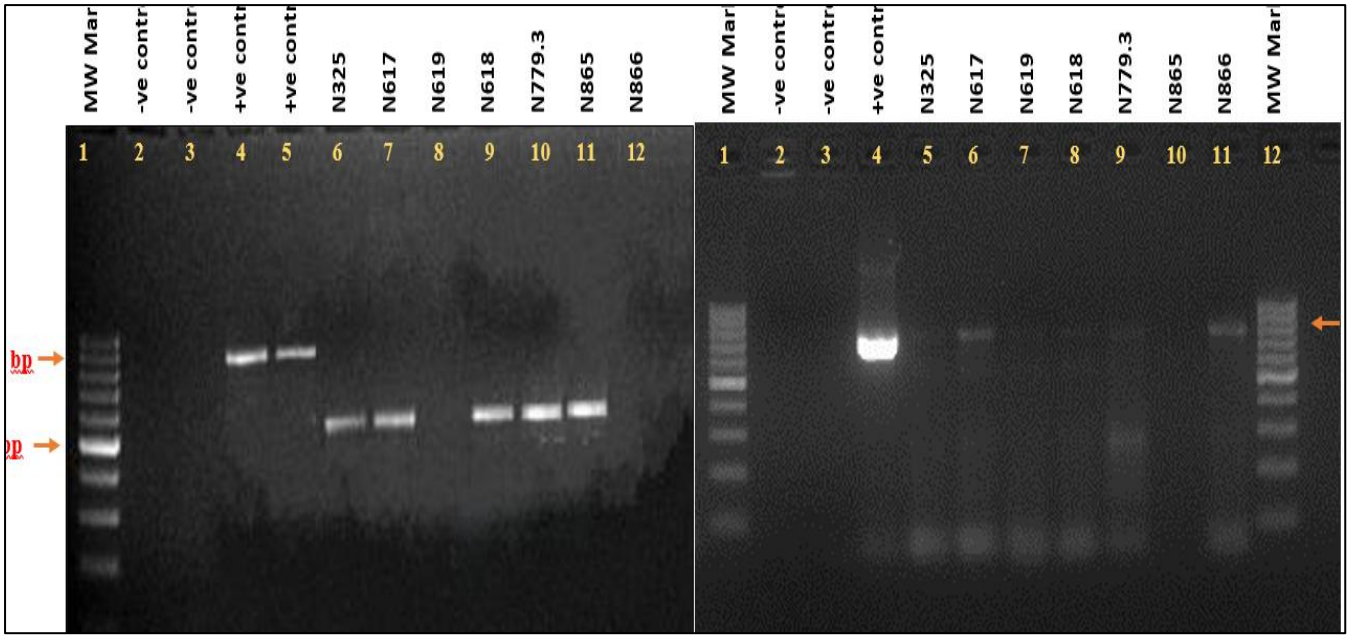


Figure 3.5: Amplification of *ITS2* and *COI* regions in *Anopheles gibbinsi* specimens using PCR, visualised on 2.5% agarose gels. A) *ITS2* PCR agarose gel. Lane 1: Molecular weight marker of 1000 bp. Lanes 2 and 3: PCR and DNA extraction negative controls. Lanes 4 and 5: *An. funestus* positive controls (~900 bp). Lanes 6 – 12: *An. gibbinsi ITS2* PCR amplicons (~507 bp). The samples in lanes 8 & 10 that did not produce amplicons were subsequently repeated. **B) *COI* PCR agarose gel**. Lanes 1 and 12: Molecular weight marker of 1000bp. Lanes 2 and 3: PCR and DNA extraction negative controls. Lanes 4: *An. funestus* positive control (~900 bp). Lanes 5 - 11: Faint *An. gibbinsi COI* PCR amplicons (~900 bp). These samples were excluded from further analysis.

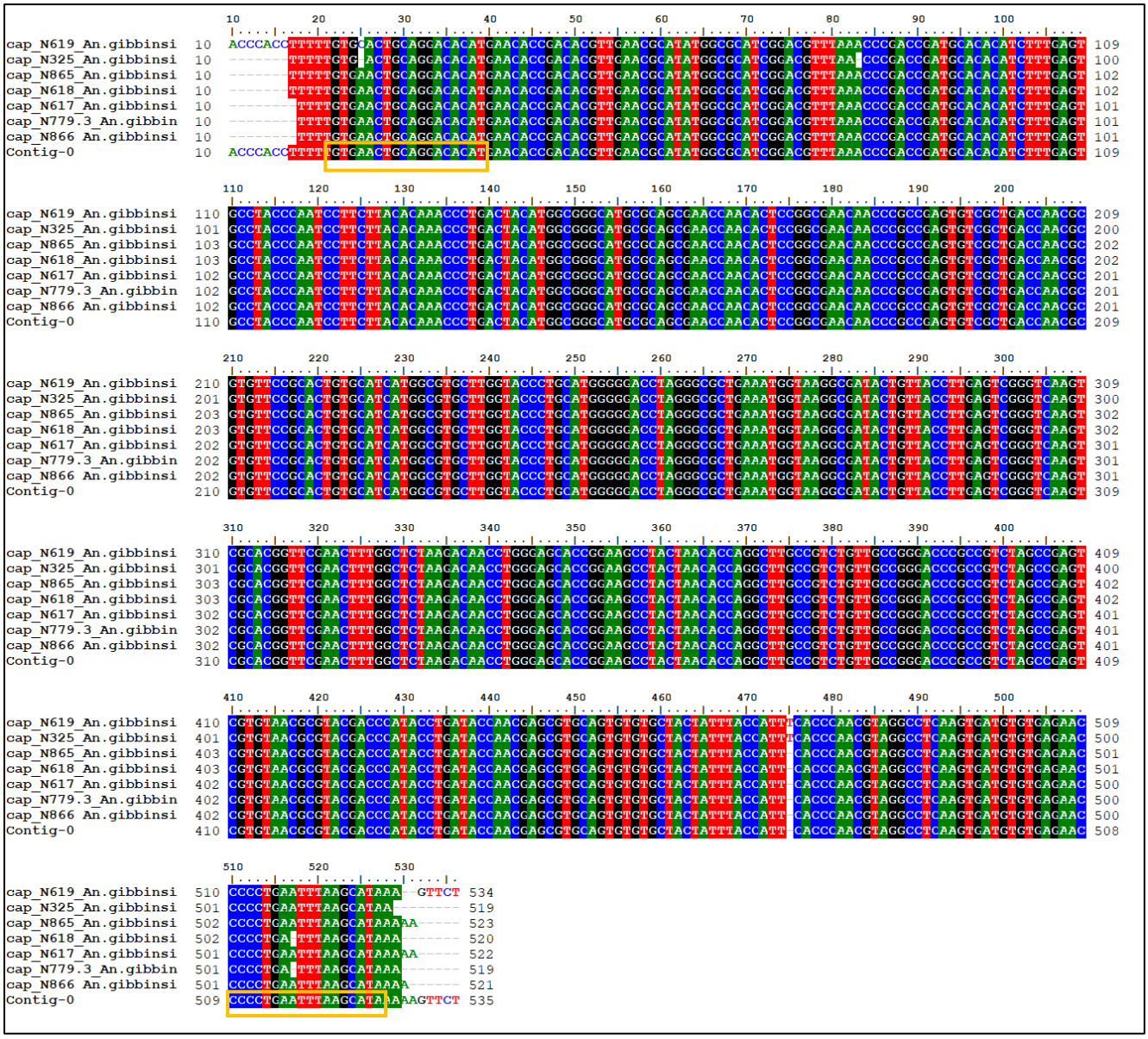


Figure 3.6: Multiple sequence alignment of the *ITS2* region from *Anopheles gibbinsi* specimens collected in Zambia. Forward and reverse sequencing reads were assembled into contiguous sequences for seven *An. gibbinsi* specimens. Sequences highlighted in yellow rectangular boxes indicate the locations of the *ITS2* forward and reverse primer binding sites employed during PCR amplification.

3.3 IDENTIFICATION OF SAMPLES FROM SOUTH AFRICA: *ANOPHELES MARSHALLII* GROUP

3.3.1 Morphological Identification (A *priori* identification)

The adult morphological characteristics, together with the immature stages observed on *An. marshallii* group families (n=4) are presented in this section. Only the live blood-fed *Anopheles marshallii* group females that were collected (**Section 2.1.3**) could be used to induce ovipositioning. Some of the females collected in the field were physically damaged and sometimes old, which limited the reliability of adult morphological identification. To overcome this, F_1 progeny were read from each family and used for morphological analysis. The individuals were preserved in silica tubes for molecular analysis. Morphological traits were studied at various life stages to ensure accurate identification and documentation of species traits. The insectary conditions were consistently maintained throughout the rearing cycles. Only specimens at clearly defined developmental stages were used for each analysis: fourth-instar larvae for larval morphology and freshly emerged adults from the F_1 generation for adult morphological measurements. By using synchronized developmental stages and maintaining consistent environmental parameters, we minimized confounding variables, such as temperature-induced morphological changes.

3.3.1.1 *Anopheles marshallii* Group Egg Morphology

The overall appearance of the *An. marshallii* group eggs that were observed were elongated and dark in colour (**Figure 3.7**) as per anopheline characteristics. During the iso-female rearing process, only a single egg clutch was visualised for each family. The microscope at the VCRL was not operational during the time that the females laid eggs, and an alternative microscope was used. Unfortunately, the resolution was not ideal, and it was difficult to conduct egg morphology accurately. Members of the *An. marshallii* group could not be confidently distinguished in this investigation. However, the egg morphology of the examined samples (**Figure 3.7 A-B**) shows a continuously open deck between the floats similar to those seen in *An. hughi* eggs **Figure 3.7C** (Lambert and Coetzee, 1982). Based on egg morphology, these families were likely to be *An. hughi*. Eggs were placed into water and allowed to hatch to allow for larval morphology identification.

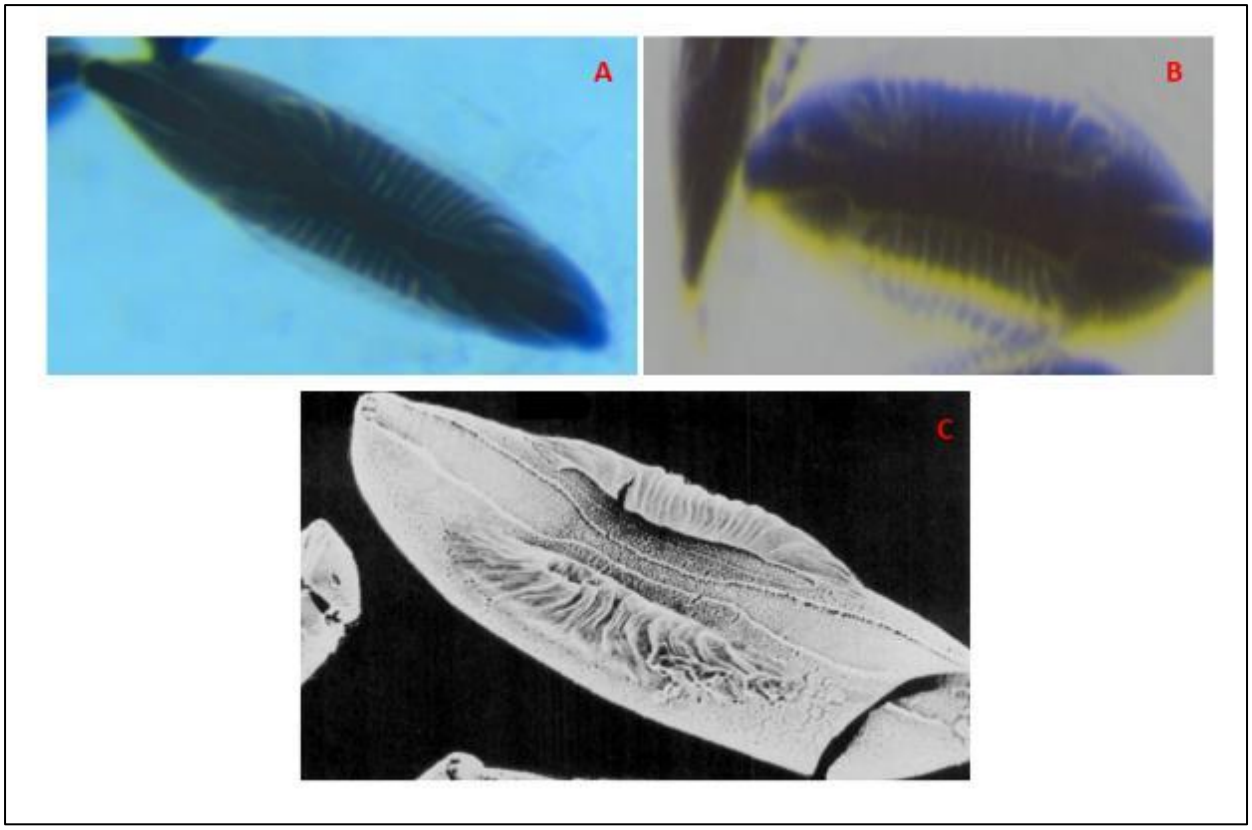


Figure 3.7: Comparative egg morphology of *Anopheles marshallii* group specimens from KZN. **A-B:** Images of eggs belonging to *Anopheles marshallii* group specimens from KZN. **C:** Scanning electron micrographs of *Anopheles hughi* eggs (Lambert and Coetzee, 1982).

3.3.1.2 *Anopheles marshallii* Group Larval Morphology

Larvae were reared through to the L4 stage (Fourth instar larvae) and mounted pelts were analysed, with a maximum of 10 individuals representing each family. Larval morphology was challenging since the larval skins were stiffened and difficult to handle, even though they were preserved in 75% to 80% ethanol. Problems with handling, mounting, and preparation techniques were resolved through a variety of troubleshooting strategies. To aid in this, protocols from Coetzee (1982) and Koekemoer (1999) were integrated. To prevent the pelts from curling and ensure that they adhered well to the microscope slide, the alcohol concentration, the duration of time the pelts were left in the clearing agent (xylene), and the quantity of mounting media (entellen) had to be adjusted. It was challenging to accurately identify distinguishing features from larval skins because some crucial morphological features of mosquito larvae became distorted during mounting, making it difficult to examine. Results from the examined larval material were inconclusive. This character was

uninformative for this analysis and therefore, excluded. **Figure 3.8** shows one of the fourth larval skins that were captured in this study.

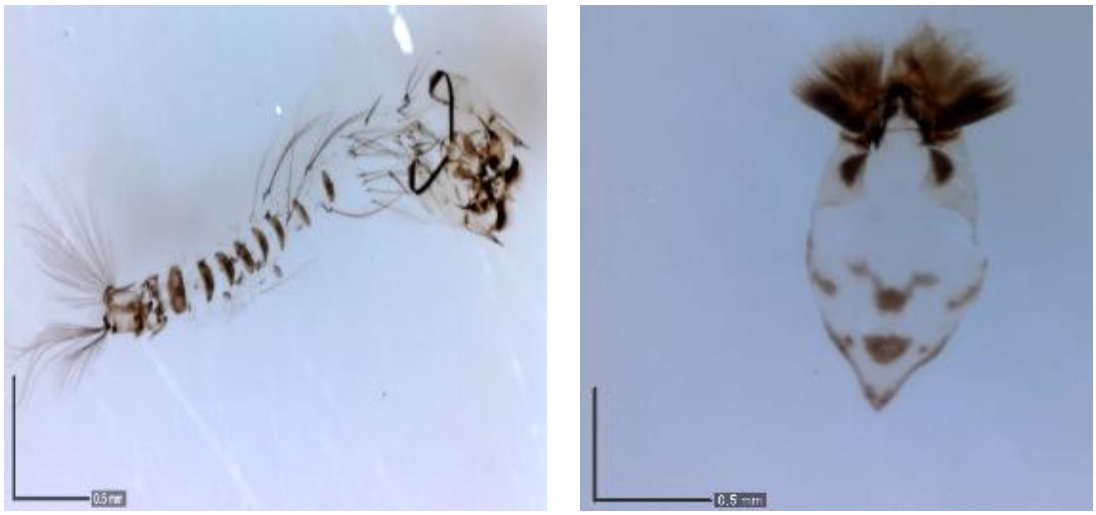


Figure 3.8: Larval morphology of fourth-instar larvae from the *Anopheles marshallii* group. **(A)** Fourth-instar larval skin of an *Anopheles marshallii* group species, showing the clypeus attached**.** **(B)** Clypeus detached from the larval skin.

3.3.1.3 *Anopheles marshallii* Group Adult Morphology

The four *An. marshallii* group families were identified using the key to adult females (Coetzee, 2020). None of the samples had lateral projecting tufts (**Figure 3.9A**). No speckling was observed on the legs (**Figure 3.9B**), and the hind tarsomeres were not entirely pale (**Figure 3.9B**). There were distinct, narrow, pale bands at the apex of hind tarsomeres 1 to 4 (**Figure 3.9C**), and hind tarsomeres 5 was entirely dark (**Figure 3.9C**). The wings showed various dark and pale spots on the costa and veins (**Figure 3.9D**). The wings showed a clear pale interruption on the 3rd main dark area (although it seemed much more reduced in some samples) with clearly defined 2nd and 1st main dark areas (**Figure 3.9E**). There were two distinct, pale spots on the upper branch of wing vein 5 (**Figure 3.9F**). The female maxillary palpus showed the apex to be pale with three pale bands (**Figure 3.9G**). The broad subapical pale band on the maxillary palps extended across the tip of the third segment and the base of the fourth segment (**Figure 3.9H**). The scutal scales of the studied individuals were similar to those of *An. marshallii s.s., An. letabensis, An. kosiensis, An. hughi*, as seen by Coetzee (2020). The scales were mainly white and varied in size, from somewhat curved to narrow and relatively broad (**Figure 3.9I**).

Figure 3.9: *Anopheles marshallii* group female morphological characters.



Figure 3.9A: Abdominal segments lacking laterally projecting tufts.

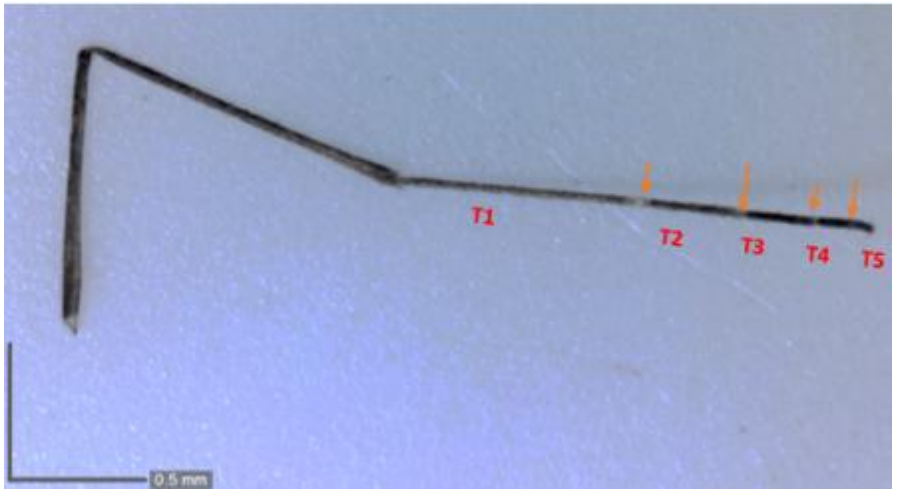


Figure 3.9B: Hind tarsomeres (T1-T5). Hindleg with pale spots on joints represented by arrows.

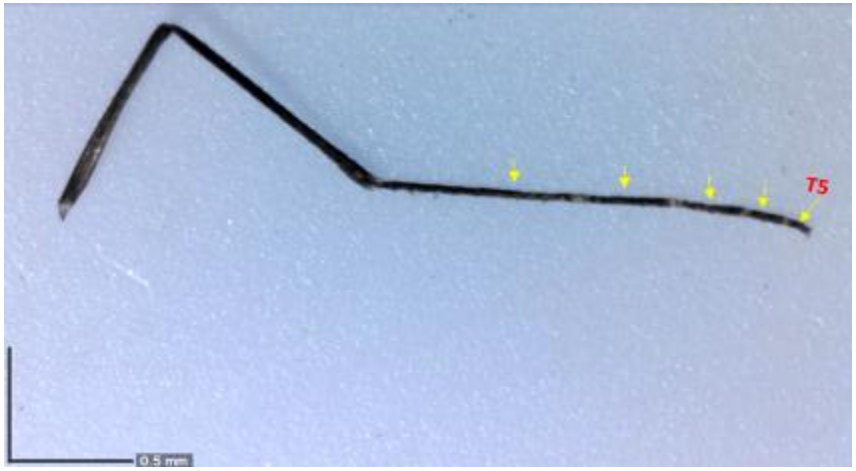


Figure 3.9C: Hind tarsomere 5 entirely dark. Apical pale bands visible on joints.

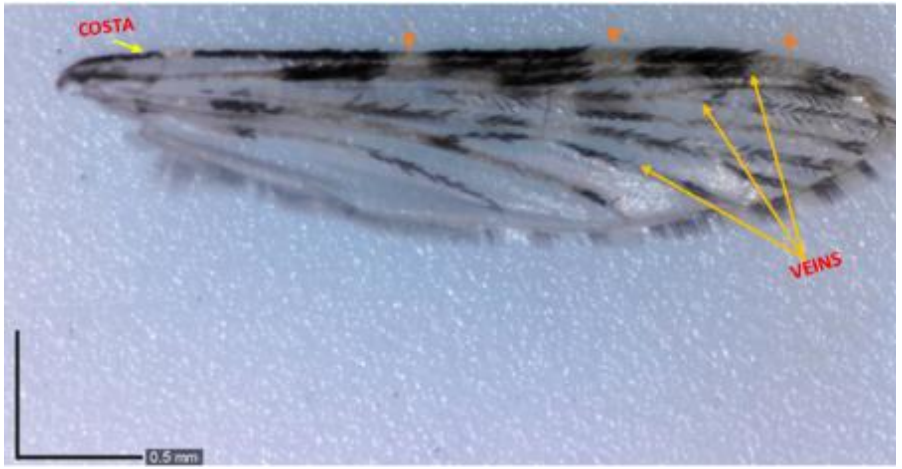


Figure 3.9D: *Anopheles marshallii* group mosquito wing showing various dark and pale spots on the costa and veins.

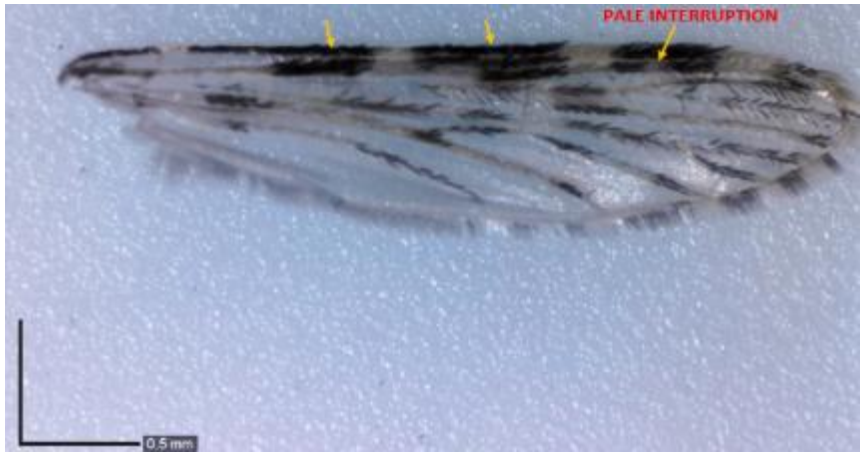


Figure 3.9E: The third main dark area on the wing with pale interruption.

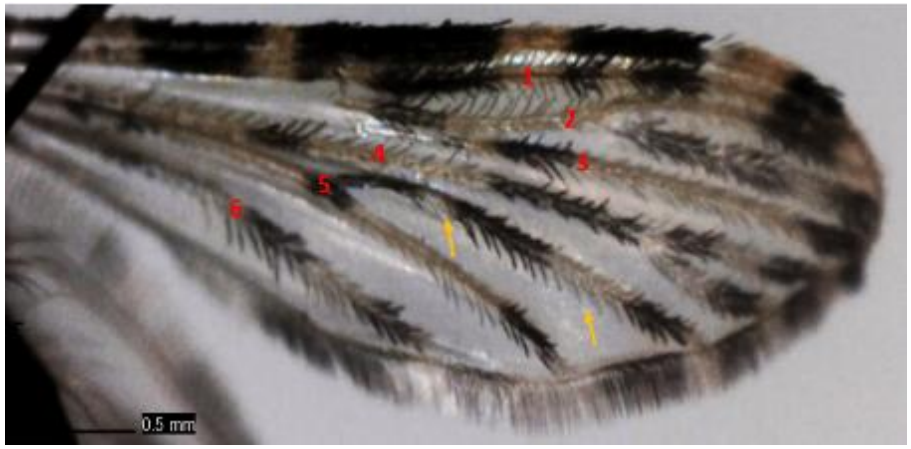


Figure 3.9F: Wing with two pale spots on the upper branch of vein 5.



Figure 3.9G: Apex of the female maxillary palpus pale with three pale bands.

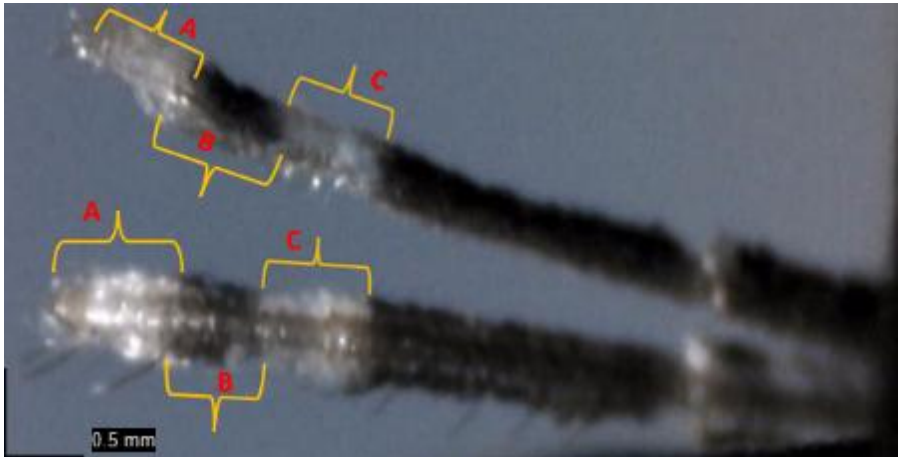


Figure 3.9H: *Anopheles marshallii* group female palps. Segment A= Apical pale band. Segment B= Apical dark band. Segment C= Subapical pale band.

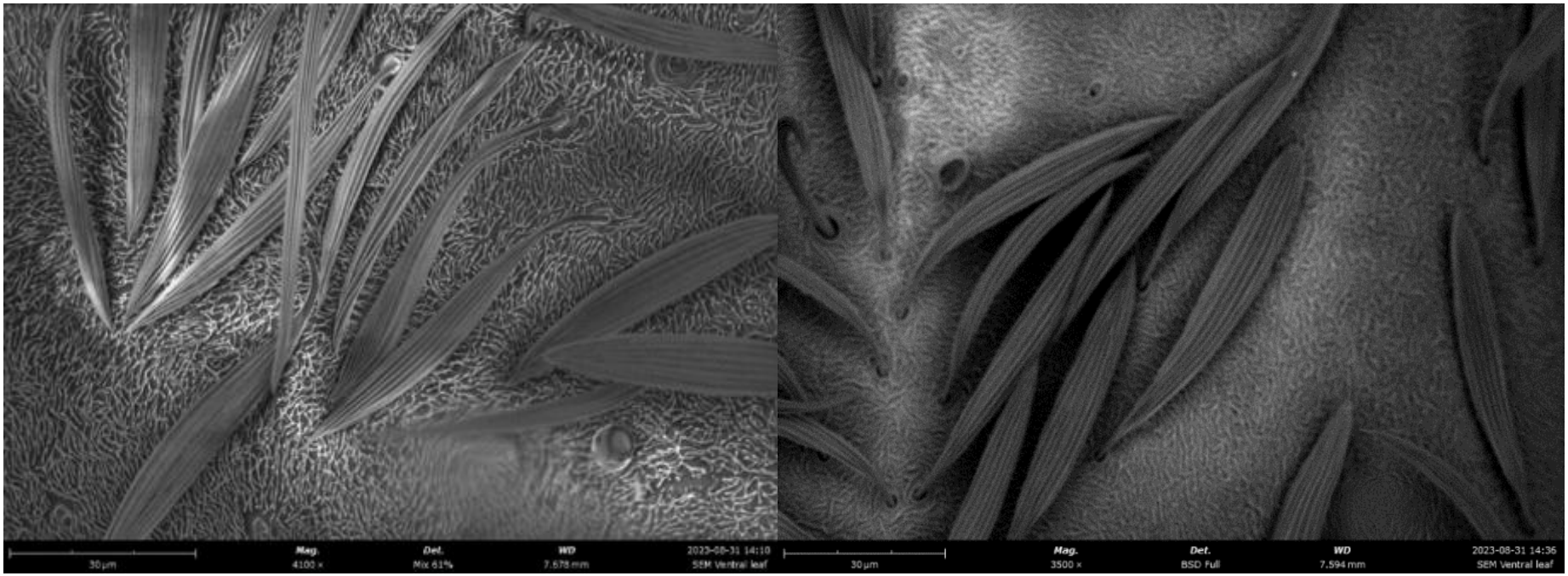


Figure 3.9I: Captured images of the scutal scales of *An. marshallii* group specimens, taken using the Scanning Electron Microscope (SEM). To analyse the scutal scales, the mosquito specimens were carefully mounted on small SEM stubs (flat metallic holders) using forceps to avoid damaging them. The stubs were handled with tweezers to prevent contamination. The specimens were positioned on the stub using a double-sided carbon tape to secure them and provide electrical conductivity. Proper orientation of the thorax was critical to capture the most informative angles of the scales for imaging. The stub-mounted specimens were placed in the SEM chamber, where a high-energy electron beam scanned the sample's surface, providing highly detailed images.

Even though it was established that these specimens might be one of the four closely related species belonging to the *An. marshallii* group: *An. marshallii s.s.*, *An. letabensis*, *An. kosiensis*, and *An. hughi*, it remains unclear what species these specimens actually are. Since conclusive species identification was not possible using adult keys (Coetzee, 2020), the individual morphological features of the legs, wings, and palps were studied in more detail, and the results are described in the next section. To correctly identify these closely related *Anopheles* species, it was important to look into the leg morphology, wing length, wing spot ratio, and palpal ratio. Subtle differences that are not immediately apparent may be revealed in the wing patterns and leg structures, which is essential when dealing with closely related species.

3.3.1.4 *Anopheles marshallii* Group Leg Morphology

Four families of wild-caught *An. marshallii* group mosquitoes, each consisting of five female F_1 progeny per family (n = 20), were examined to observe the female hind legs under an Olympus SZ61 microscope. The joints of the hind tarsomeres of all the individuals, regardless of the family they originate from, showed the presence of pale bands. Analysis of the legs was not possible in some of the samples since their legs were damaged. The damage or loss of legs may have resulted from improper or rough handling of the mosquitoes during the transfer from cages to collection tubes. The adults may have suffered damage due to prolonged confinement in the cages, and lack of timely preservation may have caused them harm. Female hind tarsomeres of the *An. marshallii* group individuals are shown in **Figure 3.10**. Using this morphological trait, no variation was identified between families or among their progenies.

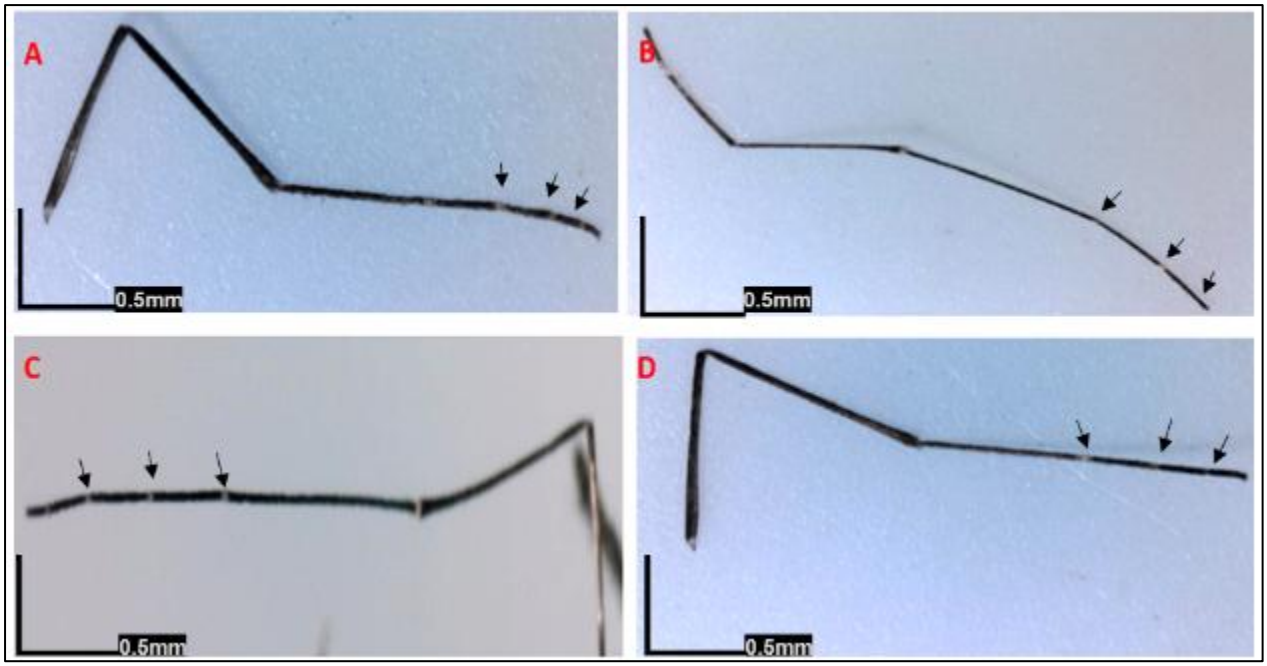


Figure 3.10: *Anopheles marshallii* group hind legs with apical pale bands on joints. **(A)** Family 63 **(B)** Family 221 **(C)** Family 289 **(D)** Family 596.

3.3.1.5 *Anopheles marshallii* Group Palp Morphology

As discussed in detail in Chapter 1 (**Section 1.6.5.4**), members of the *An. marshallii* group can be distinguished by the width of the apical dark band. The variation in length and width of the apical pale and dark bands on the maxillary palps in the *An. marshallii* group might provide more detail to differentiate between species. When it comes to closely related species like *An. marshallii s.s., An. hughi, An. kosiensis,* and *An. letabensis,* the width of the apical dark band in relation to adjacent pale bands on the palps, can be used as a diagnostic trait. Four families of wild-caught *An. marshallii* group species consisting of five female F_1 progeny per family (n = 20) were used to measure palp spots. The measurements that were taken were of the lengths and widths of the apical pale band, the apical dark band and the subapical pale band (**Figure 3.11**).

The apical dark band width for **Family 63** was found to be shorter in 4 samples than the apical and subapical pale bands, whereas in 1 sample, the apical dark band width was slightly more than the apical and subapical pale band widths. In **Family 221**, the width of the apical dark band was approximately equal to that of the apical and subapical pale band in 3 samples, but in 2 samples, the width of the apical dark band was shorter than the width of the apical and subapical pale bands. For **Family 289**, the width of the apical dark band was smaller than the width of the apical and subapical pale bands in 3 samples. In contrast, the width of the

apical dark band was slightly bigger than the width of apical and subapical pale bands in 1 sample. The apical dark band width in 1 sample was roughly the same size as the width of the apical pale band but exceeded the width of the subapical pale band. The width of the apical dark band in all 5 samples of **Family 596** was smaller than the width of the apical and subapical pale bands.

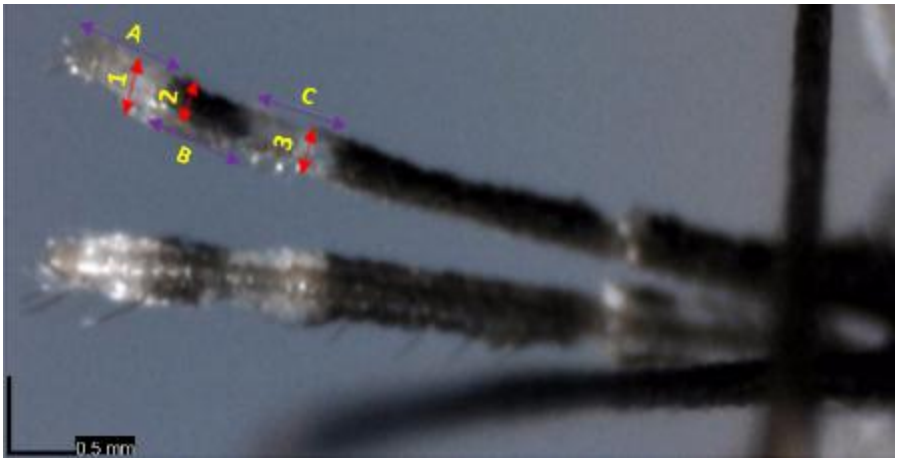


Figure 3.11: Illustration of the measured palp segments. (A) Length and (1) Width of the apical pale band. (B) Length and (2) Width of the apical dark band. (C) Length and (3) Width of the subapical pale band.

The results of the palpal measurements are given in **Table 3.1**. The apical dark band in *An. marshallii s.s.*, *An. hughi*, and *An. kosiensis* is roughly equal to the pale bands, which helps in distinguishing them apart from *An. letabensis*, where the apical dark band is somewhat narrower. One-way analysis of variance (ANOVA) was used to check for variance in this morphological character (female palps) between members of each family. No discernible variations were found between the mean palp spots among the four families (**Appendix 3E**). The mean widths and mean lengths of the palp spots did not show any significant differences between the four families (**Table 3.2**). There was no significant difference in the mean apical dark band width between the families (one-way ANOVA: $p = 0.6763$, $F = 0.5173$, $DF = 3$). A comparison of the families' means apical dark band lengths revealed no discernible differences ($p=0.8562$, $F= 0.2557$, $DF= 3$). Additionally, there was no significant difference in the width of the apical pale band between the families ($p=0.7746$, $F=0.3716$, $DF=3$), nor in the mean apical pale band length ($p=0.9625$, $F=0.0934$, $DF= 3$). The mean subapical pale band width did not significantly differ between the families ($p= 0.8793$, $F= 0.2226$, $DF=3$). Neither did the mean subapical pale band width ($p= 0.3263$, $F= 1.245$, $DF= 3$).

Table 3.1: Comparisons of palp spots (widths and lengths in mm) between the families. Data was analysed using a one-way ANOVA test. The table shows the statistical differences within the families when conducting the Tukey-HSD test.

Family	MORPHOLOGICAL FEATURES					
	1 **Mean apical dark band width ±SD (p-value)**	**2** **Mean apical pale band width ±SD (p-value)**	**3** **Mean subapical pale band width ±SD (p-value)**	**A** **Mean apical dark band length ±SD (p-value)**	**B** **Mean apical pale band length ±SD (p-value)**	**C** **Mean subapical pale band length ±SD (p-value)**
63 (n = 5)	0.1016 ± 0.02785 p=0.9995	0.1176 ± 0.02436 p=0.9418	0.1016± 0.02901 p=0.9997	0.2080 ± 0.04957 p=0.9193	0.3382 ± 0.08035 p=0.9922	0.2294 ± 0.06858 p=0.9364
221 (n = 5)	0.09980± 0.01574 p=0.7069	0.1084 ± 0.01494 p=0.8389	0.1002 ± 0.01946 p=0.3900	0.1880 ± 0.06729 p=0.9892	0.3524± 0.1107 p=0.9611	0.2514 ± 0.05210 p=0.9979
289 (n = 5)	0.1172± 0.02644 p=0.9818	0.1220 ± 0.02134 p=0.9988	0.1244 ± 0.01699 p=0.9444	0.1978 ± 0.04318 p=0.9605	0.3276 ± 0.04320 p>0.9999	0.2582 ± 0.04445 p=0.9985
596 (n = 5)	0.1112 ± 0.02964 p=0.9321	0.1244 ± 0.03749 p=0.9750	0.1162 ± 0.02630 p=0.7603	0.1824 ± 0.03293 p=0.8478	0.3308 ± 0.07384 p=0.9989	0.2522 ± 0.07038 p=0.9300
Average for four families	0.1075	0.1181	0.1106	0.1941	0.3373	0.2478

3.3.1.6 *Anopheles marshallii* Group Wing Morphology

Five individuals from each family (n=20) were used for wing measurements. To minimise conflicting results, the same researcher performed all the measurements. Since the wings were obtained from specimens that had previously undergone processing for molecular analysis, only undamaged wings with adequate structure were selected to measure the wing length and wing spot ratio. In Coetzee, Segerman, and Hunt (1987), the wing measurements played a significant role in distinguishing *An. kosiensis* from *An. marshallii s.s* and *An. letabensis*. The size of the costal spots varied noticeably amongst the species under comparison.

a) Wing spot ratio

The costal wing spots were measured and numbered according to **Figure 3.12**.

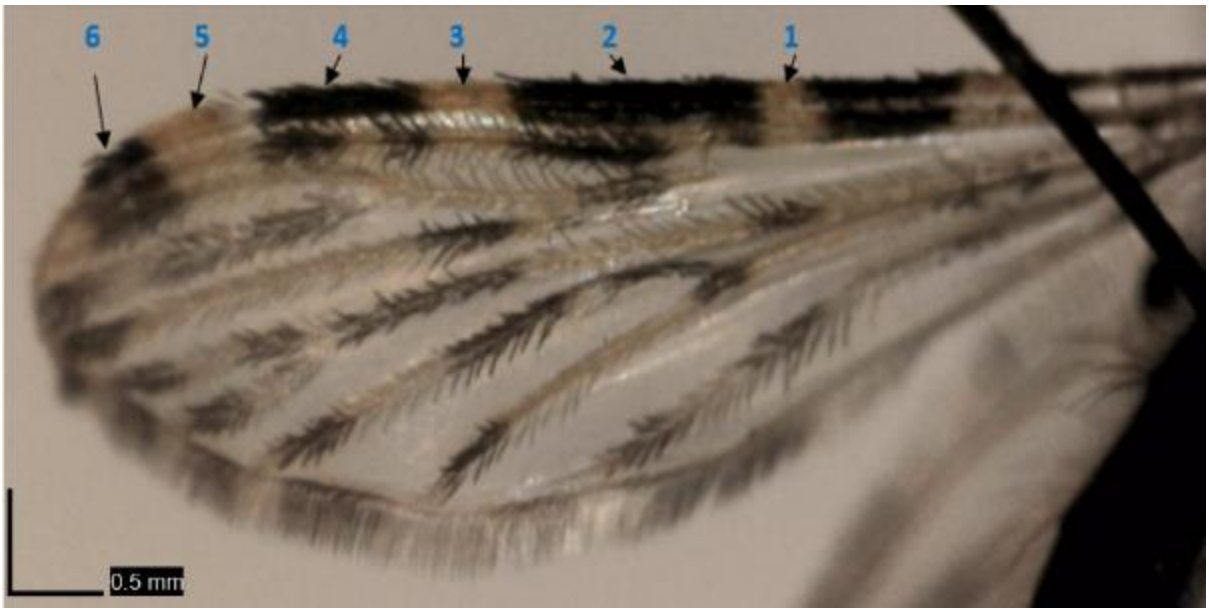


Figure 3.12: Measured costal wing spots of *Anopheles marshallii* group specimens. (1) Sector pale spot (2) Median dark spot (3) Sub-coastal pale spot (4) Pre-apical dark spot (5) Pre-apical pale spot (6) Apical dark spot.

The wing spots were measured and compared against the measurements of wing spots of the three members of the *An. marshallii* group: *An. marshallii s.s*, *An. kosiensis* and *An. hughi* found by Coetzee, Segerman and Hunt (1987) **(Table 3.2).**

Table 3.2: Measurements (mm) of wing spots of three members of the *Anopheles marshallii* group (Coetzee, Segerman and Hunt, 1987).

Wing Spot	*An. marshallii s.s. (An. pitchifordi)* holotype		*An. kosiensis* (n=25)		*An. hughi* (n=20)	
	Range	Mean	Range	Mean	Range	Mean
1	0.16, 0.16	0.16	0.094-0.159	0.13	0.073-0.165	0.11
2	0.49, 0.49	0.49	0.375-0.566	0.49	0.449-0.681	0.54
3	0.28, 0.3	0.29	0.19-0.296	0.24	0.15-0.259	0.21
4	0.4, 0.42	0.42	0.171-0.475	0.31	0.25-0.475	0.36
5	0.33, 0.33	0.33	0.2-0.3	0.25	0.175-0.284	0.23
6	0.18, 0.22	0.2	0.105-0.244	0.17	0.113-0.23	0.16
3+5	0.61, 0.63	0.62	0.394-0.569	0.48	0.356-0.543	0.45

The mean sizes of all the wing spots of the families were similar to those of *An. marshallii s.s.* The mean sizes of the sector pale spot ranged from 0.162 mm to 0.167 mm, the median dark spot from 0.047 mm to 0.048 mm, the sub-coastal pale spot from 0.28 mm to 0.29 mm, the pre-apical dark spot from 0.42 mm to 0.47 mm, the pre-apical pale spot from 0.24 mm to 0.39mm, and the apical dark spot from 0.20 mm to 0.29 mm. However, there is no absolute certainty that the individual specimens belong to *An. marshallii s.s.* because the measurements of *An. letabensis* were not included in the aforementioned study. There were no significant differences in the mean wing spot ratios of the four families, suggesting that these families could all represent a single species (One-way ANOVA: p=0.8256, F= 0.2990, DF=3) (**Table 3.3**).

Table 3.3: Wing spot measurements (mm) for morphological comparison with members of the *Anopheles marshallii* group.

Wing Feature	Family 63 n = 5		Family 221 n = 5		Family 289 n = 5		Family 596 n = 5		Average for all families
	Observed Range	Mean	Observed Range	Mean	Observed Range	Mean	Observed Range	Mean	
(1) Sector pale spot	0.161 - 0.185	0.167	0.152 - 0.169	0.162	0.128 - 0.196	0.169	0.15 - 0.201	0.167	0.1663
(2) Median dark spot	0.401 - 0.572	0.477	0.45 - 0.463	0.479	0.421 - 0.553	0.473	0.403 - 0.56	0.482	0.4780
(3) Sub-coastal pale spot	0.282 - 0.299	0.291	0.248 - 0.331	0.287	0.231 - 0.365	0.283	0.272 - 0.296	0.285	0.2867
(4) Pre-apical dark spot	0.413 - 0.499	0.447	0.426 - 0.507	0.462	0.428 - 0.474	0.448	0.332 - 0.485	0.426	0.4458
(5) Pre-apical pale spot	0.262 - 0.361	0.246	0.271 - 0.36	0.322	0.253 - 0.434	0.324	0.231 - 0.389	0.314	0.3172
(6) Apical dark spot	0.175 - 0.225	0.209	0.167 - 0.293	0.234	0.211 - 0.275	0.239	0.166 - 0.262	0.227	0.2224
Wing spot ratio (3+5/4)	1.162 - 1.557		1.22 - 1.415		1.136 - 1.686		1.21 - 1.551		-

b) Mean wing length

The wing length of an adult mosquito was measured from the axial vein to the outermost point of the first vein (**Figure 3.13**). The measurements taken of the wing length of the *An. marshallii* group showed no variation, and there were no statistical differences in the wing lengths of the examined individuals **(Figure 3.14)**. The measured wings ranged between 3.0 mm to 3.5 mm as described by Gillies and Demeilon (1968). As a result, these families could not be separated on the basis of their wing length.

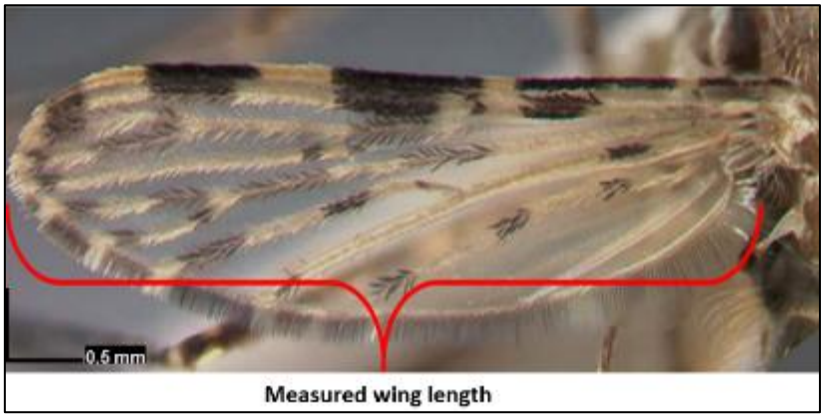


Figure 3.13: Measured wing length of *Anopheles marshallii* group specimens.

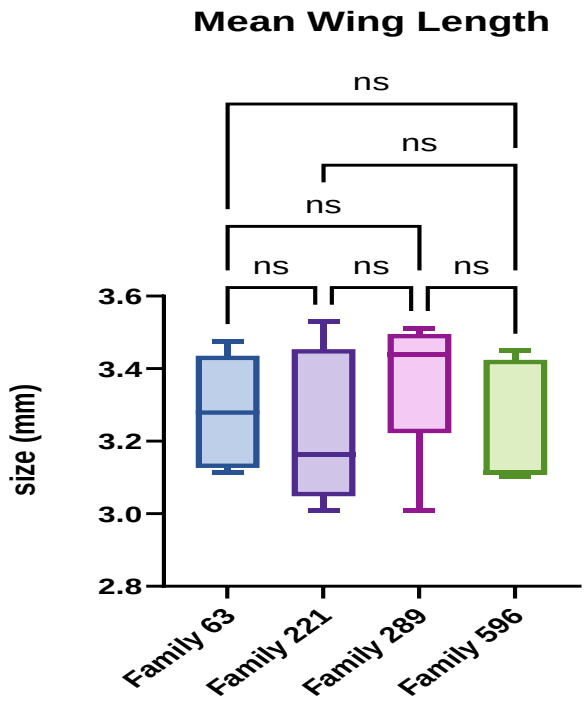


Figure 3.14: Comparison of the mean wing length between the families. Each box represents the upper and lower quartiles, with the median indicated by the line inside. The extending lines, or whiskers, illustrate the variability beyond the upper and lower quartiles in each family.

3.3.2 *Anopheles marshallii* Group Molecular Identification

3.3.2.1 *Anopheles funestus* group Species Identification

An MSc student misidentified an *An. marshallii* group sample as belonging to the *An. funestus* group, resulting in the sample being incorrectly identified as *An. leesoni* (Koekemoer *pers comm*). Subsequent morphological identification confirmed the misidentification. Additional *An. marshallii* group samples, also morphologically misidentified, did not amplify in the same species-specific PCR. Therefore, samples morphologically confirmed as *An. marshallii* group in this study were analysed using the standard *An. funestus* group PCR to better understand this variation.

The wild-caught females from which the F_1 progeny were derived had been previously identified morphologically as belonging to the *An. marshallii* group using dichotomous keys. *An. funestus* PCR assay was performed on three F_1's from each family. Each individual was classified as belonging to Species A = No amplicons or Species B = similar to diagnostic *An. leesoni* (146 bp) amplicon, while samples amplifying multiple fragments were referred to as Species C for this part of the study. The PCR results were variable across each family's progeny. An illustration of the PCR amplicons obtained is shown in **Figure 3.15.**

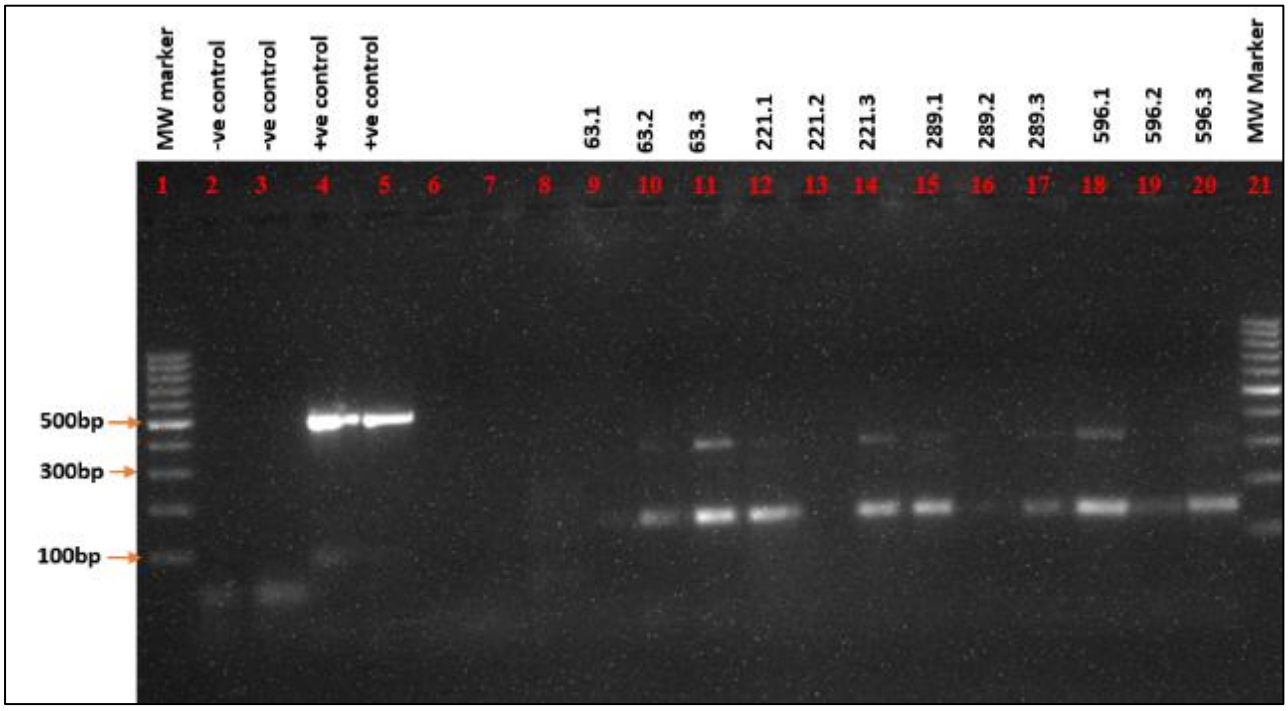


Figure 3.15: Species-specific PCR amplification of *Anopheles funestus* group on a 2.5% agarose gel stained with ethidium bromide. Lanes 1 and 21: Molecular weight marker of 1000 bp. Lanes 2 and 3: DNA extraction and PCR negative controls. Lanes 4 and 5: *An. funestus* positive controls (505

bp). Lanes 6-20: Specimens identified morphologically as belonging to the *An. marshallii* group. Lanes 9-11: (3 individuals from **Family 63**). Lanes 12-14: (3 individuals from **Family 221**). Lanes 15-17: (3 individuals from **Family 289**). Lanes 18-20: (3 individuals from **Family 596**).

A total of 95 specimens from KZN morphologically identified as *An. marshallii* group were subjected to the *An. funestus* PCR assay of Koekemoer *et al.* (2002). These included 12 samples (3 individuals per family), of the families identified as members of *An. marshallii* group. Of the overall samples, 34% (n=32) of the samples produced hybrid bands, whereas 40% (n=38) of the samples amplified as *An. leesoni*. The remaining samples, 26% (n=25) produced no amplicons. Repeats were made of the PCR samples that produced no amplicons.

To complement the PCR assay results and provide further resolution, sequencing was employed to detect species-specific DNA variations in both the ribosomal and mitochondrial regions. The *COI* and *ITS2* regions of *Anopheles* samples were amplified and subsequently sequenced to expand the DNA barcode information, thereby enhancing the available data in public repositories. A consensus sequence was generated by aligning the forward and reverse primer sequences from each mosquito. The individual consensus sequences were used to generate a multiple sequence alignment, from which conserved and variable regions were analysed across the entire length.

3.3.2.2 Sequence Variation of rDNA *ITS2* Subunit of *An. marshallii* group samples from KwaZulu-Natal

Internal Transcribed Spacer 2 (ITS2) PCR was performed on 12 mosquito samples, covering each form observed in the *An. funestus* PCR to further investigate these variations. Three individuals from each of the four families were analysed, and their resulting PCR products were sequenced. After sequencing, consensus sequences were generated for each sample, and the corresponding contigs were aligned for further analysis. The expected fragment size of the amplified *ITS2* region was approximately 500 bp (**Figure 3.16**). Upon comparison with the NCBI GenBank database, all the *ITS2* sequences showed 78% identity to the complete *ITS2* sequence of *Anopheles theileri* (Sequence ID: JN994151.1). However, the sequence divergence was significant enough to rule out the classification of the samples as *An. theileri*, suggesting that these sequences likely belong to a different species within the *Anopheles* genus.

The multiple sequence alignment of the *ITS2* rDNA sequences revealed no significant nucleotide variations among the individuals analyzed. All *ITS2* sequences generated in this study were 100% identical to each other, showing no insertions or deletions (INDELs) across the alignment. The high sequence homology observed across the aligned sequences indicated strong conservation of the *ITS2* region among the *Anopheles marshallii* group specimens, regardless of their family groupings. Additionally, no intraspecific variation was detected among the samples, as all sequences were identical, suggesting genetic uniformity within this population (**Figure 3.17**).

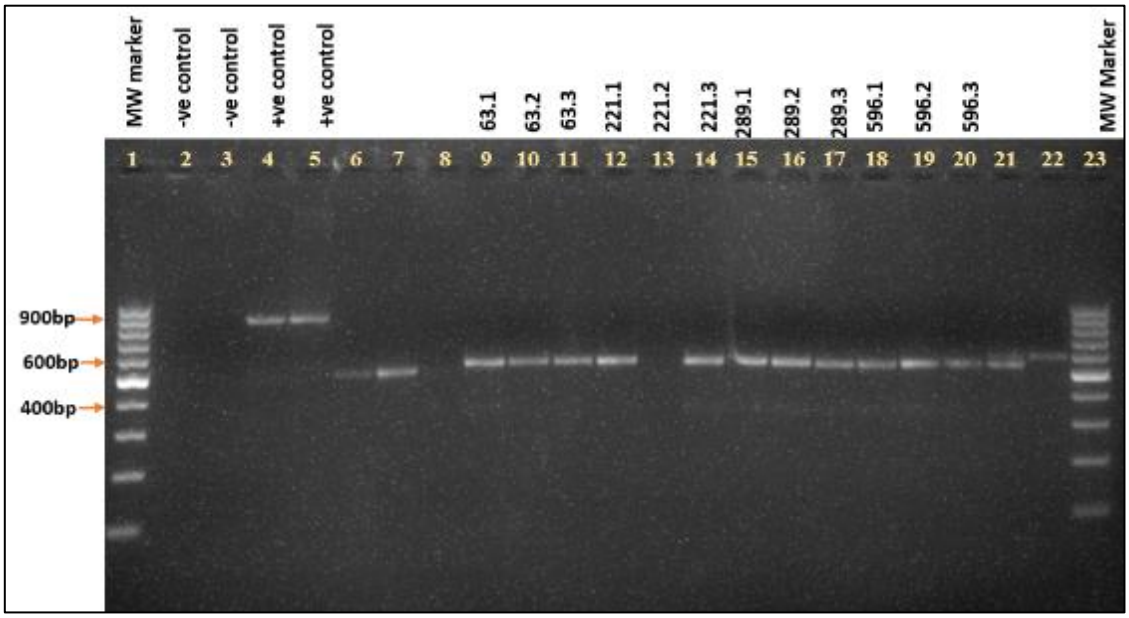


Figure 3.16: PCR amplification of the *ITS2* region in *Anopheles marshallii* group specimens, visualised on a 2.5% agarose gel. Lanes 1 and 23: Molecular weight marker of 1000 bp. Lanes 2 and 3: DNA extraction and PCR negative controls. Lanes 4 and 5: *An. funestus* positive controls (~900 bp). Lanes 9-20: *ITS2* PCR amplicons (~500 bp) from *An. marshallii* group specimens. Lanes 9-11: (3 individuals from **Family 63**). Lanes 12-14: (3 individuals from **Family 221**). Lanes 15-17: (3 individuals from **Family 289**). Lanes 18-20: (3 individuals from **Family 596**). The numerical prefixes **(63, 221, 289 and 596)** correspond to distinct mosquito families, while the suffixes **(.1, .2, .3)** denote individual specimens within each family. Samples that did not amplify were repeated. **Note:** Lanes not explicitly described in this legend correspond to samples unrelated to the analysis presented in this section.

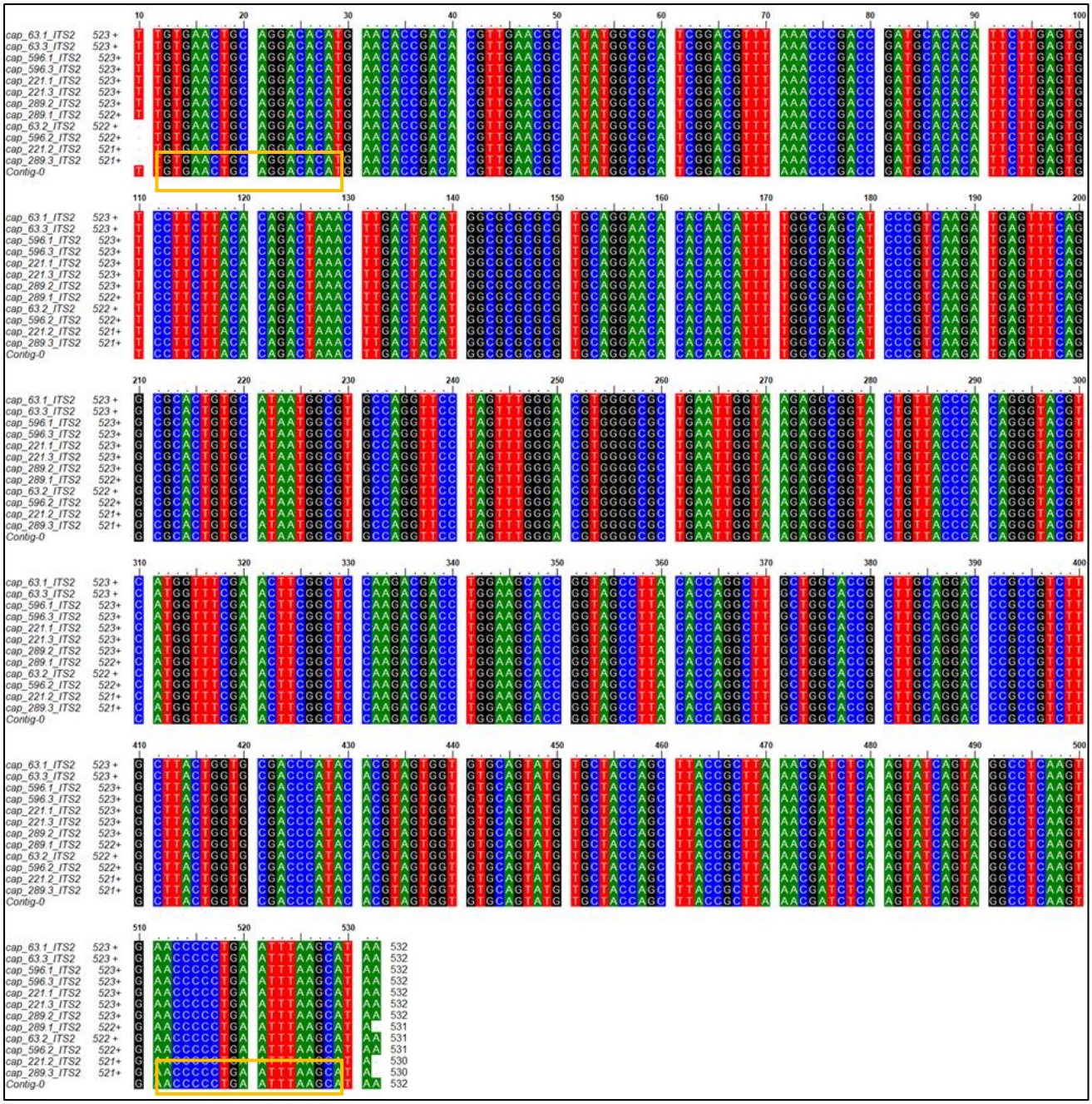


Figure 3.17: Multiple sequence alignment of the *ITS2* region from *Anopheles marshallii* group specimens. This alignment shows the *ITS2* sequences obtained from 12 *An. marshallii* group individuals, representing three specimens from each of four iso-female families. Consensus sequences were generated and aligned using BioEdit. Sequences highlighted in yellow rectangular boxes indicate the locations of the *ITS2* forward and reverse primer binding sites used during PCR amplification.

3.3.2.3 Sequence Variation of rDNA mtDNA *COI* of *An. marshallii* group samples from KwaZulu-Natal

The same 12 mosquito samples were subjected to *cytochrome c oxidase subunit I (COI)* PCR, and the PCR products were subsequently sent for Sanger sequencing. The expected size of the *COI* fragment was approximately 900 bp (**Figure 3.18**). However, during the initial PCR

run, no amplification was observed for the samples in lanes 8 and 10. These samples were repeated to verify if amplification could be achieved. The *An. funestus* positive control in lane 5 was included in the repeat run to serve as a control for amplification success. Consensus sequences were generated and subjected to a BLAST search. The analysis revealed that 10 of the *COI* sequences showed 92% similarity to the *COI* gene of *Anopheles superpictus* (Sequence ID: MT993498.1). In contrast, the remaining 2 sequences were more similar to the *COI* gene of *Anopheles aconitus* isolate (Sequence ID: HQ877378.1). Their contigs were aligned to assess sequence identity. The *COI* sequences were 99.72% identical to each other. The multiple sequence alignment indicated high homology across the 12 samples, with only minor nucleotide variations observed. Of the 720 nucleotide positions, seven sites exhibited slight differences in nucleotide composition (**Figure 3.19**). The generated *COI* sequences have been deposited in GenBank.

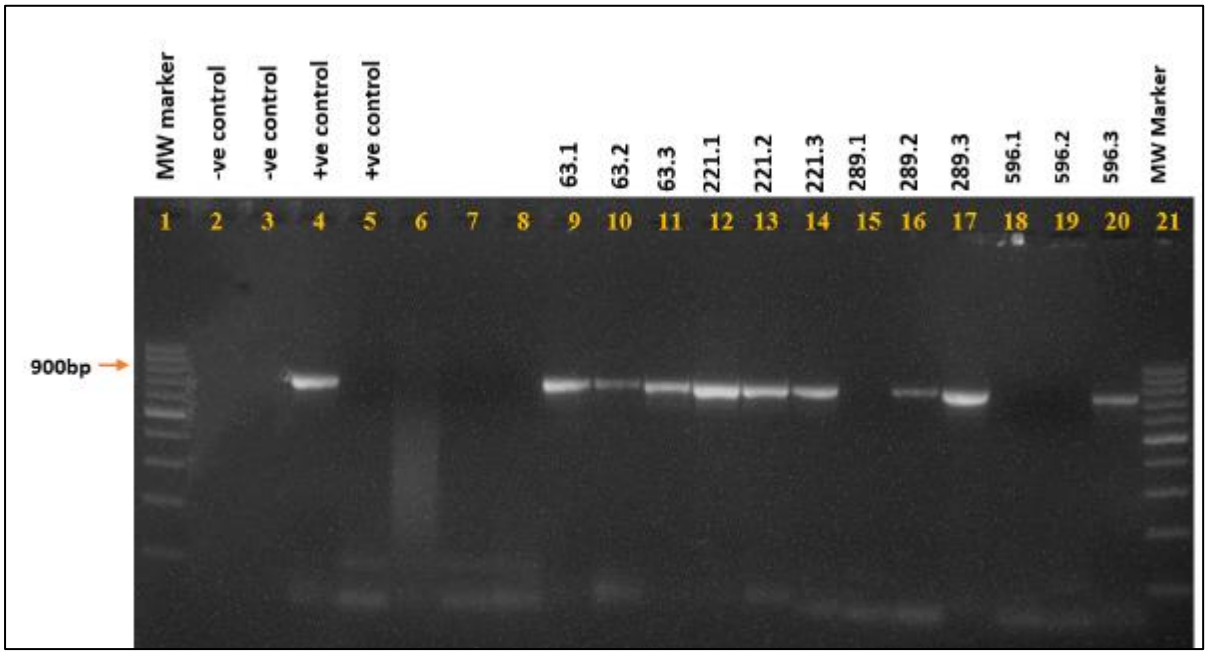


Figure 3.18: PCR amplification of the *COI* region in *Anopheles marshallii* group specimens, visualised on a 2.5% agarose gel. Lanes 1 and 21: Molecular weight marker of 1000 bp. Lanes 2 and 3: PCR and DNA extraction negative controls. Lanes 4 and 5: *An. funestus* positive controls (~900 bp). Lanes 9-20: *ITS2* PCR amplicons (~900 bp) from *An. marshallii* group specimens. Lanes 9-11: (3 individuals from **Family 63**). Lanes 12-14: (3 individuals from **Family 221**). Lanes 15-17: (3 individuals from **Family 289**). Lanes 18-20: (3 individuals from **Family 596**). The numerical prefixes **(63, 221, 289 and 596)** correspond to distinct mosquito families, while the suffixes **(.1, .2, .3)** denote individual specimens within each family. Samples that did not amplify were repeated. **Note:** Lanes not explicitly described in this legend correspond to samples unrelated to the analysis presented in this section.

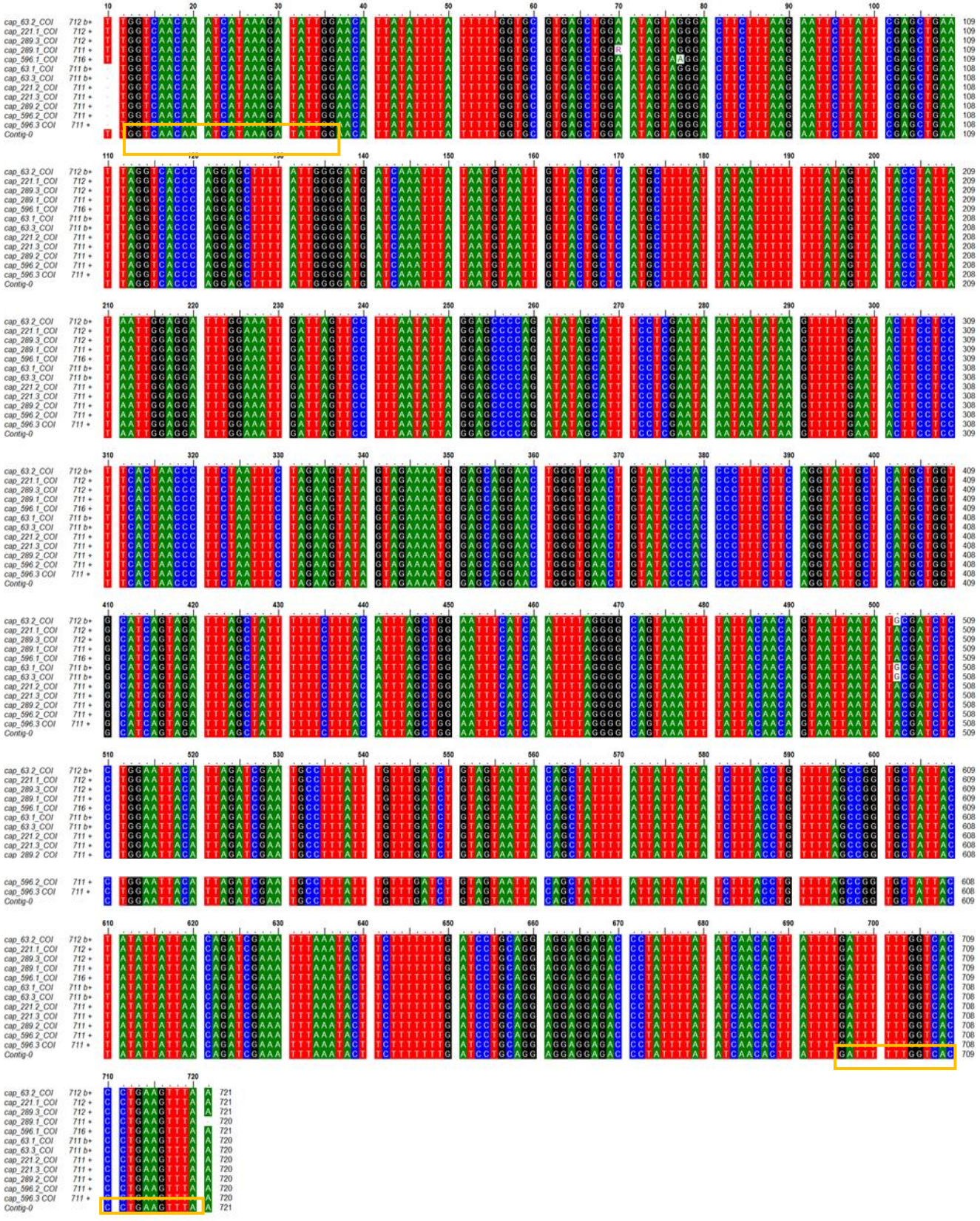


Figure 3.19: Multiple sequence alignment of the *COI* region from *Anopheles marshallii* group specimens. This alignment shows the *COI* sequences obtained from 12 *An. marshallii* group individuals, representing three specimens from each of four iso-female families. Consensus sequences

were generated and aligned using BioEdit. Sequences highlighted in yellow rectangular boxes indicate the locations of the *COI* forward and reverse primer binding sites used during PCR amplification.

3.3.2.4 Analysis of BLAST Statistics for *ITS2* and *COI* Contig Sequences in *An. marshallii* group samples from KwaZulu-Natal

The statistical data obtained from BLAST searches of *ITS2* and *COI* contig sequences from the *An. marshallii* group in the NCBI database are shown in **Table 3.4**. The *ITS2* multiple sequence alignment covered a total length of 530 bp, while that of *COI* spanned a total length of 720 bp. The percentage of the query sequence (the input sequence) that matches the subject sequence (the sequence in the database) is referred to as the "Query Coverage" (QC). The *ITS2* and *COI* regions exhibit high variability, resulting in a higher query coverage (QC) of 97-99%, with the larger portion of the query sequence being covered by the alignment. The E-value represents the number of hits one could expect to see by chance when searching a database of a specific size. The E-value of 0.0 in the *COI* sequences reflects a strong match between the query and subject sequences, indicating almost identical sequence identity. This is consistent with the fact that *COI* is a protein-coding gene, and mutations in this region are often constrained due to its functional importance. The E-value of 1e-111 seen in *ITS2* sequences signifies a highly significant match, reflecting strong similarity, but the larger E-value compared to *COI* reflects the higher degree of sequence variability typically observed in non-coding regions. The maximum percentage of identical matches between the query and subject sequences throughout the aligned region is denoted by Maximum Identity (Max ID). A greater percentage indicates a higher level of similarity. Max Score represents the overall quality and length of the alignment. A higher score generally indicates a better match with more identical or similar nucleotides, fewer gaps, and longer alignments.

Given the 100% alignment in *ITS2* and 99.72% alignment in *COI* sequences, the specimens from the different families can be confirmed as belonging to the same species. These sequences are unique *An. marshallii* group sequences and do not match the species in the available databases (NCBI, VectorBase). **Appendix 3C** shows the BLAST search results and the generated *ITS2* and *COI* accession numbers obtained for these *An. marshallii* group specimens.

Table 3.4: ***Internal Transcribed Spacer 2 and Cytochrome C Oxidase Subunit I*** **database comparisons for consensus sequences of each family used to determine species.**

Query sequence	Gene	Length	Highest Hit	QC	E-value	Max ID	Max scores
Family 63	***ITS2***	**540 bp**	*Anopheles theileri*	99%	1e-111	78.52%	418
	COI	**708 bp**	*Anopheles superpictus*	99%	0.0	92.23%	1015
Family 221	***ITS2***	**540 bp**	*Anopheles theileri*	99%	1e-111	78.52%	418
	COI	**703 bp**	*Anopheles superpictus*	99%	0.0	92.97%	1015
Family 289	***ITS2***	**540 bp**	*Anopheles theileri*	99%	1e-111	78.52%	418
	COI	**705 bp**	*Anopheles aconitus*	99%	0.0	92.12%	1021
Family 596	***ITS2***	**540 bp**	*Anopheles theileri*	97%	1e-111	78.52%	418
	COI	**710 bp**	*Anopheles superpictus*	99%	0.0	91.97%	1013

3.4 SEQUENCE ALIGNMENT OF *ITS2* AND *COI* CONTIGS IN THE *ANOPHELES MARSHALLII* GROUP AND RELATED SPECIES

The *ITS2* and *COI* contig sequences from the *An. marshallii* group families (collected in KwaZulu-Natal), along with *An. hargreavesi* and *An. gibbinsi,* from this study were subsequently aligned with *An. marshallii* group sequences from Cameroon, as well as *An. brohieri* and *An. hancocki* reference sequences found in the NCBI to assess sequence homology.

Base substitution and INDEL changes were identified in fairly substantial numbers throughout the species' *ITS2* sequence alignments (**Figure 3.20**). The nucleotide differences between the species were more pronounced in the *ITS2* alignment. The sequences at the beginning of the *ITS2* region (position 73 bp - 103 bp) are highly conserved across different *Anopheles* species. These conserved sections imply that these sequences play crucial biological roles in all species and point to a common evolutionary ancestor. However, as the sequence proceeds, variable regions appear that enable species to be distinguished from one another. These minute variations in the nucleotide sequence function as species-specific molecular markers. INDELS that further distinguish species can be seen in some sequences. The sequences of *An. hancocki* and *An. brohieri* are marginally shorter in several regions than the other sequences, suggesting possible insertions or deletions. These variations in sequence length are another indicator of species' divergence, and they highlight the differences that have accumulated as these species evolved separately.

Comparisons of the *COI* sequence alignments revealed a mixture of highly conserved and variable regions (**Figure 3.21**). The conserved nucleotides remained relatively unchanged across species due to the crucial function of the *COI* gene in the mitochondria and serve as proof of shared origins. Mutations unique to each species can be found in variable regions. As species diverge from common ancestors, these mutations accumulate and reveal information about their evolutionary pathways. Most mutations are point mutations, in which one nucleotide is substituted for another. In the *COI* gene, mutations can be classified as either synonymous, indicating that they do not alter the amino acid sequence, or nonsynonymous, indicating that they do change the amino acid sequence. Nonsynonymous mutations result in changes to the amino acid sequence that can potentially impact the protein's function, stability, or interactions. Such mutations play a critical role in evolutionary

processes, as they can introduce variations that may be subject to natural selection. The presence of INDELs results in alignment shifts, with gaps appearing in the sequence of one species relative to another. This may suggest the existence of pseudogenes, non-functional copies of *COI*, or significant evolutionary divergence.

Pairwise identity matrices displaying sequence similarity percentages among sampled species are displayed in **Table 3.5** and **Table 3.6**. While lower results indicate potential divergence, high identity scores, such as the 100% identity between *An. hancocki* and *An. brohieri* (*ITS2*) indicates close genetic ties.

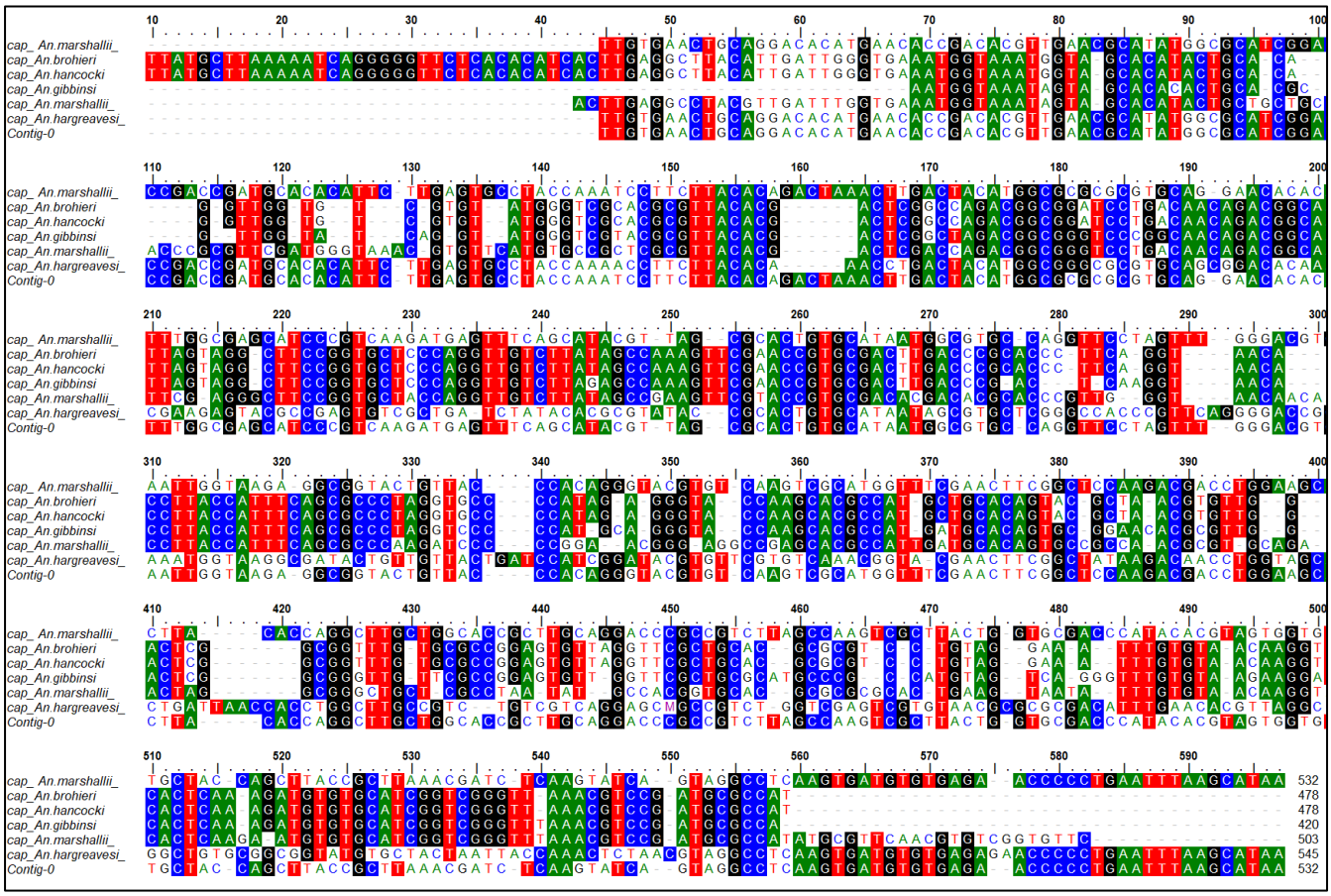


Figure 3.20: Multiple sequence alignment of the *ITS2* region from *Anopheles marshallii* group specimens and related species. This alignment compares the *ITS2* sequences of *An. marshallii* group specimens collected from KZN-South Africa, with reference sequences from *An. hargreavesi*, *An. gibbinsi*, *An. brohieri*, *An. hancocki*, and *An. marshallii* (from Cameroon).

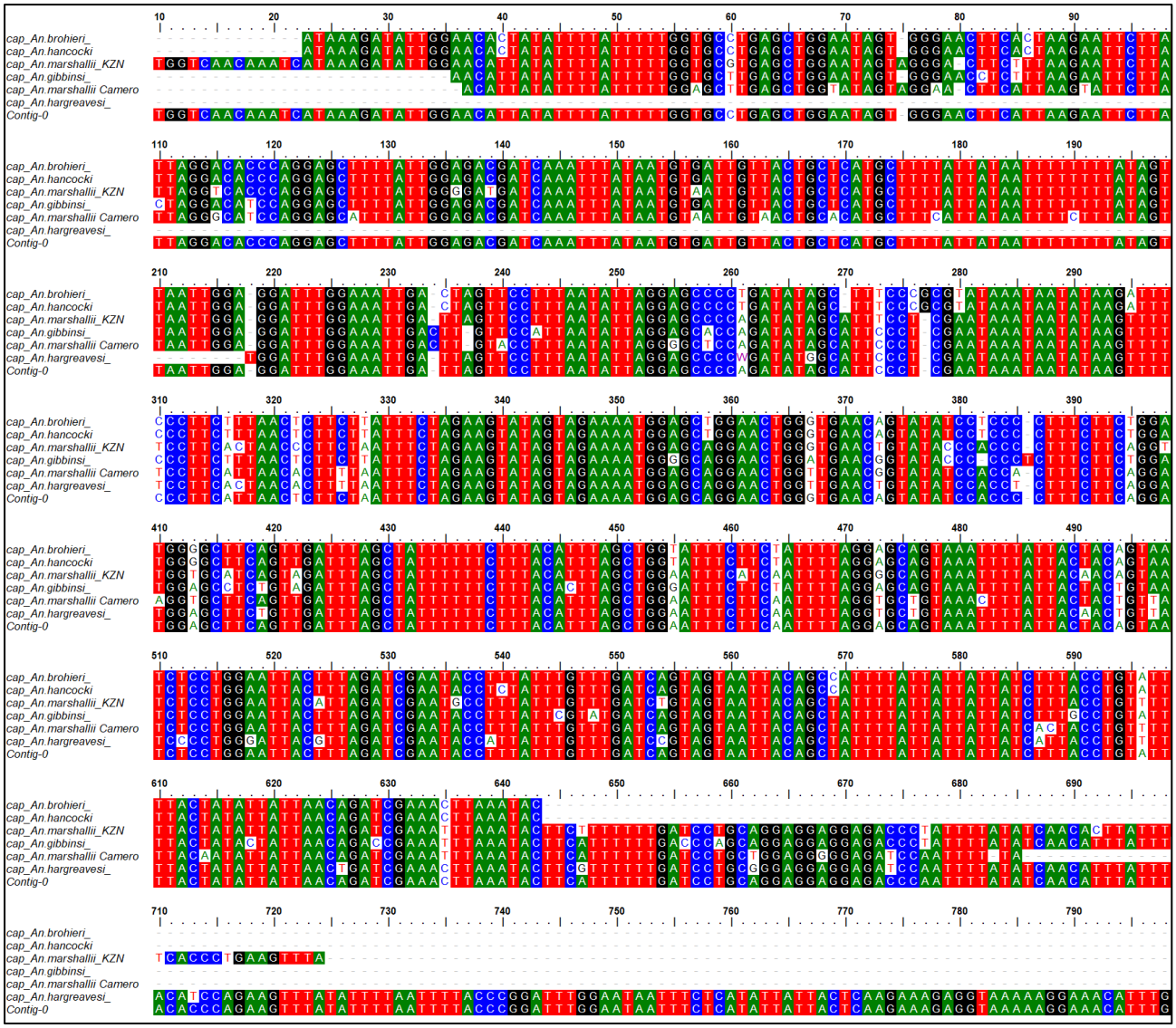


Figure 3.21: Multiple sequence alignment of the *COI* region from *Anopheles marshallii* group specimens and related species. This alignment compares the *COI* sequences of *An. marshallii* group specimens collected from KZN-South Africa, with reference sequences from *An. hargreavesi*, *An. gibbinsi*, *An. brohieri*, *An. hancocki*, and *An. marshallii* (from Cameroon).

Table 3.5: Percentage Identity (%) Matrix of *ITS2* Sequences among *Anopheles* species.

Species/Accession Number	*An. marshallii* group (KZN)	*An. brohieri*	*An. hancocki*	*An. gibbinsi*	*An. marshallii* group (Cameroon)	*An. hargreavesi*
***An. marshallii* group KZN** (PQ334736.1)	100.00	64.16	64.16	65.57	63.98	66.46
An. brohieri (MW647380.1)	64.16	100.00	100.00	84.73	76.05	71.52
An. hancocki (MW647407.1)	64.16	100.00	100.00	84.73	76.05	71.52
An. gibbinsi (OM459767.1)	65.57	84.73	84.73	100.00	73.83	71.52
***An. marshallii* group Cameroon** (MW257139.1)	63.98	76.05	76.05	73.83	100.00	79.20
An. hargreavesi (PP915781.1)	66.46	71.52	71.52	73.07	79.20	100.00

Table 3.6: Percentage Identity (%) Matrix of *COI* Sequences among *Anopheles* species.

Species/Accession Number	*An. hargreavesi*	*An. marshallii* group (Cameroon)	*An. gibbinsi*	*An. marshallii* group (KZN)	*An. brohieri*	*An. hancocki*
An. hargreavesi (PP919268.1)	100.00	93.10	89.75	92.06	90.54	90.31
***An. marshallii* group Cameroon** (OP709256.1)	93.10	100.00	90.36	90.82	91.20	91.03
An. gibbinsi (OM456806.1)	89.75	90.36	100.00	91.79	93.53	93.37
***An. marshallii* group KZN** (PQ327569.1)	92.06	90.82	91.79	100.00	92.53	92.37
An. brohieri (MW603496.1)	90.54	91.20	93.53	92.53	100.00	99.84
An. hancocki (MW603519.1)	90.31	91.03	93.37	92.37	99.84	100.00

3.5 PHYLOGENETIC ANALYSIS

Phylogenetic analysis was carried out based on molecular data using the Neighbor-Joining tree, with the evolutionary distances computed using the Maximum Composite Likelihood method. The trees were rooted with *Anopheles gambiae* as an out-group. Clade support was evaluated using bootstrap analysis with 1000 replications. Bootstrap support was categorized into three separate levels: the first category (50–74%) was considered to have low support, the second category (75–84%) has moderate support, and the third category (85–100%) has high/strong support (Felsenstein, 1985). Phylogenetic analysis involved nucleotide sequences obtained from this study, and other reference sequences were sourced from the NCBI nucleotide database (**Table 3.7**).

Table 3.7: GenBank Accession Numbers for species used for phylogenetic analysis in this study.

SPECIES	GenBank Accession Number	
	ITS2	***COI***
Anopheles brohieri	MW647380.1	MW603496.1
Anopheles gambiae	EU104648.1	MT375224.1
Anopheles gibbinsi	OM459767.1 (**This study**)	OM456806.1
Anopheles hancocki	MW647407.1	MW603519.1
Anopheles hargreavesi	PP915781.1 (**This study**)	PP919268.1 (**This study**)
***Anopheles marshallii* group (Cameroon)**	MW257139.1	OP709256.1
***Anopheles marshallii* group (KZN)**	PQ334736.1 (**This study**)	PQ327569.1 (**This study**)

The *ITS2* phylogenetic tree (**Figure 3.22**) was constructedusing the *ITS2* sequences. The tree is arranged into several clades with high support bootstrap values, each of which represents a different evolutionary lineage of the species. The *ITS2* tree clearly shows that *An. brohieri* and *An. hancocki* are clustered in the same clade. Additionally, it is evident that the other species show considerable divergence from the *An. marshallii* group isolates from KZN. The genetic distinctiveness of *An. gibbinsi, An. hargreavesi,* and *An. marshallii* group isolates from Cameroon is reflected in the formation of separate branches that diverge from other

species. The longer branch lengths of *An. gibbinsi*, *An. marshallii* group (Cameroon) and *An. hargreavesi* suggests a more ancient divergence, which is consistent with their unique ecological or geographic niches. The distinct clades formed by these species highlight the potential use of the *ITS2* region as a molecular marker.

Similarly, the constructed *COI* phylogenetic tree (**Figure 3.23**) revealed that *Anopheles brohieri* and *An. hancocki* clustered together, suggesting a strong evolutionary connection between these species. Notably, *An. marshallii* group from KZN and *An. hargreavesi* formed a clade, albeit with low bootstrap support, indicating some uncertainty in the strength of this grouping. *Anopheles gibbinsi* was positioned more distantly, highlighting its unique evolutionary trajectory, possibly with adaptations to different environmental conditions or vector dynamics. The longer branch length of *An. gibbinsi* compared to other clades suggests that this species has diverged more significantly from the others.

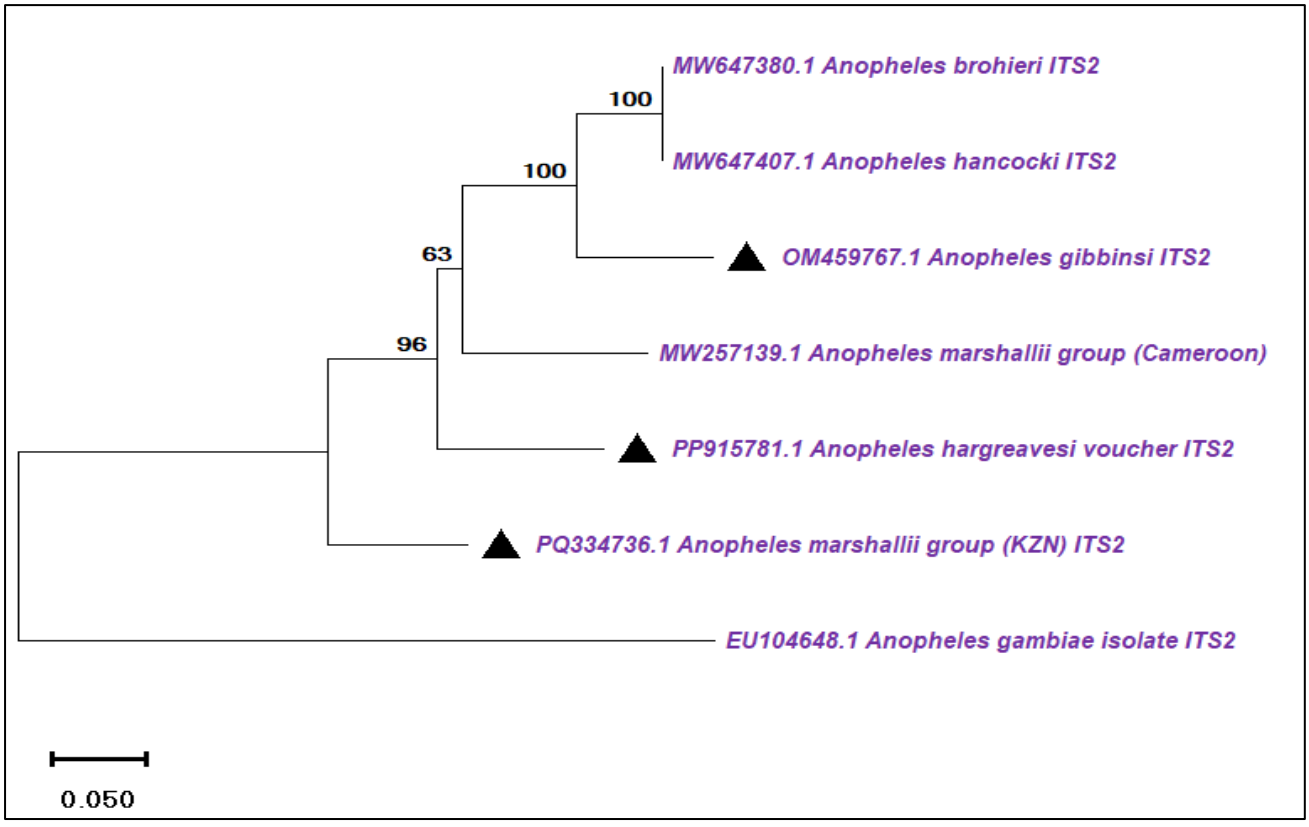


Figure 3.22: Phylogenetic tree of the *Anopheles marshallii* group and related species based on rDNA *ITS2* sequence data. The numbers displayed on branches represent the bootstrap support obtained through 1000 replications. Species along with the NCBI accession number with the triangular shape indicates the sequences generated from this study. *Anopheles gambiae* was used as the outgroup.

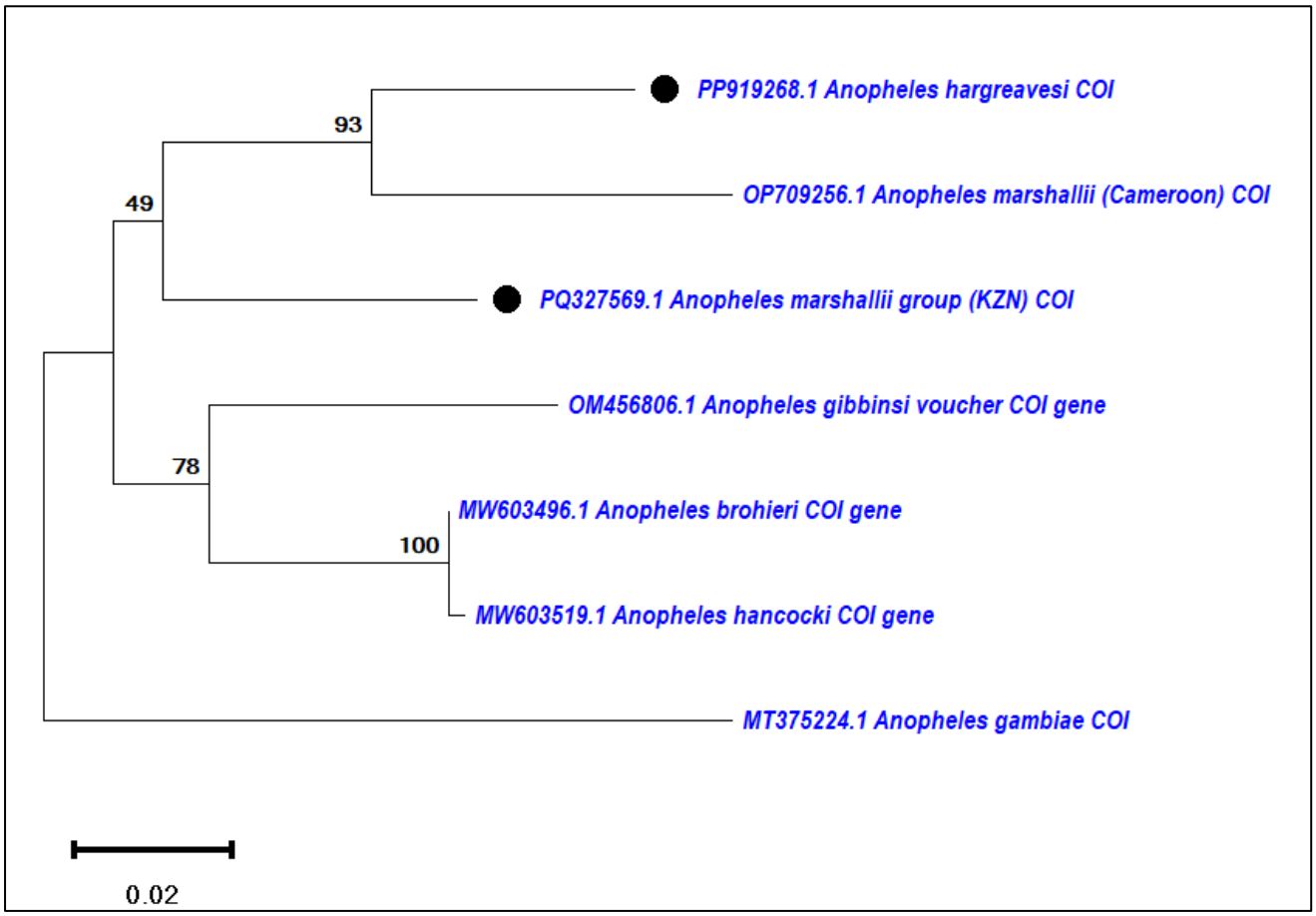


Figure 3.23: Phylogenetic tree of the *An. marshallii* group and related species based on mtDNA *COI* sequence data. The numbers displayed on branches represent the bootstrap support obtained through 1000 replications. Species along with the NCBI accession number with the circular shape indicate the sequences generated from this study. *Anopheles gambiae* was used as the outgroup.

3.6 SAMPLES FROM SOUTH AFRICA: *ANOPHELES MACULIPALPIS*

3.6.1 Morphological identification

The standard morphological dichotomous keys were used to identify female *Anopheles* species under an Olympus SZ61 microscope (Coetzee, 2020). In this study, only two wild-caught female specimens were morphologically identified as *An. maculipalpis* and sixteen were identified as *An. pretoriensis*. However sequencing revealed that the 16 *An. pretoriensis* samples were actually *An. maculipalpis* (**Section 3.4.2**). The morphology of these specimens as *An. maculipalpis* was verified by N. Venter after sequencing. This misidentification may be attributed to human error and highlights the taxonomic challenge of accurately identifying species based solely on morphology. Sequencing the misidentified specimens underscores the importance of using molecular markers (*ITS2* and *COI*) for accurate species identification, a key objective of this study. This also reinforces the need for additional morphological identification approaches since any discrepancy between morphological and molecular methods highlights the need for more morphological training.

3.6.2 *Anopheles maculipalpis* Molecular Identification

3.6.2.1 *Anopheles funestus* group Species Identification

A total of fifteen *An. maculipalpis* samples were subjected to the *An. funestus* PCR assay of Koekemoer *et al.* (1999), 67% (n=10) of the samples produced no amplicons (Species A), whereas 33% (n=5) of the samples produced multiple bands. None of the samples amplified as *An. leesoni* (**Figure 3.24**).

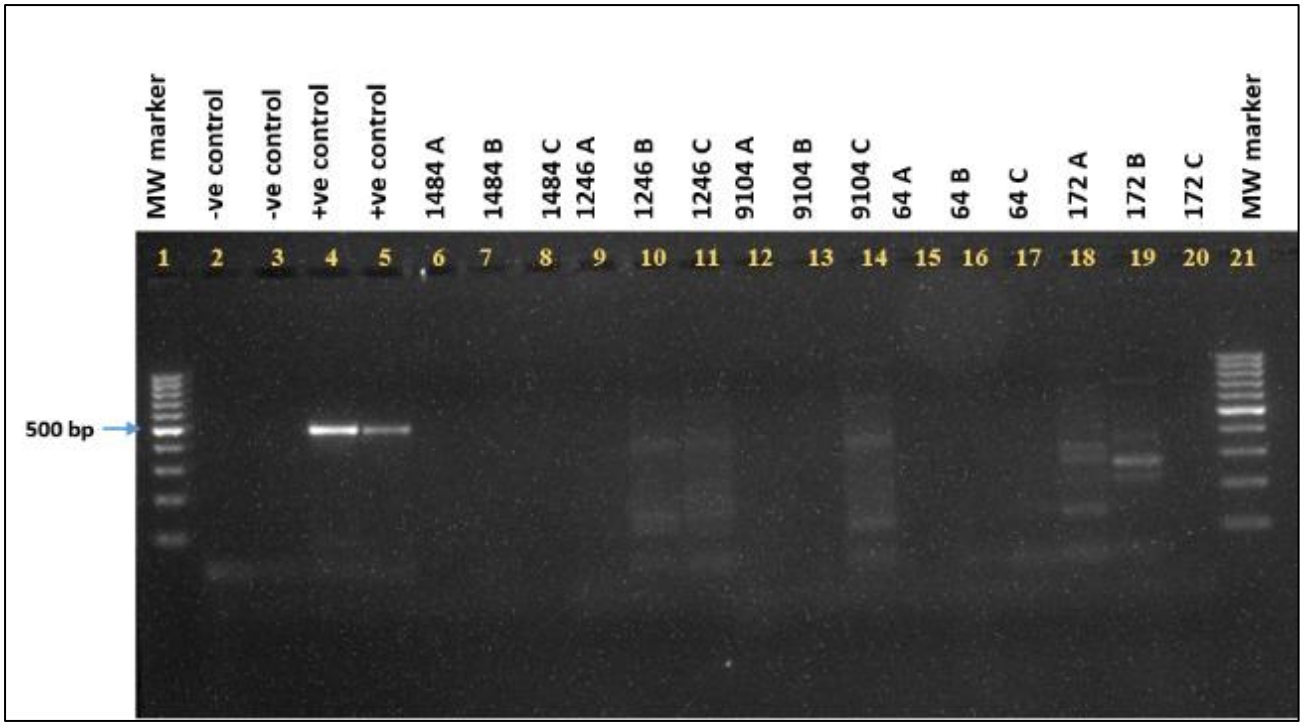


Figure 3.24: Species-specific PCR amplification of *Anopheles funestus* group on a 2.5% agarose gel stained with ethidium bromide. Lanes 1 and 21: Molecular weight marker of 1000 bp. Lanes 2 and 3: DNA extraction and PCR negative controls. Lanes 4 and 5: *An. funestus* positive controls (505 bp). Lanes 6-20: Specimens identified morphologically as *An. maculipalpis.* Lanes 6-8: (3 individuals from **Family 1484).** Lanes 9-11: (3 individuals from **Family 1246).** Lanes 12-14: (3 individuals from **Family 9104).** Lanes 15-17: (3 individuals from **Family 64).** Lanes 18-20: (3 individuals from **Family 172).** Hybrid bands were observed in lanes 10,11,14,18, and 19. The numerical prefixes **(1484, 1246, 9104, 64, 172)** correspond to distinct mosquito families, while the suffixes **(A, B, C)** denote individual specimens within each family.

3.6.2.2 Sequence Variation of rDNA *ITS2* Subunit and mtDNA *COI* of *Anopheles maculipalpis* samples from KwaZulu-Natal

ITS2 and *COI* PCR amplification were carried out on the same *An. maculipalpis* samples that were subjected to the *An. funestus* PCR assay. The *ITS2* region was successfully amplified for eight *An. maculipalpis* samples, with *ITS2* PCR fragment sizes ranging from approximately 400 bp to 610 bp (**Figure 3.25A**), while the expected *COI* size was ≈900 bp (**Figure 3.25B**). All PCR products with the different fragment sizes observed on the *ITS2* gel were sequenced as separate fragments. Although all samples being confirmed as *An. maculipalpis*, variations in the size of *ITS2* fragments were observed.

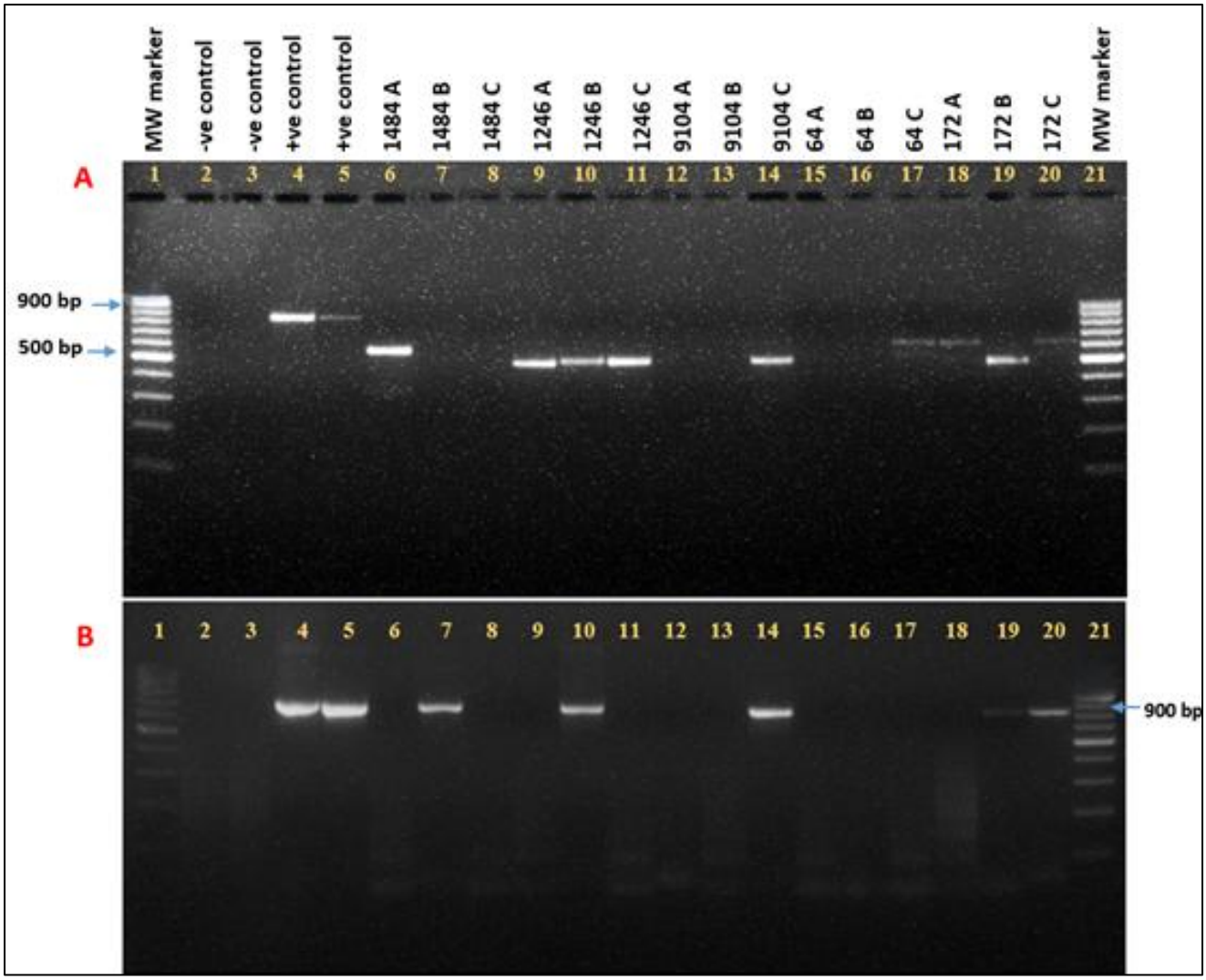


Figure 3.25: PCR amplification of the *ITS2* and *COI* region in *An. maculipalpis* specimens, visualised on a 2.5% agarose gel. A) *ITS2* PCR agarose gel. Lanes 1 and 21: Molecular weight marker of 1000 bp. Lanes 2 and 3: DNA extraction and PCR negative controls. Lanes 4 and 5: *An. funestus* positive controls (~900 bp). Lanes 6-20: *An. maculipalpis ITS2* amplicons with band sizes ranging from ~400 bp to ~610 bp. **B) *COI* PCR agarose gel**. Lane 1 and 21: Molecular weight marker of 1000 bp. Lanes 2 and 3: PCR and DNA extraction negative controls. Lanes 4 and 5: *An. funestus* positive controls (~900 bp). Lanes 6-20: *An. maculipalpis COI* PCR amplicons (~900 bp). Lanes 6-8: (3 individuals from **Family 1484).** Lanes 9-11: (3 individuals from **Family 1246).** Lanes 12-14: (3 individuals from **Family 9104).** Lanes 15-17: (3 individuals from **Family 64).** Lanes 18-20: (3 individuals from **Family 172).** Hybrid bands were observed in lanes 10, 11, 14, 18, and 19. The numerical prefixes **(1484, 1246, 9104, 64, 172)** correspond to distinct mosquito families, while the suffixes **(A, B, C)** denote individual specimens within each family.

Since the PCR products appeared on the gel as single bands, direct sequencing was done on the individual fragments without purifying them. However, this approach may have contributed to the observed variation in *ITS2* fragment sizes by potentially sequencing mixed or co-amplified *ITS2* variants that were not isolated before sequencing. Following the

sequencing of the *ITS2* region, the acquired forward sequences were of good quality, while reverse sequences exhibited poor quality. The sequences appeared to be "mixed" due to an INDEL event at the start of the *ITS2-B* read, which caused the enzyme to sequence the two alleles simultaneously (Al-Shuhaib and Hashim, 2023). Although the INDEL event interfered with the sequencing, the high quality of the forward reads were suitable for a blast search, and the gene of interest was accurate. This discrepancy in sequence quality impacted the ability to generate consensus sequences from the forward, and reverse reads, as high-quality sequences from both directions are typically required to create reliable consensus sequences. The poor quality of the reverse sequences also prevented the construction of sense strand contigs, which are essential for accurate multiple sequence alignments of the *ITS2* region. The poor quality of the reverse sequences in the *ITS2* sequencing may be attributed to primer-related issues if they failed to bind effectively, which could result in incomplete or noisy sequence reads.

The NCBI BLAST search results (**Appendix 3D**) revealed that the *ITS2* sequences with fragment sizes of ≈410bp and ≈500bp fragments showed a high degree of similarity with *Anopheles maculipalpis* isolate KH08 *internal transcribed spacer 2* (Sequence ID: MT408571.1) with a sequence identity of >99%. Similarly, the *ITS2* sequences that produced fragments ranging from ≈400bp and ≈610bp had a 99% sequence identity to *Anopheles maculipalpis* haplotype, *Internal Transcribed Spacer 2*, region. (Sequence ID: KR014835.1). An *ITS2* sequence alignment was performed using only the forward nucleotide sequences, which varied in length **(Figure 3.26).** The alignment revealed a high degree of similarity among the samples morphologically identified as *An. maculipalpis*, with nucleotide differences observed at only two positions. The nucleotide code Y positioned at 69 base pairs represents either a C (cytosine) or T (thymine).

All *COI* specimens had an NCBI BLAST result of *An. maculipalpis* mitochondrion (Sequence ID: NC_064606.1) with a 100% nucleotide identity. For the *COI* alignment, both DNA strands (*COI-F* and *COI-R*) were used to generate contigs, increasing the reliability of the sequencing data **(Figure 3.27).** The sequences were similar with minor nucleotide differences in eleven positions. There were two M and R base substitutions and one Y and K base substitutions at different sites. Overall, the species exhibited the least number of variable sites and significant genetic homogeneity with regard to the *ITS2* and *COI* sequences. **Appendix 3D** shows the BLAST search results and the generated *COI* accession numbers obtained for these *An. maculipalpis* specimens.

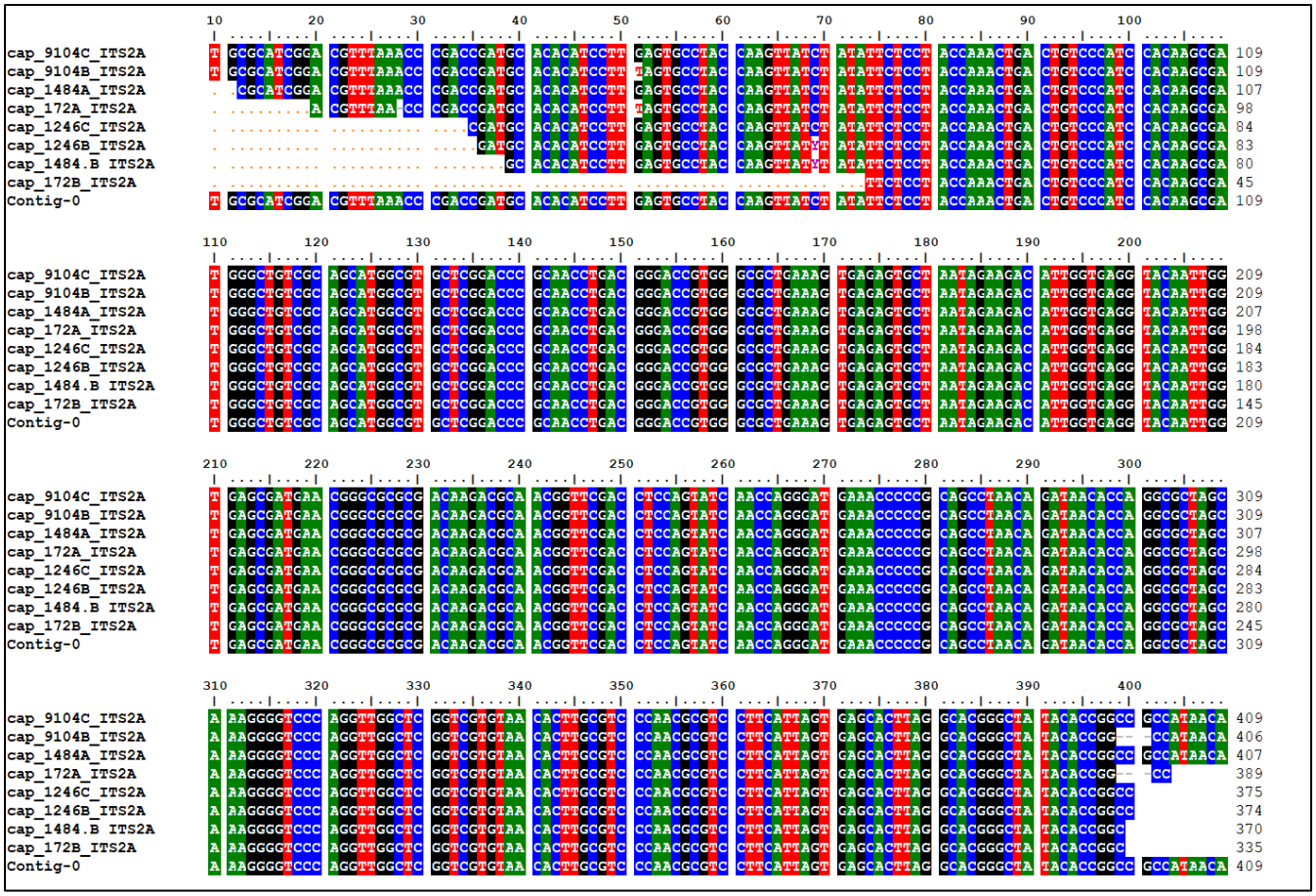


Figure 3.26: Alignment of *ITS2* nucleotide sequences from *Anopheles maculipalpis* samples collected in KwaZulu-Natal. This alignment shows the *ITS2* sequences obtained from 8 *An. maculipalpis* individuals, representing specimens from each of the families. The alignment was performed using forward sequences only due to poor quality of reverse reads.



Figure 3.27: Multiple sequence alignment of the *COI* region from *Anopheles maculipalpis* group specimens. This alignment shows the *COI* sequences obtained from 8 *An. maculipalpis* individuals, representing three specimens from each of the families. Consensus sequences were generated and aligned using BioEdit. Sequences highlighted in yellow rectangular boxes indicate the locations of the *COI* forward and reverse primer binding sites used during PCR amplification.

3.7 SPOROZOITE DETECTION IN *ANOPHELES MARSHALLII* GROUP AND *ANOPHELES MACULIPALPIS*

Field-collected female mosquitoes were examined for the presence of *Plasmodium* using the hydrolysis probe assay (TaqMan assay), which utilizes Taq DNA polymerase's "5 - 3" exonuclease activity. A total of 82 *An. marshallii* group and 10 *An. maculipalpis* female specimens were analysed. Of the 92 analysed samples, only 9% (n=8) of the *An. marshallii* group samples initially showed positive results (Ct value <30, RFU value >500). However, upon repeating the assay to confirm the presence of sporozoites, these samples resulted in false positives **(Table 3.8).** Subsequent PCR tests on these specimens returned negative results, indicating no true sporozoite infections. Therefore, none of the specimens tested positive for sporozoite infections. Despite the fact that none of the specimens had a positive *Plasmodium* infection test, the absence of detected infections does not preclude the possibility of ongoing malaria transmission in the study area.

Table 3.8: Summary of *Plasmodium* infectivity results.

Species	N (Sample size)	Bass PCR+	False Bass PCR+	Bass PCR-
An. marshallii group	82	0	7	82
An. maculipalpis	10	0	0	10
Total	92	0 (0%)	7 (7.6%)	92 (100%)

CHAPTER FOUR
DISCUSSION

This study investigated the characteristics of understudied *Anopheles* species may be involved in malaria transmission cycles utilising both morphological and DNA-based methods. Although less extensively studied compared to other prominent malaria vectors like *Anopheles gambiae* and *An. funestus,* emerging evidence suggests that the *An. marshallii* group may play a role in malaria transmission in certain regions where it is present. The primary objective of this study was to accurately identify *An. marshallii* group species in South Africa using *a priori* identification methods based on morphological characteristics and molecular techniques. This synergistic approach has proven vital in characterising other *Anopheles* species and offers valuable insights into the species' potential as a malaria vector.

4.1 MORPHOLOGICAL ANALYSIS

Despite the high number of *Anopheles* females collected from various sampling sites, colonising and rearing mosquito species in a laboratory setting proved challenging. Despite being supplied with a blood meal, many female mosquitoes failed to feed successfully, leading to poor egg production. Among the females that laid eggs, hatch rates were notably low, likely due to a combination of environmental and physiological factors, such as fluctuating temperatures and humidity levels in the insectary during the experimental period. Thermal stress likely contributed to the low egg survival rates observed, given the elevated and unstable temperature conditions in the insectary at the NICD during the experimental period. Although specific temperature data were not recorded, it was noted that the insectary often exceeded the ideal rearing range of 25°C ± 2°C. High temperatures are known to negatively affect the viability of *Anopheles* eggs by accelerating desiccation, shortening the pre-hatching phase, and disrupting embryonic development (Clements, 1992). These factors may have negatively impacted feeding behaviour and egg viability. However, other factors likely contributed to the low hatch rates, including the age and physiological state of the field-collected females, possible incomplete insemination, and stress caused by transport and handling. Such stress can suppress blood-feeding responses and impact reproductive output, making colonisation in the laboratory particularly difficult for wild-caught mosquitoes. These

variables likely contributed to low feeding success and decreased fecundity. Such influences have been reported in previous studies on *Anopheles* reproductive biology and egg viability (Yaro *et al.,* 2006; Impoivil *et al.,* 2007; Ghosh *et al.,* 2024; Ottih & Tripet, 2024).

In this study, four families belonging to the *Anopheles marshallii* group were studied in depth. While the specimens exhibited wide morphological variation, they were assigned to the *An. marshallii* group. However, the precise identification of each family to the species level remained unresolved, highlighting the limitations of morphological methods in differentiating closely related species within species complexes. The morphological analyses carried out in this study did not yield conclusive results for species-level identification of the *An. marshallii* group families. The use of egg and larval morphology for identifying *An. marshallii* group samples presented various issues that limited their usefulness as a diagnostic tool in this study. Due to the limited availability of egg clutches, there was insufficient detail to accurately assess variability in egg morphology within the *An. marshallii* group. This limited sample size may not capture the whole aspects of morphological characteristics, which could lead to the omission of distinctive traits that could be present in a larger sample set. It was difficult to capture the fine structural details of the eggs due to the poor resolution of the microscope used to observe egg morphology during the investigation **(see Figure 3.7).** High-resolution imaging, like scanning electron microscopy (SEM), is frequently needed to observe egg morphology in order to precisely view distinguishing characteristics like surface texturing or float structure. The quality of the egg images would have appeared better had they been examined under a SEM. Without this level of detail, identifying subtle differences that could distinguish species was challenging. Unfortunately, due to time constraints and a limited number of eggs, the eggs were placed into water immediately to allow for egg hatching. Future studies should prioritise SEM examination for the egg morphology. During the study, larval specimens were preserved in ethanol, which sometimes led to stiffened or distorted samples and loss of structural integrity **(see Figure 3.8).** Important morphological characteristics were obscured by this handling procedure, which led to an erroneous examination of these specimens. This suggests that if morphological data are to be utilised for identification, then consistent rearing and preservation procedures are necessary to allow for accurate and reliable identification, ensuring that important diagnostic traits are preserved and observable for proper taxonomic analysis.

The adult morphological traits (leg, palp, wing), while informative, failed to provide distinct diagnostic features that could reliably separate species within the *An. marshallii* group

specimens from KZN. Despite the tarsal segment markings, which are generally helpful in identifying species, no clear distinctions were found amongst the *An. marshallii* group families **(see Figure 3.10).** Similarly, no discernible variation in apical banding patterns that could facilitate species identification was observed in the palps (**see Table 3.1**). Palps are recognised for their diagnostic potential in other *Anopheles* species complexes, such as *An. gambiae s.l.* and *An. melas* (Bryan, 1980; Annan *et al.,* 2015). Furthermore, wing morphology, which is commonly employed due to its conserved characteristics and venation patterns, failed to distinguish between the *An. marshallii* group families from this study. This may be attributed to the high degree of morphological similarity among sibling species within the group, which makes it difficult to separate species using traditional keys because many of their diagnostic features overlap or lie within a small range of variation. Additionally, environmental factors like temperature may have contributed to morphological plasticity, which obscures actual genetic differences and makes it challenging to identify species based solely on phenotype.

Earlier studies have found that geometric morphometrics approaches based on wing shape and wing venation analysis can aid in identifying members among the *Anopheles* species group and complex, such as the three species of the *An. maculatus* group (Chaiphongpachara *et al*., 2019) and two species of the *An. minimus* complex (Chatpiyaphat *et al*., 2021*).* The geometric morphometric analysis results from a study conducted by Chaiphongpachara *et al.* (2022) clearly distinguished *An. baimaii* and *An. dirus* (sibling species of the *An. dirus* complex) based on the wing shape. It was determined that this is a useful technique for accurately identifying the species of these two malaria vectors. Wing size, on the other hand, was found to be more susceptible to environmental fluctuations and need to be interpreted cautiously in these kinds of investigations.

In this study, wing length, morphology, and wing spot ratios were examined to assess variation among female *An. marshallii* group mosquitoes, however, the specimens analysed here showed no notable differences in wing length **(see Table 3.2).** This lack of variation can likely be attributed to the similar environmental conditions in both the natural collection sites and the insectary where the offspring were reared, although no direct quantitative measurements of temperature and humidity were recorded during rearing. Consistent body size, as influenced by environmental factors, is known to correlate with wing length, which likely accounts for the uniformity observed in the wing measurements of these specimens. It is conceivable that the quality of the larval food may have affected the wing and palp

measurements in this study, since the overall size of adult mosquitoes can be significantly influenced by the larval diet and quality of the larvae, with larger adults generally being produced by better-fed larvae (Damiens *et al*., 2014; Tuno *et al*., 2023). Larger adults that result from enhanced nutrition would have longer wings and increased wing spot ratios, which could have an impact on the species-specific morphological traits that are typically used for identification. Barreaux *et al.* (2016) reported that elevating larval rearing temperatures from 23°C to 31°C caused a significant reduction in adult wing length. Numerous studies have shown a positive correlation between larval nutrition and adult wing length in *Anopheles* species. In a study conducted by Vantaux *et al.* (2016), *Anopheles gambiae* larvae with limited food availability produced adults with considerably smaller wings than those that were given adequate food. Likewise, Valerio *et al.* (2016) found that a greater amount of larval diet led to longer wing lengths in both male and female *Anopheles gambiae*. This variation underscores the need to take into account elements like diet that could affect morphometric data and affect species identification or comparisons.

Wing morphology was combined with other morphological characters, such as the egg and larval features, to provide an extensive and accurate assessment of species identity. Integrating multiple characters enhances the accuracy and reliability of species identification. However, no clear separation between the families using the egg, larval and adult characteristics could be achieved. These findings highlight the challenges of morphological identification, especially for cryptic species where subtle morphological differences can be difficult to discern.

Despite the challenges presented by missing and/or incomplete body parts (legs and wings) in *An. hargreavesi* and *An. gibbinsi* samples, morphological identification was eventually successful for these samples. *Anopheles gibbinsi* was identified based on distinctive morphological traits, such as pale bands on the palps and particular markings on wing veins, whereas *An. hargreavesi* samples were identified morphologically using scale morphology. This does, however, draw attention to a drawback of morphology-based species identification techniques, as damaged samples may result in incorrect identification or the inability to confirm identity. This study relied on the expertise of a few skilled individuals to confirm the morphological identification of *An. gibbinsi* and *An. hargreavesi* samples, and without their input morphological identification would most likely have been inaccurate. Only a handful of trained taxonomists have the expertise required for high-accuracy identification, leading to

excessive reliance on these few experts. *Anopheles maculipalpis* specimens being misidentified as *An. pretoriensis* also highlights the challenges posed by the limited availability of trained taxonomists in the field. Without enough trained professionals, accurate species identification is compromised, which can impact the reliability of field data and vector control strategies.

4.2 MOLECULAR ANALYSIS

4.2.1 Sequence Analysis

The other goal of this study was to generate a DNA barcode database for the *An. marshallii* group and other anopheline species, using a combination of iso-female lines and molecular techniques. Although morphological analysis was used for initial species identification, a greater resolution of genetic diversity and evolutionary relationships among the examined populations was made possible by DNA sequencing. Understanding the distribution and vectorial potential of species is mainly dependent on accurately identifying them among morphologically similar groups or complexes. Therefore, DNA sequencing was used as an attempt to discriminate the families belonging to the *An. marshallii* group. Currently, there is no rapid or accurate method of identifying *An. marshallii* group species, which poses a challenge for surveillance studies involving the group.

Numerous studies have examined the effectiveness of *ITS2* and *COI* loci in detecting different species of *Anopheles* from various regions. The *ITS2* region is commonly used for species identification due to its variability and evolutionary conservation. Compared to other rDNA regions, it shows greater sequence diversity, which qualifies it for phylogenetic and species-level identification. *Anopheles* species that are cryptic or closely related can be distinguished from one another using *ITS2* sequencing data. This is especially helpful in detecting sibling species complexes or newly discovered species. The *ITS2* region has been used to differentiate between different species of *Anopheles* mosquitoes, including the *An. dirus* complex (Walton *et al*., 1999), *An. funestus* group (Koekemoer *et al*., 2002), *An. hyrcanus* group (Li *et al*., 2005) and *An. maculatus* group (Ma *et al*., 2006). This gene has been proven to be more effective than the *COI* gene. The *COI* gene has the highest level of nucleotide divergence and consists of both highly conserved and variable regions (Burton and

Lee, 1994; Zang and Hewitt, 1997). Due to their limited ability to repair DNA replication errors, mitochondria experience a faster mtDNA mutation rate than nuclear DNA (Allio, *et al*., 2017). This comparatively greater mutation rate in many vertebrates has made it a useful marker for researching relatedness patterns among species populations (Walton *et al*., 1999). In the present study, both *ITS2* and *COI* loci were employed to differentiate species within the *An. marshallii* group, revealing insights that morphological methods alone could not provide.

In this study, the *Anopheles funestus* PCR assay (Koekemoer *et al.*, 2002) was used to complement the *ITS2* and *COI* sequencing in order to detect species-specific DNA variations in both the ribosomal and mitochondrial regions. The PCR results provided valuable insights into the species composition of the *An. marshallii* group specimens collected from KZN. Some of the specimens produced hybrid bands, suggesting the possibility of mixed-species amplification or the presence of closely related species. Some specimens amplified as *An. leesoni*, indicating that these specimens, despite being identified morphologically as *An. marshallii* group may belong to another species. This underscores the difficulty in distinguishing between closely related species within the *An. marshallii* group. Some samples did not produce amplicons, which may be due to DNA degradation affecting the efficiency of the PCR process or the assay's lack of species specificity for those particular specimens. Degraded DNA results in fragmented templates, which decreases the efficiency of PCR amplification. In this study, fresh F_1 samples from iso-female families were successfully amplified, whereas several field-collected adult samples, which had been stored for long periods, failed to amplify. This indicates that DNA degradation may be a significant issue. The *An. funestus* PCR assay, while valuable for preliminary species screening, was not definitive across diverse species groups. This reinforces the need for additional molecular techniques, such as DNA sequencing, to provide more accurate species identification.

It was established from the sequencing results that the *An. marshallii* group specimens from KZN possessed a low level of DNA variation across both *ITS2* and *COI* markers. The *ITS2* sequences were 99.5 - 100% identical across the four iso-female lines, while the *COI* sequences showed greater than 98% identity, with only a few variable nucleotide positions observed across a 745 bp alignment. These findings strongly suggest that the specimens likely belong to a single species, given their high inter-individual sequence similarity. This could be explained by the fact that the specimens share a great deal of rDNA and mtDNA

indicating that they are the same species. This is likely due to the geographic proximity of the sample populations in northern KZN, which could facilitate gene flow. The limited divergence observed in the *COI* sequences suggests a high level of conservation, perhaps because of selective pressures that preserve gene integrity across the species. The individual specimens that were compared in this context are closely related and may have undergone recent divergence, but there may not have been sufficient time for mutations to accumulate and generate significant variation in the *ITS2* and *COI* regions. The phylogenetic trees generated using both *ITS2* and *COI* data further support this, as all KZN specimens formed a single well-supported clade (bootstrap values > 90%) distinct from other known African *An. marshallii* group species **(see Figure 3.22 - 3.23).** Interestingly, the *ITS2* sequences showed a 78% match with *An. theileri* reflecting a level of genetic similarity between this species and *An. marshallii* group specimens. This could be the result of historical taxonomic confusion, as *An. brohieri* (a member of the *An. marshallii* group) was often treated synonymously with *An. theileri*. Studies on their morphology and genetics suggested that the two species are closely related and likely share a common ancestor (Green, 1981; Gillies and Coetzee, 1987). It is possible that *An. brohieri* sequences were deposited into the GenBank as *An. theileri* since the species are often treated as synonyms. The species names picked up when the *ITS2* and *COI* consensus sequence were queried against the NCBI database using BLASTn do not fall under the *An. marshallii* group, which could suggest that the available data in the database may be incomplete, and the correct name might not be linked to the morphological information. This could be due to missing or outdated information leading to discrepancies between morphological identification and the listed name following sequencing. Such challenges are exacerbated by the lack of reference sequences in public databases like GenBank for many species, limiting the ability to definitively confirm species identities using molecular data.

Hybridisation events may have made it difficult to differentiate between *An. marshallii* group species using molecular markers, as genetic material could have been exchanged between them. These closely related species have similar sequences, possibly due to incomplete evolutionary sorting or hybridisation that reduces the ability to distinguish species. Similar findings using mtDNA have been reported in previous studies. According to Fontaine *et al.* (2015), the mtDNA displayed patterns that were compatible with continuous gene flow between *An. arabiensis* and *An. gambiae* or *An. coluzzii*, and they also discovered widespread introgression amongst *An. gambiae* complex species. This study also corroborates previous

research that showed low genetic variation in *An. stephensi* populations that were collected from two different cities in Saudi Arabia (Munawar *et al*., 2020). The results were obtained by using the analysis of the *ITS2* and *COI* markers. According to the researchers, these findings were caused by widespread gene flow and ecotype adaptations with limited intraspecific variation.

Low genetic variation was also found in *An. hargreavesi ITS2* and *COI* sequences. This high degree of homology can be attributed to the fact that these species share a common ancestor, as a result, they retain many similarities in their genetic sequences due to their shared evolutionary heritage. Confirmation of identification proved challenging in the absence of reference sequences for *An. hargreavesi* in publicly accessible databases. The lack of published genetic sequences for *An. hargreavesi* illustrates a common issue when working with understudied species, where novel sequences might be listed under different or outdated names. It is common for new species to be described without having their genetic sequences published, especially if they have not been studied in great detail. However, there is also a possibility that these sequences have been published under a different name. This underscores the drawbacks of using currently available databases for molecular identification. The lack of existing *ITS2* or *COI* sequences for *An. hargreavesi* meant that the sequencing data could not be directly matched to GenBank records or compared with published phylogenies. This reduced the strength of our conclusions regarding the exact taxonomic position and molecular identity of the specimens. While the sequence data were internally consistent, showing >98% identity across individuals, the possibility that specimens represent a misidentified or closely related taxon could not be excluded.

The *ITS2* region of *An. gibbinsi* showed high homology, with a 100% match to "*Anopheles sp. 6*" from Kenya that was published in earlier research (Cooke *et al*., 2015; Gebhardt *et al*., 2022), suggesting these two are the same species. The designation of *An. gibbinsi* as *Anopheles sp. 6* indicates that this species is in the process of being formally described, and it provides more background to this understudied taxon. This, however, emphasises how ambiguous species names can be during taxonomic description processes.

Variations were observed in the size of *ITS2* fragments of *An. maculipalpis* samples despite all samples being confirmed as *An. maculipalpis*. These differences may be attributed to several factors. The *ITS2* region can exhibit genetic diversity among individuals of the same species that manifests as insertions or deletions in non-coding areas, leading to variations in

fragment length. Furthermore, the *ITS2* region is a component of the ribosomal DNA, which is found throughout the genome in many copies. Because of the heterogeneity of these multicopy genes, distinct copies within an individual may amplify fragments with slightly varying sizes.

Across the broader species alignment, the high level of sequence variation, particularly in the *ITS2* region, highlights its utility as a marker for uncovering genetic diversity and facilitating species differentiation. The *ITS2* alignment exhibits considerable sequence diversity, as seen by the substantial number of base substitutions and frequent INDEL events found across the alignment, resulting in significant length variation between sequences. Despite this variability, some areas of the *ITS2* region showed conservation, especially those connected to primer binding sites or retained functional motifs. Both point mutations and INDEL events contribute to this diversity, providing genetic markers for species differentiation. In contrast, the *COI* sequence alignment revealed a complex pattern characterised by a combination of highly conserved and variable regions among the aligned *Anopheles* species. These conserved regions are likely essential for maintaining the structural and functional integrity of the *COI* gene, as well as for precise species identification and phylogenetic analysis. Additionally, variable areas that showed notable sequence diversity throughout the *Anopheles* species were apparent in the *COI* alignment. These varying locations can be a reflection of past demographic trends, selective forces operating on various mosquito populations, or evolutionary adaptations. Some of the sequences in the study showed unusual combinations of INDELs and base substitutions, suggesting the presence of novel genetic variations, whereas other sequences closely matched existing reference sequences. This variability indicates the evolutionary processes that shape these species and emphasises the role of the *COI* gene, despite being more conserved than *ITS2,* in revealing deeper evolutionary relationships.

4.2.2 Phylogenetic Relationship

The phylogenetic trees generated from *ITS2* and *COI* sequences offer valuable perspectives into the genetic diversity and evolutionary relationships among *Anopheles* species in the study. The significant degree of sequence diversity in the *ITS2* region was reflected in the formation of multiple well-supported clades in the tree. This indicates a significant degree of sequence diversity in the *ITS2* region, making it a reliable molecular marker for distinguishing species within the *An. marshallii* group. *Anopheles brohieri* and *An. hancocki*

are nested together in the tree despite their phenotypic differences. This suggests that these species share a recent common ancestor. The clustering of *An. brohieri* and *An. hancocki* in the same clade raises the possibility of cryptic speciation, where these species might be more closely related than previously thought based on morphological characteristics alone. *Anopheles gibbinsi, An. hargreavesi* and *An. marshallii* group isolates formed separate branches on the tree, suggesting substantial genetic distinctiveness. This could suggest these species have been evolving independently for longer periods, accumulating mutations that differentiate them genetically. The divergence observed reflects their unique evolutionary trajectories, which may correspond to differences in geographic distributions. *Anopheles gibbinsi* specimens from Zambia were grouped separately from other species in the tree, while *An. hargreavesi* from Nigeria formed a distinct clade. Additionally, *An. marshallii* group specimens collected from KZN (South Africa) exhibited unique *ITS2* sequences that did not align with any existing reference. These regional variations in sampling sites might indicate past geographic isolation or ecological specialisation that led to lineage divergence. Despite being morphologically similar, these species can be distinguished from one another by the unique mutations they have accrued in the *ITS2* region.

The *COI* phylogenetic tree also displays *An. brohieri* and *An. hancocki* clustering together. The idea that these species have a close evolutionary relationship is supported by this consistency across these markers. Their shared evolutionary lineage is reflected in both mitochondrial and ribosomal DNA, despite their morphological differences. The *COI* tree, while informative, shows some inconsistencies compared to the *ITS2* tree. The grouping of *An. marshallii* group and *An. hargreavesi* in a single clade shows some considerable genetic similarity, but the poor bootstrap support suggests uncertainty in the strength of this relationship. This might be the result of inadequate lineage sorting, hybridisation events, or the low variance in *COI* sequences between these species. This suggests that *COI* may not be as reliable as *ITS2* for distinguishing closely related species within this group. These results highlight the complexity of *Anopheles* taxonomy and the importance of thorough molecular research in order to better understand species variety and evolutionary relationships.

4.2.3 Sporozoite Detection

An essential part of malaria control programs involves determining the sporozoite rates in mosquito vectors, which enables evaluation of the risk of transmission and the effectiveness of any control measures. The hydrolysis probe assay has been found to be the most sensitive and most specific of all the previously evaluated assays using genomic DNA samples for all four *Plasmodium* species (Bass *et al*., 2018). Since the test is highly specific, there is a small chance that the tested samples could give positive results. It is difficult to explain why some of the *An. marshallii* group samples falsely tested positive for *Plasmodium.* One possibility is that the assay detected a similar antigen that is not *Plasmodium* but is present in the mosquito. Results from the assay could have been falsely positive due to a cross-reaction with mosquito DNA. This may occur if the assay's primers significantly resemble sequences found in the mosquito genome, leading to non-specific amplification. Another possibility could be contamination with *Plasmodium* DNA from external sources during sample processing and DNA extraction may have taken place. However, this is highly unlikely because the laboratory adheres to strict contamination control procedures. Furthermore, negative controls were included in every PCR run, and all yielded negative results, confirming that no cross-contamination occurred during the assays. Some mosquito species carry commensal or symbiotic microbes in their tissues, including in their guts. If the genetic sequences of these organisms are not sufficiently differentiated from those of *Plasmodium* during molecular testing, it could result in false-positive results. To mitigate false positives, it is advisable to retest all positive samples by re-running the qPCR assay. This can confirm the reproducibility of results and help distinguish true positives from sporadic background signals or artefacts. Primers and probes should be regularly validated and optimised against mosquito genomes and known non-target DNA. This ensures specificity and reduces the likelihood of cross-reactivity, especially in field-collected samples that may contain complex DNA backgrounds. Sequencing can also assist in determining the true identity of the amplified DNA.

Previous studies have shown that zoophilic mosquito species in Africa can have false-positive *Plasmodium* infections, which can have detrimental effects on vector control (Sylla *et al*., 2000; Koekemoer *et al.,* 2001; Bigoga *et al.,* 2007; Mouatcho *et al*., 2007). Detecting false positives can lead to inaccurate assessments of malaria risk in affected regions, potentially resulting in a misallocation of resources for vector control strategies and public health interventions. Unnecessary public health responses such as mass insecticide spraying

campaigns or community-wide prophylactic treatment programs may inadvertently harm non-target organisms or disrupt ecological relationships, leading to unintended consequences for biodiversity and ecosystem functioning. This can erode public trust in the accuracy and reliability of mosquito surveillance and control efforts. This loss of confidence may undermine community participation in malaria control programs and hinder public health authorities' ability to communicate and implement disease control measures effectively.

Furthermore, accurately detecting sporozoites is crucial for evaluating secondary malaria vectors, such as those in the *An. marshallii* group, as they can still contribute to low-level or residual malaria transmission, particularly in regions where primary vectors have been suppressed through control interventions (Afrane *et al.*, 2016). These secondary vectors often display exophilic or zoophilic behaviours, making them difficult to target with standard indoor strategies like IRS and ITNs (Russell *et al.,* 2011; Sougoufara *et al*., 2020; Carnevale and Manguin, 2021). Their role in ongoing transmission might be overlooked if they are misidentified or wrongly assumed to be non-infective due to detection errors. This highlights the need for highly specific and sensitive detection tools, especially when assessing the transmission potential of understudied species. Understanding the infection status of these vectors essential for formulating comprehensive malaria control programs that do not leave any vector unaddressed

4.3 FUTURE DIRECTIONS

The majority of African malaria vectors have comparatively well-studied biology. Numerous studies on their life cycles, mating patterns, and behaviours have made it possible to create targeted control methods such as indoor residual spraying (IRS) and insecticide-treated nets (ITNs). However, malaria is still endemic throughout Africa due to difficulties in distinguishing malaria vectors that are part of species complexes. The *Anopheles marshallii* group remains less understood, which could present challenges for vector control in areas where it may be present. Understanding the role that the *An. marshallii* group plays in malaria transmission requires accurate species identification. The methodology used in this study has been applied to many other species complexes in the genus *Anopheles*, however, despite the rigorous methodology employed, the results of the *An. marshallii* group species identification was inconclusive. While several specimens were identified at the group level, definitive species identification proved challenging. None of the morphological characters investigated resulted in a clear distinction between the *An. marshallii* group families. The

measured wing spots, wing lengths and palp spots did not provide a clear distinction to completely differentiate *An. marshallii* group families.

Improved methodologies are needed to address the complexity of *An. marshallii* group species identification, as the current findings do not give a clear species distinction. With the morphological results being inconclusive, it would be ideal to turn the focus to cytogenetic approaches (Lambert, 1979; Lambert and Coetzee, 1982) for the identification of members of the *An. marshallii* group as additional research. Previous studies by Lambert (1979) and Lambert & Coetzee (1982) have shown that chromosomal inversion patterns in polytene chromosomes can differentiate members of the *An. marshallii* group. These findings serve as a reference point for developing updated taxonomic tools. Future research could use polytene chromosome analysis on wild-caught iso-female lines to strengthen species delimitation within this group. However, it is important to acknowledge that cytogenetic analyses can be time-consuming and require specialised infrastructure, well-preserved half-gravid females, and technical expertise in salivary gland dissection and chromosomal preparation, resources that were beyond the scope of this study.

While this study applied the dual approach, several methodological considerations warrant discussion. The data acquired from this study shows that molecular characterisation of mosquito species yields results that are more reliable than morphological tools. Hence, there should be more capacity to utilise molecular techniques. To enhance the precision of species identification, a PCR-based technique that offers a dependable and precise way of differentiating *An. marshallii* group species ought to be developed. However, the primary method for detecting malaria vectors should always be morphological identification, with molecular assays always used to confirm the results. Future research should also explore additional molecular techniques to enhance species-level resolution, particularly for cryptic taxa in the *An. marshallii* group. Methods like multi-locus sequencing, microsatellite genotyping, and next-generation sequencing (NGS) can reveal population structures and cryptic divergences when morphological traits are unclear (Ndo *et al.,* 2010; Campos *et al.,* 2022). Although these techniques are resource-intensive, they can provide high-throughput and accurate species identification, overcoming limitations of single-locus barcoding. Additionally, molecular protein profiling using Matrix-Assisted Laser Desorption/Ionization Time-Of-Flight Mass Spectrometry (MALDI-TOF MS) is a valuable tool for mosquito species identification (Müller *et al.,* 2013; Karisa *et al.,* 2024). Its key advantages include

requiring minimal tissue samples, rapid processing times, and being cost-effective. In future studies, integrating protein profiling with DNA methods would be advantageous. Further research with larger sample sizes will be conducted in order to better comprehend the genetic diversity and vectorial potential of these understudied *Anopheles* species. Future surveillance initiatives and sequencing studies can focus on confirming the accurate species identification of *An. marshallii* group specimens and mapping their geographic distribution with the aid of the sequences produced in this study for confirmed *An. marshallii* group species from KwaZulu-Natal (KZN).

CHAPTER FIVE
CONCLUSIONS

This study sought to molecularly characterise understudied *Anopheles* species from South Africa, focusing on the *Anopheles marshallii* group. The significance of utilising morphological identifications in conjunction with molecular assays, particularly in regions with a high vector diversity and limited morphological reference material, has been demonstrated by this study. Significant discrepancies between the initial morphological identification and the molecular confirmation were identified by sequencing data. The risk of relying solely on morphological identification was highlighted by the fact that specimens that were mistakenly recognized as *An. pretoriensis* based on morphological identification were later identified as the *An. maculipalpis* species using a molecular technique. These findings underscore the risk of relying solely on morphological tools for species identification, especially in the presence of cryptic or morphologically similar species. Morphological misidentifications may occur due to various factors, including biological, technical, and human-related ones.

Certain *Anopheles* species are cryptic, which means that although they differ genetically, they are morphologically identical or very similar (Harbach, 2013). Individuals with limited expertise may overlook subtle distinguishing features or misinterpret morphological characteristics. Accurate morphological identification often requires individuals with specialized training and experience who can observe fine morphological details. However, there is still a severe lack of expertise in taxonomy and morphological identification.

Numerous studies indicate a worldwide decrease in taxonomic skills and training resources (Hopkins and Freckleton, 2002; Tautz *et al.*, 2003; Engel *et al.*, 2021). These researchers highlight a taxonomic impediment: a lack of proficient taxonomists, obstructing biodiversity studies and vector monitoring. The authors emphasise that although molecular and digital technologies have advanced the discipline, they cannot replace the essential knowledge, skills, and experience of expert taxonomists. They stress the importance of building taxonomic capacity, particularly in developing areas where vector-borne diseases are prevalent. This study reinforces the importance of strengthening training in traditional taxonomic skills, as they are essential for correctly identifying species. Misidentifications emanating from morphological identification might have detrimental implications when assessing a species' bionomic features, vector status relationships, and malaria control effects (Stevensons *et al*., 2012; Davidson, 2019; Zhang *et al*., 2022).The accuracy of species identification is significantly improved when morphological identification is complemented with molecular techniques such as PCR, DNA barcoding, and sequencing to confirm species identity and identify cryptic species. The disparity between molecular and morphological identification emphasises how important it is to incorporate molecular methods to better distinguish between vector species, particularly in regions with considerable vector diversity (Zhang *et al.*, 2022).

This study recommends the use of DNA barcode sequences for effective identification and determination of evolutionary relationships among mosquito species. The two main genetic markers used in this study were the *ITS2* and the *COI* gene. These genetic markers are particularly useful for species-level resolution due to their high degree of sensitivity, making it possible to identify all variants in the relevant genes, therefore, misidentification of species is rare. Among molecular markers, the *COI* gene used in DNA barcoding is preferred for effective species identification and phylogenetic inference among mosquito species due to its broad taxonomic utility, ease of amplification, high interspecific resolution, and availability in global reference databases. While DNA barcoding is an effective tool, it has certain limitations. For instance, false negatives can arise from degraded DNA or primer mismatches that hinder successful amplification (Beebe, 2018). Similarly, the presence of pseudogenes or hybridisation events may complicate sequence interpretation (Choochote *et al.*, 2014; Pramasivan *et al*, 2022). Furthermore, relying solely on a single marker such as *COI* might not adequately resolve species complexes where *COI* divergence is minimal. Therefore,

utilising multilocus approaches that combine mitochondrial and nuclear markers like *ITS2* can enhance resolution and accuracy.

It is important to note that implementing molecular techniques in a field setting presents practical challenges. These challenges include the need for laboratory infrastructure, skilled personnel, high-quality reagents, and funding for sequencing (Gupta *et al.*, 2024; Alghamdi, 2025). Furthermore, shipping samples to specialised laboratories may introduce delays or contamination risks. Therefore, while molecular tools enhance resolution and accuracy, their widespread use requires sustainable investment in training, infrastructure, and regional sequencing capacity. Despite these limitations, in this study DNA sequencing allowed for a more thorough understanding of genetic diversity and evolutionary relationships among the specimens under study, even though morphological analysis provided initial species identification. The integration of molecular tools into routine surveillance programs can be a good way of limiting distribution or eliminating vectors as it offers vital insights into the precise vector species involved in the transmission of malaria by differentiating closely related species, and it can help monitor changes in vector distribution brought on by environmental changes or insecticide resistance (Hemingway *et al.*, 2016). Ultimately, this improved surveillance will in turn reduce malaria transmission by enabling more targeted and efficient control measures.

REFERENCES

Adam, J. P. (1956). Fauna and biological notes on *Anopheles* in the region of Yaounde and malaria transmission in the forestry area of Southern Cameroon. *Bulletin de la Société de Pathologie Exotique*, 49(1), 210-220.

Adeola, A. M., Botai, O. J., Olwoch, J. M., Rautenbach, C. D. W., Adisa, O. M., Taiwo, O. J., and Kalumba, A. M. (2016). Environmental factors and population at risk of malaria in Nkomazi municipality, South Africa. *Tropical Medicine and International Health*, 21(5), 675-686.

Adum, P., Agyare, V. A., Owusu-Marfo, J., and Agyeman, Y. N. (2023). Knowledge, attitude and practices of malaria preventive measures among mothers with children under five years in a rural setting of Ghana. *Malaria Journal*, 22(1), 268.

Afrane, Y. A., Bonizzoni, M., and Yan, G. (2016). Secondary malaria vectors of sub-Saharan Africa: threat to malaria elimination on the continent? *IntechOpen - Current Topics in Malaria*, 473-490.

Alberts, B., Johnson, A., and Lewis J. (2002). Molecular Biology of the Cell. 4th edition. *New York: Garland Science. From DNA to RNA.* Available from: https://www.ncbi.nlm.nih.gov/books/NBK26887/

Alghamdi, R. (2025). Bridging the gaps: prioritizing research strategies for enhanced malaria control and elimination. *Journal of Vector Borne Diseases*, 62(1), 24-38.

Allio, R., Donega, S., Galtier, N., and Nabholz, B. (2017). Large variation in the ratio of mitochondrial to nuclear mutation rate across animals: implications for genetic diversity and the use of mitochondrial DNA as a molecular marker. *Molecular Biology and Evolution*, 34(11), 2762-2772.

Al-Shuhaib, M. B. S., and Hashim, H. O. (2023). Mastering DNA chromatogram analysis in Sanger sequencing for reliable clinical analysis. *Journal of Genetic Engineering and Biotechnology*, 21(1), 115.

Annan, A. A., Kruppa, T. F., Adjei, O., and Garms, R. (2015). Palp ratio as a field identification tool for two members of the *Anopheles gambiae* complex in Ghana (*A. melas* and *A. gambiae*). *Parasites and Vectors*, 8:295

Antonio-Nkondjio, C., Kerah, C. H., Simard, F., Awono-Ambene, P., Chouaibou, M., Tchuinkam, T., and Fontenille, D. (2006). Complexity of the malaria vectorial system in Cameroon: contribution of secondary vectors to malaria transmission. *Journal of Medical Entomology*, 43(6), 1215-1221.

Antonio-Nkondjio, C., Simard, F., Awono-Ambene, P., Ngassam, P., Toto, J. C., Tchuinkam, T., and Fontenille, D. (2005). Malaria vectors and urbanization in the equatorial forest region of south Cameroon. *Transactions of the Royal Society of Tropical Medicine and Hygiene*, 99(5), 347-354.

Artemov, G. N., Gordeev, M. I., Kokhanenko, A. A., Moskaev, A. V., Velichevskaya, A. I., Stegniy, V. N., and Sharakhova, M. V. (2018). A standard photomap of ovarian nurse cell chromosomes and inversion polymorphism in *Anopheles beklemishevi*. *Parasites and Vectors*, 11, 1-9.

Asmare, Y., Wale, M., and Adem, S. (2022). Larval *Anopheles* species composition and diversity at different habitats and seasons of Gondar Zuria District, Ethiopia. *Journal of Tropical Medicine*, 9767155.

Ayala, F. J., and Powell, J. R. (1972). Allozymes as diagnostic characters of sibling species of Drosophila. *Proceedings of the National Academy of Sciences*, 69(5), 1094-1096.

Ayala, F. J., Powell, J. R., Tracey, M. L., Mourão, C. A., and Pérez-Salas, S. (1972). Enzyme variability in the *Drosophila willistoni* group. IV. Genic variation in natural populations of *Drosophila willistoni*. *Genetics*, 70(1), 113-139.

Bafort, J.M. (1985). *Anopheles marshallii s.l.*, a secondary vector of malaria in Africa. *Transactions of the Royal Society of Tropical Medicine and Hygiene* and *International Health*, 79(4), 566–567.

Baimai, V. (1975). Heterochromatin and multiple inversions in a *Drosophila* chromosome. *Canadian Journal of Genetics and Cytology*, 17(1), 15-20.

Barber, M. A., Olinger, M. T., and Putnam, P. (1931). Studies on malaria in southern Nigeria. *Annals of Tropical Medicine and Parasitology*, 25(3-4), 461-508.

Barrón, M. G., Paupy, C., Rahola, N., Akone-Ella, O., Ngangue, M. F., Wilson-Bahun, T. A., and Ayala, D. (2019). A new species in the major malaria vector complex sheds light on reticulated species evolution. *Scientific Reports*, 9(1), 14753.

Bass, C., Nikou, D., Blagborough, A. M., Vontas, J., Sinden, R. E., Williamson, M. S., and Field, L. M. (2008). PCR-based detection of *Plasmodium* in *Anopheles* mosquitoes: a comparison of a new high-throughput assay with existing methods. *Malaria Journal*, 7, 177.

Batovska, J., Blacket, M.J., Brown, K. and Lynch, S.E. (2016). Molecular identification of mosquitoes (Diptera: Culicidae) in southeastern Australia. *Ecology and Evolution*, 6(9), 3001-3011.

Becker, N., Petric, D., Zgomba, M., Boase, C., Madon, M., Dahl, C. and Kaiser, A. (2010). Mosquitoes and their control. *Springer, Heidelbeg*, 577.

Beebe, N. W. (2018). DNA barcoding mosquitoes: advice for potential prospectors. *Parasitology*, 145(5), 622-633.

Beebe, N. W., Ellis, J. T., Cooper, R. D., and Saul, A. (1999). DNA sequence analysis of the ribosomal DNA *ITS2* region for the *Anopheles punctulatus* group of mosquitoes. *Insect Molecular Biology*, 8(3), 381-390.

Bickford, D., Lohman, D. J., Sodhi, N. S., Ng, P. K., Meier, R., Winker, K., and Das, I. (2007). Cryptic species as a window on diversity and conservation. *Trends in Ecology and Evolution*, 22(3), 148-155.

Bigoga, J. D., Manga, L., Titanji, V. P., Coetzee, M., and Leke, R. G. (2007). Malaria vectors and transmission dynamics in coastal south-western Cameroon. *Malaria Journal*, 6, 1-12.

Brooke, B., Koekemoer, L., Coetzee, M., Kruger, P., and Urbach, J. (2013). Malaria vector control in South Africa: vector control. *South African Medical Journal*, 103(10), 784-788.

Brooke, B.D., Raman, J., Frean, J., Rundle, K., Maartens, F., Misiani, E., Mabuza, A., Barnes, K.I., Moonasar, D.P., and Dlamini, Q. (2020). Implementing malaria control in South Africa, Eswatini and southern Mozambique during the COVID-19 pandemic. *South African Medical Journal*, 110(11), 1072–1076.

Bryan, J. H. (1980). Use of the palpal ratio and the number of pale bands on the palps in separating *Anopheles gambiae s.s* Giles and *Anopheles melas* Theobald (Diptera: Culicidae). *Mosquito Systematics*, 12, 155-163.

Burton, R. S., and Lee, B. N. (1994). Nuclear and mitochondrial gene genealogies and allozyme polymorphism across a major phylogeographic break in the copepod *Tigriopus californicus*. *Proceedings of the National Academy of Sciences*, 91(11), 5197-5201.

Carnevale, P., and Manguin, S. (2021). Review of issues on residual malaria transmission. *The Journal of Infectious Diseases*, 223(2), S61-S80.

Carter, T.E., Yared, S., Gebresilassie, A., Bonnell, V., Damodaran, L., Lopez, K., Ibrahim, M., Mohammed, S. and Janies, D. (2019). First detection of *Anopheles stephensi* Liston, 1901 (Diptera: Culicidae) in Ethiopia using molecular and morphological approaches. *Acta Tropica*, 188, 180–186.

Chaiphongpachara, T., and Laojun, S. (2019). Variation over time in wing size and shape of the coastal malaria vector *Anopheles* (Cellia) *epiroticus* Linton and Harbach (Diptera: Culicidae) in Samut Songkhram, Thailand. *Journal of Advanced Veterinary and Animal Research*, 6(2), 208.

Chaiphongpachara, T., Changbunjong, T., Laojun, S., Sumruayphol, S., Suwandittakul, N., Kuntawong, K., and Pimsuka, S. (2022). Geometric morphometric and molecular techniques for discriminating among three cryptic species of the *Anopheles barbirostris* complex (Diptera: Culicidae) in Thailand. *Heliyon*, 8(10), 11261.

Chan, A., Chiang, L.P., Hapuarachchi, H.C., Tan, C.H., Pang, S.C., Lee, R., Lee, K.S., and Lam-Phua, S.G. (2014). DNA barcoding: Complementing morphological identification of mosquito species in Singapore. *Parasites and Vectors*, 7(569).

Chatpiyaphat, K., Sumruayphol, S., Dujardin, J. P., Samung, Y., Phayakkaphon, A., Cui, L., Sriwichai, P., *et al.* (2021). Geometric morphometrics to distinguish the cryptic species *Anopheles minimus* and *An. harrisoni* in malaria hot spot villages, western Thailand. *Medical and Veterinary Entomology*, 35(3), 293-301.

Choi, K.S., Christian, R., Nardini, L., Wood, O.R., Agubuzo, E., Muleba, M., Munyati, S., Makuwaza, A., Koekemoer, L.L., Brooke, B.D., Hunt, R.H. and Coetzee, M. (2014). Insecticide Resistance and role in Malaria Transmission of *Anopheles funestus* populations from Zambia and Zimbabwe. *Parasites and Vectors*, 7(464).

Choochote, W., Min, G. S., Intapan, P. M., Tantrawatpan, C., Saeung, A., and Lulitanond, V. (2014). Evidence to support natural hybridization between *Anopheles sinensis* and *Anopheles kleini* (Diptera: Culicidae): Possibly a significant mechanism for gene introgression in sympatric populations. *Parasites and Vectors*, 7, 1-13.

Chwatt, L. B., and Gockel, C. W. (1960). A study of the blood-feeding patterns of *Anopheles* mosquitos through precipitin tests. Results of collaborative work for the period 1955-59 and their application to malaria eradication programmes. *Bulletin of the World Health Organization*, 22(6), 685-720.

Ciubotariu, I. I., Jones, C. M., Kobayashi, T., Bobanga, T., Muleba, M., Pringle, J. C., and Norris, D. (2020). Genetic diversity of *Anopheles coustani* (Diptera: Culicidae) in malaria transmission foci in Southern and Central Africa. *Journal of Medical Entomology*, 57(6), 1782-1792.

Coetzee, M. (1982). A taxonomic and genetical study of the *Anopheles coustani* group of mosquitoes in Southern Africa. (Doctoral dissertation, University of the Witwatersrand).

Coetzee, M. (2020). Key to the females of Afrotropical *Anopheles* mosquitoes (Diptera: Culicidae). *Malaria Journal*, 19, 70.

Coetzee, M., and Koekemoer, L. L. (2013). Molecular systematics and insecticide resistance in the major African malaria vector *Anopheles funestus*. *Annual Review of Entomology*, 58, 393-412.

Coetzee, M., and Sueur, D. L. (1988). Effects of salinity on the larvae of some Afrotropical *anopheline* mosquitoes. *Medical and Veterinary Entomology*, 2(4), 385-390.

Coetzee, M., Kruger, P., Hunt, R.H., Durrheim, D.N., Urbach, J. and Hansford, C.F. (2013). Malaria in South Africa: 110 years of learning to control the disease. *South African Medical Journal*, 103(10), 770–778.

Coetzee, M., Segerman, J., and Hunt, R. H. (1987). Description of a new species *Anopheles* (Cellia) *kosiensis* (Diptera: Culicidae) from Zululand, South Africa. *Systematic Entomology*, 12(1), 23-28.

Cohuet, A., Simard, F., Toto, J.C., Kengne, P., Coetzee, M. and Fontenille, D. (2003). Species identification within the *Anopheles funestus* group of malaria vectors in Cameroon and evidence for a new species. *American Journal of Tropical Medicine and Hygiene*, 69(2), 200-205.

Coleman, A. W. (2003). *ITS2* is a double-edged tool for eukaryote evolutionary comparisons. *Trends in Genetics*, 19(7), 370-375.

Coluzzi, M., Sabatini, A., Petrarca, V., and Di Deco, M. A. (1979). Chromosomal differentiation and adaptation to human environments in the *Anopheles* gambiae complex. *Transactions of the Royal Society of Tropical Medicine and Hygiene*, 73(5), 483-497.

Connolly, J. B. (2023). Defining transformation events for gene drive in species complexes. Available from: [https://doi.org/10.21203/rs.3.rs-2806607/v1]

Cooke, M. K., Kahindi, S. C., Oriango, R. M., Owaga, C., Ayoma, E., Mabuka, D., and Stevenson, J. (2015). 'A bite before bed': exposure to malaria vectors outside the times of net use in the highlands of western Kenya. *Malaria Journal*, 14, 259.

Cornel, A. J., Porter, C. H., and Collins, F. H. (1996). Polymerase chain reaction species diagnostic assay for *Anopheles quadrimaculatus* cryptic species (Diptera: Culicidae) based on ribosomal DNA *ITS2* sequences. *Journal of Medical Entomology*, 33(1), 109-116.

Dahan-Moss, Y., Hendershot, A., Dhoogra, M., Julius, H., Zawada, J., Kaiser, M., and Koekemoer, L. L. (2020). Member species of the *Anopheles gambiae* complex can be misidentified as *Anopheles leesoni*. *Malaria Journal*, 19, 89.

Dahan-Moss, Y., Jamesboy, E., Lobb, L., Letinic, B., Zawada, J., Langa, Z., Brooke, B., *et al.* (2021). Malaria Vector Surveillance Report, South Africa, January–December 2020. *NICD Public Health Surveillance Bulletin*. Available from: [https://www.nicd.ac.za/wp-content/uploads/2022/12/MALARIA-VECTOR-SURVEILLANCE-REPORT-SOUTH-AFRICA-JANUARY-%E2%80%93-DECEMBER-2021.pdf]

Dahan-Moss, Y., Matamba, A., Jamesboy, E., Munhenga, G., Riddin, M., Shanahan, M., Guarido, M., Lobb, L., Mazarire, T., *et al.* (2022). Malaria vector surveillance report, South Africa, January-December 2021. *NICD Public Health Surveillance Bulletin*. Available from: [https://www.phbsa.ac.za/wp-content/uploads/2024/02/PHBSA-Malaria-vector-surveillance-report-2022.pdf]

Damiens, D., Benedict, M. Q., Wille, M., and Gilles, J. R. L. (2014). An inexpensive and effective larval diet for *Anopheles arabiensis* (Diptera: Culicidae): eat like a horse, a bird, or a fish? *Journal of Medical Entomology*, 49(5), 1001-1011.

Dandalo, L.C., Brooke, B.D., Munhenga, G., Lobb, L.N., Zikhali, J., Ngxongo, S.P., Zikhali, P.M., Msimang, S., Wood, O.R., and Mofokeng, M. (2017). Population dynamics and *Plasmodium falciparum* (Haemosporida: *Plasmodiidae*) infectivity rates for the malaria vector *Anopheles arabiensis* (Diptera: Culicidae) at Mamfene, KwaZulu-Natal, South Africa. *Journal of Medical Entomology*, 54(6), 1758–1766.

Davidson, J. R. (2019). Informing Vector-Borne Disease Intervention Strategies in Biodiversity Hotspots: Indonesia. (Doctoral dissertation). University of Notre Dame.

De Meillon, B. (1951). Species and varieties of malaria vectors in Africa and their bionomics. *Bulletin of the World Health Organization*, 4(3), 419-441.

De Meillon, B., and Pereira, M. D. C. (1940). Notes on Some Anophelines (Dipt. Culicidae) from Portuguese East Africa. *Mozambique Docum Trimestral*, (23), 69-83.

Dia, I., Guelbeogo, M. W., and Ayala, D. (2013). Advances and perspectives in the study of the malaria mosquito *Anopheles funestus*. *Anopheles mosquitoes-New Insights into Malaria Vectors*, 10, 55389.

Erlank, E., Koekemoer, L.L. and Coetzee, M. (2018). The importance of morphological identification of African anopheline mosquitoes (Diptera: Culicidae) for malaria control programmes. *Malaria Journal*, 17(43).

Evans. (1938). Mosquitoes of the Ethiopian Region. Larval Bionomics of Mosquitoes and Taxonomy of Culicine Larvae. *Annals of Tropical Medicine and Parasitology*, 30, 533.

Felsenstein, J. (1981). Evolutionary trees from DNA sequences: a maximum likelihood approach. *Journal of Molecular Evolution*, 17, 368-376.

Fontaine, M. C., Pease, J. B., Steele, A., Waterhouse, R. M., Neafsey, D. E., Sharakhov, I. V., and Besansky, N. J. (2015). Extensive introgression in a malaria vector species complex revealed by phylogenomics. *Science*, 347(6217), 1258524.

Frézal, L. and Leblois, R. (2008). Four years of DNA barcoding: Current advances and prospects. *Infection, Genetics and Evolution*, 8(5), 727–736.

Garros, C., and Dujardin, J. P. (2013). Genetic and phenetic approaches to *Anopheles* systematics. *Anopheles Mosquitoes: New Insights into Malaria Vectors. Rijeka: InTech*, 81-105.

Gebhardt, M. E., Krizek, R. S., Coetzee, M., Koekemoer, L. L., Dahan-Moss, Y., Mbewe, D., and Southern Africa International Centers of Excellence for Malaria Research. (2022). Expanded geographic distribution and host preference of *Anopheles gibbinsi* (*Anopheles species 6*) in northern Zambia. *Malaria Journal*, 21(1), 211.

Gerbi, S. A. (1986). The evolution of eukaryotic ribosomal DNA. *Biosystems*, 19(4), 247-258.

Gillies, M.T. and De Meillon B. (1968). The Anophelinae of Africa south of the Sahara (Ethiopian zoogeographical region). Johannesburg: *South African Institute for Medical Research*, 54, 1-343.

Gillies, M.T., and Coetzee, M. (1987). A supplement to the Anophelinae of Africa south of the Sahara (Afrotropical Region). *South African Institute for Medical Research*, 55, 1–143.

Ginzinger, D. G. (2002). Gene quantification using real-time quantitative PCR: an emerging technology hits the mainstream. *Experimental Hematology*, 30(6), 503-512

Gonzalez, I. L., Gorski, J. L., Campen, T. J., Dorney, D. J., Erickson, J. M., Sylvester, J. E., and Schmickel, R. D. (1985). Variation among human 28S ribosomal RNA genes. *Proceedings of the National Academy of Sciences*, 82(22), 7666-7670.

Green, C. A. (1970). Identifications of member species of the *Anopheles gambiae* complex in the Zambesi valley. *Central African Journal of Medicine*, 16(9), 207-209.

Green, C. A. (1981). Malaria epidemiology and anopheline cytogenetics. In Cytogenetics and genetics of vectors: proceedings of a symposium of the XVIth International Congress of Entomolog. *Elsevier Biomedical Press*, 21-29.

Green, C. A., and Hunt, R. H. (1980). Interpretation of variation in ovarian polytene chromosomes of *Anopheles funestus* Giles, *A. parensis* Gillies, and *A. aruni*? *Genetica*, 187–195.

Gupta, H., Sharma, S., Gilyazova, I., and Satyamoorthy, K. (2024). Molecular tools are crucial for malaria elimination. *Molecular Biology Reports*, 51(1), 555.

Hackett, B.J., Gimnig, J., Guelbeogo, W., Costantini, C., Koekemoer, L.L., Coetzee, M., Collins, F.H. and Besansky, N.J. (2000). Ribosomal *DNA internal transcribed spacer (ITS2)* sequences differentiate *Anopheles funestus* and *An. rivulorum*, and uncover a cryptic taxon. *Insect Molecular Biology*, 9(4), 369–374.

Hadebe, M. T., Malgwi, S. A., and Okpeku, M. (2023). Revolutionizing Malaria Vector Control: The Importance of Accurate Species Identification through Enhanced Molecular Capacity. *Microorganisms*, 12(1), 82.

Hall, T. A. (1999). BioEdit: a user-friendly biological sequence alignment editor and analysis program for Windows 95/98/NT. In *Nucleic Acids Symposium Series*, 41(41), 95-98).

Hamon, J., and Mouchet, J. (1961). Secondary vectors of human malaria in Africa. *Medecine Tropicale*, 21, 643-660.

Hamon, J., Sales, S., Coz, J., Ouedraogo, C. S., Dyemkouma, A., and Diallo, B. (1964). Observations on the dietary preferences of mosquitoes from the République de Haute-Volta. *Bulletin de la Société de Pathologie Exotique*, 57, 1133-1150.

Harbach, R. E. (1994). Review of the internal classification of the genus *Anopheles* (Diptera: Culicidae): the foundation for comparative systematics and phylogenetic research. *Bulletin of Entomological Research*, 84(3), 331-342.

Harbach, R. E. (2003). Mosquito systematics: from organisms to molecules--a tribute to Kenneth L. Knight. *Journal of the American Mosquito Control Association*, 19(4), 452-460.

Harbach, R. E. (2004). The classification of genus *Anopheles* (Diptera: Culicidae): a working hypothesis of phylogenetic relationships. *Bulletin of Entomological Research*, 94(6), 537-553.

Hay, S. I., Okiro, E. A., Gething, P. W., Patil, A. P., Tatem, A. J., Guerra, C. A., and Snow, R. W. (2010). Estimating the global clinical burden of *Plasmodium falciparum* malaria in 2007. *PloS Medicine*, 7(6), 1000290.

Hebert, P. D., and Gregory, T. R. (2005). The promise of DNA barcoding for taxonomy. *Systematic Biology*, 54(5), 852-859.

Hebert, P. D., Ratnasingham, S., and De Waard, J. R. (2003). Barcoding animal life: cytochrome c oxidase subunit 1 divergences among closely related species. *Proceedings of the Royal Society of London. Series B: Biological Sciences*, 270(1), 96-99.

Heid, C. A., Stevens, J., Livak, K. J., and Williams, P. M. (1996). Real-time quantitative PCR. *Genome Research*, 6(10), 986-994.

Hemingway, J., Ranson, H., Magill, A., Kolaczinski, J., Fornadel, C., Gimnig, J., and Hamon, N. (2016). Averting a malaria disaster: will insecticide resistance derail malaria control? *The Lancet*, 387(10029), 1785-1788.

Hong, S., Bunge, J., Leslin, C., Jeon, S., and Epstein, S. S. (2009). Polymerase chain reaction primers miss half of rRNA microbial diversity. *The ISME journal*, 3(12), 1365-1373.

Hunt, R. H. (1973). A cytological technique for the study of *Anopheles gambiae* complex. *Parassitologia*, 15(2), 137-9.

Hunt, R. H., and Coetzee, M. (1986). Field sampling of *Anopheles* mosquitos for correlated cytogenic, electrophoretic and morphological studies. *Bulletin of the World Health Organization*, 64(6), 897.

Hunt, R.H. and Coetzee M. (1989). A parasitological, cytogenetic and biochemical study of *Anopheles gambiae* (Diptera: Culicidae) from the People's Republic of Congo. *South African Medical Journal*, 76, 362-364.

Ingram, A., and De Meillon, B. (1927). A Mosquito Survey of Certain Parts of South Africa, with Special Reference to the Carriers of Malaria and their Control. *Publications of the South African Institute for Medical Research***,** 22, 1-81.

Iyiola, O. A., Kamaldeen-Ibrahim, A. T., Shaibu, R. D., Shittu, O., Fadipe, T. O., Adelaja, O. J., and Afolabi, H. A. (2021). Molecular characterization and phylogenetic analysis of collected mosquitoes (Diptera: Culicidae) from Northcentral Nigeria using mitochondrial *COI* and ribosomal *IGS* gene regions. *The Journal of Basic and Applied Zoology*, 82, 59.

Jones, C. M., Ciubotariu, I. I., Muleba, M., Lupiya, J., Mbewe, D., Simubali, L., and Norris, D. E. (2021). Multiple novel clades of anopheline mosquitoes caught outdoors in northern Zambia. *Frontiers in Tropical Diseases*, 2, 780664.

Jourdain, F., Picard, M., Sulesco, T., Haddad, N., Harrat, Z., Sawalha, S. S., and Robert, V. (2018). Identification of mosquitoes (Diptera: Culicidae): an external quality assessment of medical entomology laboratories in the MediLabSecure Network. *Parasites and Vectors*, 11, 553.

Kleinhans, I., Mahanjana, S., Els, F., Mabona, M., Pitso, L. A., Malatje, G., and Raman, J. (2024). The prevalence and distribution of malaria in Mpumalanga Province before and during COVID-19 (2017-2022). *South African Medical Journal*, 114(8), 29-36.

Knowlton, N. (1986). Cryptic and sibling species among the decapod Crustacea. *Journal of Crustacean Biology*, 6(3), 356-363.

Koekemoer, L.L, Lochouarn, L., Hunt, R. H., and Coetzee, M. (1999). Single-strand conformation polymorphism analysis for identification of four members of the *Anopheles funestus* (Diptera: Culicidae) group. *Journal of Medical Entomology*, 36(2), 125-130.

Koekemoer, L.L., (1999). Systematic studies on the *Anopheles funestus* (Diptera: Culicidae) group in Southern Africa. Doctoral Thesis. University of the Witwatersrand.

Koekemoer, L.L., Kamau, L., Coetzee, M. and Hunt, R.H. (2002). A cocktail polymerase chain reaction assay to identify members of the *Anopheles funestus* (Diptera: Culicidae) group. *The American Journal of Tropical Medicine and Hygiene*, 66(6), 804–811.

Koekemoer, L.L., Rankoe, E.M., la Grange, J.P., Govere, J. and Coetzee, M. (2001). False detection of *Plasmodium falciparum* sporozoites in *Anopheles marshallii* group mosquitoes. *Journal of the American Mosquito Control Association,* 17(3), 160–165.

Kress, W. J., and Erickson, D. L. (2008). DNA barcodes: genes, genomics, and bioinformatics. *Proceedings of the National Academy of Sciences*, 105(8), 2761-2762.

Kumar, S., Stecher, G., and Tamura, K. (2016). MEGA7: Molecular Evolutionary Genetics Analysis version 7.0 for bigger datasets. *Molecular Biology and Evolution*, 33(7), 1870-1874.

Kwi, P. N., Ewane, E. E., Moyeh, M. N., Tangi, L. N., Ntui, V. N., Zeukeng, F., and Apinjoh, T. O. (2022). Diversity and behavioral activity of *Anopheles* mosquitoes on the slopes of Mount Cameroon. *Parasites and Vectors*, 15(1), 344.

Lambert, D. M. (1979). *Anopheles marshallii* (Theobald) is a complex of species. *Mosquito Systematics,* 11(3), 173–178.

Lambert, D. M. (1983). A population genetical study of the African mosquito *Anopheles marshallii* (Theobald). *Evolution*, 484-495.

Lambert, D. M., and Coetzee, M. (1982). A dual genetical and taxonomic approach to the resolution of the mosquito taxon, *Anopheles* (Cellia) *marshallii* (Culicidae). *Systematic Entomology*, 7(3), 321-332.

Lambert, D.M. (1981). Cytogenetic evidence of a possible fourth cryptic species within the taxon *Anopheles marshallii* (Theobald) (Diptera: Culicidae) from Northern Natal. Mosquito Systematics, 13(2), 168–175.

Li, C., Lee, J. S., Groebner, J. L., Kim, H. C., Klein, T. A., O'Guinn, M. L., and Wilkerson, R. C. (2005). A newly recognized species in the *Anopheles Hyrcanus* Group and molecular identification of related species from the Republic of South Korea (Diptera: Culicidae). *Zootaxa*, 939(1), 1-8.

Lips, M. (1960). Anophelines of the Congo. 3. Fauna from Caves and Rock Clefts. Distribution, Medical Importance and Review of the Literature. *Rivista di Parassitologia*, 21(4), 289-306.

Lobo, N. F., Laurent, B. S., Sikaala, C. H., Hamainza, B., Chanda, J., Chinula, D., and Collins, F. H. (2015). Unexpected diversity of *Anopheles* species in Eastern Zambia:

implications for evaluating vector behavior and interventions using molecular tools. *Scientific Reports*, 5(1), 17952.

Loonen, J. A., Dery, D. B., Musaka, B. Z., Bandibabone, J. B., Bousema, T., van Lenthe, M., and Koenraadt, C. J. (2020). Identification of main malaria vectors and their insecticide resistance profile in internally displaced and indigenous communities in Eastern Democratic Republic of the Congo (DRC). *Malaria Journal*, 19, 1-10.

Ma, Y., Li, S., and Xu, J. (2006). Molecular identification and phylogeny of the *Maculatus* group of *Anopheles* mosquitoes (Diptera: Culicidae) based on nuclear and mitochondrial DNA sequences. *Acta Tropica*, 99(2-3), 272-280.

Macgregor, M. E. (1924). Report on the Anophelinae of Mauritius, and on certain Aspects of Malaria in the Colony, with Recommendations for a New Anti-malaria Campaign, London. 48.

Mahon, R. J., Green, C. A., and Hunt, R. H. (1976). Diagnostic allozymes for routine identification of adults of the *Anopheles gambiae* complex (Diptera, Culicidae). *Bulletin of Entomological Research*, 66(1), 25-31.

Mahon, R. J., Green, C. A., and Hunt, R. H. (1976). Diagnostic allozymes for routine identification of adults of the *Anopheles gambiae* complex (Diptera, Culicidae). *Bulletin of Entomological Research*, 66(1), 25-31.

Makunin, A., Korlević, P., Park, N., Goodwin, S., Waterhouse, R. M., von Wyschetzki, K., and Lawniczak, M. K. (2022). A targeted amplicon sequencing panel to simultaneously identify mosquito species and *Plasmodium* presence across the entire *Anopheles* genus. *Molecular Ecology Resources*, 22(1), 28-44.

Martin, D. P., Lemey, P., and Posada, D. (2011). Analysing recombination in nucleotide sequences. *Molecular Ecology Resources*, 11(6), 943-955.

Mattingly, P. F. (1955). Towards a zoogeography of the mosquitoes. Towards a zoogeography of the mosquitoes. *Publ. Syst. Ass.*, 4, 17-36.

Mayr, E. (1969) In: Principle of Systematic Zoology. New York: McGraw-Hill. *Scientific Publishes*, 83-88.

Miles, S. J. (1979). A biochemical key to adult members of the *Anopheles gambiae* group of species (Diptera: Culicidae). *Journal of Medical Entomology*, 15(3), 297-299.

Mishra, A. K., Bharti, P. K., Vishwakarma, A., Nisar, S., Rajvanshi, H., Sharma, R. K., and Lal, A. A. (2020). A study of malaria vector surveillance as part of the Malaria Elimination Demonstration Project in Mandla, Madhya Pradesh. *Malaria Journal*, 19, 447.

Mouatcho, J.C., Hargreaves, K., Koekemoer, L L., Brooke, B.D., Oliver, S.V., Hunt, R.H. and Coetzee, M. (2007). Indoor collections of the *Anopheles funestus* group (Diptera: Culicidae) in sprayed houses in northern KwaZulu-Natal, South Africa. *Malaria Journal*, 6, 30.

Mouchet, J., Carnevale, P., Coosemans, M., Julvez, J., Manguin, S., Richard-Lenoble, D., and Sircoulon, J. (2004). Biodiversity of malaria worldwide. *Editions John Libbey Eurotext, Montrouge*, France, 3-352.

Müller, P., Pflüger, V., Wittwer, M., Ziegler, D., Chandre, F., Simard, F., and Lengeler, C. (2013). Identification of cryptic *Anopheles* mosquito species by molecular protein profiling. *PLoS One*, 8(2), e57486.

Munawar, K., Saleh, A., Afzal, M., Qasim, M., Khan, K. A., Zafar, M. I., and Khater, E. I. (2020). Molecular characterization and phylogenetic analysis of anopheline (Anophelinae: Culicidae) mosquitoes of the Oriental and Afrotropical Zoogeographic zones in Saudi Arabia. *Acta Tropica*, 207, e105494.

Munhenga, G., Oliver, S. V., Lobb, L. N., Mazarire, T. T., Mashatola, T., and Brooke, B. D. (2022). Malaria risk and receptivity: Continuing development of insecticide resistance in the major malaria vector *Anopheles arabiensis* in northern KwaZulu-Natal, South Africa. *South African Journal of Science*, 118(3-4), 1-7.

Murugan, K., Vadivalagan, C., Karthika, P., Panneerselvam, C., Paulpandi, M., Subramaniam, J., and Benelli, G. (2016). DNA barcoding and molecular evolution of mosquito vectors of medical and veterinary importance. *Parasitology Research*, 115, 107-121.

Nyirakanani, C., Chibvongodze, R., Kariuki, L., Habtu, M., Masika, M., Mukoko, D., and Njunwa, K. J. (2017). Characterization of malaria vectors in Huye District, southern Rwanda. *Tanzania Journal of Health Research*, 19(3).

Oaks Jr, S. C., Mitchell, V. S., Pearson, G. W., and Carpenter, C. C. (1991). Vector biology, ecology, and control. In *Malaria: Obstacles and Opportunities*. National Academies Press (US). Available from: [https://www.ncbi.nlm.nih.gov/books/NBK234322/]

Odero, J. O., Nambunga, I. H., Wangrawa, D. W., Badolo, A., Weetman, D., Koekemoer, L. L., and Baldini, F. (2023). Advances in the genetic characterization of the malaria vector, *Anopheles funestus*, and implications for improved surveillance and control. *Malaria Journal*, 22(1), 230.

Ogola, E. O., Fillinger, U., Ondiba, I. M., Villinger, J., Masiga, D. K., Torto, B., and Tchouassi, D. P. (2018). Insights into malaria transmission among *Anopheles funestus* mosquitoes, Kenya. *Parasites and Vectors*, 11, 1-10.

Oyegoke, O. O., Maharaj, L., Akoniyon, O. P., Kwoji, I., Roux, A. T., Adewumi, T. S., and Okpeku, M. (2022). Malaria diagnostic methods with the elimination goal in view. *Parasitology Research*, 121(7), 1867-1885.

Panda, D., and Barik, T. K. (2020). Unravelling mosquito species complex through DNA barcodes: complementing morphological identification for accurate discrimination. *Molecular Identification of Mosquito Vectors and Their Management*, 1-21.

Paskewitz, S.M. and Collins, F.H. (1997). PCR amplification of insect ribosomal DNA. In Crampton J.M., Beard C.B. and Louis C. (editors), *The Molecular Biology of Insect Disease Vectors*, *Springer*, *Dordrecht*, 374-383.

Pramasivan, S., Liew, J. W. K., Jeyaprakasam, N. K., Low, V. L., Ngui, R., and Vythilingam, I. (2022). Multiplex PCR assay for the identification of four species of the *Anopheles leucosphyrus* sub-group in Malaysia. *Insects*, 13(2), 195.

Raman, J., Morris, N., Frean, J., Brooke, B., Blumberg, L., Kruger, P., and Moonasar, D. (2016). Reviewing South Africa's malaria elimination strategy (2012–2018): progress, challenges and priorities. *Malaria Journal*, 15, 438.

Rants'o, T. A., Koekemoer, L. L., and Van Zyl, R. L. (2023). In vitro and in silico analysis of the *Anopheles anticholinesterase* activity of terpenoids. *Parasitology International*, 93, 102713.

Rathnayake, R. A. S., Wedage, W. M. M., Muthukumarana, L. S., and De Silva, B. G. (2023). Genetic diversity, phylogenetic and phylogeographic analysis of *Anopheles culicifacies* species complex using *ITS2* and *COI* sequences. *PloS one*, 18(8), e0290178.

Rattanarithikul, R., and Green, C. A. (1986). Formal recognition of the species of the *Anopheles maculatus group* (Diptera: Culicidae) occurring in Thailand, including the descriptions of two new species and a preliminary key to females. *Mosquito Systems*, 18(3), 4.

Rattanarithikul, R., and Harbach, R. E. (1991). *Anopheles maculatus* (Diptera: Culicidae) from the type locality of Hong Kong and two new species of the *Maculatus* Complex from the Philippines. *Mosq Syst*, 22(3), 160-83.

Reid, E. T., and Woods, R. W. (1957). Anopheline Mosquitoes of Southern Rhodesia: a general Survey. *Proceedings and Transactions of the Rhodesia Scientific Association*, 45.

Rodrigues, M. S., Morelli, K. A., and Jansen, A. M. (2017). *Cytochrome c oxidase subunit 1* gene as a DNA barcode for discriminating *Trypanosoma cruzi* DTUs and closely related species. *Parasites and Vectors*, 10, 488.

Russell, T. L., Govella, N. J., Azizi, S., Drakeley, C. J., Kachur, S. P., and Killeen, G. F. (2011). Increased proportions of outdoor feeding among residual malaria vector populations following increased use of insecticide-treated nets in rural Tanzania. *Malaria Journal*, 10, 1-10.

Saccone, C., De Giorgi, C., Gissi, C., Pesole, G., and Reyes, A. (1999). Evolutionary genomics in Metazoa: the mitochondrial DNA as a model system. *Gene*, 238(1), 195-209.

Sáez, A. G., and Lozano, E. (2005). Body doubles. *Nature*, 433(7022), 110-111.

Scott, J.A., Brogdon, W.G. and Collins, F.H. (1993). Identification of single specimens of the *Anopheles Gambiae* complex by the Polymerase Chain Reaction. *The American Journal of Tropical Medicine and Hygiene*, 49(4), 520–529.

Service, M. and Towson, H. (2002). The *Anopheles* vector. *Essential Malariology*. 4, 59–84.

Sharakhov, I. V., Sharakhova, M. V., Mbogo, C. M., Koekemoer, L. L., and Yan, G. (2001). Linear and spatial organization of polytene chromosomes of the African malaria mosquito *Anopheles funestus*. *Genetics*, 159(1), 211-218.

Sharakhova, M. V., Antonio-Nkondjio, C., Xia, A., Ndo, C., AWONO-AMBENE, P., Simard, F., and Sharakhov, I. V. (2014). Polymorphic chromosomal inversions in *Anopheles moucheti*, a major malaria vector in Central Africa. *Medical and Veterinary Entomology*, 28(3), 337-340.

Singh, B. and Daneshvar, C. (2013). Human infections and detection of *Plasmodium knowlesi*. *Clinical Microbiology Reviews*, 26(2), 165–184.

Singh, B. N. (2016). The genus Drosophila is characterized by a large number of sibling species showing evolutionary significance. *Journal of genetics*, 95, 1053-1064.

Sinka, M. E., Bangs, M. J., Manguin, S., Coetzee, M., Mbogo, C. M., Hemingway, J., and Hay, S. I. (2010). The dominant *Anopheles* vectors of human malaria in Africa, Europe and the Middle East: occurrence data, distribution maps and bionomic précis. *Parasites and Vectors*, 3, 1-34.

Sinka, M.E., Bangs, M.J., Manguin, S., Rubio-Palis, Y., Chareonviriyaphap, T., Coetzee, M., Mbogo, C.M., Hemingway, J., Patil, A.P., Temperley, W.H., Gething, P.W., Kabaria, C.W., Burkot, T.R., Harbach, R.E. and Hay, S.I. (2012). A global map of dominant malaria vectors. *Parasites and Vectors*, 5(69).

Sougoufara, S., Ottih, E. C., and Tripet, F. (2020*).* The need for new vector control approaches targeting outdoor biting Anopheline malaria vector communities. *Parasites and Vectors*, 13, 1-15.

Spillings, B.L., Brooke, B.D., Koekemoer, L.L., Chiphwanya, J., Coetzee, M. and Hunt, R.H. (2009). A new species concealed by *Anopheles funestus* Giles, a major malaria vector in Africa. *The American Journal of Tropical Medicine and Hygiene*, 81(3), 510–515.

St Laurent, B. S., Cooke, M., Krishnankutty, S. M., Asih, P., Mueller, J. D., Kahindi, S., and Stevenson, J. C. (2016). Molecular characterization reveals diverse and unknown malaria vectors in the western Kenyan highlands. *The American Journal of Tropical Medicine and Hygiene*, 94(2), 327.

Stevenson, J. C., Pinchoff, J., Muleba, M., Lupiya, J., Chilusu, H., Mwelwa, I., and Southern Africa International Centers of Excellence in Malaria Research. (2016). Spatio-temporal heterogeneity of malaria vectors in northern Zambia: implications for vector control. *Parasites and Vectors*, 9, 510.

Stevenson, J., Laurent, B. S., Lobo, N. F., Cooke, M. K., Kahindi, S. C., Oriango, R. M., and Drakeley, C. (2012). Novel vectors of malaria parasite in the western highlands of Kenya. *Emerging Infectious Diseases*, 18(9), 1547.

Subbarao, S. K., Nanda, N., Vasantha, K., Dua, V. K., Malhotra, M. S., Yadav, R. S., and Sharma, V. P. (1994). Cytogenetic evidence for three sibling species in *Anopheles fluviatilis* (Diptera: Culicidae). *Annals of the Entomological Society of America*, 87(1), 116-121.

Suzuki, M. T., and Giovannoni, S. J. (1996). Bias caused by template annealing in the amplification of mixtures of 16S rRNA genes by PCR. *Applied and Environmental Microbiology*, 62(2), 625-630.

Sylla, E., Lell, B., Jürgen F.J. Kun, Peter G., Kun, J., and Kremsner, P. (2000). Mosquito distribution and entomological inoculation rates in three malaria-endemic areas in Gabon, *Transactions of The Royal Society of Tropical Medicine and Hygiene*, 94(6), 652–656.

Theobald, F.V. (1903). A monograph of the Culicidae of the World. London, England: British Museum (Natural History). *Printed by William Clowes and Sons, Limited*, 3(28).

Tobe, S. S., Kitchener, A. C., and Linacre, A. M. (2010). Reconstructing mammalian phylogenies: a detailed comparison of the *cytochrome b* and *cytochrome oxidase subunit I* mitochondrial genes. *PloS One*, 5(11), e14156.

Trivedi, S., Aloufi, A. A., Rehman, H., Saggu, S., and Ghosh, S. K. (2016). DNA barcoding: tool for assessing species identification in Reptilia. *J Entomol Zool Stud*, *4*(1), 332-337.

Tuno, N., Farjana, T., Uchida, Y., Iyori, M., and Yoshida, S. (2023). Effects of Temperature and Nutrition during the Larval Period on Life History Traits in an Invasive Malaria Vector *Anopheles stephensi*. *Insects*, 14(6), 543.

Vaucel, M. and Campourcy, A. (1943) Rev. Sci. Mid. Pharm. *Bulletin of the World Health Organization*. 419-441.

Vezenegho, S. B. (2012). Systematic study of the new *Anopheles funestus-like* species from Malawi (Doctoral dissertation). University of the Witwatersrand.

Vincke, I. H., and Leleup, N. (1949). Description of the Pupa, Larvae and Egg of *Anopheles* concolor. *Revue de Zoologie et de Botanique Africaines*, 42(3), 245-247.

Walton, C., Handley, J. M., Kuvangkadilok, C., Collins, F. H., Harbach, R. E., Baimai, V., and Butlin, R. K. (1999). Identification of five species of the *Anopheles dir*us complex from Thailand, using allele-specific polymerase chain reaction. *Medical and Veterinary Entomology*, 13(1), 24-32.

Walton, C., Sharpe, R. G., Pritchard, S. J., Thelwell, N. J., and Butlin, R. K. (1999). Molecular identification of mosquito species, *Biological Journal of the Linnean Society*, 68(1-2), 241–256.

Walton, C., Somboon, P., O'loughlin, S. M., Zhang, S., Harbach, R. E., Linton, Y. M., and Butlin, R. K. (2007). Genetic diversity and molecular identification of mosquito species in the *Anopheles maculatus* group using the *ITS2* region of rDNA. *Infection, Genetics and Evolution*, 7(1), 93-102.

Weetman, D., Steen, K., Rippon, E. J., Mawejje, H. D., Donnelly, M. J., and Wilding, C. S. (2014). Contemporary gene flow between wild *An. gambiae ss* and *An. arabiensis*. *Parasites and Vectors*, 7, 345.

White, B. J., Collins, F. H. and Besansky, N. J. (2011). Evolution of *Anopheles gambiae* in Relation to Humans and Malaria. *Annual Review of Ecology, Evolution, and Systematics*, 42, 111–132

Whittaker, C., Hamlet, A., Sherrard-Smith, E., Winskill, P., Cuomo-Dannenburg, G., Walker, P. G., and Churcher, T. S. (2023). Seasonal dynamics of *Anopheles stephensi* and its implications for mosquito detection and emergent malaria control in the Horn of Africa. *Proceedings of the National Academy of Sciences*, 120(8), e2216142120.

Wilkerson, R. C., Reinert, J. F., and Li, C. (2004). Ribosomal DNA *ITS2* sequences differentiate six species in the *Anopheles crucians* complex (Diptera: Culicidae). *Journal of Medical Entomology*, 41(3), 392-401.

World Health Organization (WHO). (2022). World Malaria Report 2022. Geneva: World Health Organization. Available from: [https://www.who.int/teams/global-malaria-programme/reports/world-malaria-report-2022]

World Health Organization (WHO). (2023). World Malaria Report 2023. Geneva: World Health Organization. Available from: [https://www.who.int/teams/global-malaria-programme/reports/world-malaria-report-2023]

Zengenene, M. P., Munhenga, G., Okumu, F., and Koekemoer, L. L. (2022). Effect of larval density and additional anchoring surface on the life-history traits of a laboratory colonised *Anopheles funestus* strain. *Medical and Veterinary Entomology*, 36(2), 168-175.

Zhang, C., Luo, C., Yang, R., Yang, Y., Guo, X., Deng, Y., and Zhang, Y. (2022). Morphological and molecular identification reveals a high diversity of Anopheles species in the forest region of the Cambodia–Laos border. *Parasites and Vectors*, 15(1), 94.

Zhang, D. X., and Hewitt, G. M. (1997). Assessment of the universality and utility of a set of conserved mitochondrial *COI* primers in insects. *Insect Molecular Biology*, 6(2), 143-150.

Zheng, X. L. (2020). Unveiling mosquito cryptic species and their reproductive isolation. *Insect Molecular Biology*, 29(6), 499-510.

APPENDICES

Appendix 1A: Morphological Differences in Egg Stages

Species name	Floats	Decks
An. austenii	Unknown	Unknown
An. berghei	Unknown	Unknown
An. brohieri	Unknown	Unknown
An. gibbinsi	Slightly bigger than that of *An. marshallii s.s.* The chorion appears to be discontinuous between the floats.	The size of the deck and accordingly the length of the frill are very variable.
An. hancocki	Closely resembles *An. funestus* eggs but may be distinguished by the very fine sculpturing of the chorion, floats with 13-15 ridges.	No information
An. hargreavesi	Floats with 14-18 air cells. 2 well developed frills that each form a complete oval surrounding the polar enclosed areas.	No information
An. harperi	Unknown	Unknown
An. hughi*	Floats well separated	Differs from *An. marshallii s.s.* and *An. hughi* in that it has a continuous, open single deck between the floats.
An. kosiensis*	Same as *An. hughi*	Same as *An. hughi*, occasionally with a closed deck.
An. letabensis*	Floats well separated	With 2 polar decks as in *An. marshallii s.s*, but with openings of decks slightly more rounded.
An. marshallii*	Floats are close together. The floats occupy the middle two-thirds of the egg.	With two decks. Each deck extends along the whole dorsal surface surrounded by a narrow frill.

An. mortiauxi	Unknown	Unknown
An. mousinhoi*	Unknown	Unknown
An. njombiensis	Unknown	Unknown
An. seydeli*	Similar to *An. marshallii s.s.*	With 3 decks
An. upemba	Unknown	Unknown

(Gillies and De Meillon, 1968; Gillies and Coetzee, 1987).

No information = Mosquito feature has been studied, but no data was recorded.

Unknown = The mosquito feature has yet to be looked into.

***** *Anopheles marshallii* group species found in South Africa.

Appendix 1B: Morphological differences in Larval stages of the *An. marshallii* group.

Species name	Clypeal hairs	Shoulder hairs	Mesopleural hairs	Palmate hairs	Abdominal plates	Saddle hairs
***An. austenii** **	Inner: simple or rarely bifid. Outer: long as inner, bifid or with 3-4 branches.	Well separated, on large basal tubercles.	Same as in *An. marshallii s.s.*	1st abdominal undifferentiated, 2nd-7th with abrupt shoulders, filaments typically short and spiky but sometimes longer.	The outline of the main plate is irregular. Three accessory plates present on most segments.	With 3-5 branches.
An. berghei	Unknown	Unknown	Unknown	Unknown	Unknown	Unknown
An. brohieri	No information	No information	No information	No information	Main abdominal plates wider. 3 accessory abdominal plates sometimes present.	No information
An. gibbinsi	Inner: short, widely spaced basally. Outer: similar to inner but slightly shorter.	No information	No information	1st undifferentiated. 2nd partly differentiated, 3rd-7th with often rather short blunt filaments.	Variable.	No information
An. hancocki	Inner: long and finely pointed. Outer: rather stout, abruptly pointed.	Well-developed, basal tubercles fused.	Both long hairs are simple, small basal spine.	1st abdominal is developed but smaller than the rest of the abdomen.	Moderately developed in width. One accessory plate is present.	Short, apically with 5 or more branches.
An. hargreavesi	Inner: long, simple, drawn out to a fine point. Outer: about half as long as the inner.	On moderately large pigmented bases, which may be fused.	Same as in *An. marshallii s.s.*	1st abdominal poorly developed, leaflets narrow. 2nd-7th abdominal fully developed. Filaments are long and finely drawn.	Moderately developed, pale, slightly more than twice as wide as deep. One accessory plate is present.	Long and simple or occasionally bifid.

An. harperi	Inner: simple, normal length. Outer: more or less than half length of inner.	With bases either fused or separate.	No information	1st abdominal differentiated. 2nd very narrow but differentiated, 3rd-7th well developed, shoulders and filaments variable.	The main plate equals two-thirds of the distance between palmate hairs. One accessory plate is present.	Long and simple.
An. hughi*	Posterior hair (seta 4-C) simple.	Median hair (seta 2-P) with 8-13 branches.	No information	No information	With 8-13 branches, arising mainly from one side of the stem of the hair.	No information
An. kosiensis*	Resembles *An. hughi*.	Resembles *An. hughi*.	No information	Resembles *An. hughi* but the larval thoracic palmate seta (seta 3-T) is significantly smaller. However, counting the number of leaflets on this seta is difficult.	Resembles *An. hughi*	No information
An. letabensis*	Posterior hair (seta 4-C) simple.	Has 9-14 branches, mounted on a small tubercle.	No information	No information	No information	No information
An. marshallii*	Inner: simple, widely spaced basally. Outer: slightly more the length of the inner.	Well-developed on well-formed tubercles, which are usually separated.	Both long hairs are simple, small basal spine.	Subject to variation. Filaments are usually short and pointed, but it may be longer.	The width of segment 5 is more than half the distance between the palmate hairs. One accessory plate.	Short and with at least 5 branches.
An. mortiauxi	Unknown	Unknown	Unknown	Unknown	Unknown	Unknown

An. mousinhoi*	All clypeal hairs are simple, much as in *An. marshallii s.s.* except that the posterior hair is relatively shorter.	Basal tubercles developed and placed close together.	Similar to *An. marshallii s.s.*	1st abdominal differentiated. 2nd abdominal is narrow and undifferentiated. 3rd-7th fully developed with delicate filaments variable in length.	Large, almost the distance between the palmate hairs on segment 5. One accessory plate present.	Long and simple.
An. njombiensis	Inner: simple. Outer: Half as inner. Posterior: slightly longer than outer.	Mounted on large, unfused tubercles.	Basal spines are small.	3rd-7th fully developed, with very short filaments,2nd with 14 narrow, lanceolate leaflets.	Deep with almost two-thirds distance between palmates. A single accessory plate present on segments 2-7.	With 3-4 branches
An. seydeli*	Inner: relatively short, about one-third the length of the fronto-clypeus. Outer: very short and stumpy.	No information	Same as *An. marshallii s.s.*	Leaflets with distinct shoulders and pronounced filaments are present on segment 1. Broad leaflets with serrated shoulders and short, pointed filaments on segments 3–7.	Same as *An. marshallii s.s.*	Short and much branched.
An. upemba	Unknown	Unknown	Unknown	Unknown	Unknown	Unknown

No information = Mosquito feature has been studied, but no data was recorded.

Unknown = The mosquito feature has yet to be looked into.

***** *Anopheles marshallii* group species found in South Africa.

(Gillies and De Meillon, 1968; Gillies and Coetzee, 1987).

Appendix 1C: Morphological Differences in Pupal Stages

Species name	Paddle fringe	Setal differences
***An. austenii** **	Consisting of small spines changing progressively into fine hairs, extending two-thirds distance to base, not beyond apical hair.	Hair on segments I-V with 3-5 branches, nearly as long as segment. Segments l-VII with l-2 branches, shorter than segment.
An. berghei	Unknown	Unknown
An. brohieri	Unknown	Unknown
An. gibbinsi	Differs from *An. marshallii s.s* in the apical paddle hair being short.	Hair on segments V-VII being shorter than the segments.
An. hancocki	Extends two-thirds distance to base, composed of spines changing gradually to hairs, continued beyond apical hair. Apical hair long and strongly hooked.	Hair on segments III-IV with 7-8 branches, on V-VII simple or bifid and almost as long as segment. Segments III-IV with 6-8 branches, V-VII with 3-7 branches.
An. hargreavesi	Extends less than half-way to base, composed of spines changing abruptly to hairs, continued beyond apical hair by a few fine hairs. Apical hair short and straight.	Hair on segments III-VII with 2-5 branches. Segment III-VII with 1-5 branches.
An. harperi	Extends half-way to base, composed of spines changing gradually to hairs, not continued beyond apical hair. Apical hair straight and relatively short.	Hair on segments V-VI short with 4-7 branches, on VII simple or bifid and longer than segment. V-VI with 3-5 branches, on VII with 2-4. Segments V and VI progressively shorter.
***An. hughi** **	Same as *An. letabensis* but extending a shorter distance beyond apical hair.	Setal counts differing from those of *An. marshallii s.s.* and *An. letabensis* at numerous sites.
***An. kosiensis** **	Resembles *An. hughi.*	The number of setae beyond seta (1-P) on the inner border of the paddle, ranges from 18 to 32. Seta 5-V has 5-9 branches. Seta (7-VI) is mainly simple.
***An. letabensis** **	Same as in *An. marshallii s.s.* but more extensive, with more than 20 very fine hairs beyond apical hair.	Setae as in *An. marshallii s.s.* except that seta 3-II is simple or bifid.

An. marshallii*	Extending half-way to base, composed of spines. A few fine hairs beyond apical hair. Apical hair curved, about quarter length of paddle.	Segments III-IV with 6-9 branches. Segments V-VII with 3 branches.
An. mortiauxi	Unknown	Unknown
An. mousinhoi*	Same as in *An. marshallii s.s.*	Differs from that of *An. marshallii s.s.* in hair 1, which is very short and delicate with 5-8 branches on segment IV, 3-8 on segments V and VI.
An. njombiensis	Extends less than half-way to base, composed of spines changing more or less gradually into hairs, not continued beyond apical hair. Apical paddle hair long and hooked.	Hair on segments III-VII with 2-6 branches, on segments III-VII with 3-6 branches.
An. seydeli*	Extends two-thirds to based, composed of spines changing gradually to hairs, continued past apex. Apical hair long and hooked.	Hairs on segments III-IV with 6-7 and 5-6 branches. On V-VII simple and about as long as segment. Hair on segments III-VII with 6-10 branches. Segments V and IV progressively shorter.
An. upemba	Unknown	Unknown

No information = Mosquito feature has been studied, but no data was recorded.

Unknown = The mosquito feature has yet to be looked into.

***** *Anopheles marshallii* group species found in South Africa.

(Gillies and De Meillon, 1968; Gillies and Coetzee, 1987).

Appendix 2A: DNA extraction mastermix calculations using the ZyGEM prepGEM® Insect kit

Reagants	**1X reaction**
10X buffer black	**1.0 µl**
PrepGEM enzyme	**0.25 µl**
PCR water	**8.75 µl**
Total:	**10.0 µl**

Supplier: (Cat No.: PUN1000, ZyGEM™, New Zealand)

Appendix 2B: Standard mastermix calculations for *An. funestus* PCR (Koekemoer *et al.*, 2002, Cohuet *et al.*, 2003).

PCR components	**1X reaction**	**Cat. Number and Supplier**
10x PCR buffer	1.25 µl	ALE2493, Separations, South Africa
dNTPs (2.5 mM)	1 µl	AJ30387A, Separations, South Africa
$MgCl_2$ (25 mM)	0.75 µl	ALE2495A, Separations, South Africa
Universal primer (3.3pmol/µl)	1 µl	201012-024-H6, Inqaba Biotec
An. funestus primer (3.3pmol/µl)	1 µl	201012-024-H7, Inqaba Biotec
An. leesoni primer (3.3pmol/µl)	1 µl	201012-024-H11, Inqaba Biotec
An. parensis primer (3.3pmol/µl)	1 µl	201012-024-H10, Inqaba Biotec
An. rivolurum primer (3.3pmol/µl)	1 µl	201012-024-H9, Inqaba Biotec
An. rivolurum-like primer (3.3pmol/µl)	1 µl	201012-024-H12, Inqaba Biotec
An. vaneedeni primer (3.3pmol/µl)	1 µl	201013-014-A3, Inqaba Biotec
Taq-polymerase (5 units/µl)	0.1 µl	ALE2492A, Separations, South Africa
dH_2O	1.9 µl	–
DNA template	0.5 µl	-
Total:	**12.5 µl**	–

Appendix 2C: Protocol for 1X TAE Buffer

1. Preparation of a 0.5 M EDTA stock solution

- Weigh out 186.1g of EDTA disodium salt (MW=372.24 g/mol).
- Dissolve in 800 ml deionized water and adjust the pH to 8.0 with solid sodium hydroxide (NaOH) pellets.
- Stir vigorously using a magnetic stirrer.

2. Preparation of 50X TAE buffer

- Weigh out 242g of Tris-base (MW = 121.14 g/mol).
- Dissolve in approximately 700 ml of deionized water.
- Add 57.1 ml of 100 % glacial acid (or acetic acid).
- Add 100 milliliters of 0.5 M EDTA (pH 8.0)
- Adjust the solution to a final volume of 1 litre
- Store stock solution at room temperature

3. Preparation of 1X TAE working solution

- Dilute 20 ml 50X TAE stock into 980ml distilled water.

4. Preparation of 2.5% Agarose Gel

- Measure 10g of Agarose gel powder.
- Add the powder to 400 ml of 1X TAE buffer and microwave for 3-4 minutes until the agarose is completely dissolved.
- Allow the agarose solution to cool down.
- Add 12 µl ethidium bromide and swirl.
- Pour the agarose into a gel tray with the well combs in place.
- Let sit at room temperature for 30-60 minutes until it has completely solidified.

Appendix 2D: HotSHOT DNA Extraction Protocol

1. Buffer Preparation

Alkaline Lysis Buffer (pH 12)

1. For 100 ml of alkaline lysis buffer, add:

- 25 ml of 100 mM NaOH (Cat no. 30385, ACE, South Africa)
- 0.4 ml of 50 mM Na_2EDTA (Lot no. 1052966, Sigma Aldrich, South Africa)
- 74.6 ml of distilled H_2O

Neutralising Solution (pH 5)

1. For 100 ml of neutralising solution, add:

- 630 mg of Tris-HCl (Lot no. 3255466, EMD Millipore Corporation, South Africa)
- 100 ml of distilled H_2O

2. Procedure

Notes before starting

- Turn on the heating block before starting the procedure and set the temperature to 95°C.

1. Dissect the head and thorax of each mosquito and add to individual 1.5 ml Eppendorf tubes.

2. Aliquot 50 µl of alkaline lysis buffer into each tube.

3. Using a sterile pestle, grind the head and thorax of each mosquito until completely homogenised. If there are multiple samples, use the magnetic beads to grind the samples in the TissueLyser II.

4. Incubate for 30 minutes at 95°C.

5. Allow to cool on ice for 3-4 minutes.

5. Add 50 µl neutralising solution to each tube.

6. Vortex and briefly centrifuge the tubes.

7. Use 2 µl of extracted DNA for PCR or freeze at –20°C for long-term storage.

Appendix 2E: TaqMan PCR protocol for detecting *Plasmodium* species (Bass *et al*., 2008).

PCR Reagents	1X	Cat. Number and Supplier
IQ Supermix	10µl	1708860, BioRad, SA
PlasF (10µM)	1.6µl	4304970, Thermo Scientific, SA
PlasR (10µM)	1.6µl	4304970, Thermo Scientific, SA
PlasF probe (10µM)	0.6µl	4316034, Thermo Scientific, SA
OVM+ probe (10µM)	0.4µl	4316034, Thermo Scientific, SA
dH_2O	3.8µl	-
DNA	2µl	-
Total	**20µl**	**-**

- Add 18µl of master mix to each well and 2µl DNA to each well.
- Seal the reaction tube/plate and centrifuge briefly.

Note:

- **The final concentration of probes and primers are as follows:**

  800nM of each primer

  300nM of probe PlasF

  200nM of probe OVM+

Cycling conditions:

- 10 minutes at 95°C
- 40 cycles of 95°C for 10 seconds and 60°C for 45 seconds

Plate Read:

- **VIC-** yellow (530nm excitation and 555nm emission)
- **FAM –** green (470nm excitation and 510 emission)

Appendix 2F: DNeasy Blood and Tissue Extraction Kit

1. A whole mosquito tissue was placed in a 1.5ml microcentrifuge tube and cut into small pieces.
2. 180 µl buffer ATL and 20 µl proteinase K were added to the tube.
3. The mixture was placed in a shaking water bath and incubated at 56 °C for ±3 hours or until the tissue was completely lysed.
4. 200 µl buffer AL was added to the mixture and vortexed. The tube was incubated for 10 minutes at 56 °C.
5. 200 µl ethanol (96 %) was added to the tube and vortexed for 10 seconds.
6. The mixture was then pipetted into a spin column with a 2 ml collection tube and centrifuged at 8000rpm for 1 minute. The flow-through was discarded, and the spin column was replaced with a new collection tube.
7. 500 µl buffer AW1 was added to the mixture. The tube was centrifuged at 8 000 rpm for 1 minute. The flow-through was discarded, and the spin column was replaced with a new collection tube.
8. 500 µl buffer AW2 was added to the mixture. The tube was centrifuged at 14 000 rpm for 3 minutes. The flow-through was discarded, and the spin column was replaced with a new collection tube.
9. The DNA was eluted by adding 200 ul buffer AE to the centre of the spin column membrane. The tube was allowed to sit for 1 minute at room temperature (15-25°C).
10. The tube was centrifuged for 1 minute at 8 000 rpm.
11. The recovered DNA was used immediately or stored at -20 °C.

Supplier: Qiagen, DNeasy Blood and Tissue kit (Lot no. 172045050).

Appendix 3: The *ITS2* and *COI* sequences generated during this study have been deposited in GenBank under the following accession numbers:

Sample ID	**Morphology**	***ITS2* Fragment**	***ITS2* Accession Number**	***COI* fragment**	***COI* Accession Number**
H9	*An. hargreavesi*	≈485 bp - ≈560 bp	PP915781	≈900 bp	PP919268
H10	*An. hargreavesi*	≈485 bp - ≈560 bp	PP915782	≈900 bp	PP919269
H55	*An. hargreavesi*	≈485 bp - ≈560 bp	PP915783	≈900 bp	PP919270
H58	*An. hargreavesi*	≈485 bp - ≈560 bp	PP915784	≈900 bp	PP919271
H59	*An. hargreavesi*	≈485 bp - ≈560 bp	PP915785	≈900 bp	PP919272
N325	*Anopheles gibbinsi*	≈507 bp	PQ399842	———	———
N617	*Anopheles gibbinsi*	≈507 bp	OM459764.1	———	———
N618	*Anopheles gibbinsi*	≈507 bp	OM459765.1	———	———
N619	*Anopheles gibbinsi*	≈507 bp	PQ399843	———	———
N779.3	*Anopheles gibbinsi*	≈507 bp	OM459767.1	———	———
N865	*Anopheles gibbinsi*	≈507 bp	OM459768.1	———	———
N866	*Anopheles gibbinsi*	≈507 bp	PQ399844	———	———
63.1	*An. marshallii group*	≈500 bp	PQ334736	≈900 bp	PQ327569
63.2	*An. marshallii group*	≈500 bp	PQ334737	≈900 bp	PQ327570
63.3	*An. marshallii group*	≈500 bp	PQ334738	≈900 bp	PQ327571
221.1	*An. marshallii group*	≈500 bp	PQ334739	≈900 bp	PQ327572
221.2	*An. marshallii group*	≈500 bp	PQ334740	≈900 bp	PQ327573
221.3	*An. marshallii group*	≈500 bp	PQ334741	≈900 bp	PQ327574

289.1	*An. marshallii group*	≈500 bp	PQ334742	≈900 bp	PQ327575
289.2	*An. marshallii group*	≈500 bp	PQ334743	≈900 bp	PQ327576
289.3	*An. marshallii group*	≈500 bp	PQ334744	≈900 bp	PQ327577
596.1	*An. marshallii group*	≈500 bp	PQ334745	≈900 bp	PQ327578
596.2	*An. marshallii group*	≈500 bp	PQ334746	≈900 bp	PQ327579
596.3	*An. marshallii group*	≈500 bp	PQ334747	≈900 bp	PQ327580
1246B	*An. maculipalpis*	≈410 bp	———	≈900 bp	PQ326959
1246C	*An. maculipalpis*	≈400 bp	———	≈900 bp	PQ326960
9104B	*An. maculipalpis*	≈400 bp	———	≈900 bp	PQ326961
9104C	*An. maculipalpis*	≈400 bp	———	≈900 bp	PQ326962
172A	*An. maculipalpis*	≈610 bp	———	≈900 bp	PQ326963
172B	*An. maculipalpis*	≈500 bp	———	≈900 bp	PQ326964
1484A	*An. maculipalpis*	≈500 bp	———	≈900 bp	PQ326965
1484B	*An. maculipalpis*	≈490 bp	———	≈900 bp	PQ326966

Appendix 3A: *An. hargreavesi* sequences BLAST Results and Accession Numbers.

Sample ID Morphology	Morphology	*ITS2* Blast Results	Accession Number	*COI* Blast Results	Accession Number
H9	***An. hargreavesi***	***Anopheles marshallii* isolate** Sequence ID: MW257139.1 406/503(81%)	PP915781	***Anopheles marshallii* mitochondrion** Sequence ID: NC_064607.1 612/650(94%)	PP919268
H10	***An. hargreavesi***	***Anopheles marshallii* isolate** Sequence ID: MK592084.1 437/543(80%)	PP915782	***Anopheles marshallii* mitochondrion** Sequence ID: NC_064607.1 666/715(93%)	PP919269
H55	***An. hargreavesi***	***Anopheles marshallii* isolate** Sequence ID: MK592084.1 430/523(80%)	PP915783	***Anopheles marshallii* mitochondrion** Sequence ID: NC_064607.1 660/715(93%)	PP919270
H58	***An. hargreavesi***	***Anopheles marshallii* isolate** Sequence ID: MW257139.1 407/503(81%)	PP915784	***Anopheles marshallii* mitochondrion** Sequence ID: NC_064607.1 671/717(94%)	PP919271
H59	***An. hargreavesi***	***Anopheles marshallii* isolate** Sequence ID: MW257138.1 407/503(81%)	PP915785	***Anopheles marshallii* mitochondrion** Sequence ID: NC_064607.1 671/717(94%)	PP919272

Appendix 3B: *An. gibbinsi* sequences BLAST Results and Accession Numbers.

Sample ID	Morphology	*ITS2* Blast Results	Accession Number
N325	***Anopheles gibbinsi***	***Anopheles sp. 6* BSL-2014** Sequence ID: KJ522818.1 506/510(99%)	PQ399842
N617	***Anopheles gibbinsi***	***Anopheles sp. 6* BSL-2014** Sequence ID: KJ522818.1 508/513(99%)	OM459764.1
N618	***Anopheles gibbinsi***	***Anopheles sp. 6* BSL-2014** Sequence ID: KJ522818.1 505/512(99%)	OM459765.1
N619	***Anopheles gibbinsi***	***Anopheles sp. 6 BSL-2014*** Sequence ID: KJ522818.1 506/511(99%)	PQ399843
N779.3	***Anopheles gibbinsi***	***Anopheles sp. 6* BSL-2014** Sequence ID: KJ522818.1 435/457(95%)	OM459767.1
N865	***Anopheles gibbinsi***	***Anopheles sp. 6* BSL-2014** Sequence ID: KJ522818.1 508/517(98%)	OM459768.1
N866	***Anopheles gibbinsi***	***Anopheles sp. 6* BSL-2014** Sequence ID: KJ522818.1 507/512(99%)	PQ399844

Appendix 3C:

i. *Anopheles marshallii* group sequences BLAST Results and Accession Numbers.

Specimen ID	Morphology	*ITS2* Blast Results	Accession Number	*COI* Blast Results	Accession Number
63.1	***An. marshallii group***	*Anopheles theileri.* Sequence ID: JN994151.1 423/540(78%)	PQ334736	*Anopheles superpictus (COX1)* gene. Sequence ID: MT993498.1 648/707(92%)	PQ327569
63.2	***An. marshallii group***	*Anopheles theileri.* Sequence ID: JN994151.1 424/540(79%)	PQ334737	*Anopheles superpictus (COX1)* gene. Sequence ID: MT993498.1 653/707(92%)	PQ327570
63.3	***An. marshallii group***	*Anopheles theileri.* Sequence ID: JN994151.1 427/544(78%	PQ334738	*Anopheles superpictus (COX1)* gene. Sequence ID: MT993498.1 653/709(92%)	PQ327571
221.1	***An. marshallii group***	*Anopheles theileri.* Sequence ID: JN994151.1 425/541(79%)	PQ334739	*Anopheles superpictus (COX1)* gene. Sequence ID: MT993498.1 649/705(92%)	PQ327572
221.2	***An. marshallii group***	*Anopheles theileri.* Sequence ID: JN994151.1 425/541(79%)	PQ334740	*Anopheles superpictus (COX1)* gene. Sequence ID: MT993498.1 647/705(92%)	PQ327573
221.3	***An. marshallii group***	*Anopheles theileri.* Sequence ID: JN994151.1 424/540(79%)	PQ334741	*Anopheles superpictus (COX1)* gene. *Sequence ID: MT993498.1 653/708(92%)*	PQ327574
289.1	***An. marshallii group***	*Anopheles theileri.* Sequence ID: JN994151.1 424/540(79%)	PQ334742	*Anopheles aconitus* isolate (*COXI*) gene. Sequence ID: HQ877378.1 651/708(92%)	PQ327575
289.2	***An. marshallii group***	*Anopheles theileri.* Sequence ID: JN994151.1 419/535(78%)	PQ334743	*Anopheles aconitus* isolates (*COXI*) gene. Sequence ID: HQ877378.1 653/708(92%)	PQ327576
289.3	***An. marshallii group***	*Anopheles theileri.* Sequence ID: JN994151.1 424/540(79%)	PQ334744	*Anopheles superpictus (COX1)* gene. Sequence ID: MT993498.1 646/705(92%)	PQ327577
596.1	***An. marshallii group***	*Anopheles theileri.* Sequence ID: JN994151.1 426/542(79%)	PQ334745	*Anopheles superpictus (COX1)* gene. Sequence ID: MT993498.1 650/712(91%)	PQ327578

596.2	***An. marshallii group***	*Anopheles theileri.* Sequence ID: JN994151.1 424/542(78%)	PQ334746	*Anopheles superpictus (COX1)* gene. Sequence ID: MT993498.1 653/707(92%)	PQ327579
596.3	***An. marshallii group***	*Anopheles theileri.* Sequence ID: JN994151.1 424/540(79%)	PQ334747	*Anopheles superpictus (COX1)* gene. Sequence ID: MT993498.1 652/710(92%)	PQ327580

ii. *ITS2* and *COI* contig sequences of *An. marshallii* group samples from KwaZulu-Natal. Primer sites highlighted.

>ITS2 Contig Sequence Length: 530 bp

TTGTGAACTGCAGGACACATGAACACCGACACGTTGAACGCATATGGCGCATCGGACGTTTAAACCCGACCGATGCACACATTCTTGAGTGCCTACCAAATCCTTC
TTACACAGACTAAACTTGACTACATGGCGCGCGCGTGCAGGAACACACAACATTTTGGCGAGCATCCCGTCAAGATGAGTTTCAGCATACGTTAGCGCACTGTGCA
TAATGGCGTGCCAGGTTCCTAGTTTGGGACGTGGGGCGCTGAATTGGTAAGAGGCGGTACTGTTACCCACAGGGTACGTGTCAAGTCGCATGGTTTCGAACTTCGG
CTCCAAGACGACCTGGAAGCACCGGTAGCCTTACACCAGGCTTGCTGGCACCGCTTGCAGGACCCGCCGTCTTAGCCAAGTCGCTTACTGGTGCGACCCATACACG
TAGTGGTGTGCAGTATGTGCTACCAGCTTACCGCTTAAACGATCTCAAGTATCAGTAGGCCTCAAGTGATGTGTGAGAACCCCCTGAATTTAAGCATAA

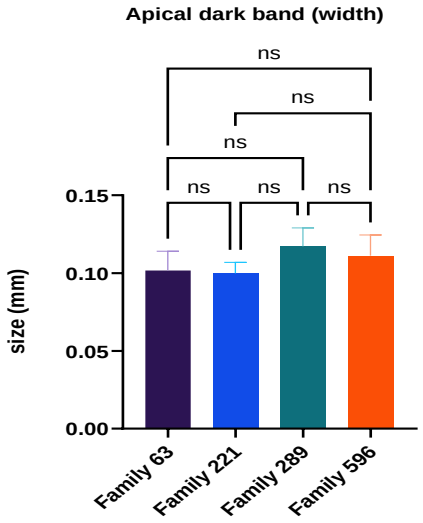
>COI Contig Sequence Length: 711 bp

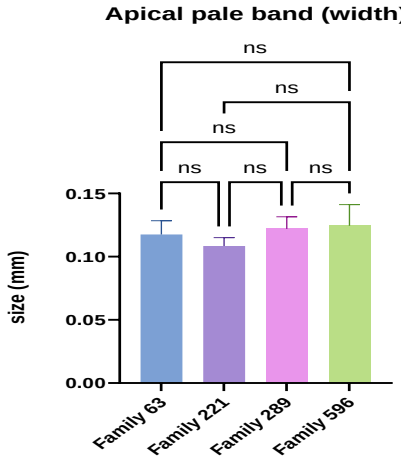
TTGGTCAACAAATCATAAAGATATTGGAACATTATATTTTATTTTTGGTGCGTGAGCTGGAATAGTAGGGACTTCTTTAAGAATTCTTATTCGAGCTGAATTAGGT
CACCCAGGAGCTTTTATTGGGGATGATCAAATTTATAATGTAATTGTTACTGCTCATGCTTTTATTATAATTTTTTTTATAGTTATACCTATTATAATTGGAGGAT
TTGGAAATTGATTAGTTCCTTTAATATTAGGAGCCCCAGATATAGCATTTCCTCGAATAAATAATATAAGTTTTTGAATACTTCCTCCTTCACTAACCCTTCTAAT
TTCTAGAAGTATAGTAGAAAATGGAGCAGGAACTGGGTGAACTGTATACCCACCCCTTTCTTCAGGTATTGCTCATGCTGGTGCATCAGTAGATTTAGCTATTTTT
TCTTTACATTTAGCTGGAATTTCATCAATTTTAGGGGCAGTAAATTTTATTACAACAGTAATTAATATACGATCTCCTGGAATTACATTAGATCGAATGCCTTTAT
TTGTTTGATCTGTAGTAATTACAGCTATTTTATTATTATTATCTTTACCTGTTTTAGCCGGTGCTATTACTATATTATTAACAGATCGAAATTTAAATACTTCTTT
TTTTGATCCTGCAGGAGGAGGAGACCCTATTTTATATCAACACTTATTTTGATTTTTTGGTCACCCTGAAGTTTA

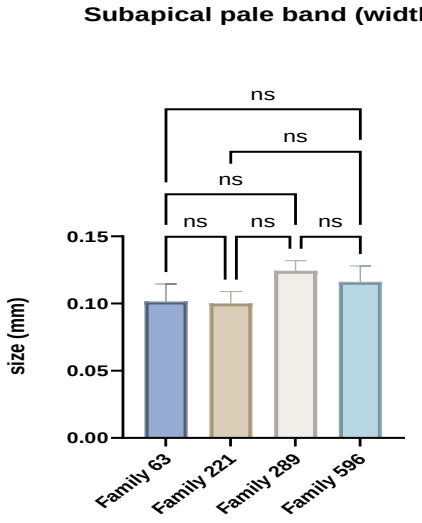
Appendix 3D: *An. maculipalpis* sequences BLAST Results and Accession Numbers.

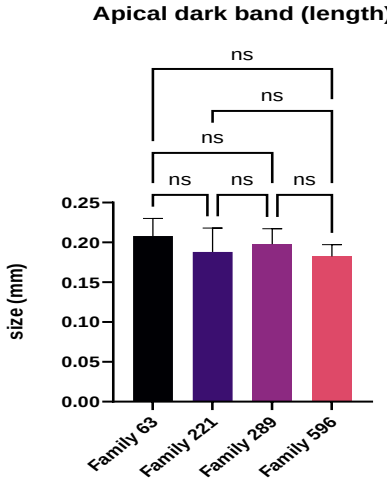
Specimen ID	Morphology	*ITS2* BLAST Results	Accession Number	*COI* Blast Results	Accession Number
1246B	***An. maculipalpis***	*Anopheles maculipalpis* isolate. Sequence ID: MT408571.1 364/365(99%)	———	*Anopheles maculipalpis* isolate *(COI)* gene, Sequence ID: MK776734.1 662/665(99%)	PQ326959
1246C	***An. maculipalpis***	*Anopheles maculipalpis* isolate. Sequence ID: MT408571.1 366/367(99%)	———	*Anopheles maculipalpis* isolate *(COI)* gene. Sequence ID: MK776734.1 666/666(100%)	PQ326960
9104F	***An. maculipalpis***	*Anopheles maculipalpis* isolate. Sequence ID: MK592039.1. 396/401(99%)	———	*Anopheles maculipalpis* isolate *(COI)* gene Sequence ID: MK776734.1 457/458(99%)	PQ326961
9104G	***An. maculipalpis***	*Anopheles maculipalpis* isolate. Sequence ID: MT408571.1 404/404(100%)	———	*Anopheles maculipalpis* isolate *(COI)* gene. Sequence ID: MK776734.1 664/664(100%)	PQ326962
172A	***An. maculipalpis***	*Anopheles maculipalpis* haplotype. Sequence ID: 379/383(99%)	———	*Anopheles maculipalpis* mitochondrion. Sequence ID: NC_064606.1 695/707(98%)	PQ326963
172B	***An. maculipalpis***	*Anopheles maculipalpis* isolate. Sequence ID: MT408571.1. 327/327(100%)	———	*Anopheles maculipalpis* mitochondrion. Sequence ID: NC_064606.1 696/709(98%)	PQ326964
1484A	***An. maculipalpis***	*Anopheles maculipalpis* isolate. Sequence ID: MT408571.1 398/399(99%)	———	*Anopheles maculipalpis* mitochondrion. Sequence ID: NC_064606.1 691/698(99%)	PQ326965
1484B	***An. maculipalpis***	*Anopheles maculipalpis* isolate. Sequence ID: MT408571.1 361/361(100%)	———	*Anopheles maculipalpis* mitochondrial *COI* gene. Sequence ID: LC473600.1 578/579(99%)	PQ326966

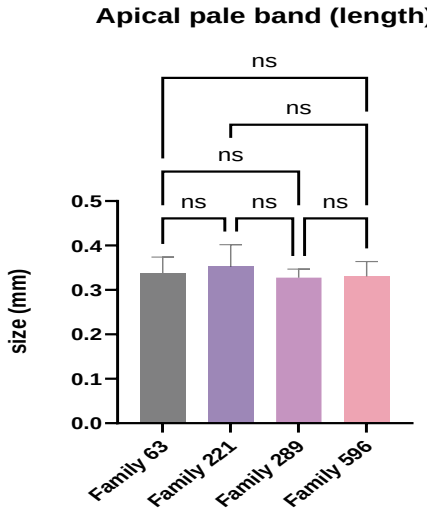
Appendix 3E: ANOVA graphs for comparisons of palp spots (widths and lengths) across the *An. marshallii* group families.

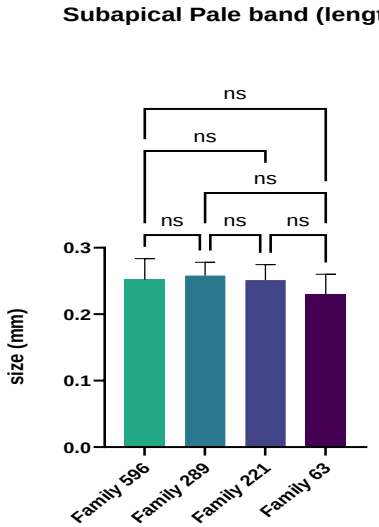












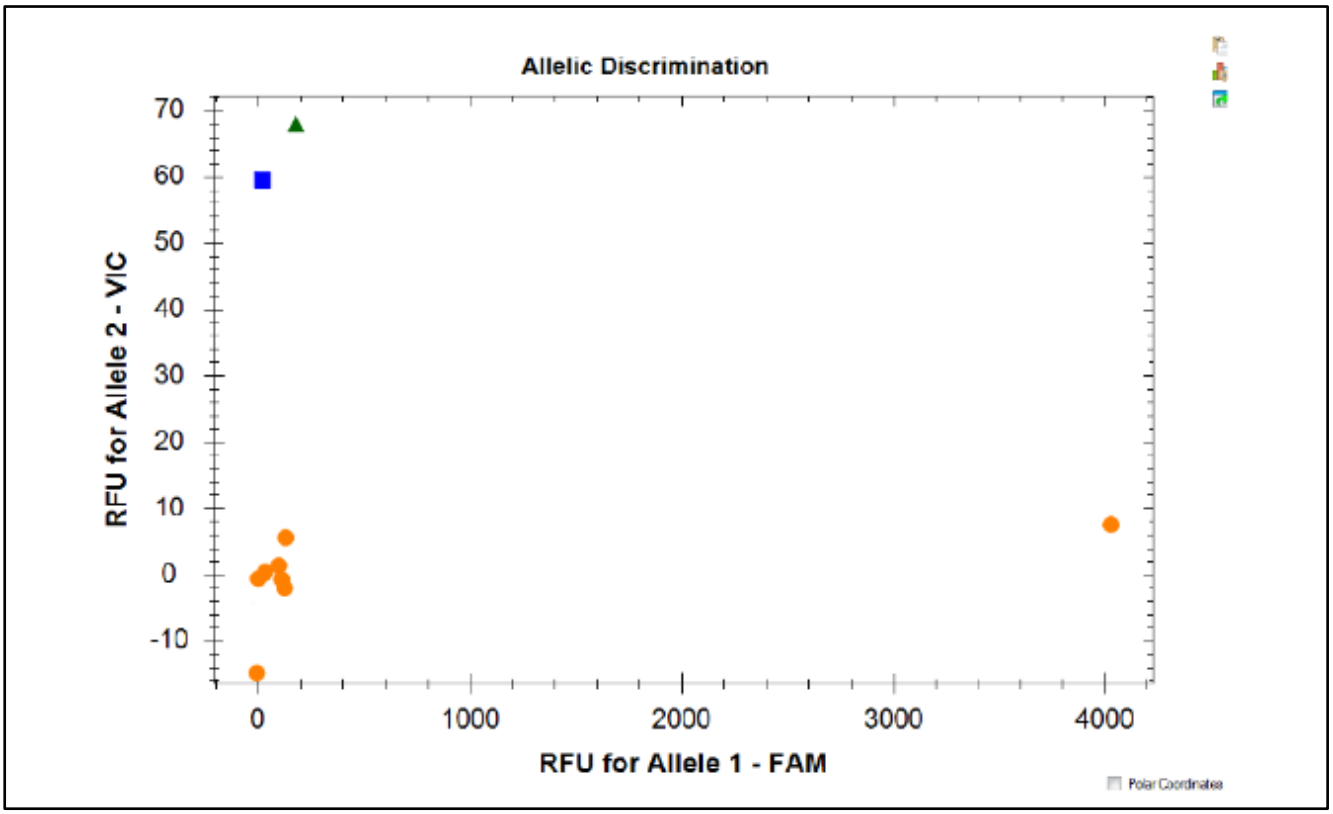
Appendix 3F: Palp spots raw data for adult females of the *Anopheles marshallii* group Width and Length measured in mm.

Sample ID	Apical dark band (Width)	Apical Pale band (Width)	Subapical Pale band (Width)	Apical dark band (Length)	Apical pale band (Length)	Subapical Pale band (Length)
63.1	0.083	0.085	0.066	0.144	0.224	0.155
63.2	0.091	0.13	0.105	0.211	0.421	0.256
63.3	0.091	0.103	0.1	0.187	0.341	0.204
63.4	0.151	0.148	0.146	0.28	0.405	0.334
63.6	0.092	0.122	0.091	0.218	0.3	0.198
Mean	0.1016	0.1176	0.1016	0.208	0.3382	0.2294
221.1	0.099	0.12	0.086	0.213	0.452	0.273
221.2	0.088	0.104	0.085	0.111	0.33	0.222
221.3	0.114	0.122	0.122	0.236	0.338	0.181
221.4	0.117	0.111	0.121	0.258	0.456	0.318
221.5	0.081	0.085	0.087	0.122	0.186	0.263
Mean	0.0998	0.1084	0.1002	0.188	0.3524	0.2514
289.2	0.129	0.118	0.152	0.205	0.369	0.33
289.3	0.153	0.156	0.128	0.253	0.268	0.244
289.5	0.12	0.127	0.11	0.222	0.361	0.234
289.6	0.099	0.102	0.12	0.158	0.298	0.215
289.7	0.085	0.107	0.112	0.151	0.342	0.268
Mean	0.1172	0.122	0.1244	0.1978	0.3276	0.2582
596.1	0.072	0.082	0.082	0.166	0.264	0.175
596.2	0.135	0.125	0.121	0.185	0.352	0.244
596.3	0.104	0.108	0.108	0.192	0.327	0.257
596.4	0.099	0.123	0.115	0.229	0.267	0.22
596.6	0.146	0.184	0.155	0.14	0.444	0.365
Mean	0.1112	0.1244	0.1162	0.1824	0.3308	0.2522

Appendix 3G: Wing length raw data for adult females of *Anopheles marshallii* group Length of wing spots measured in mm.

Sample ID	Wing Length	1. Sector pale spot	2. Median dark spot	3. Sub-coastal pale spot	4. Pre-apical dark spot	5. Pre-apical pale spot	6. Apical dark spot	Pale scales (White/Creamy)	Pale interruption in preapical dark spot (Distinct /Indistinct)
63.1	3.139	0.177	0.469	0.282	0.413	0.361	0.218	Predominantly white	Distinct
63.3	3.114	0.143	0.572	0.299	0.472	0.262	0.175	Creamy	Distinct
63.4	3.279	0.185	0.403	0.286	0.438	0.325	0.21	Predominantly white	Distinct
63.6	3.395	0.169	0.401	0.292	0.413	0.311	0.225	Creamy	Distinct
63.7	3.476	0.161	0.54	0.297	0.499	0.283	0.218	Predominantly white	Indistinct
Mean	3.281	0.167	0.477	0.2912	0.447	0.3084	0.2092		
221.1	3.529	0.166	0.463	0.331	0.498	0.339	0.237	Creamy	Distinct
221.2	3.089	0.158	0.456	0.31	0.507	0.357	0.293	Creamy	Indistinct
221.3	3.164	0.169	0.468	0.248	0.426	0.271	0.217	Creamy	Distinct
221.5	3.008	0.152	0.56	0.279	0.432	0.287	0.167	Creamy	Distinct
221.7	3.379	0.164	0.45	0.271	0.446	0.36	0.258	Creamy	Indistinct
Mean	3.234	0.1618	0.4794	0.2878	0.4618	0.3228	0.2344		
289.1	3.437	0.196	0.467	0.332	0.455	0.381	0.219	Creamy	Distinct
289.2	3.479	0.128	0.553	0.365	0.474	0.434	0.174	Creamy	Indistinct
289.3	3.44	0.163	0.478	0.231	0.459	0.297	0.214	Creamy	Distinct
289.4	3.008	0.171	0.448	0.231	0.426	0.253	0.275	Creamy	Distinct
289.5	3.512	0.187	0.421	0.255	0.428	0.253	0.211	Creamy	Distinct
Mean	3.375	0.169	0.4734	0.2828	0.4484	0.3236	0.2186		
596.1	3.102	0.201	0.403	0.282	0.41	0.291	0.201	Creamy	Indistinct
596.2	3.114	0.157	0.409	0.296	0.485	0.289	0.257	Creamy	Distinct
596.3	3.4	0.15	0.499	0.289	0.425	0.37	0.25	Creamy	Distinct
596.4	3.449	0.162	0.56	0.286	0.477	0.389	0.262	Creamy	Indistinct
596.6	3.114	0.166	0.54	0.272	0.332	0.231	0.166	Creamy	Indistinct
Mean	3.236	0.1672	0.4822	0.285	0.4258	0.314	0.2272		

Appendix 3H: Results of the repeat TaqMan assay on samples that initially tested positive for the presence of sporozoites.



Appendix 4A: Plagiarism Declaration

UNIVERSITY OF THE WITWATERSRAND, JOHANNESBURG

FACULTY OF HEALTH SCIENCES

PLAGIARISM DECLARATION TO BE SIGNED BY ALL HIGHER DEGREE STUDENTS

SENATE PLAGIARISM POLICY: APPENDIX ONE

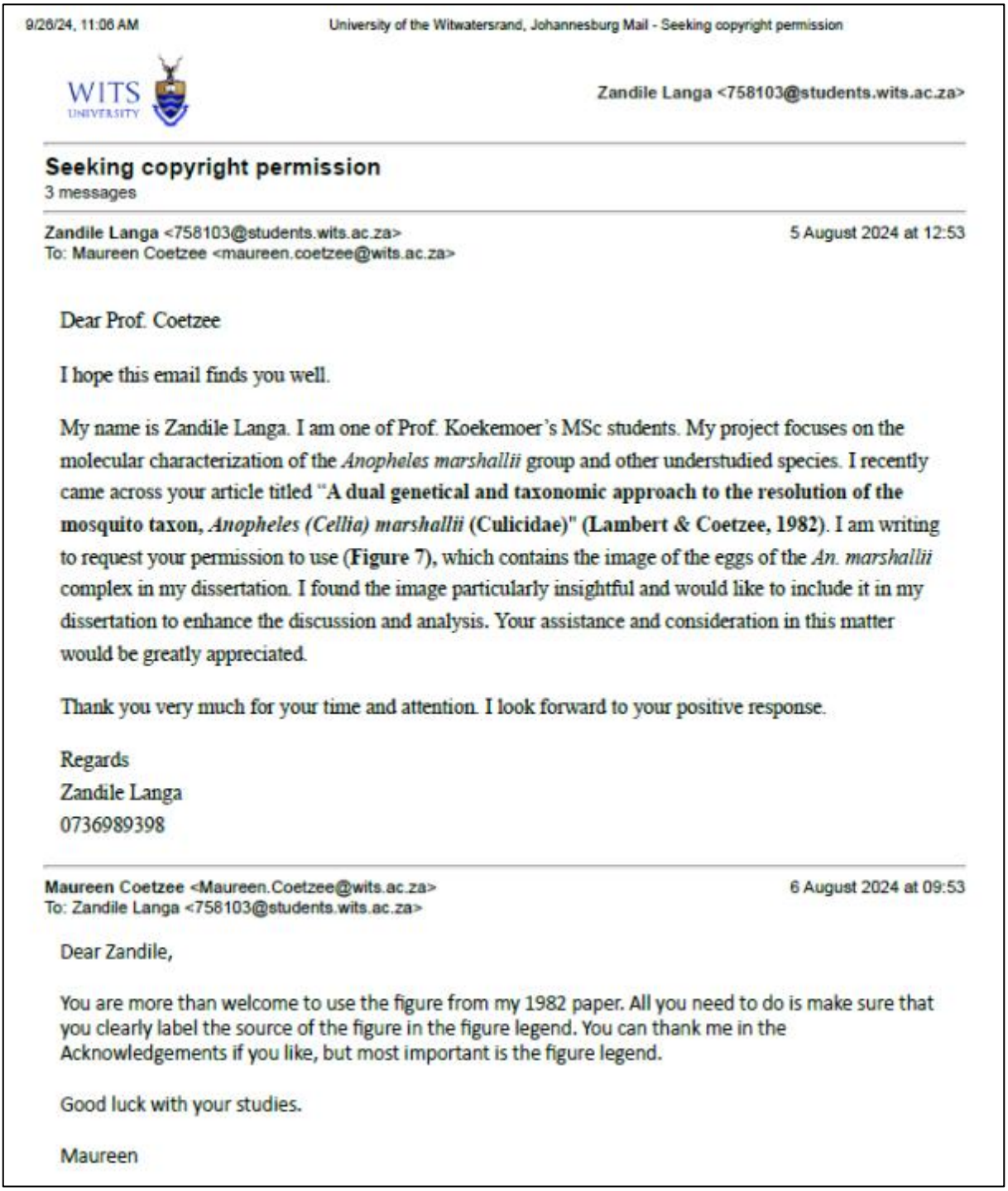
I **ZANDILE LANGA** (Student number: **758103)** am a student registered for the degree of **MASTER OF SCIENCE IN MEDICINE** in the academic year **2024**.

I hereby declare the following:

- I am aware that plagiarism (the use of someone else's work without their permission and/or without acknowledging the original source) is wrong.
- I confirm that the work submitted for assessment for the above degree is my own unaided work except where I have explicitly indicated otherwise.
- I have followed the required conventions in referencing the thoughts and ideas of others.
- I understand that the University of the Witwatersrand may take disciplinary action against me if there is a belief that this is not my own unaided work or that I have failed to acknowledge the source of the ideas or words in my writing.
- I have included as an appendix a report from "Turnitin" (or other approved plagiarism detection) software indicating the level of plagiarism in my research document.

Signature: Z. Langa Date: **02 December 2024**

Appendix 4B: Copyright permission to use Figure 7 from Lambert and Coetzee, 1982. (Figure 3.7C in Section 3.3.1 of this dissertation).



9/26/24, 11:08 AM University of the Witwatersrand, Johannesburg Mail - Seeking copyright permission

WITS UNIVERSITY

Zandile Langa <758103@students.wits.ac.za>

Seeking copyright permission

3 messages

Zandile Langa <758103@students.wits.ac.za> 5 August 2024 at 12:53
To: Maureen Coetzee <maureen.coetzee@wits.ac.za>

Dear Prof. Coetzee

I hope this email finds you well.

My name is Zandile Langa. I am one of Prof. Koekemoer's MSc students. My project focuses on the molecular characterization of the *Anopheles marshallii* group and other understudied species. I recently came across your article titled "**A dual genetical and taxonomic approach to the resolution of the mosquito taxon, *Anopheles (Cellia) marshallii* (Culicidae)" (Lambert & Coetzee, 1982)**. I am writing to request your permission to use (**Figure 7**), which contains the image of the eggs of the *An. marshallii* complex in my dissertation. I found the image particularly insightful and would like to include it in my dissertation to enhance the discussion and analysis. Your assistance and consideration in this matter would be greatly appreciated.

Thank you very much for your time and attention. I look forward to your positive response.

Regards
Zandile Langa
0736989398

Maureen Coetzee <Maureen.Coetzee@wits.ac.za> 6 August 2024 at 09:53
To: Zandile Langa <758103@students.wits.ac.za>

Dear Zandile,

You are more than welcome to use the figure from my 1982 paper. All you need to do is make sure that you clearly label the source of the figure in the figure legend. You can thank me in the Acknowledgements if you like, but most important is the figure legend.

Good luck with your studies.

Maureen